

A Translational Study in Pancreatic Neuroendocrine Neoplasms

Dr Kate Young

University of London

MD(Res)

Co-Primary Supervisors:

Dr Naureen Starling and Dr Anguraj Sadanandam

Backup Supervisor: Ian Chau

IRS Partner: David Cunningham

The Royal Marsden NHS Foundation Trust &

The Institute of Cancer Research

Declaration

I confirm that the work presented in this thesis is my own.

Dr Kate Young

Word Count excluding references: 43,559

Abstract

Pancreatic Neuroendocrine Neoplasms (PanNENs) are rare, highly heterogeneous tumours. There have been significant recent advances in our knowledge of genomic events underlying their pathogenesis. However, treatment decisions remain largely based on tumour stage and grade which is inadequate, the current classification paradigm failing to capture the significant heterogeneity in tumour biology.

The first aim of my thesis was to establish a large registry for PanNENs and then clinically phenotype the patients included. The next aim was to develop a novel assay to subtype PanNENs, based on our previously derived PanNETassigner molecular subtypes, and to establish if the subtypes assigned were prognostic.

The PanNEN registry and PanNETassigner assay were successfully developed. Clinical data and tissue samples from the registry were used to test, validate and refine this assay. The assay demonstrated that the metastasis-like primary-1 subtype (MLP-1) was associated with a poor prognosis.

Novel therapeutic options are required in PanNENs and trials of immunotherapy are underway, although knowledge of the immune microenvironment in this disease is lacking. The last aim of my thesis was therefore to describe immune related gene expression across the PanNETassigner molecular subtypes.

The poor prognosis MLP-1 subtype had an immune high phenotype, associated with hypoxic tumours and signalling within damage-associated molecular pattern pathways. The immune gene expression profile demonstrated generates the hypothesis that the MLP-1 subtype may be more amenable to an immunotherapeutic approach than other subtypes.

Overall, my thesis demonstrates that molecular subtyping can be used to provide valuable additional information both regarding prognosis and the immune microenvironment in PanNENs. The assays and hypotheses developed here now require additional testing in pre-clinical mechanistic studies, larger cohorts of patients and prospective clinical trials. With such further validation the PanNETassigner subtypes may pave a way forward for a more personalised approach for patients with this rare tumour type.

Contents

Declaration.....	2
Abstract	3
Contents	4
Tables.....	8
Figures.....	9
Publications and Presentations	11
Awards.....	12
1 Introduction.....	13
1.1 Epidemiology of Pancreatic Neuroendocrine Neoplasms	13
1.2 Clinical Features and Diagnosis of PanNENs	16
1.3 Staging of PanNENs	18
1.4 Histopathological Classification of PanNENs	19
1.5 Molecular Biology and Subtypes of PanNENs.....	24
1.6 Current Treatment of PanNENs	27
1.7 Biomarkers in PanNENs	31
1.8 Hypothesis	38
1.9 Research Aims	39
2 Establishing a PanNEN Registry (PaNACeA study).....	40
Abstract.....	40
2.1 Background and Rationale.....	42
2.2 Methods.....	43
2.2.1 Securing Funding.....	43
2.2.2 Patient and Public Involvement.....	43
2.2.3 PaNACeA Study Set up and management.....	44
2.2.4 PanNEN Registry Design.....	45
2.2.5 Consent	45
2.2.6 Clinical Data Collection	46
2.2.7 Tissue Collection and Histological Assessments.....	46
2.2.8 Statistical Analyses	46
2.2.9 Overview of my role	47
2.3 Results.....	48
2.3.1 Clinical Data Collection, Tissue Retrieval and Central Review	48
2.3.2 Patient Demographics across the entire cohort.....	50
2.3.3 Tumour and Disease Characteristics across the entire cohort	50

2.3.4	Differences in Characteristics of the RM and Verona Cohorts.....	52
2.3.5	Baseline Symptoms and Investigations.....	53
2.3.6	Systemic Treatment.....	55
2.3.7	Survival Analyses.....	56
2.3.8	Assessment of Heterogeneity across and within Grades.....	60
2.4	Discussion.....	62
3	Development of the PanNETassigner Assay.....	68
	Abstract.....	68
3.1	Background and Rationale.....	70
3.2	Methods.....	74
3.2.1	PanNEN Tissue Samples and Clinical Data.....	74
3.2.2	228 gene PanNETassigner NanoString Assay Development.....	77
3.2.3	Wet Lab Techniques.....	77
3.2.4	Bioinformatics Techniques.....	79
3.2.5	Overview of my role.....	82
3.3	Results.....	85
3.3.1	Initial Testing of 228 gene PanNETassigner NanoString Assay (n=48)	85
3.3.2	Suitability of the NanoString platform.....	85
3.3.3	Further Testing of the 228 Gene Assay (n=96).....	87
3.3.4	Subtyping using the 228 gene Assay (n=144).....	89
3.3.5	Development of the Refined 78 gene Nano-PanNET Assay.....	92
3.3.6	Survival Analysis according to PanNETassigner Subtype.....	95
3.3.7	Validation of the 78 Gene Nano-PanNET Assay using FFPE samples from the Verona Cohort (n=44).....	101
3.3.8	Validation of 78 gene panel centroids with RNAseq data (n=98)..	103
3.3.9	Validation of 78 gene Nano-PanNET Assay using FFPE samples from the Royal Marsden Cohort as a real world example (n=27).....	104
3.3.10	Inclusion of 2 Erroneous Samples and Additional Bioinformatics Assessments Completed.....	105
3.4	Discussion.....	107
4	The Immune Landscape of PanNENs.....	115
	Abstract.....	115
4.1	Background and Rationale.....	117
4.2	Methods.....	120
4.2.1	PanNEN Patient Samples.....	120
4.2.2	Wet Lab Techniques.....	123

4.2.3	Bioinformatics Techniques	124
4.2.4	Overview of my role	127
4.3	Results.....	130
4.3.1	Preliminary Work: NanoString Immune Profiling Assay reveals differential immune gene expression across PanNETassigner subtypes (n=48)	130
4.3.2	Preliminary work: NanoString analyses reveal MLP subtype has a high Immune Cell Abundance and is enriched for multiple immune pathways	131
4.3.3	Immune related gene expression is not dependent upon grade of disease, liver metastases or genetic mutations	133
4.3.4	Differential expression of immune related genes according to PanNETassigner subtype	136
4.3.5	MLP-1 subtype demonstrates a highly diverse pattern of immune gene expression.....	139
4.3.6	MLP-1 Subtype is enriched for Hypoxia and Necroptosis genes ..	140
4.3.7	MLP-1 is enriched for genes associated with the DAMP pathway, Toll-Like Receptors and Dendritic Cells.....	143
4.3.8	MLP-1 Subtype is enriched for genes associated with multiple aspects of the immune response.....	144
4.3.9	MLP-1 Subtype is enriched for the genes of multiple immune cell types	146
4.3.10	MLP-1 tumours display elements of both immune stimulation and immunosuppression	149
4.3.11	Validation Cohorts support patterns of immune cell gene expression in Microarray Cohort.....	150
4.3.12	Other PanNETassigner subtypes demonstrate different enrichment patterns	152
4.3.13	Multiplex IHC demonstrates increased macrophage density in MLP-1	155
4.3.14	Key Immunotherapy Targets are enriched in MLP-1	157
4.3.15	Deficient Mismatch Repair (MMR) not associated with PanNETassigner subtypes.....	159
4.3.16	MLP Subtype enriched for Expanded Immune Signature across all cohorts	159
4.4	Discussion	163
5	Conclusions	171
	References	175
	Acknowledgements.....	197
	Appendices	199

Appendix 1	199
Appendix 1.1 Abbreviations used in this thesis.....	199
Appendix 2	203
Appendix 2.1 PaNACeA Study Protocol.....	203
Appendix 3	221
Appendix 3.1 Supplementary Table 3.1 228 Gene Panel for PanNETassigner Nanostring Assay.....	221
Appendix 3.2 Supplementary Table 3.2 Refined 78 Gene PanNETassigner Panel and Centroids.....	227
Appendix 3.3 Supplementary Table 3.3 RM Cohort FFPE Sample Details.	229
Appendix 3.4 SEQTOR study Translational Project documents.	231
Appendix 4	237
Appendix 4.1 Supplementary Table 4.1 132 differentially expressed immune genes according to PanNETassigner subtype, classified according to subtype with highest expression.....	237
Appendix 4.2 Supplementary Table 4.2 GSEA Report for MLP-1 using C7 Gene Sets.....	241
Appendix 4.3 Supplementary Table 4.3 MMR status for RMH PanNET cohort (n=24)	242

Tables

Table 1.1 Functional Syndromes Associated with PanNENs.....	17
Table 1.2 ENETs /8 th edition AJCC TNM Classifications	18
Table 1.3 Selected Studies demonstrating the prognostic value of WHO grade in PanNETs	22
Table 1.4 Selected studies demonstrating the prognostic value of alternate Ki-67 index cut-offs in PanNETs.....	23
Table 1.5 WHO Classification of GEP-NENs from 2010 and 2017	24
Table 1.6 Range of Treatment Options available for Advanced PanNET	30
Table 1.7 Selected Potential Prognostic Biomarkers investigated in PanNEN.....	33
Table 2.1 Patient Demographics and Baseline Disease Characteristics.....	51
Table 2.2 Baseline Symptoms and Investigations	54
Table 2.3 Median OS, 2 year and 5 year survival rates	58
Table 2.4 Univariate Analysis	59
Table 2.5 Multivariate Analysis.....	59
Table 2.6 Heterogeneity across and within grades.....	60
Table 3.1 Subtypes Assigned using Microarray Data and 228 gene Assay (n=19)	87
Table 4.1 Selected Immunotherapy Trials in PanNENs registered on ClinicalTrials.gov.....	118
Table 4.2 Selected Studies of Potential Immune Biomarkers in GEP-NENs.....	119
Table 4.3 Summary characteristics for Microarray Cohort.....	134
Table 4.4 PanNETassigner Subtypes, Immune Properties and Potential Treatment Approaches.....	162

Figures

Figure 1.1 Incidence (A), Prevalence (B) and Median OS according to Stage and Grade (C) for PanNEN Patients (1973-2012)	15
Figure 1.2 Examples of poorly and well differentiated GEP-NENs.....	20
Figure 1.3 PanNETassigner Molecular Subtypes	26
Figure 2.1 Clinical Data and Tissue Collection for the Verona Cohort	48
Figure 2.2 Clinical Data and Tissue Collection for the RM Cohort	49
Figure 2.3 Proportions of patients according to ENETS Stage	52
Figure 2.4 Baseline Symptoms in RM Cohort (n=77)	53
Figure 2.5 Systemic Treatments Administered in the RM Cohort	55
Figure 2.6 Chemotherapy Regimens Administered in RM cohort	55
Figure 2.7 OS in all patients (All grades/Stages)	57
Figure 2.8 OS according to ENETs stage (combined I/II/III vs. IV)	57
Figure 2.9 OS according to WHO 2010 Grade	58
Figure 3.1 nCounter Elements™ Tag Complex	72
Figure 3.2 NanoString Hybridization and Decoding Process	73
Figure 3.3 Overview of Tissue Samples and Analyses Performed	75
Figure 3.4 Overview of the project to develop, refine and validate a novel PanNETassigner NanoString Assay.....	76
Figure 3.5 Macrodissection Process	78
Figure 3.6 Strong Concordance between subtypes derived from Microarray data and NanoString data (iLVM)	86
Figure 3.7 Heatmap of gene expression data from the 228 gene Assay.....	88
Figure 3.8 Technical Reproducibility of the 228 gene Assay	88
Figure 3.9 Genes with $\geq 20\%$ zero expression removed from analysis.....	89
Figure 3.10 exploBATCH analysis of batch effect for 228 Gene Assay	90
Figure 3.11 Cophenetic and Silhouette Analyses as part of NMF.....	91
Figure 3.12 Single Run Silhouette to determine most representative samples for further analysis of PanNETassigner subtypes	91
Figure 3.13 SAM used to derive refined 78 gene Nano-PanNET Assay	92
Figure 3.14 PAM Centroids for Refined 78 gene Nano-PanNET Assay.....	93
Figure 3.15 Heatmap of Expression of selected 78 genes (n=113)	94
Figure 3.16 Distribution of (A) PanNETassigner Subtypes and (B) WHO 2010 Grades (n=97).....	95
Figure 3.17 OS according to PanNETassigner Subtype (n=97).....	96
Figure 3.18 OS according to WHO 2010 Grade (n=97)	97
Figure 3.19 WHO 2010 Grade according to PanNETassigner Subtype.....	98
Figure 3.20 OS according to PanNETassigner subtype for Grade 1 Patients.....	99
Figure 3.21 OS according to PanNETassigner subtype for Grade 2 patients	100
Figure 3.22 OS according to PanNETassigner subtype for Grade 1 and 2 patients	101
Figure 3.23 Correlation between the expression of the refined panel of 78 genes in fresh frozen and FFPE patient samples (n=37)	102
Figure 3.24 Concordance of PanNETassigner subtypes assigned using FFPE and Fresh Frozen Tissue by NanoString assay (n=37)	102
Figure 3.25 Concordance between subtypes assigned using 78 gene panel centroids with RNAseq data (fresh frozen) and using NanoString assay data (fresh frozen) (n=98)	103

Figure 3.26 78 gene Nano-PanNET Assay Results for RM Cohort (n=12)	105
Figure 4.1 Overview of PanNEN Samples and Analyses Conducted	122
Figure 4.2 Heatmap to demonstrate enrichment of the MLP Subtype for Immune Related Gene Expression	130
Figure 4.3 Heatmap to demonstrate the enrichment of the Preliminary Expanded Immune Signature in the MLP vs. the Intermediate Subtype (n=32).....	131
Figure 4.4 Box Plots to demonstrate enriched Immune Cell Abundance across multiple cell types in the MLP vs. Intermediate Subtype	132
Figure 4.5 NSolver Immune Pathway Scores increased in MLP subtype	132
Figure 4.6 Immune Related Gene Expression According to Clinical Parameters of Importance and PanNETassigner Subtype	135
Figure 4.7 PanNETassigner Subtypes and Immune Related Gene Expression.	138
Figure 4.8 High Diversity of Immune Gene Expression in MLP-1 Subtype	140
Figure 4.9 Enrichment of MLP-1 Subtype for Hypoxia and Necroptosis Genes.	142
Figure 4.10 Enrichment of the MLP-1 pathway for DAMP pathway genes.....	145
Figure 4.11 Enrichment of the MLP-1 Subtype for genes associated with multiple immune cell types	148
Figure 4.12 ssGSEA Analyses for Validation Cohorts	151
Figure 4.13 Immune Enrichment Patterns in Intermediate and MLP-2.....	154
Figure 4.14 Multiplex IHC (mIHC) supports Macrophage enrichment of MLP-1 subtype	156
Figure 4.15 Key Immunotherapy Targets enriched in the MLP-1 subtype	158
Figure 4.16 Expanded Immune Signature Enrichment in MLP-1 and MLP-2.....	160
Figure 4.17 Pathways of Immune Enrichment and Potential Therapeutic Opportunities in the MLP-1 Subtype.....	161

Publications and Presentations

- **Young K**, Lawlor RT, Patil Yet al. Immune Landscape and Therapeutic Potentials in Pancreatic Neuroendocrine Tumours determined by Molecular Subtypes and Hypoxia-associated Pathways. Manuscript in preparation.
- Sadanandam A, **Young K**, Lawlor R et al. Immune Characteristics of Pancreatic Neuroendocrine Tumours According to Grade and Molecular Subtypes. Oral Presentation ENETS 2019, Barcelona
- Sadanandam A, **Young K**, Nyamundanda G et al. Development of a multiplex biomarker assay to subtype pancreatic neuroendocrine tumours (PanNETs) with distinct prognosis and mutations. Oral Presentation ENETS 2018, Barcelona
- **Young K**, Ragulan C, Nyamundanda G et al. Immune Landscape of Pancreatic Neuroendocrine Tumours (PanNETs). Proffered Paper (Oral) presentation ESMO 2017, Madrid
- **Young K**, Morganstein D, Sadanandam A and Starling N. A translational study in Gastroenteropancreatic Neuroendocrine tumours (GEP-NETs) to validate and assess a new molecular classification (PaNACeA). Poster presentation, NIHR Trainee Meeting: Research Leaders of the Future, Leeds
- **Young K**, Morano F, Morganstein D et al. A single institution experience of treating gastroenteropancreatic neuroendocrine tumours (GEP-NETs) over the last 10 years: the Royal Marsden Hospital (RM) experience. Poster presentation at UKINETS meeting, Royal College of Physicians, London
- **Young K**, Iyer R, Morganstein D et al. Pancreatic Neuroendocrine Tumours: a review. *Future Oncol* (2015),11(5), 853–864

Awards

- Ronald Raven Bequest awarded to attend Neuroendocrine Tumour Research Foundation Symposium. K Young (2017)
- ESMO Travel Grant awarded for proffered oral paper. K Young (2017)
- BRC Flagship Grant: PaNACeA- A translational study in GEP-NETs to validate and assess a novel molecular classification. (£224,910). K. Young, A. Sadanandam, D. Morganstein and N. Starling (CI). (2015)
- UKINETS Travel Grant awarded for high scoring abstract. K Young (2015)

1 Introduction

1.1 Epidemiology of Pancreatic Neuroendocrine Neoplasms

Neuroendocrine neoplasms (NENs) are rare and heterogeneous tumours with widely varying morphologies and behaviours. NENs arise in multiple organs, originating in different neuroendocrine cells across the body. Over 65% occur in the GI tract, known as Gastroenteropancreatic (GEP) NENs¹. Whilst GEP-NENs remain a rare cancer, their incidence has significantly increased in recent decades to 5.25/100,000/year, according to Surveillance, Epidemiology and End Results (SEER) program data². Moreover, as many GEP-NENs are slow growing, with a reasonable length of survival even with metastatic disease, their prevalence is relatively high and rising^{3,4,5}.

This rising incidence of GEP-NENs has been documented across the globe^{6,7,8,9}. The aetiology for this increase is likely multifactorial, attributed to an aging population, improved detection due to the growing use of screening endoscopies and cross-sectional imaging, improved data capture by registries and an increased awareness of the disease both in the medical and in the general population^{3,4}.

Pancreatic neuroendocrine neoplasms (PanNENs) are the 3rd most common GEP-NEN, after small bowel and rectal NENs, with an incidence of 0.33-0.48/100,000/year^{6,3} (Figure 1.1 A and B). After Pancreatic Ductal Adenocarcinoma (PDAC), PanNENs are the second most common epithelial cancer of the pancreas, with an overall mortality rate of 60%^{10,11}.

Sporadic PanNENs can present at any age, but the highest incidence is found in patients between the ages of 30 and 60, with no significant difference in incidence between men and women¹². In the past, a large proportion of PanNENs were thought to be functional, secreting hormones resulting in specific patterns of symptoms. However, as diagnostic techniques have improved and more non-functional tumours are being

identified, it is now believed that over 60% of PanNENs are non-functional¹³.

Overall survival (OS) varies significantly between patients, from under 1 to over 20 years, and is influenced by a number of factors including disease stage (Figure 1.1 C). Although PanNENs tend to be slow growing, in the region of 60% of patients will have nodal metastases at diagnosis, and 30% will have liver metastases¹⁴. 5-year survival ranges from 60-100% for localised disease to 25% for metastatic disease¹⁵. In dedicated centres the 5-year survival for metastatic disease can be over 60%, highlighting the importance of specialised care for this rare tumour type¹⁵. Although relatively good in oncological terms, these prognoses remain life-limiting for the majority and significantly worse for many patients.

Figure 1.1 Incidence (A), Prevalence (B) and Median OS according to Stage and Grade (C) for PanNEN Patients (1973-2012)

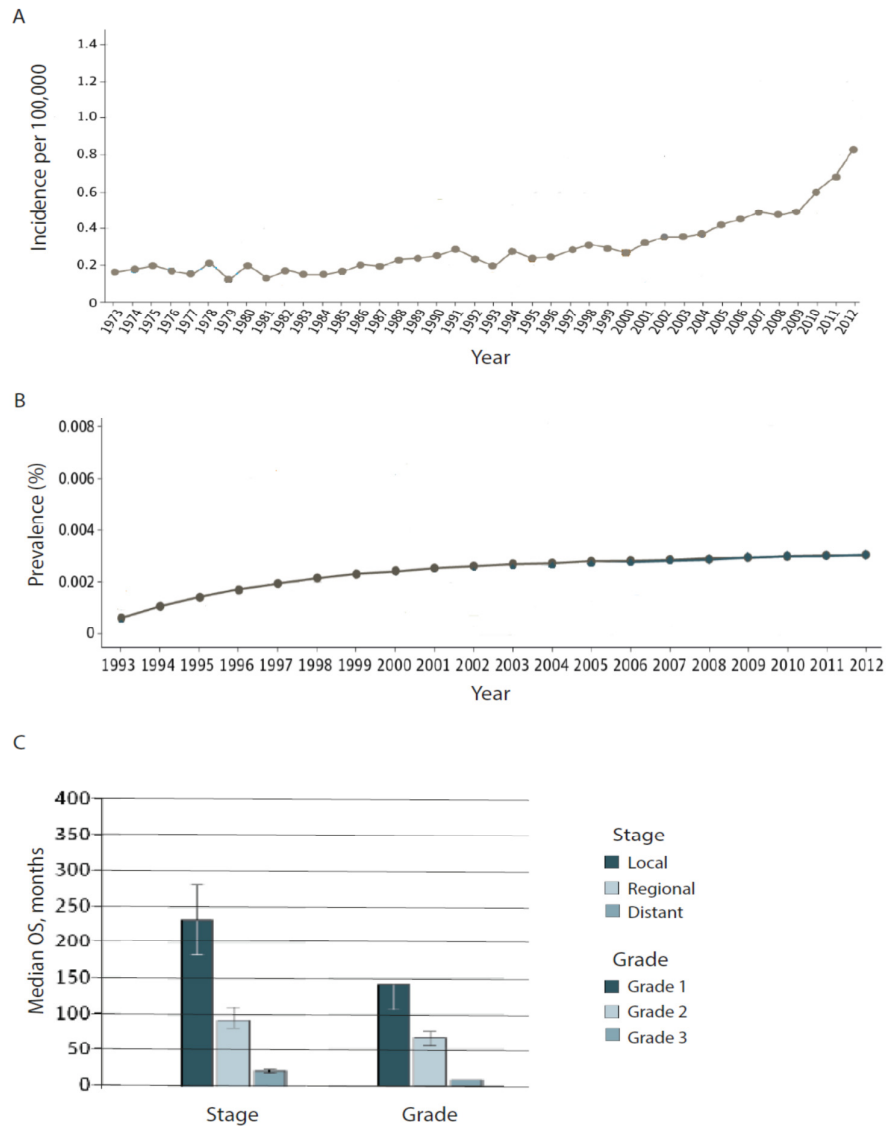


Figure 1.1 is modified from Trends in the Incidence, Prevalence, and Survival Outcomes in Patients With Neuroendocrine Tumors in the United States (JAMA Oncol.2017;3(10):1335-1342.doi:10.1001/jamaoncol.2017.0589)

1.2 Clinical Features and Diagnosis of PanNENs

As with all NETs, presenting symptoms for PanNENs may be initially mild and non-specific such as abdominal pain, nausea, weight loss and anaemia. Pain can be caused by mass effect from the primary tumour itself or from liver capsule pain, due to metastatic liver disease. For patients with non-functional tumours a high index of suspicion is therefore required and diagnosis may be delayed for many years¹⁶. Patients with functional tumours, may have specific patterns of symptoms according to the peptide hormone released, making them more easily recognisable (Table 1.1)¹⁷.

The 4 classic functional PanNENs are Insulinomas, Gastrinomas, Glucagonomas and VIPomas¹⁸. Insulinomas and Gastrinomas tend to be diagnosed earlier, due to the significant symptoms caused by large volumes of peptides released, whereas Glucagonomas and VIPomas may be diagnosed later. Other functional tumours, such as somatostatinomas, GRFomas, ACTHomas, PTHrPomas and PanNETs causing Carcinoid syndrome, are less common¹⁷.

The diagnosis of a PanNEN is based on the clinical picture, blood and urine tests for secreted peptides and amines, a variety of imaging modalities, including somatostatin receptor (SSTR) scintigraphy or SSTR PET/CT scans for well differentiated NENs, and histopathology¹⁹. Both European and American NET societies have published extensive guidelines regarding the diagnostic pathway^{13,20,21}. These investigations enable the patient's tumour to be classified according to tumour type, grade and stage, which in turn facilitates risk stratification and treatment planning. However, there are significant limitations regarding the precision of the current classification paradigm and its ability to personalise treatment planning in this very heterogeneous disease.

Table 1.1 Functional Syndromes Associated with PanNENs

Tumour (Syndrome)	Symptoms	Associated Peptide	Incidence (per million/year)
Insulinoma (Hypoglycaemia syndrome)	Confusion, sweating, dizziness, weakness, unconsciousness, relief with eating	Insulin	1-2
Gastrinoma (Zollinger-Ellison syndrome)	Diarrhoea with or without severe peptic ulceration	Gastrin	1-2
Glucagonoma (Glucagonoma Syndrome)	Necrolytic migratory erythema, weight loss, diabetes mellitus, stomatitis, diarrhoea, DVT, depression	Glucagon	0.1
VIPoma (Verner-Morrison Syndrome)	Profuse watery diarrhoea and marked hypokalaemia, hypochlorhydria	Vasointestinal polypeptide (VIP)	0.1
Somatostatinoma (questionable if syndrome exists)	Cholelithiasis, weight loss, diarrhoea, steatorrhoea, diabetes mellitus, achlorhydria	Somatostatin	<0.1
ACTHoma (Cushing's Syndrome)	Weight gain, round face, menstrual changes, hirsutism, hypertension, bruising, depression, dorsal fat pad, abnormal glucose tolerance	ACTH (Adrenocorticotrophic hormone)	<0.1
PTHrPomas (Hypercalcaemia)	Symptoms due to raised calcium	PTHrP (Parathyroid hormone related peptide)	<0.1
GRFoma (Acromegaly)	Enlarged hands and feet, coarsened facial features, thickened skin, excessive sweating, skin tags, fatigue and muscle weakness	GRF(Growth hormone releasing factor)	Unknown
Carcinoid Syndrome	Dry flushing, palpitations, diarrhoea, abdominal pain, wheezing, carcinoid heart disease, pellagra	Serotonin	< 50 total cases

1.3 Staging of PanNENs

A number of different staging systems have been proposed for PanNETs, the European Neuroendocrine Tumour Society (ENETs) and the American Joint Committee on Cancer/ Union for International Cancer Control (AJCC/UICC) TNM classifications being the most commonly used²². Whilst both have been shown to be prognostic, the ENETs PanNET specific classification previously demonstrated superiority over the 7th edition AJCC system in predicting patient outcomes²². The AJCC classification was subsequently altered, introducing a PanNET specific system, to bring it closer to the ENETs classification in the 8th edition in 2017 (Table 1.2).

Table 1.2 ENETs /8th edition AJCC TNM Classifications

	ENETs and AJCC/UICC 8th Edition*
Tx	Tumour cannot be assessed
T0	No evidence of primary tumour
T1	Tumour limited to the pancreas, <2 cm
T2	Tumour limited to the pancreas, 2 to 4 cm
T3	Tumour limited to the pancreas, >4 cm; or tumour invading the duodenum or common bile duct
T4	Tumour invading adjacent organs (stomach, spleen, colon, adrenal gland) or the wall of large vessels (celiac axis or the superior mesenteric artery)
Nx	Regional lymph nodes cannot be assessed
N0	No regional lymph node involvement
N1	Regional lymph node involvement
M0	No distant metastasis
M1	Distant metastases
Stage I	T1 N0 M0
Stage IIA	T2 N0 M0
Stage IIB	T3 N0 M0
Stage IIIA	T4 N0 M0
Stage IIIB	Any T N1 M0
Stage IV	Any T Any N M1

**Note PanNECs are staged separately in AJCC system, alongside PDAC*

The prognostic ability of the ENETs/8th edition AJCC has been since compared to the 8th edition AJCC classification for exocrine pancreatic cancer (EPC), which includes an N2 category for involvement of ≥ 4 regional lymph nodes. This analysis concluded that the EPC classification was superior, although noted that the differences were minimal²³. A further modified ENETs classification with prognostic significance has also been proposed, with slightly altered staging groups²⁴.

A clear consensus staging system to avoid confusion, to ensure guidelines are appropriately followed and to enable accurate comparable research would be ideal, but it is not yet clear which classification will fill this space. At present, it is reasonable to use the ENETs/8th edition AJCC classification and indeed this is referred to in current guidelines¹³. Whichever staging system is ultimately used, its prognostic ability is complemented by histopathological grading of the tumour.

1.4 Histopathological Classification of PanNENs

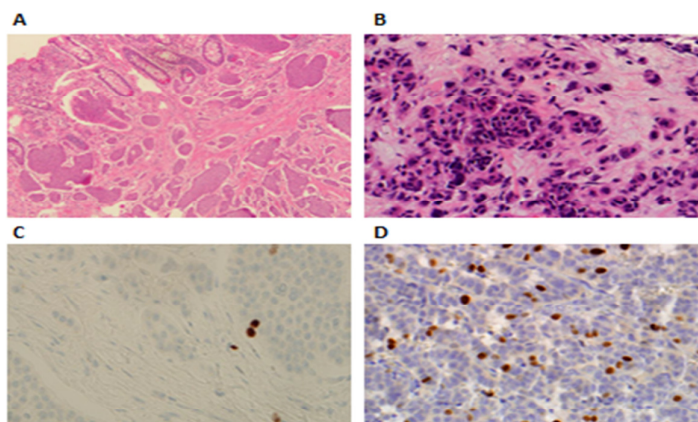
To improve the classification and management of heterogeneous GEP-NENs the ENETs devised a grading system, adopted by the World Health Organisation (WHO) in 2010²². In this tiered classification, NENs are divided into 3 grades, according to various histopathological features and the tumour's proliferative index, assessed by Ki-67% or Mitotic Index (MI). The Ki-67 Index is a measure of active cell cycling using monoclonal antibody staining and the MI is an assessment of the proportion of cells with visible chromosomes²⁵.

The main division in the WHO classification is between well and poorly differentiated tumours; the former grouped as grade 1/2 NETs and the latter labelled grade 3 Neuroendocrine Carcinomas (NECs). The 3 grades have been demonstrated to have prognostic significance across multiple studies, with grade 1 tumours (Ki-67<3%) having the best prognosis and grade 3 tumours (Ki-67>20%) the worst^{26,11} (Table 1.3 and Figure 1.2).

This split between well and poorly differentiated tumours also appears to be biologically relevant as clear differences have been documented in genetic

alterations between the two groups. Well differentiated NETs may have mutations including *MEN1*, *DAXX/ATRX*, *TSC* and *NF1* but poorly differentiated NECs are more likely to have *p53*, *CDKN2A* or *RB* mutations, or share alterations associated with PDAC such as *KRAS* or *SMAD4* mutations^{27,28,29}.

Figure 1.2 Examples of poorly and well differentiated GEP-NENs



Haematoxylin and Eosin (H&E) staining showing a well differentiated (A) and a poorly differentiated GEP-NEN (B). Ki-67 monoclonal antibody staining demonstrating a tumour with a low Ki-67 index (C) and a high Ki-67 index (D). Images provided by histopathologist Monica Terlizzo.

Whilst the WHO grading system has significant value, there remains substantial heterogeneity of disease behaviour within the grades. Further, there is controversy as to the optimum Ki-67 cut-offs used to assign grade, with various alternative cut-offs proposed in the literature (Table 1.4). For example, a number of groups have advocated a higher Ki-67 threshold for grade 2 disease, at 5%, which may improve the prognostic value of the classification or subdividing grade 3 disease at a Ki-67 of 55%^{30,31,32}.

The heterogeneity within the classification system was in part recognised by the WHO, who published an update to their 2010 classification in 2017, adding a 3rd well differentiated NET subgroup, NET grade 3¹². Tumour samples classified as NET grade 3 are well differentiated but have a Ki-67 > 20% (Table 1.5). Patients within this new NET grade 3 subgroup are

reported to have a somewhat worse prognosis than grade 2 NET patients, but a better prognosis than grade 3 NEC patients³³. However, the WHO 2017 update did not alter the Ki-67 cut-off between grade 1 and 2 disease, or include any maximum Ki-67% for the new grade 3 PanNET group and the problem of heterogeneity within grades persists.

Table 1.3 Selected Studies demonstrating the prognostic value of WHO grade in PanNETs

Study Population (n)	Ki-67 cut-offs investigated	Endpoint	Prognostic Significance	Reference (Year)
PanNET (61) Non-functional	2%	OS	Prognostic in univariate analysis	La Rosa et al.³⁴ (1995)
PanNET (324) Mixed	2%	OS	Prognostic on multivariate analysis	Ekeblad et al.¹¹ (2008)
Foregut NET (PanNET 131) Mixed	≤2%, 3-20% and >20%	OS	Prognostic on multivariate analysis	Pape et al.³⁵ (2008)
GEP-NET (PanNET 288) Mixed	≤2% vs. >20%	OS	Prognostic on multivariate analysis	Garcia-Carbonero et al.³⁶ (2010)
PanNET (131) Mixed	≤2%, 3-20% and >20%	OS	Prognostic on univariate but not multivariate analysis	Khan et al.³⁷ (2013)
PanNET (166) Non-functional	≤2%, 3-20% and >20%	OS	Prognostic on multivariate analysis	Bu et al.³⁸ (2018)

Table 1.4 Selected studies demonstrating the prognostic value of alternate Ki-67 index cut-offs in PanNETs

Study Population (n)	Ki-67 cut-offs investigated	Endpoint	Prognostic Significance	Reference (Year)
PanNET (54) Functional and Non-functional	5%	OS	Prognostic on multivariate analysis	Pelosi et al.³⁹ (1996)
PanNET (274) Resected	≤5%, 6-20% and >20%	OS	Prognostic on multivariate analysis	Scarpa et al.²⁶ (2010)
PanNET (202) Advanced	5%	PFS	Prognostic on multivariate analysis	Panzuto et al.⁴⁰ (2011)
PanNET (1072) Resected	4.85%	OS	Prognostic on multivariate analysis	Rindi et al.⁴¹ (2012)
PanNET (131) Mixed	≤5%, 6-20% and >20%	OS	Prognostic on multivariate analysis	Khan et al.³⁷ (2013)
GI-NEC (305) Mixed	55%	OS	Prognostic on univariate but not on multivariate analysis	Sorbye et al.⁴² (2013)

Table 1.5 WHO Classification of GEP-NENs from 2010 and 2017

WHO 2010			WHO 2017		
Differentiation	Grade	Ki67	Differentiation	Grade	Ki67
Well Differentiated NET	NET Grade 1	<3%	Well Differentiated NEN	NET Grade 1	<3%
	NET Grade 2	3-20%		NET Grade 2	3-20%
				NET Grade 3	>20%
Poorly Differentiated NEC	NEC Grade 3 (small cell or large cell)	>20%	Poorly Differentiated NEN	NEC Grade 3 (small cell or large cell)	>20%

In clinic, this heterogeneity of disease behaviour within grades causes significant problems. It may manifest as a patient having a lower grade tumour (1/2) which behaves more like a grade 3 tumour and perhaps should be treated more aggressively upfront and vice versa. However, currently there is no way to predict such disease behaviour at baseline or to determine which patients may require treatment intensification or indeed de-escalation, sparing them unnecessary treatment and attendant side effects. There is a clear unmet clinical need for novel prognostic and predictive markers to complement grade and stage, guide prognostication and support individualised treatment decisions.

1.5 Molecular Biology and Subtypes of PanNENs

The majority of pNENs are sporadic, but they may occur as part of one of the familial cancer syndromes, such as Multiple Endocrine Neoplasia 1 (MEN1), Von Hippel Lindau (VHL), Neurofibromatosis type 1 and Tuberous sclerosis¹⁸. Studying the genetic mutations seen in these syndromes and the molecular profiling of sporadic PanNENs have been key steps in understanding the development and progression of these tumours, with whole-genome analysis recently published²⁹.

Recurrent genetic alterations have been described in four main pathways in sporadic PanNETs: telomere maintenance (*DAXX/ATRX*), chromatin remodelling (*SETD2, ARID1A, MLL3*), mTOR pathway activation (*PTEN*,

TSC1/2, *DEPDC5*) and DNA damage repair (*CHEK2*, *BRCA2*, *MUTYH*, *ATM*), with *MEN1* inactivation influencing all four pathways^{28, 29}.

Chromosomal instability (CIN) has also been noted as a feature of GEP-NETs^{43,44}. It has been suggested that in PanNET CIN may be a result of mutations in *MEN1/DAXX/ATRX* leading to chromosomal gains and losses⁴⁴. Interestingly, high levels of CIN appear to be associated with a trend towards improved prognosis in PanNET but a poorer prognosis in small intestinal (SI) NET, although these results require additional mechanistic studies and validation in a larger population^{44,43}.

As for CIN, attempts have been made to associate mutations and other molecular features with prognosis or treatment response in PanNENs, but the majority of studies have been small and retrospective in nature, often covering mixed populations, with at times conflicting results⁴⁵. Strong, clinically relevant conclusions cannot yet be drawn. For example *DAXX/ATRX* mutations and alternative lengthening of telomeres (ALT) have been associated with a poor prognosis across a number of studies^{29,46,47, 48} but with an improved prognosis in one study²⁸ and with no significant difference in survival in analysis of the PanNET patients in the RADIANT trials⁴⁴.

Due to the complexity and heterogeneity of NENs, a number of groups have elected to take an integrated approach to studying their molecular biology, defining molecular or transcriptomic subtypes.

One group used DNA microarray analysis, quantitative real-time PCR and hierarchical clustering in a small group of PanNETs (n=19) to reveal a 'benign' and 'malignant' cluster, which correlated with the WHO histopathological classifications used at the time, being well-differentiated endocrine tumours (WDET) and well-differentiated endocrine carcinomas (WDECs)⁴⁹. Molecular subtypes have also been reported in SI-NETs and in pulmonary NENs, where they were found to have prognostic significance^{43,50}.

Our laboratory previously defined 3 molecular subtypes in sporadic PanNENs based on an integrated analysis of gene expression (221 genes),

microRNA (30 miRs) and mutations (targeted mutational profiles of *MEN1*, *DAXX/ATRX*, *TSC2*, *PTEN* and *ATM*), collectively named the PanNETassigner signature⁵¹. The existence of these three transcriptional subtypes was supported by Scarpa et al. who reported three similar subtypes using RNA-sequencing²⁹.

The three PanNETassigner subtypes, Metastasis-like-primary (MLP), Insulinoma-like and Intermediate, each have specific features as described below (Figure 1.3). As yet their prognostic significance has not been assessed, although the MLP subtype was found to be associated with metastases⁵¹.

Figure 1.3 PanNETassigner Molecular Subtypes

PanNETassigner Subtypes		
MLP	Insulinoma-like	Intermediate
38% of patients	25% of patients	37% of patients
Usually Non functional	Usually Functional	Usually Non functional
High Metastatic Potential	Low Metastatic Potential	Moderate Metastatic Potential
Grade 1/2/3	Grade 1/2	Grade 1/2
DAXX, ATRX, TSC2, PTEN, ATM mutations	TSC2, PTEN, ATM mutations	MEN1, DAXX/ATRX mutations

The association noted between these molecular subtypes and grade of disease is particularly interesting. grade 1/2 PanNETs are heterogeneous, associated with all three molecular subtypes, whereas grade 3 tumours are predominantly associated with the MLP subtype.

These data led to the hypothesis that subtyping using the PanNETassigner signature may be able to facilitate patient stratification, in addition to grade and stage. For example, potentially being used to select those grade 1/2 patients falling into the MLP subtype, whose disease biology may cause the tumour to behave more aggressively than would be expected according to grade alone (see Chapters 2 and 3).

1.6 Current Treatment of PanNENs

PanNET survival increased from 2000-2004 to 2009-2012 (HR 0.56, 95% CI 0.44-0.70)³. This may be in part due to the increased number of active treatments available, thanks to a number of large, international studies, conducted despite the inherent difficulties associated with research into rare diseases. However, the impact of lead time bias due to improved detection and length time bias in light of the indolent nature of many PanNETs should not be overlooked.

To help clinicians navigate the increasing complex PanNEN treatment landscape, extensive guidelines have been published, both in Europe, with UKINETS and ENETS guidelines in 2012 and 2016 respectively, and in America, with the North American NET Society (NANETS) guidelines updated in 2013 and the NCCN guidelines which are currently being updated^{13,20,52,53}. The treatment paradigms outlined are largely based upon grade and stage of disease, alongside tumour functionality and somatostatin receptor (SSR) status, as there are no other validated prognostic and/or predictive biomarkers routinely used in clinical practice.

Treatment is aimed at controlling tumour growth and functional symptoms. Surgery remains the only curative treatment, but PanNEN patients frequently present with advanced disease, when this is often impossible. When surgery is not an option, patients with grade 3 NECs tend to be treated aggressively with immediate platinum-based chemotherapy doublets, whereas patients with grade 1 and 2 NETs, are frequently treated with a less aggressive approach. Initially a combination of watchful waiting and somatostatin analogues (SSAs) may be used, before more intensive treatment with chemotherapy (including streptozocin, dacarbazine, doxorubicin, 5FU and temozolomide), targeted agents (sunitinib and everolimus), peptide receptor radionuclide therapy (PRRT) and targeted liver metastasis treatments when initial treatment fails (Table 1.6).

The best treatment for grade 3 NET disease is not yet clear, but it has been suggested that streptozocin and temozolomide regimens be used, rather

than cisplatin based doublets, and that other treatment options considered for grade 1 and 2 patients be considered, in light of grade 3 NET's similar molecular profile and SSR expression^{13,54}. Patients with functional disease are treated with SSAs and other therapies targeted to the specific functional syndrome in question.

There is a lack of trial evidence directly comparing active treatments or their sequencing and meta-analyses of existing trial data are limited by the variations in patient populations and response criteria⁵⁵. There are also difficulties associated with assessing the effectiveness of therapies for well differentiated NETs, due to the more indolent nature of the disease, disease stabilisation rather than objective shrinkage as a response and PanNET's relatively long survival, making survival assessments challenging.

Despite the variety of treatment options available for PanNENs, novel therapeutics are urgently required, particularly for those patients with more aggressive or advanced disease. Patients should be encouraged to enter clinical trials where available and a broad range of trials are currently ongoing for PanNEN patients, including trials of immunotherapy.

Early data from a small number of immunotherapy studies suggest that a proportion of PanNET patients may benefit from such treatments. For example, the KEYNOTE 028 study of Pembrolizumab reported a clinical benefit in PD-L1 positive PanNET patients (NCT02054806)⁵⁶. As for all PanNEN treatments, biomarkers are required to define the patients most likely to benefit from an immunotherapeutic approach and a more in-depth understanding of the immune landscape in this disease is required to inform potential future combination studies, to enable a higher proportion of patients to respond (see Chapter 4).

As yet, there is no gold standard treatment, clear order of therapies or strong evidence base to determine which patients may benefit from the more aggressive treatment options earlier, according to clinical, pathological or molecular characteristics. Decisions are made based on disease bulk, stability of disease, the side effect profile of particular therapeutics, patient preferences and the availability of particular

treatments. Novel biomarkers which could help to predict the behaviour of PanNETs, alongside grade and stage, would be a highly clinically relevant addition to the treatment paradigm. This need for novel biomarkers has been highlighted as a priority in consensus meetings of leaders in the field, both in America and in Europe in recent years^{57,58}.

Table 1.6 Range of Treatment Options available for Advanced PanNET

Therapy	Situation	Benefit	Toxicity	Key Trial
Watch and Wait	G1/2 stable disease	No toxicity	N/A	N/A
Somatostatin Analogues Ocreotide Lanreotide	G1/low G2 (Ki-67<10%), low tumour burden, stable disease, minimal symptoms due to tumour bulk (Note Octreotide trial in midgut only)	Control hormone secretion in functional tumours, increased PFS, long acting preparations	Well tolerated, nausea, bloating, steatorrhoea, glucose intolerance, gallstones	PROMID ⁵⁹ CLARINET ⁶⁰
Targeted Treatments Sunitinib	Progressive G1/G2 but not overly symptomatic patient	Increased PFS,	Infections, myelosuppression, thyroid dysfunction, hypoglycaemia, psychiatric disorders, headache, taste changes, cardiac disorders, hypertension, thromboembolism, bleeding, GI disorders including perforation, rash, hand-foot skin reactions, skin discolouration, arthralgia, proteinuria, renal impairment, delayed wound healing	Raymond et al. ⁶¹
Targeted Treatments Everolimus	Progressive G1/G2 but not overly symptomatic patient	Increased PFS, Control of refractory hypoglycaemia	Infections, myelosuppression, hyperglycaemia, insomnia, rash, headache, bleeding, hypertension, thromboembolism, pneumonitis, GI disorders, arthralgia, proteinuria, cough, diabetes, stomatitis, hypercholesterolaemia, oedema, epistaxis, liver dysfunction	RADIANT-2 ⁶² RADIANT-3 ⁶³
Chemotherapy STZ/5FU, Doxorubicin/5FU CAPTEM, Cisplatin Doublets (NEC)	Progressive or bulky G1/G2, G3 NEN, symptomatic patient	Increased PFS and higher objective response rates	Standard chemotherapy toxicities dependent upon regimen, including myelosuppression, nausea, hair loss, and renal dysfunction	Moertel et al. ⁶⁴ ⁶⁵ Kouvaraki et al. ⁶⁶ Dilz et al. ⁶⁷ Kunz et al. ⁶⁸ Sorbye et al. ⁴²
Peptide Receptor Radionuclide Therapy (PRRT)	Progressive, SSTR positive PanNET (NETTER-1 midgut only)	Improved PFS	Neutropenia, thrombocytopenia and lymphopenia, hepatic and renal dysfunction, leukaemia, myelodysplastic syndrome	NETTER-1 ⁶⁹ Brabander et al. ⁷⁰
Liver Directed Therapy Surgery/ Embolisation	Uncontrolled functional, non-functional with symptomatic liver disease	Control symptoms	Surgical complications and high risk of recurrence	Limited trials De Baere et al. ⁷¹

1.7 Biomarkers in PanNENs

Due to the heterogeneity of PanNEN disease behaviour discussed and wide range of potential treatment options, there is a significant unmet need for novel biomarkers in clinic^{57,58}. Biomarkers are required to facilitate early diagnosis, aid prognostication, predict and detect recurrence after surgery, and predict and monitor response to treatment.

Current PanNEN guidelines recommend the use of stage and grade as prognostic biomarkers and also suggest the use of a number of biomarkers to aid diagnosis and in some cases follow-up^{13,21,72}. These include CgA, pancreatic peptide (PP) and Neuron Specific Enolase (NSE), although all three have significant limitations and relatively poor sensitivity and specificity⁷³.

To date, the majority of biomarkers studied for PanNENs have been monoanalytes, considering just one variable such as CgA, NSE or PP. It has been suggested that multianalyte biomarkers may become more important in the future in this disease due to their more multidimensional nature⁵⁷. It also seems likely that a multi-modal approach will be required, incorporating molecular imaging, which has been employed to good effect in the field of theranostics in NENs, alongside tissue and serum based assays.

Novel Prognostic Biomarkers

As the prediction of prognosis in PanNENs is so difficult, for well differentiated PanNETs in particular, much effort has been made to identify new prognostic biomarkers to complement grade and staging. Many novel biomarkers have been investigated, with some of the most promising including circulating tumour cells (CTCs) and molecular assays for variables such as the presence of ALT, or particular microRNAs (miRNAs), although their clinical significance is as yet uncertain (Table 1.7). Further mechanistic research and prospective validation is required for all of these potential biomarkers before they could be taken forward into clinical

practice. To date, therefore, grade and stage remain the only validated prognostic biomarkers routinely used.

It is to be hoped that prospective longitudinal trials such as the Uppsala University Biomarker Study of Pancreatic Neuroendocrine Tumours (NCT03741517), the Princess Margaret Hospital NET-SEQ study (NCT02586844) and the Royal Marsden PaC-MAn Study (NCT03840460) will shed further light on key biological changes in PanNENs throughout the course of the disease and in response to treatment, highlighting further potential biomarkers and clarifying the clinical significance of those already being considered.

Table 1.7 Selected Potential Prognostic Biomarkers investigated in PanNEN

Marker	Details	References
Chromogranin A (CgA)	Elevated baseline CgA associated with reduced PFS and OS and CgA a prognostic factor for patients treated with everolimus BUT false elevations associated with PPIs, renal/hepatic impairment, hypertension etc. Poorly differentiated disease less likely to secrete CgA and association with poor prognosis not consistent through all studies	11,74,75,76,59
Pancreastatin	Elevation of baseline pancreastatin associated with poor PFS/OS for resected PanNET or post chemoembolization and an increase in pancreastatin after starting SSAs associated with poor prognosis BUT assay not widely available and can be non-specific	77,78
Neuron specific enolase (NSE)	Elevated versus non-elevated baseline NSE associated with reduced PFS and OS	74
<i>MEN1</i> and <i>DAXX/ATRX</i>	Mutations in <i>DAXX/ATRX</i> with or without <i>MEN1</i> mutations associated with increased OS BUT <i>DAXX/ATRX</i> mutations and alternative lengthening of telomeres (ALT) have also been associated with a poor prognosis across a number of studies	28,29,46,47,48
<i>mTOR</i>	High expression of <i>mTOR</i> or its activated downstream targets associated with adverse clinical outcomes	79
<i>PTEN/ TSC1/ TSC2/ DEPDC5</i>	<i>PTEN, TSC2, TSC1</i> and <i>DEPDC5</i> loss of function mutations have all been associated with a reduction in OS	48,29,80
CDKN1B (p27)	Loss of CDKN1B expression associated with decreased survival in GEP-NETs	81
CTCs	≥ 1 CTC in 7.5ml blood associated with reduced PFS and OS and changes in CTCs associated with OS in various NETs including PanNETs, best prognostic group being patients with 0 CTCs before and after treatment	82,76
Chromosomal instability (CIN)	Higher CIN demonstrated trend towards increased OS in PanNET patients	44
CK19	In a number of studies CK19 expression correlates with PanNET OS BUT not in all studies, only when detected with the RCK108 antibody and mainly in insulinomas	83,84
SSTR2a	Tissue SSTR-2a but not SSTR-5 expression associated with improved OS	85
<i>KIT</i>	<i>KIT</i> expression associated with low OS on univariate but not multivariate analyses	84
MicroRNAs (miR)	miR-21 overexpression correlated with high Ki-67 and liver metastases	86,87

Imaging Biomarkers

Due to the difficulties associated with evaluating disease stabilisation as a treatment response using standard measures, such as RECIST, and the indolent behaviour of many NENs, there has been much interest in the use of functional imaging. This has been aided by the expression of SSTRs in GEP-NETs, which may be targeted by radionuclides attached to somatostatin analogues.

⁶⁸Gallium (Ga) PET (DOTATATE/TOC/NOC) has demonstrated its superiority over Octreoscan and is now regarded as the gold standard SRS in NENs^{88,13}. Both ⁶⁸Ga-DOTATATE and ⁶⁸Ga-DOTANOC PET scans have been demonstrated to have prognostic value in advanced NETs, including PanNETs^{89,90,91}. This result is not surprising as well differentiated, low grade tumours tend to have the highest avidity on ⁶⁸Ga-PET scans. However, this causes difficulties in assessing higher grade tumours and in interpreting response to treatment, as a reduction in avidity may represent a treatment response or grade progression in the tumour. Therefore ⁶⁸Ga-PET scans are most useful for aiding clinical decision making for grade 1/2 NETs, particularly as a predictive biomarker regarding PRRT eligibility and SSA treatment, but not as helpful for determining treatment response or for NEC patients.

FDG-PET scans are complementary to ⁶⁸Ga-PET scans as they are more likely to be positive in tumours with high rates of proliferation, grade 3 NET and NEC. A positive FDG-PET scan has been associated with rapidly progressive disease and reduced OS in advanced GEP-NETs^{92,93}. Due to their contrasting qualities it has been suggested that results from the two types of PET scan, ⁶⁸Ga and FDG, be combined as a "NETPET score" of 1-5⁹⁴. This score has prognostic value with the patients with ⁶⁸Ga negative and FDG positive disease, a score of 5, having the poorest prognosis, although further validation is required⁹⁴.

Predictive biomarkers

In addition to the aforementioned SRS and PRRT/SSA treatment, a range of predictive biomarkers have been considered in PanNENs. Biomarkers which could predict response to systemic treatments for patients with advanced PanNEN are particularly appealing. Such biomarkers would enable patients to be spared significant potential side effects, not to mention the considerable costs to the provider, should the treatment be deemed unlikely to be of benefit.

For the targeted agents sunitinib and everolimus, multiple biomarkers have been considered, although as yet none are used in clinical practice.

Potential predictors of clinical outcome for sunitinib include baseline levels of stromal cell-derived factor-1 α (SDF-1 α) and soluble vascular endothelial growth factor receptor-2 (sVEGFR-2)^{95,73}. For everolimus, however, levels of baseline VEGF pathway biomarkers were not predictive of efficacy in the RADIANT-3 trial population⁹⁶. Low baseline VEGF-A, placental growth factor (PIGF), and sVEGFR-1 were identified as potential prognostic factors for PanNET progression on everolimus⁹⁶. Early data has also suggested that assessment using IHC for p-AKT in patient tissue may be used to select patients with activity within the PI3K/AKT/mTOR pathway required for everolimus efficacy, but this requires further investigation⁹⁷.

The methylation pattern of the DNA damage repair enzyme O-6-methylguanine-DNA methyltransferase (MGMT) and a subsequent reduction in its expression has been associated with an increased sensitivity to alkylating chemotherapy drugs such as temozolomide⁹⁸. In PanNETs, MGMT promoter hypermethylation and low MGMT expression has been associated with response to temozolomide^{99,100}. Further prospective testing is required before MGMT testing could be incorporated into the guidelines but this approach has been used in other tumour types, such as glioblastoma¹⁰¹.

The potential predictive biomarkers discussed above are all monoanalytes, usually investigated based on an understanding of the specific treatment's mechanism of action. The NETest, initially developed as an mRNA based

liquid biopsy to diagnose NENs, is a potential predictive biomarker with a different approach¹⁰². The multianalyte assay measures the expression of 51 genes in 1ml of blood and provides a score of disease status: high, intermediate or low, based on an algorithmic analysis¹⁰³. The NETest has been reported to have a high specificity and high sensitivity, both 94%, in detecting PanNEN¹⁰⁴.

To expand the utility of the NETest, Modlin et al. completed a regulatory network analysis and identified 8 gene “omic” clusters with relevance in NET biology. The activity within these clusters is used to scale the NETest score with a view to better defining an individual tumour’s biology¹⁰³. The updated NETest has now been investigated in a number of clinical settings beyond diagnosis in pancreatic and other NENs. In a small GEP-NET study (n=35) the test was able to predict residual/recurrent disease after surgery¹⁰⁵ and in another GEP-NET study (n=28) to predict disease progression on SSA approximately 5 months before progressive disease was visible on routine imaging¹⁰⁶. More recently, the NETest was combined with grade and used as a PRRT predictive quotient (PPQ) with an accuracy of >90% at predicting efficacy of PRRT treatment in NETs¹⁰⁷. Whilst the blood based NETest appears to have great potential for clinical use, as yet it is not clear how it may best be used to guide clinical management; for example, it is not clear whether stopping treatment when the NETest predicts disease progression prior to its appearance on imaging would be beneficial, particularly when treatment lines may be limited. Further validation of the NETest in a larger cohort is awaited, with a prospective study of “clinical utility” in 200 GEP-NET and pulmonary NET patients due to complete in December 2020 (NCT02948946).

Another novel approach to predictive biomarkers has been to consider a metabonomic phenotyping strategy for NENs. In one small study of mixed NENs (n=28) differences in hippurate metabolism measured in urine samples were used to differentiate between SI-NET and PanNET, between functional and non-functional tumours and between metastatic and localised disease¹⁰⁸.

The number and variety of approaches to find novel biomarkers for PanNENs underline the need and determination in the field to improve the current classification paradigm, to enable more personalised treatment, based on a patient's disease biology, to overcome the challenges caused by the inherent heterogeneity in this disease.

1.8 Hypothesis

The clear unmet clinical need for novel biomarkers to enable individualised risk-adapted therapeutic strategies for PanNEN patients, alongside the opportunity to investigate whether the PanNETassigner molecular subtypes previously defined by our laboratory could help meet this need, led to my thesis.

Novel therapeutic approaches are also required for PanNENs, with immunotherapy an obvious area for exploration. However, as yet little is known about the immune landscape in PanNENs. My thesis therefore also considers immune related gene expression in PanNENs and how this is stratified by the PanNETassigner molecular subtypes.

The hypothesis for my thesis is that the PanNETassigner molecular subtypes may be used to refine prognostication, improve classification and provide a means to divide patients with different immune phenotypes for PanNEN patients.

1.9 Research Aims

To test this hypothesis my thesis has the following aims:

1. To establish a large, well annotated clinical registry for PanNENs (Chapter 2)
2. To clinically phenotype and assess disease heterogeneity in the patients included in this registry (Chapter 2)
3. To develop and validate a novel gene expression assay based on the PanNETassigner molecular signature and subtypes (Chapter 3)
4. To assess the prognostic significance of the molecular subtype assigned by this assay in PanNEN patients from the registry (Chapter 3)
5. To describe immune related gene expression across the PanNETassigner molecular subtypes, and consider possible causes for differential expression and any potential therapeutic opportunities this may afford (Chapter 4)

2 Establishing a PanNEN Registry (PaNACeA study)

Abstract

Objective

The unmet need for novel biomarkers to enable a more personalised approach for PanNEN patients is accepted with worldwide consensus in the field. Due to the rarity of PanNENs, it has been difficult to conduct the translational studies required to develop such biomarkers. This is due to a lack of robust datasets including both tissue samples and matched clinical data. We therefore sought to establish such a dedicated PanNEN registry, including patients of all grades and stages of disease.

Design

The PaNACeA study was developed to support the retrospective collection of clinical data and matched tissue for this PanNEN registry. The registry covered two sites, the Royal Marsden Hospital (RM), London and the ARC-NET Research Centre, Verona University. For the RM cohort, all of the patients diagnosed with PanNEN between 1st Jan 2004 and 1st September 2014 were included (n=77). The Verona cohort consisted of 2 groups of patients (n=205). 45 patients were part of a legacy collection from previous pathology studies conducted at the ARC-NET centre, collected between 1988 and 2005. The remaining 160 patients were consecutively recruited and consented between 2011 and 2014 under the ARC-NET biobank protocol. A prospective analysis of tumour grade was performed on tumour samples where possible. The entire registry was clinically phenotyped. Survival analyses were conducted using Kaplan-Meier methodology. Cox-proportional hazards regression analysis was used in univariate and multivariate analyses.

Results

Clinical data was collected for 282 patients and tissue samples for 257. Patient characteristics were consistent with those previously published

(median age 56, 56% men, over 90% sporadic and 80% non-functional tumours). The RM and Verona cohorts differed with regard to stage of disease and surgical intervention, with a much larger proportion of the RM cohort having advanced disease (70% stage IV versus 17% in the Verona cohort) and a smaller proportion of the RM cohort having curative intent surgery (29% versus 100% in the Verona cohort).

The median follow up for the entire cohort was 31 months, median OS was 79 months and the 5 year survival rate was 59%. For grade 2 patients there was a large range in OS with an IQR of 3.6-8 years.

On multivariate analysis stage (stage IV vs. Stage I/II/III) ($p < 0.001$) and grade ($p < 0.009$) were independent poor prognostic factors. For the whole cohort, as Ki-67 index increased by 1 unit the risk of death increased by 1.3%.

Conclusion

A large international registry for PanNEN clinical data and tissue was successfully developed. The consistency with previously published data across patient characteristics and survival analyses provides assurance that the dataset is of good quality and representative of PanNENs more generally. As such, the registry provides a robust sample set for biomarker correlation to be discussed in the next chapters.

Whilst stage and grade were independently prognostic in registry patients, Ki-67 analyses also demonstrated the arbitrary nature of dividing patients into grades using this continuous variable. The clinical phenotyping and survival analyses here once more note the substantial heterogeneity in this disease, particularly regarding survival for grade 2 patients. There remains a significant unmet clinical need for biomarkers to allow clinicians and patients to navigate this heterogeneity in grade 2 disease. These data therefore highlight the need to develop novel means of stratifying patients according to their disease biology and provide support for the further investigation of a potential role for the PanNETassigner molecular subtypes in this setting.

2.1 Background and Rationale

Research into rare cancers is challenging, and as a result outcomes for patients with such tumours are often worse than for those with more common malignancies¹⁰⁹. Many studies to date have understandably grouped together a wide variety of NENs from different sites, to ease recruitment and increase sample size. However, it has become apparent that even NENs originating from subtly different sites in the gastrointestinal tract may represent very different diseases, making it sometimes difficult to deduce clinically relevant findings, even from studies restricted to GEP-NENs¹¹⁰.

PanNENs themselves are a highly heterogeneous group. As outlined in Chapter 1, this heterogeneity has driven a search for reliable biomarkers to improve prognostication and enable a more tailored approach to treatment selection. As developing biomarkers has been established as a key area of unmet need in PanNENs, large robust datasets of tumour samples and matched clinical data devoted specifically to this disease are of the utmost importance, to enable the required translational work⁵⁸.

To this end, we sought to establish a large registry dedicated to PanNENs, collecting patient data and tissue samples from the Royal Marsden Hospital (RM) and ARC-NET, Verona. This registry aimed to include patients with all stages and grades of disease, who had received a wide range of treatments. Data obtained would be used to understand the heterogeneity of PanNEN disease behaviour in registry patients. Clinical phenotyping would be conducted to ensure that the patients included were representative of PanNEN patients more broadly, which in turn would support the application of any conclusions from subsequent translational work to a wider PanNEN population.

This chapter outlines the development of the retrospective PaNACeA study, under which the registry was established, and the analysis of the clinical phenotyping data obtained.

2.2 Methods

2.2.1 Securing Funding

With support from Naureen Starling and Anguraj Sadanandam, the Chief Investigator (CI) and scientific lead for the study, respectively, I wrote a successful application for an NIHR Biomedical Research Centre (BRC) flagship grant as a co-applicant. The PaNACeA study (**P**ancreatic **N**euroendocrine **A**ssigner signature **C**lass **A**ssessment) was awarded £224, 910 (BRC no. 910 A144 (W92360)).

Funding for the ARC-NET biobank was provided by the Italian Ministry of Research, Association of Cancer Research and Foundation for Diseases of the Pancreas.

2.2.2 Patient and Public Involvement

I approached the NET Patient Foundation charity to request their opinion on and input into our funding application for the PaNACeA study and a PanNEN registry. Having reviewed the project they provided the following statement of support:

“On reading the proposal for the study I feel that the premise of the study resonates well with the current situation. Classification of these complex tumours has aided general pathways for care but the unique individual nature of each patient does require a more in-depth approach. Grade 2 NETS are a difficult group where variation in the presentation is quite extensive. Low Ki-67 with aggressive nature vs. 15% Ki-67 with relatively indolent behaviour in some cases. The question is why? We wholly support your research proposal as will the NET patient community, who through research have shown that their greatest fear is the fear of the unknown / the future. By gaining an understanding of what tumour type they have and the implications of their individual tumour we will be able to give some indications as to what the future may hold. I look forward to the involvement of the NET patient community with this study.” Catherine Bouvier – Director

I subsequently set up a patient focus group of 4 NET patients who kindly provided opinions on the priority research questions, the lay summary, protocol and plans for dissemination of the results of the study.

2.2.3 PaNACeA Study Set up and management

With the support of the GI unit clinical trials team, I then set up the PaNACeA study (Protocol in Appendix 2.1). Study set up included:

- Preparing the RM Committee for Clinical Research (CCR) application and presenting the study at the CCR meeting to obtain approval following scientific peer and research governance review (CCR4476, 18/04/2016)
- Liaising with the Research Ethics Committee (REC) and obtaining approval (16/LO/0984, 27/05/2016)
- Completing the Integrated Research Application System (IRAS) application and obtaining HRA approval (194534, 08/08/2016)
- Writing the protocol
- Setting up the clinical databases (for clinical and histopathology data)
- Setting up the Material Transfer agreement and the contract with ARC-NET, Verona

Once the PaNACeA study opened (September 2016), I was the trial physician. My responsibilities in this role included:

- Day-to-day oversight of the study, including working with the biological specimens co-ordinators to ensure sample retrieval
- Liaising with the team in Verona regarding tissue samples and to support consistent clinical data collection
- Liaising with the finance teams at the ICR and RM and managing the study budget
- Preparing reports for Trial Management Group Meetings (TMG) and BRC and REC Annual Progress Reports (APR)
- Preparing study amendments
- Collecting clinical data for RM patients

- Laboratory work as detailed in Chapters 3 and 4

2.2.4 PanNEN Registry Design

PaNACeA is a retrospective translational tissue collection study. The study includes separate registries for both PanNEN and non-pancreatic GEP-NEN patients but only data from the PanNEN registry are included in this thesis (Protocol in Appendix 2.1).

Primary objective

- To establish a large international registry of clinical data and matched tissue samples, dedicated to PanNEN patients.

Secondary Objectives

- To clinically phenotype all patients included in the registry
- To assess the impact of stage, grade and other clinical variables on survival for registry patients

Inclusion Criteria for PanNEN registry

- Histological diagnosis of PanNEN
- Treatment received at RM or ARC-NET, Verona
- Tissue sample available and/ or clinical data available

Exclusion Criteria for PanNEN registry

- Other primary cancer at or before diagnosis

2.2.5 Consent

In this study the data and tissue are link-anonymised. The Human Tissue Authority (HTA) code of practice for consent states that if the tissue is anonymised then tissue taken from living patients that does not have consent for future research may be used in ethically approved research projects without the patient's consent (HTA: Code of Practice 1 on Consent, from paragraph 127 to 129). Hence, as agreed with the REC, we did not routinely seek specific consent for the purpose of this study. The patients

included from the Verona biobank were routinely consented prior to surgery, as part of the biobank protocol.

2.2.6 Clinical Data Collection

I devised a database for clinical data collection and then collected and checked the clinical data for the RM patients. I liaised with Rita Lawlor, ARC-NET Verona, to arrange the clinical data collection for the Verona patients and then combined the two datasets.

Essential data fields included patient demographics, symptoms leading to diagnosis, tumour size, tumour functionality, baseline investigations, tumour differentiation, Ki-67 index, staging, treatment and survival.

2.2.7 Tissue Collection and Histological Assessments

PanNEN tumour tissue (fresh frozen and/or Formalin Fixed Paraffin Embedded (FFPE)) was collected, where available. Tumour sections were submitted for immunohistochemical (IHC) examination by an expert pathologist (for RM cohort patients by Monica Terlizzo/ Daniel Nava Rodrigues and for Verona cohort patients by the ARC-NET pathology team). Slides were reviewed and cut as described in section 3.2.3. Ki-67 index, differentiation and MI were analysed to determine tumour grade according to the WHO 2010/2017 classification. Ki-67 was analysed on 2,000 tumour cells in an area of high staining and expressed as a percentage of stained cells. MI was assessed according to standard ENETs criteria. On light microscopy, mitotic figures were evaluated in at least 40 high power fields (HPF), with results expressed by the number of mitoses per 10 HPF. We elected to use the WHO 2010/2017 Ki-67 recommended cut-offs for grade, with grade 2 disease having a Ki-67 index between 3% and 20%, rather than the 5% cut-off proposed by a number of groups^{26,37}. In light of the debates surrounding the optimum cut-offs we also analysed Ki-67 as a continuous variable.

2.2.8 Statistical Analyses

I wrote the statistical analysis plan (SAP) in conjunction with statistician Ria Kalaitzaki (see protocol in Appendix 2.1 for full details).

Sample size

Sample size was limited by the number of patients who were treated for PanNENs at the Royal Marsden Hospital and at the University of Verona within the site specific time points, and for whom clinical data and/or tumour tissue was available for analysis. Since the registry opened we have had the opportunity to develop an additional collaboration with Dr. Raj Srirajskanthan's team, Kings College Hospital. This collaboration will enable the collection of clinical data and FFPE samples for another cohort of approximately 300 PanNEN cases, including 150 resections and 30 patients with grade 3 PanNEC. I wrote an amendment to the PaNACeA protocol to include this additional cohort and with trial coordinator Richard Crux arranged for regulatory approval (Substantial amendment 1, approved 02/11/2018). I have since liaised with the team at Kings to ensure consistent clinical data collection and tissue preparation. As the first 40 samples were received in the Sadanandam laboratory in April 2019, they will not be included in this thesis.

Analysis

Statisticians Henry Nanji and Ria Kalaitzaki performed the survival analyses and I completed the clinical phenotyping analysis and interpreted the results. The majority of the statistical analysis is descriptive, reported using percentages. Categorical data were described using counts and percentages and compared using the Chi-squared (χ^2) test. Continuous data were described using medians and inter-quartile ranges (IQR). Means were compared using a two-sided, paired T-Test. A two sided p value of less than 0.05 was considered statistically significant. Survival analyses were conducted using Kaplan-Meier methodology. Overall survival (OS) was defined as time from the date of diagnosis to death of any cause. Cox-proportional hazards regression analysis was used in univariate and multivariate analyses.

2.2.9 Overview of my role

As described above, I secured funding for, set up and subsequently managed the PaNACeA study and PanNEN registry. Dr Naureen Starling, as the CI for the study had overall oversight.

2.3 Results

2.3.1 Clinical Data Collection, Tissue Retrieval and Central Review

Clinical data were collected for 282 patients. For the RM cohort, all of the patients diagnosed with PanNEN between 1st Jan 2004 and 1st September 2014 were included (n=77). The Verona cohort consisted of 2 groups of patients (n=205). 45 patients were part of a legacy collection from previous pathology studies conducted at ARC-NET (1988- 2005). The remaining 160 patients were consecutively recruited and consented under the ARC-NET biobank protocol (2011-2014). Whilst clinical data was matched for the majority of variables, data was missing for a small number of categories in the Verona cohort (ethnicity, baseline investigations, symptoms and treatments). Thus some analyses are for the whole cohort whilst others are specific to the RM cohort.

Tissue was collected for 257 patients (FFPE samples for 57 RM patients and fresh frozen samples for 200 Verona patients, with FFPE tissue also available for 44 Verona patients) (Figures 2.1 and 2.2). For the Verona cohort, central histopathology review had been conducted prospectively for all tissue. For the RM cohort we planned to conduct a similar central review. However, due to challenges collecting the tissue, grade was ultimately assigned from central Ki-67 review for 10 patients, from central MI review using H&E slides for 8 patients, and from the original diagnostic histopathology reports for 44 patients and grade remained unknown for 15 patients (Figure 2.2).

Figure 2.1 Clinical Data and Tissue Collection for the Verona Cohort

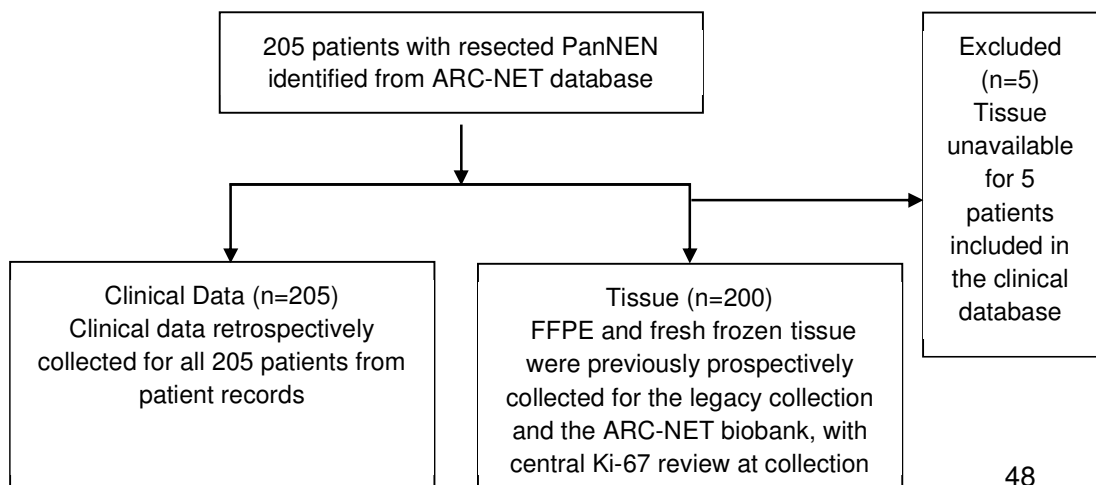
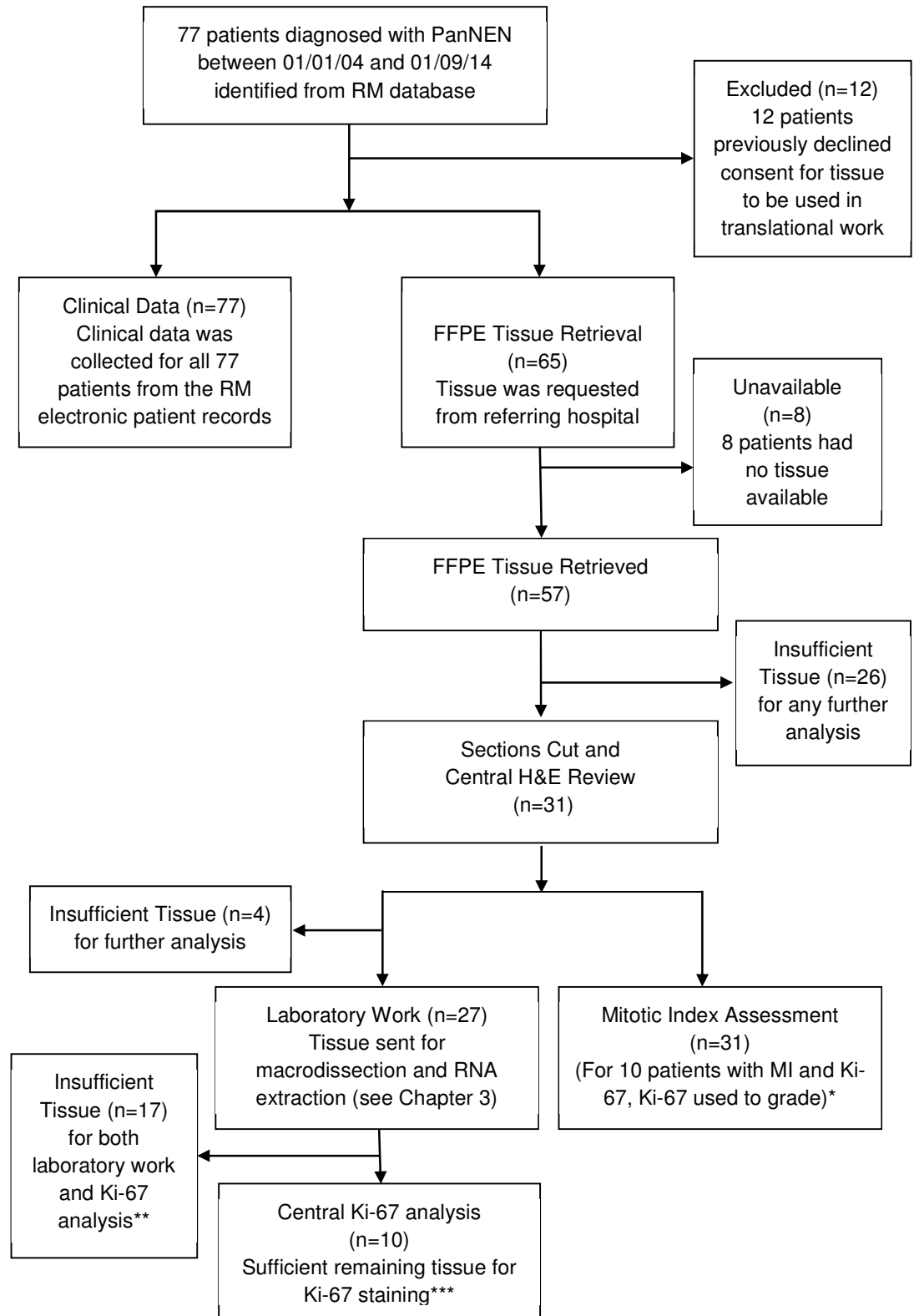


Figure 2.2 Clinical Data and Tissue Collection for the RM Cohort



** For the 21 patients graded by MI, 8 had previously unknown grades, 11 original grades were concordant with central review and 2 discordant. When discordant, the original grades were used.*

***When there was limited tissue available, tissue for laboratory analyses was prioritised over central histopathology review*

**** For the 10 patients graded by Ki-67 index, 2 had previously unknown grades, 6 original grades were concordant with central review and 2 were discordant. When discordant the original grades were used.*

2.3.2 Patient Demographics across the entire cohort

The patients had a median age of 56 years and there was a slightly higher proportion of men (56%) compared to women (44%). For the patients where ethnicity had been documented, there was a higher representation of white patients (81%) compared to other ethnic backgrounds. The vast majority of patients had sporadic disease (92.5%). For those patients with familial disease, MEN1 was the most frequently documented familial syndrome (48%) (Table 2.1)

2.3.3 Tumour and Disease Characteristics across the entire cohort

The proportion of patients with WHO 2010 grade I and 2 disease was similar (44% and 41% respectively), with a smaller number having grade 3 disease (8%). Of the patients with grade 3 disease, using the WHO 2017 classification, 52% had a poorly differentiated tumour (grade 3 NEC) and 43% had a well differentiated tumour (G3 NET) (Table 2.1).

Overall, the number of patients with Stage III and IV disease was similar at approximately 30% each. Fewer patients had Stage I and II disease (15% and 24% respectively). 38% of patients with non-metastatic disease had nodal involvement at baseline. 31% of patients had metastatic disease at baseline, with 29% of all patients having metastatic liver disease. 80% of the patients in the registry had curative intent surgery.

Table 2.1 Patient Demographics and Baseline Disease Characteristics

Characteristic	All Patients (n=282)	RM (n=77) (%)	Verona (n=205) (%)	p value (RM vs. Verona)
Age at diagnosis*				
Median (range)	56 (17-87)	63 (17-87)	56 (17-84)	p= 0.15
Sex*				
Male	156 (56%)	42 (55%)	114 (56%)	p= 0.84
Female	125 (44%)	35 (45%)	90 (44%)	
Ethnicity **				
White	56 (81%)	56 (81%)	N/A	N/A
Asian	7 (10%)	7 (10%)		
Black	5 (7%)	5 (7%)		
Mixed	1 (1%)	1 (1%)		
Sporadic/ Familial***				
Familial	21 (7.5%)	0 (0%)	21 (10%)	p=0.003
Sporadic	259 (92.5%)	77 (100%)	182 (90%)	
Familial Syndrome †				
MEN1 10 (48%)	10 (48%)	0 (0%)	10 (48%)	N/A
VHL 3 (14%)	3 (14%)	0 (0%)	3 (14%)	
Not documented 8 (38%)	8 (38%)	0 (0%)	8 (38%)	
Grade				
Grade 1	124 (44%)	27 (35%)	97 (47%)	p<0.001
Grade 2	117 (41%)	23 (30%)	94 (46%)	
Grade 3	23 (8%)	12 (16%)	11 (5%)	
Unknown	18 (6%)	15 (19%)	3 (1%)	
Grade 3 NET/NEC**				
G3 NET	10 (43%)	0 (0%)	10 (90%)	N/A
G3 NEC	12 (52%)	11 (92%)	1 (10%)	
G3 differentiation unknown	1 (4%)	1 (8%)	0 (0%)	
Differentiation				
Well	258 (92%)	56 (72%)	202 (99%)	p<0.001
Poorly	12 (4%)	11 (14%)	1 (<1%)	
Unknown	12 (4%)	10 (13%)	2 (1%)	
Stage				
I	41 (15%)	5 (6%)	36 (18%)	p<0.001
II	67 (24%)	11 (14%)	56 (27%)	
III	80 (28%)	5 (6%)	75 (37%)	
IV	88 (31%)	54 (70%)	34 (17%)	
Unknown	6 (2%)	2 (3%)	4 (2%)	
N1 at diagnosis (Stage I-IIIb) ***				
Stage IIIb	72 (38%)	4 (19%)	68 (41%)	p=0.05
Stage I/II/IIIa	116 (62%)	17 (81%)	99 (59%)	
Liver Metastasis at diagnosis				
Yes	81 (29%)	47 (61%)	34 (17%)	p<0.001
No	199 (71%)	30 (39%)	169 (82%)	
Unknown	2 (1%)	0 (0%)	2 (1%)	
Curative Intent Surgery				
Yes	227 (80%)	22 (29%)	205 (100%)	p<0.001
No	55 (20%)	55 (71%)	0 (0%)	

* n=281 **n=69 ***n=280 † n=21 †† n=23 ††† n=188

Note percentages in the table have been rounded. Categorical data were described using counts and percentages and compared using the χ^2 test. Continuous data were described using medians and means were compared using T-Test.

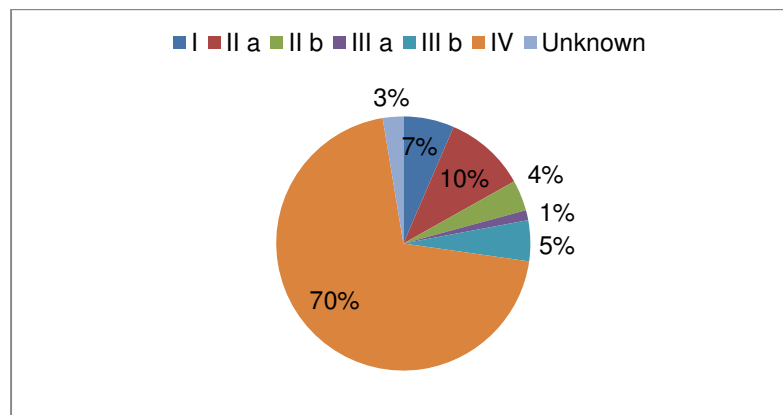
2.3.4 Differences in Characteristics of the RM and Verona Cohorts

The demographics of the RM and Verona cohort were well matched regarding age and sex. A higher proportion of the Verona cohort had a familial syndrome ($p=0.003$).

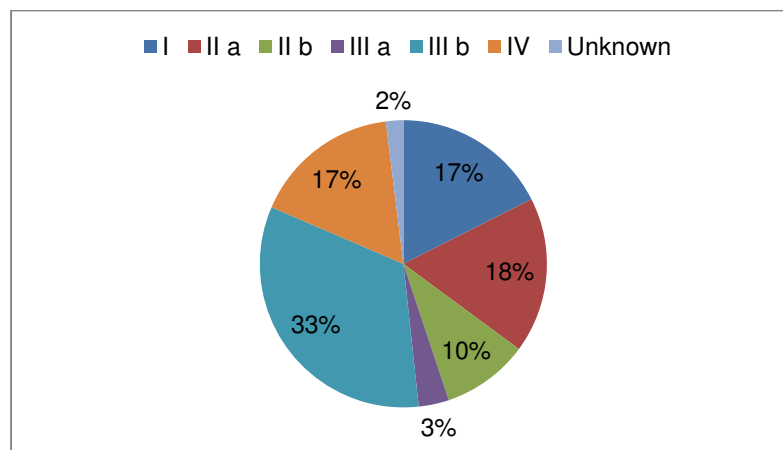
As would be expected due to the origins of the cohorts, the characteristics of the RM and Verona cohorts differed substantially when considering stage or grade of disease and curative intent surgery (all $p < 0.001$). All of the patients in the Verona cohort underwent curative intent surgery, with only 17% having metastatic disease. In the RM cohort, the majority of patients presented with advanced disease (70% metastatic) and less than 30% had curative intent surgery (Table 2.1 and Figure 2.3).

Figure 2.3 Proportions of patients according to ENETS Stage

A RM Cohort (n=77)



B Verona Cohort (n=205)



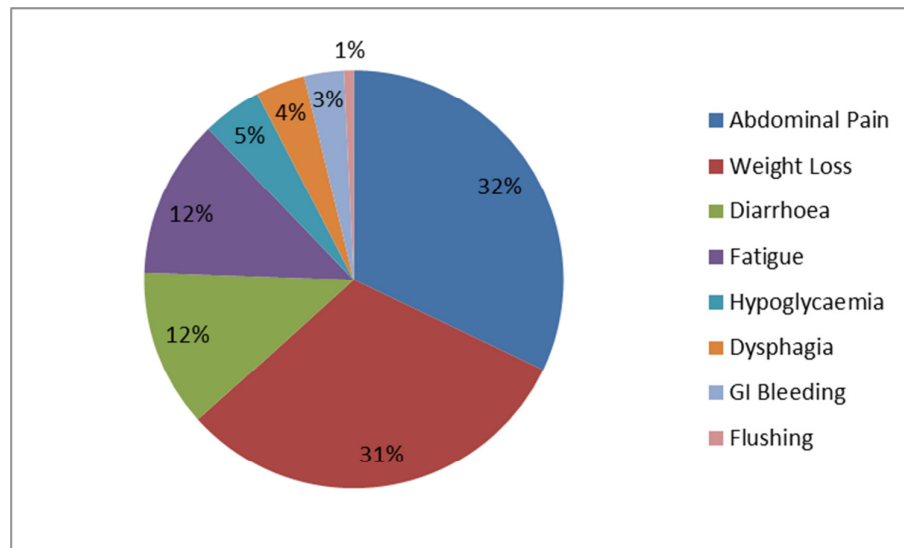
2.3.5 Baseline Symptoms and Investigations

Baseline symptoms and investigations were assessed in the RM cohort, and apart from functionality which was assessed across all 282 patients (Table 2.2). The majority of patients had non-functional disease (79%). For patients with functional disease, insulin was the most frequently secreted hormone (43%).

88% of RM patients reported at least one symptom at diagnosis (Figure 2.4). Abdominal pain and weight loss were each reported by over 50% patients, with diarrhoea and fatigue in over 20%.

Chromogranin A and B (CgA and B) were measured in 82% of the RM cohort. CgA was elevated in a higher proportion of patients than CgB (62% vs. 33%). All of the RM patients had a baseline CT with a high proportion (74%) also having Somatostatin Receptor Scintigraphy (SRS). Endoscopic Ultrasound Scans (EUS), Magnetic Resonance Imaging (MRI) and Positron Emission Tomography scans (PET) were used less frequently (Table 2.2).

Figure 2.4 Baseline Symptoms in RM Cohort (n=77)



68/77 RM cohort patients reported baseline symptoms. Between them these 68 patients reported 131 symptoms, which are shown in the pie-chart above, divided into 8 categories. Abdominal pain and weight loss were the most common symptoms, each experienced by over 50% patients as outlined in Table 2.2.

Table 2.2 Baseline Symptoms and Investigations

Characteristic	n=77(%)
Functionality*	
Functional	56 (20%)
Non-Functional	229 (79%)
Unknown	3 (1%)
Hormone Secreted if Functional **	
Insulin	24 (43%)
Gastrin	15 (27%)
Glucagon	8 (14%)
ACTH/Cortisol	3 (5%)
Somatostatin	3 (5%)
PP	1 (2%)
Serotonin	1 (2%)
VIP	1 (2%)
Symptoms	
Yes	68 (88%)
No	9 (12%)
Symptoms reported	
Abdominal Pain	42 (55%)
Weight Loss	41 (53%)
Diarrhoea	16 (21%)
Fatigue	16 (21%)
Hypoglycaemia	6 (8%)
Dysphagia	5 (6%)
GI Bleeding	4 (5%)
Flushing	1 (1%)
Chromogranin A ***	
Elevated	39 (62%)
Normal	24 (38%)
Chromogranin B ***	
Elevated	21 (33%)
Normal	42 (67%)
Baseline Imaging Investigations	
CT Yes	77 (100%)
No	0 (0%)
SRS Yes	57 (74%)
No	20 (26%)
MRI Yes	18 (23%)
No	59 (77%)
EUS Yes	14 (18%)
No	63 (82%)
PET Yes	13 (17%)
No	64 (83%)

*n=282 **n=56 ***n=63

2.3.6 Systemic Treatment

Data on systemic treatments administered was only available in the RM cohort (n=77). The most common treatments were chemotherapy, SSAs and watchful waiting, but a broad range of treatments were given (Figure 2.5). For those patients who received chemotherapy, multiple different regimens were used (Figure 2.6).

Figure 2.5 Systemic Treatments Administered in the RM Cohort

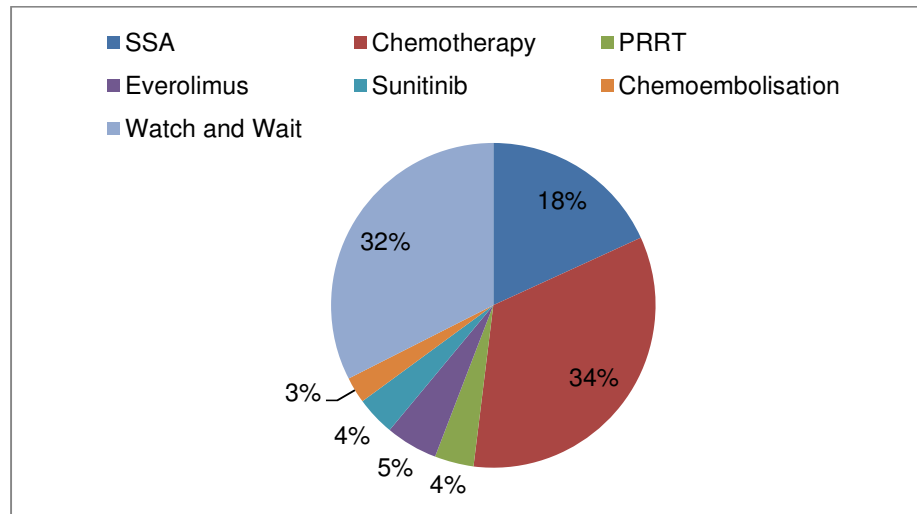
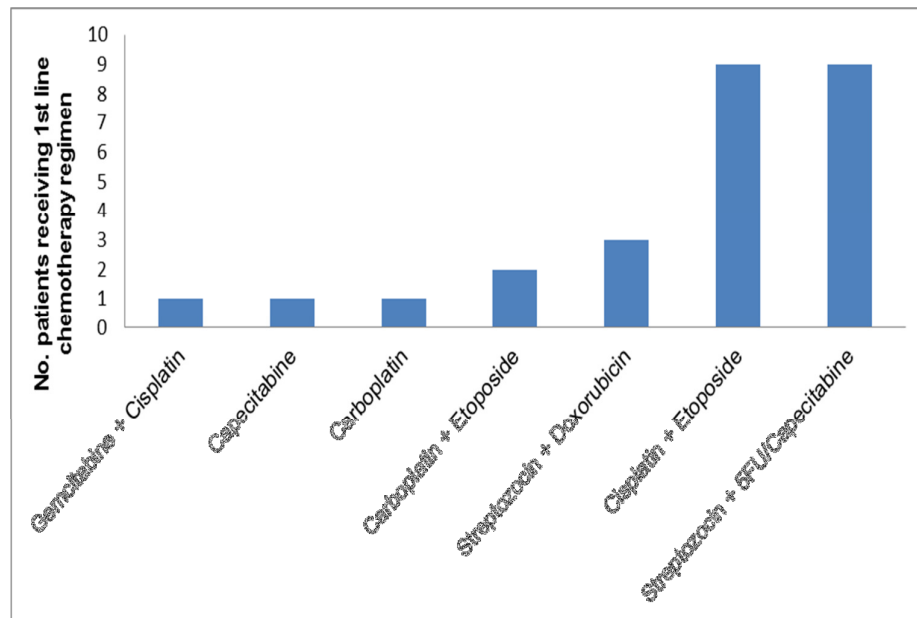


Figure 2.6 Chemotherapy Regimens Administered in RM cohort



2.3.7 Survival Analyses

For the entire cohort (n=282), 63 (22%) of the patients were dead and 186 (66%) were alive at the time of analysis, with 33 (12%) lost to follow up. Of the 33 patients lost to follow up censoring data was available for 7 patients. Survival data was therefore available for 256 patients overall.

Median follow up was 31 months. According to site, the median follow up was 45.3 months for RM and 27 months for Verona. As would be expected due to the different characteristics of the 2 cohorts and the longer follow up for the RM cohort, the death rate was higher in the RM cohort at 56% compared to the Verona cohort at 10%.

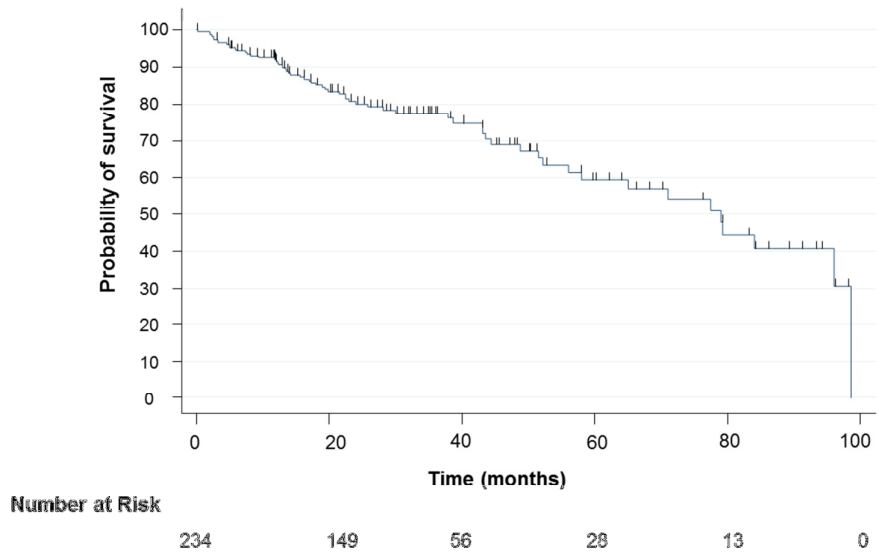
The last death occurred at 98.5 months for a RM patient and no other later deaths occurred except for one ARC-NET patient at 262 months. Due to the high influence of this data point, which stretched the observations, the analysis time was truncated at 100 months (~8 years). This reduced the number of patients included in the survival analyses by 22, from 256 to 234. In the 100 months' time period, 62 deaths were observed (43 in the RM cohort and 19 in the Verona cohort).

Data for 234 patients were used to conduct the following survival analyses.

Median Overall Survival (OS)

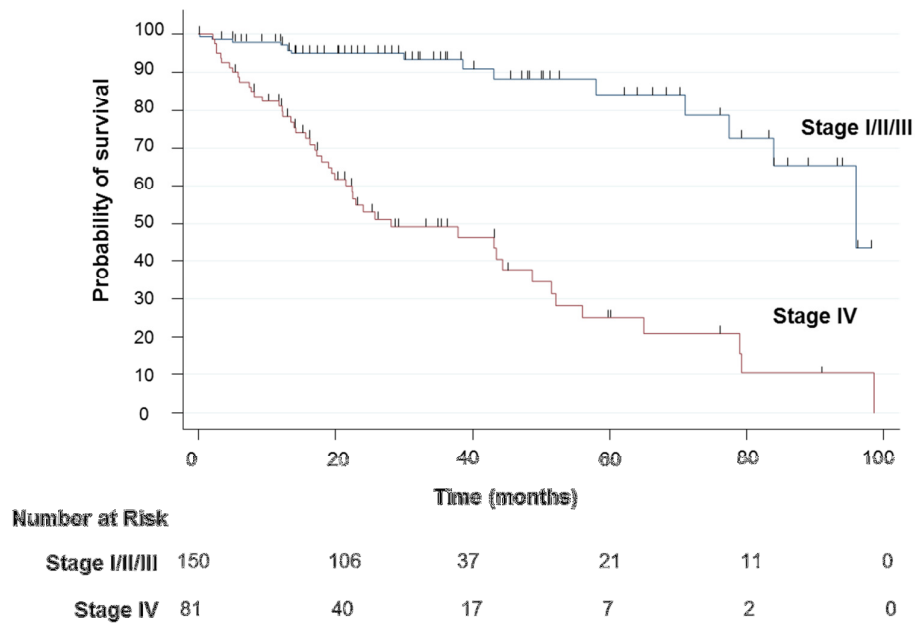
OS was assessed for the entire cohort and according to stage and grade (Figures 2.7-2.9 and Table 2.3). Survival time of living patients was censored on the last date a patient was known to be alive or lost to follow-up. Median OS for the entire cohort was 79 months (95% CI 50.0-NE). Due to the low number of deaths occurring in ENETS stages I, II, III, these were combined and investigated versus stage IV disease. Survival was improved for stages I/II/III combined compared to stage IV and this was statistically significant (log-rank test $p < 0.001$). There was also a statistically significant difference in OS for the three grades (log-rank test $p < 0.001$).

Figure 2.7 OS in all patients (All grades/Stages)



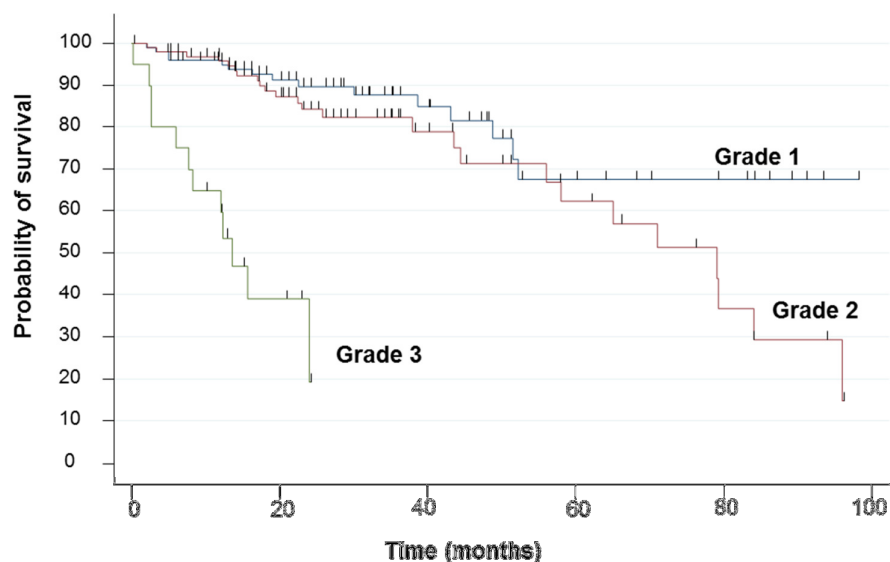
Note analysis time was truncated at 100 months

Figure 2.8 OS according to ENETs stage (combined I/II/III vs. IV)



Note analysis time was truncated at 100 months

Figure 2.9 OS according to WHO 2010 Grade



Number at Risk		Time (months)					
		0	20	40	60	80	100
Grade 1	102	69	29	13	7	0	
Grade 2	98	68	23	13	5	0	
Grade 3	20	5	0	0	0	0	

Note analysis time was truncated at 100 months

Table 2.3 Median OS, 2 year and 5 year survival rates

	Median (months) (95% CI)	2 year (%) (95% CI)	5 year (%) (95% CI)
Entire Cohort			
(n=234)	79 (50.0-NE)	80.1 (73.6-85.1)	59.3 (47.8-69.1)
According to Stage			
I/II/III (n=150)	96 (84.0-NE)	95.1 (89.8-97.6)	84.3 (69.3-92.3)
IV (n=81)	28.1 (19.8-48.7)	52.9 (40.3-64.1)	25.1 (13.0-39.2)
According to Grade			
Grade 1 (n=102)	NE (NE)	89 (80.9-94.5)	67.5 (47.5-81.3)
Grade 2 (n=98)	79 (56-96)	84.2 (74.1-90.6)	62.1 (43.1-76.5)
Grade 3 (n=20)	13.5 (6-NE)	19.5 (1.6-52.4)	NE (NE)

Univariate Analysis

On univariate analysis grade, baseline lymph node involvement/ liver metastases and stage were identified as statistically significant poor prognostic factors (Table 2.4). Results were adjusted for cohort of origin (RM/ Verona).

Table 2.4 Univariate Analysis

Variables	HR	95% CI	p value
Grade			
Grade 1	1.00		
Grade 2	2.05	1.19 - 3.53	0.03
Grade 3	13.19	6.35 - 27.43	<0.001
N1 at diagnosis			
No	1.00		
Yes	2.25	1.45 - 3.49	0.002
Liver Metastasis at diagnosis			
No	1.00		
Yes	2.76	1.69 – 4.51	0.001
Stage			
I/II/III	1.00		
IV	4.22	2.43 – 7.30	<0.001
Elevated baseline CgA/ B			
Not Elevated	1.00		
Elevated	1.18	0.56 - 2.47	0.657

Multivariate Analysis

Stage and grade were the only factors found to be significant at the 5% level on multivariate analysis (Table 2.5).

Table 2.5 Multivariate Analysis

Variable	HR	95% CI	p value
Stage			
I/II/III	1.00		
IV	4.12	1.97 - 8.64	<0.001
Grade			
			[<0.009] ¹
Grade 1	1.00		
Grade 2	1.37	0.69 – 2.73	0.359
Grade 3	4.43	1.67 – 11.7	0.003

¹: overall effect

The risk of death was 12% higher for patients with ENETs stage IV disease compared to stages I/II/III (log-rank $p < 0.001$).

A higher grade was also associated with an increased risk of death (HR increased from 1 to 1.37 to 4.43 relative to the reference group, grade 1, log-rank $p < 0.001$). Although the HR was not significant when grade 2 was compared to grade 1 disease ($p=0.359$).

As Ki-67 index increased by 1 unit, with all other variables held constant, the risk of death increased by 1.3%.

2.3.8 Assessment of Heterogeneity across and within Grades

There was a statistically significant difference between grades for all of the variables listed in Table 2.6.

Table 2.6 Heterogeneity across and within grades

Variable	Grade 1	Grade 2	Grade 3	Significance*
Disease Extent (n=264)				
I/II/III	105 (85%)	72 (61%)	8 (35%)	$p < 0.001$
IV	18 (15%)	43 (37%)	15 (65%)	
Unknown	1 (<1%)	2 (2%)	0 (0%)	
N1 at diagnosis (Stages I-IIIb) (n=185)				
Yes	26 (25%)	39 (54%)	7 (88%)	$p < 0.001$
No	79 (75%)	33 (46%)	1 (13%)	
Liver Metastases at diagnosis (n=274)				
Yes	17 (13%)	44 (38%)	10 (43%)	$p < 0.001$
No	117 (87%)	73 (62%)	13 (57%)	
Curative Intent Surgery (n=277)				
Yes	112 (90%)	98 (82%)	12 (35%)	$p < 0.001$
No	12 (10%)	21 (18%)	22 (65%)	
Median OS (n=220)				
Median	NE	79	13.5	$p < 0.001^{**}$
IQR	(51.5-NE)	(44.4-96)	(6-24)	
Tumour Size (n=201) (mm)				
Median	29	45	35	$p < 0.001$ for G1 vs. G2***
Mean	31	48	39	
IQR	15-45	30-69	25-50	

* Categorical data described as counts and percentages and compared using X^2 test, continuous data described with medians and means, with means compared using T-Test.

**Survival differences compared using log-rank test

***G1 vs. G3 and G2 vs. G3 not significant

However, a wide range of behaviour was also evident within each grade, particularly within grade 2 disease (Table 2.6). For example, whilst the majority of localised grade 1 patients had node negative disease and the majority of localised grade 3 patients had nodal involvement, for the grade 2 patients there was a roughly even division (54% with nodal involvement vs. 46% node negative). Further, although the majority of grade 2 patients had localised disease, a sizeable minority had metastatic disease (37%). Grade 2 patients also had a wide range of tumour sizes (IQR 30-69mm) and a large range in OS, with an IQR of between 3.6 years and 8 years. These data highlight the substantial heterogeneity of disease behaviour within grade 2 patients.

2.4 Discussion

In this chapter, I have described the set-up of a large, international PanNEN registry (within the PaNACeA study) and presented clinical phenotyping and survival analyses for the 282 patients included to date.

Clinical data was collected across the 2 study centres, RM and ARC-NET, Verona for patients diagnosed with PanNEN between 1988 and 2014. The majority of the data was collected for the entire registry, with baseline symptoms, investigations and treatments being specific to the RM cohort.

The characteristics of the 2 cohorts differed significantly, as all of the patients in the Verona cohort (n=205) had undergone curative intent resections, whereas the majority of the RM cohort patients (n=77) had advanced, metastatic disease (70%) and had systemic treatment rather than surgery. As such, the two cohorts are complementary, covering a broader range of disease than either would have done alone.

The demographics reported for the entire PanNEN registry (n=282) are consistent with published literature, with a median age of diagnosis of 56 years, a roughly equal split between men and women, a large majority of patients having non-functional, sporadic disease, with MEN1 being the most common of the familial cancer syndromes documented and insulin the most commonly secreted hormone^{111,14,41,112,113}.

Tumour and disease characteristics were also assessed across the entire cohort (n=282). Using the WHO 2010/17 Ki-67 cut-offs outlined, there was a smaller percentage of grade 3 tumours (8%) versus grade 1 and 2 tumours (44% and 41% respectively). Tumour differentiation fits this pattern, with the vast majority of patients having well differentiated disease (92%). This distribution of grade and differentiation is as expected, as 205/282 patients were from the Verona cohort where all patients underwent curative intent resections. A large, international cohort of 1072 PanNEN patients who had undergone surgery reported a similar distribution with 6.8% grade 3 patients⁴¹.

The distribution of stage across the whole cohort is also broadly consistent with the literature, with perhaps a slightly higher frequency of stage III and IV patients^{14,41,112}. This is likely to be due to the influence of the RM cohort as the majority of patients in the RM cohort had stage IV disease (70%) versus only 17% of the Verona cohort. In the Verona cohort, a relatively large percentage of patients had stage IIIb disease (37%).

The high proportion of patients with stage IIIb (any T N1 M0) disease is reflected in the percentage of patients with nodal disease at baseline, with 38% patients with localised disease having nodal involvement. Most patients (67%) had localised disease at baseline and the majority of patients who presented with stage IV disease had liver metastases (81/88, 92%). This observation is consistent with studies reporting the liver as the most frequent site of metastasis for GEP-NETs^{14,114}.

PanNEN symptoms are often non-specific, contributing to diagnostic delays and often incorrect initial diagnoses^{16,17,18}. Within the RM cohort, where the majority of patients had metastatic non-functional disease, 88% of patients reported at least one symptom at baseline. The top 4 symptoms reported here, abdominal pain, weight loss, diarrhoea and fatigue are non-specific, as expected. All 6 RM patients with insulinomas reported symptoms of hypoglycaemia, highlighting the more symptomatic pattern observed with functional tumours.

CgA/B were assessed in 82% of the RM cohort at baseline. CgA was elevated in almost twice as many patients as CgB (62% vs. 33%). As the patients in the RM cohort were diagnosed between 2004 and 2014, CgB was routinely measured for the majority. However, more recently the routine measurement of CgB has fallen out of practice due to its limited utility¹¹⁵. That only 33% of cases in the RM cohort had an elevated CgB supports this decision. CgA is still routinely measured and is recommended as a circulating biomarker by the ENETS consensus guidelines 2016¹³. Although CgA performed better than CgB in the RM cohort only 62% patients had a baseline elevation, supporting the need for improved

biomarkers in this disease and agreeing with concerns raised in the literature about the performance of CgA¹¹⁶⁻¹¹⁸.

All of the patients in the Verona cohort had curative intent surgery versus only 29% in the RM cohort. This low proportion of patients undergoing an operation in the RM cohort is understandable as patients would commonly be referred to RM for systemic treatment, with more advanced disease. It is likely this low percentage of operated patients will have contributed to the survival figures for the RM cohort, as radical surgery has been linked to improved survival in PanNET¹¹.

Systemic treatment data was only available in the RM cohort. The range of systemic therapies received by the 77 RM patients highlights the complexity of treating PanNENs. If anything the situation for patients today is even more complex as, for the majority of the RM cohort everolimus, sunitinib and PRRT were not treatment options at the time. Studies such as SEQTOR, where the optimum sequencing of everolimus and chemotherapy is being investigated, may help to clarify the treatment paradigm. Yet, what is really required are prognostic and predictive biomarkers to help select therapy for those patients who require it, whilst sparing the others toxicity from unnecessary or ineffective treatments.

Survival analyses were conducted across the whole registry. At a median follow up of 31 months, 63 (22%) patients had died, 186 (66%) were still alive and 33 (22%) patients were lost to follow up. As would be expected, the death rate was higher in the mainly metastatic RM cohort at 56%, compared to the Verona cohort at 10%.

The median OS (79 months) and 2 and 5 year survival rates (80% and 59% respectively) reported are comparable to other PanNEN studies and SEER registry data, particularly when noting the high proportions of stage IIIb and IV patients^{37,119,14}.

Due to the low number of deaths occurring in patients with ENETS stage I, II and III disease, these were combined and investigated together versus stage IV disease. Survival was improved for stages I-III compared to stage IV disease ($p < 0.001$). Stage IV disease remained a poor prognostic factor

on multivariate analysis, associated with a 12% higher risk of death than stage I-III disease. As for OS, the 2 and 5 year survival rates for early and advanced disease are in line with the literature^{14,119}.

Using the WHO recommended Ki-67 cut-offs for grade, there was a statistically significant difference in OS across the three grades ($p < 0.001$) but 5 year survival rates were very similar between grade 1 and 2 disease (67% and 62%) demonstrating the difficulties of assigning prognosis in well differentiated PanNETs. Whilst grade overall was prognostic on multivariate analysis ($p < 0.009$), the Hazard Ratio (HR) was not significant for grade 2 versus grade 1 disease, as previously described by Scarpa et al. and leading to the proposal for a 5% cut-off¹¹⁹.

When, however, Ki-67 was assessed as a continuous variable there was a 1.3% increase in the risk of death for each 1% increase in Ki-67 index. This level of increased risk of death is akin to that previously presented, where a 1% increase in Ki-67 was linked to a 2% increased risk of metastasis. This study reported a hazard ratio for progression of 1.02 for each increasing unit in Ki-67% unit ($p < .001$)⁴⁰.

Analysing Ki-67 in this manner makes both biological and statistical sense as Ki-67 is a continuous variable and dichotomization of such variables may result in reduced power in regression models and loss of information regarding individual differences¹²⁰. This analysis demonstrates that grade is a purely arbitrary division and again highlights the need for improved methods of sub-dividing PanNEN patients with biological relevance and prognostic significance.

The limitations of dividing PanNEN patients into grades based on these arbitrary limits are particularly evident for grade 2 patients. This group of patients demonstrates substantial heterogeneity of disease behaviour in the registry patients, with an OS IQR of between 3.6 years and 8 years.

The PanNEN registry has a number of limitations. To include as many PanNEN patients with matched clinical data and tissue as possible, the data collected here encompassed a broad time period (1988-2014). The available treatments varied significantly over the time period, which may

have impacted upon OS. Further, patients' disease was reported and classified differently at various time points, creating challenges for consistent data collection.

These challenges of consistent data collection underline the importance of minimum dataset documentation for all patients, particularly for those with rare diseases. In recent years, the various guidelines including PanNENs have recognised this and frequently specified a minimal dataset for inclusion in pathology and staging reports for PanNENs^{12,72,121}.

Consistent data collection, histopathology techniques and reporting were all made more challenging by the PanNEN registry encompassing 2 sites in different countries. However, as discussed above, minimum datasets will make such studies easier in the future. The development of ENETS Centres of Excellence (CoE) across Europe since 2009 has also supported a more standardised approach and will continue to facilitate such international collaboration, essential for studies in this rare disease.

Another limitation is the retrospective nature of the PanNEN registry. Collecting both data and tissue samples retrospectively can be problematic, especially over a long time period. This is highlighted by the lower than expected number of tissue samples available for the RM cohort for central histopathology review or further analysis. The development of prospective biobanks, such as the ARC-NET protocol, is therefore of paramount importance to enable high quality translational work. Since working on the PanNEN registry, with CI oversight (Naureen Starling), I set up the PaC-MAN Study to support the prospective collection of tissue and other samples from patients with newly diagnosed PanNEN.

Notwithstanding these limitations, the PanNEN registry described here, including clinical data for 282 patients and matched tissue for 227 patients, is a valuable resource for this rare tumour type. In light of the consistency with previous PanNEN studies regarding patient demographics, tumour and disease characteristics and survival analyses, the clinical phenotyping of the registry provides assurance that the dataset is of good quality and

representative of a wider population. As such, the registry provides a robust sample set for biomarker correlation, to be discussed in the next chapters.

Whilst stage and grade were independently prognostic, Ki-67 analyses also demonstrated the arbitrary nature of dividing patients into grades using this continuous variable. The clinical phenotyping and survival analyses reported here once more note the significant heterogeneity in this disease, particularly for grade 2 patients. There remains a significant unmet clinical need for biomarkers to enable clinicians and patients to navigate this heterogeneity in grade 2 disease. These data therefore highlight the need to develop novel means of stratifying patients according to disease biology, in addition to stage and grade, and provide support for further investigation of the potential role of the PanNETassigner molecular subtypes in this setting (Chapter 3).

3 Development of the PanNETassigner Assay

Abstract

Objective

Treatment decisions in PanNENs are currently determined by grade and stage of disease. However, as demonstrated in Chapter 2 and elsewhere, grade is an arbitrary measure and, due to the significant level of within grade heterogeneity of disease behaviour, particularly for grade 2 patients, this paradigm is inadequate. Gene expression signatures have been used extensively in other tumour types to guide treatment decisions. A similar index for PanNENs, to improve patient prognostication and classification, would be highly clinically relevant. The aim of this chapter was to develop and validate a novel gene expression assay based on the PanNETassigner molecular subtypes previously defined by our laboratory, and then to assess the prognostic significance of the subtypes assigned by this assay.

Design

A custom assay of 228 genes was developed using the NanoString nCounter gene expression platform, based on the PanNETassigner signature. The ability of this novel PanNETassigner NanoString assay to derive subtypes was assessed in a training set of PanNEN patient samples (n=48). The concordance of subtypes derived using the novel assay with subtypes previously derived using microarray was assessed (n=19). The assay was tested in a further 96 fresh frozen samples and reproducibility was assessed. Significance Analysis of Microarrays (SAM) was performed to refine the 228 gene PanNETassigner assay to 78 robust genes and centroids were derived for each subtype. The refined assay, called the Nano-PanNET assay, was then validated using FFPE tissue (n=58). An RNAseq validation cohort (n=98) was also used to assess the centroids derived and concordance between platforms and between FFPE and fresh frozen tissue was assessed. Prognosis according to PanNETassigner subtype assigned was evaluated using Kaplan-Meier methodology.

Results

A novel 228 gene PanNETassigner NanoString assay was successfully developed and demonstrated to have 95% concordance with previous subtyping results using the microarray platform. Replicates confirmed assay reproducibility. A refined 78 gene Nano-PanNET assay was developed and validated using FFPE tumour tissue. The analyses demonstrated 91% concordance of gene expression using the refined 78 gene assay in fresh frozen and FFPE samples. 92% concordance was demonstrated across RNAseq and NanoString platforms, using the 78 gene centroids. Survival analyses revealed that patients assigned the MLP-1 subtype had a poor prognosis, with a 5 year survival rate of 60%, whilst patients with the Insulinoma-like subtype had a good prognosis, 5 year survival rate 100%.

Conclusion

A novel robust 78 gene Nano-PanNET assay has been developed which can subtype patient samples using both fresh frozen and FFPE tissue. Patients assigned the MLP-1 subtype have been demonstrated to have a poor prognosis, with a 15% lower 5 year survival rate than any of the other PanNETassigner molecular subtypes. Approximately 20% of PanNENs fall into the MLP-1 subtype and this subtype is represented across all 3 PanNEN grades. Additional validation in a larger cohort is now required to establish if the Nano-PanNET assay developed here is prognostic on multivariate analysis and could be optimised for use in clinic. If so, the Nano-PanNET assay may potentially be used to improve current classification strategies, enabling a more personalised approach for PanNEN patients.

3.1 Background and Rationale

As previously outlined, treatment decisions for PanNEN patients are currently based on stage and grade of disease, alongside functionality and SSTR status, as there are no other validated prognostic and/or predictive biomarkers routinely used in clinical practice for patient stratification. Yet there is significant heterogeneity of clinical behaviour within grades and controversy remains as to the optimum Ki-67 index cut-offs^{30,31,32}.

From data presented in Chapter 2, for patients in the PanNEN registry, risk of death increased overall by 1.3% per unit increase in Ki-67% value, irrespective of grade of disease. This demonstrates again that Ki-67 is a continuous variable for risk of death and that dividing patients into 3 grades according to fixed Ki-67 cut-offs is an arbitrary division, rather than a separation of disease according to distinct biological differences. Further, patients with grade 2 disease demonstrated highly heterogeneous disease behaviour with an OS IQR of 3.6-8 years. There is therefore an unmet clinical need for novel biomarkers which can separate patients according to their tumours' biology and to complement grade to predict prognosis and guide treatment decisions for PanNEN patients.

Our laboratory previously defined 3 PanNEN molecular subtypes, based on an integrated analysis of gene expression, microRNA and mutations, and collectively named the PanNETassigner signature (see Chapter 1). The subtypes described are Insulinoma-like, Intermediate and metastasis like primary (MLP), which can be sub-divided into MLP-1 and MLP-2. The prognostic value of these molecular subtypes has not previously been examined, although metastatic disease was found to be associated with the MLP subtype⁵¹.

Associations between these subtypes and grade of disease were previously investigated. Grade 1 and 2 PanNETs were found to be heterogeneous, variably associating with all three molecular subtypes, whereas grade 3 tumours were exclusively associated with the MLP subtypes⁵¹. These data and the association of the MLP subtype with metastases, led to the

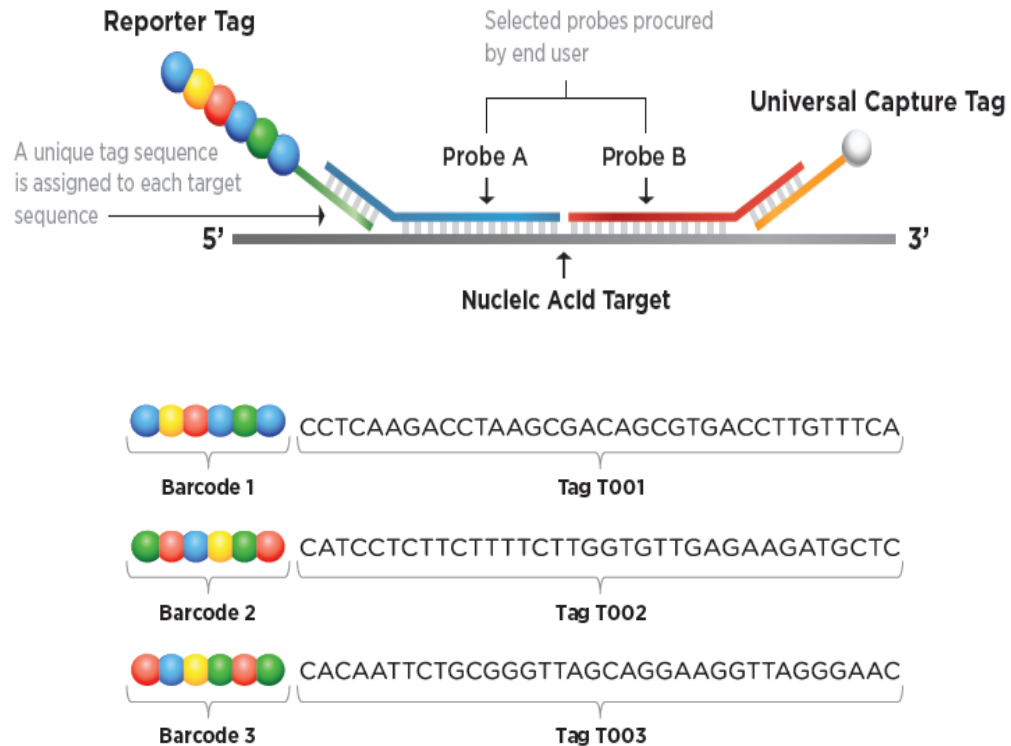
hypothesis that our molecular classification of PanNEN into subtypes may provide a useful tool for additional patient stratification, according to tumour biology.

Expression signatures have been used extensively in other tumour types, particularly breast cancer. The Prosigna test measures risk of recurrence¹²² and the breast cancer Genomic Grade Index predicts response to chemotherapy and separates subtypes of breast cancer¹²³. The Breast Cancer Index (BCI) stratifies breast cancer patients into three risk groups and provides an assessment of tumour recurrence¹²⁴. A similar index for GEP-NETs, to improve patient prognostication and classification, would be highly clinically relevant.

Various platforms have been used to develop such clinical assays, including the NanoString nCounter system. This platform uses digital molecular barcoding to enable the detection and quantification of the expression of up to 800 genes in a single sample. NanoString supplies a range of standard assays (including the immune profiling panel used in Chapter 4) but also allows researchers to design their own custom assays, using the ElementsTM technology program.

For such custom assays, nCounter ElementsTM supply a TagSet, consisting of a fluorescently labelled reporter tag and a biotinylated universal capture tag, and the target-specific oligonucleotide probe pairs (A and B) are supplied by the researcher to match their genes of interest. The reporter tags and capture tags hybridize to the target specific oligonucleotide probes A and B, which in turn hybridize to the RNA target. The complete structure is known as a tag complex (Figure 3.1).

Figure 3.1 nCounter Elements™ Tag Complex



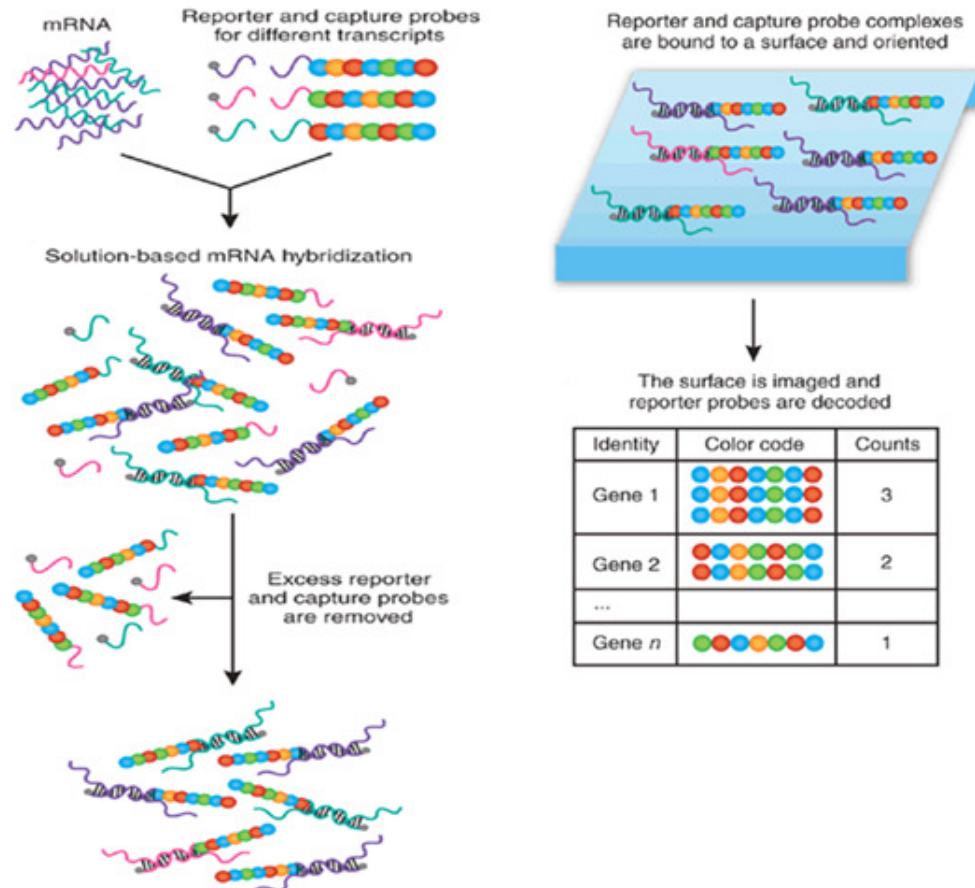
Modified from NanoString Elements™ training slide set (Sept 2016)

The unique pattern of six colour spots on each reporter tag create the barcodes required for data collection and the capture tag facilitates immobilisation of the hybridized complex in an nCounter cartridge, which is imaged using a digital analyser. As the assay uses direct digital detection of messenger RNA (mRNA), both reverse transcription and amplification of complementary DNA (cDNA) using polymerase chain reaction (PCR) are not required, eliminating potential amplification bias. Gene expression is measured by counting the number of times a barcode for a specific gene is detected (Figure 3.2).

This platform has been demonstrated to be favourable over various other techniques based upon a number of features including sensitivity, technical reproducibility, robustness (particularly with low quality FFPE samples), and in light of its practicality as a lower cost clinical application¹²⁵. Further the technology has already been used to develop a number of clinical assays

across multiple tumour types, including the aforementioned Prosigna Breast Cancer Prognostic Test^{126,127,128,129,130,131}.

Figure 3.2 NanoString Hybridization and Decoding Process



Modified from NanoString Elements™ training slide set (Sept 2016)

The first aim of this chapter was to develop, refine and validate a novel gene expression assay based on the PanNETassigner molecular subtypes using the nCounter platform.

The second aim was to use this Nano-PanNET assay to assess the prognostic significance of the PanNETassigner subtypes in a sizeable cohort of PanNEN patients. The ultimate ambition was to establish if the Nano-PanNET assay could potentially, with further validation, be used to refine the current classification paradigm, to enable a more personalised approach to treatment for PanNEN patients.

3.2 Methods

3.2.1 PanNEN Tissue Samples and Clinical Data

PanNEN tissue samples and matched clinical data were collected from ARC-NET, Verona and RM, London, within the PanNEN registry (PaNACeA study CCR4476, Research Ethics Committee approval reference 16/LO/0984, May 2016) as described in Chapter 2. Microarray gene expression data from work previously conducted by our lab was also used for validation purposes and these samples are described as the Microarray cohort (n=19).

Verona Cohort

RNA isolated from fresh frozen tissue was provided for 200 patients from the Verona cohort. RNA isolated from matched normal pancreatic tissue was provided for 20 of these patients. RNA from selected samples was used for NanoString (n=144) and RNAseq analyses (n=98). For 44 patients, RNA extracted from FFPE tissue was also provided, which was used for NanoString analyses alone.

RM Cohort

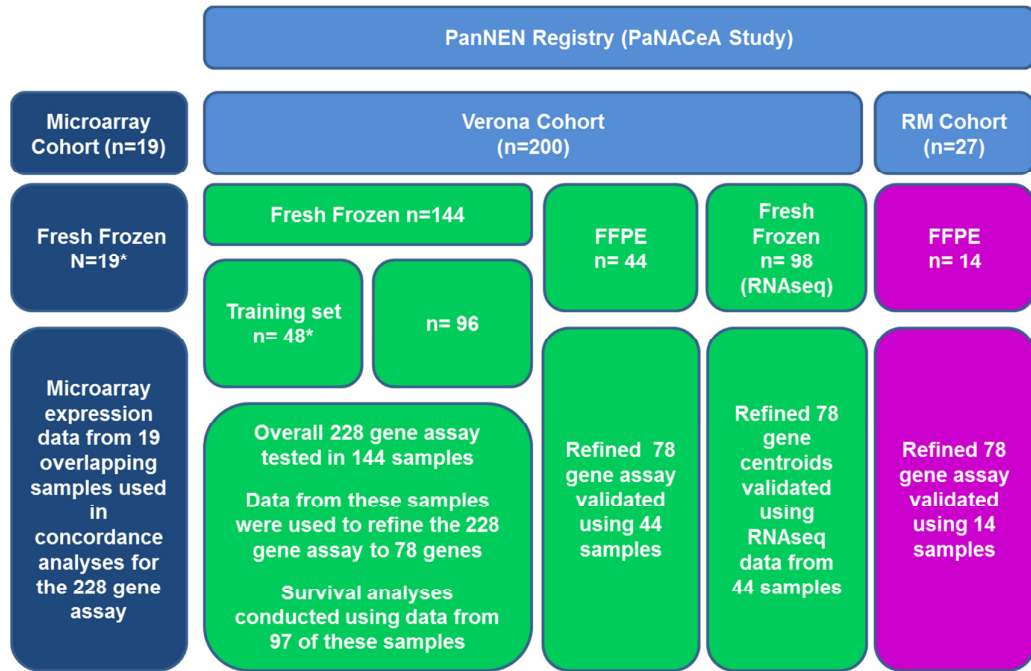
27 FFPE samples were collected as described in Chapter 2 (Figure 2.2). RNA was extracted and used for NanoString analyses.

Microarray Cohort

The PanNEN gene expression data for the Microarray cohort was originally from Missiaglia and colleagues, Verona (GEO Omnibus ID GSE73338; ref 34), and had been used by our lab previously in the original development of the PanNETassigner molecular subtypes^{51,80}. Gene expression in this cohort was assessed using an 18.5 K Human oligo-microarray from the Ohio State University Cancer Centre and analysed using R and Bioconductor as described^{132,133,134}. Data from the 19 samples which overlapped with samples from the Verona cohort were used in validation analyses.

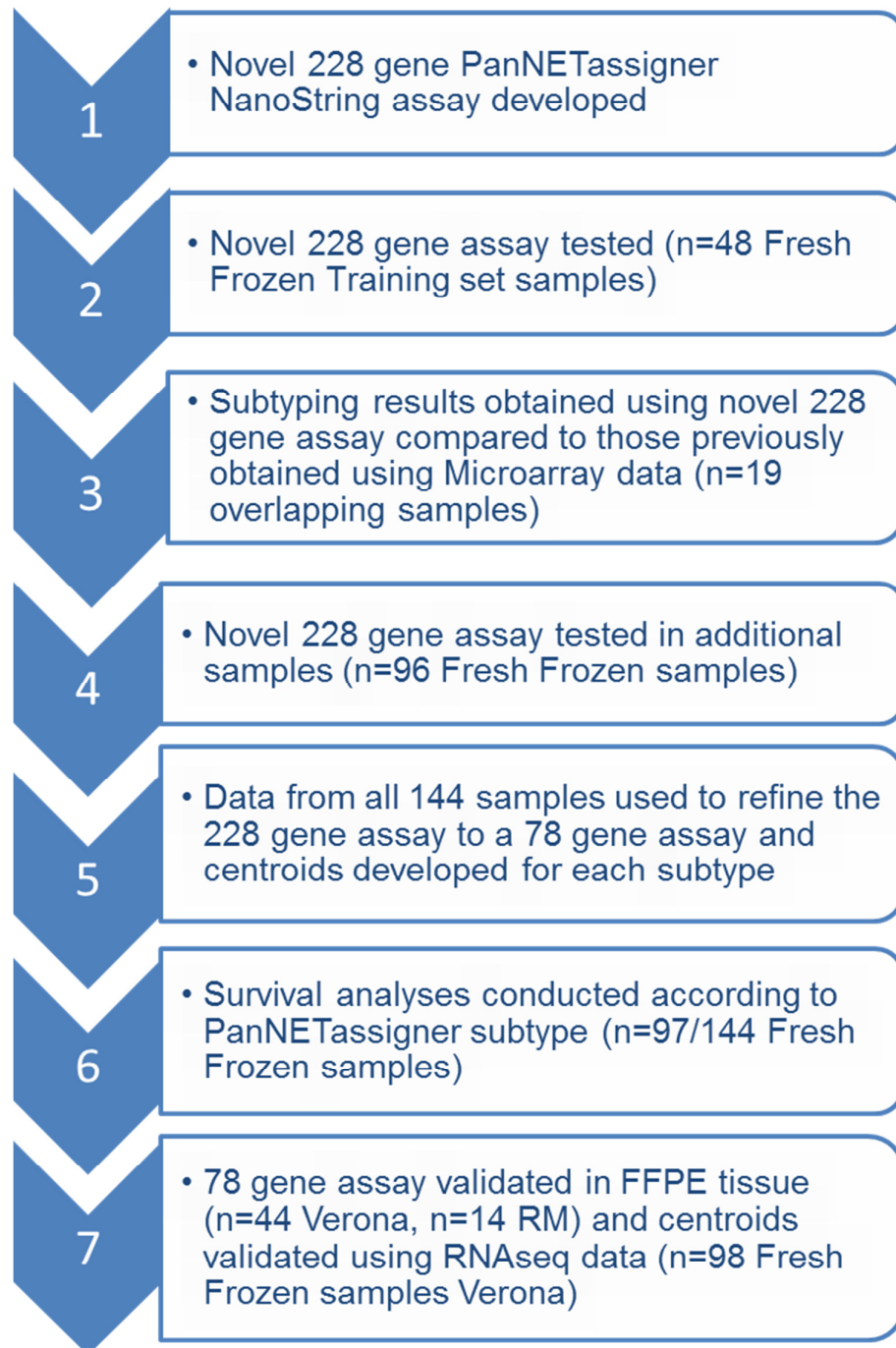
Figure 3.3 details the analyses carried out across these samples and Figure 3.4 provides an overview of the steps involved in the development of the PanNETassigner assay.

Figure 3.3 Overview of Tissue Samples and Analyses Performed



**19 samples overlapped between the Microarray and Verona cohorts*

Figure 3.4 Overview of the project to develop, refine and validate a novel PanNETassigner NanoString Assay



3.2.2 228 gene PanNETassigner NanoString Assay Development

A panel of 228 genes (including 30 housekeeping genes) was selected for a NanoString Elements™ custom assay, based on our PanNETassigner signature⁵¹. Target specific probes were designed by NanoString. Probes were checked using Basic Local Alignment Search Tool (BLAST), an algorithm for comparing biological sequence information with established sequence databases, to confirm identity and optimum isoform coverage. Final probes were selected and ordered from Integrated DNA Technologies and the corresponding TagSets from NanoString Technologies.

3.2.3 Wet Lab Techniques

Nucleic Acid Extraction and quality/quantity assessment

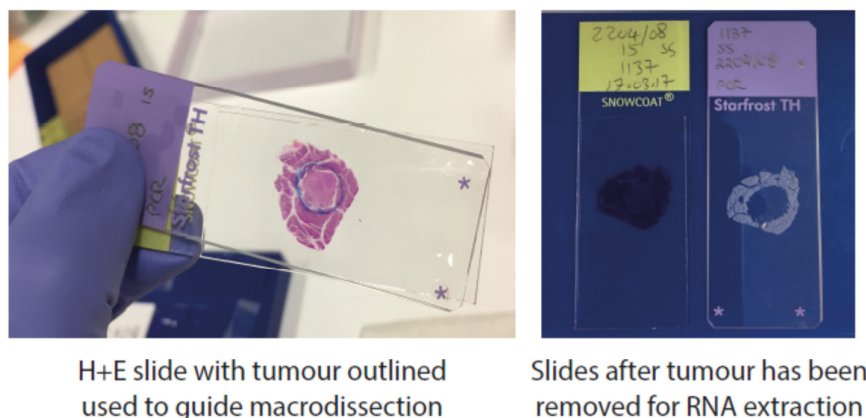
For the RM cohort samples, haematoxylin and eosin (H&E) slides cut from tissue blocks successfully obtained through the PanNEN registry were assessed by an experienced Gastrointestinal Histopathologist (Monica Terlizzo), as described in the slide protocol below. If tumour content was limited, slides for RNA extraction were prioritised over slides for central histopathology review.

Protocol for PanNEN registry slides

1. 1x H&E slide cut for each available block
2. Histopathologist reviewed (tumour content/cellularity) and advised which block to use.
3. Histopathologist outlined tumour on the H&E slide for the chosen block to enable macrodissection before RNA extraction
4. Biological specimens team then cut the chosen block as follows:
 - H&E (4 micron thick) 1st slide
 - 1 slide for Ki-67
 - 5-7 slides (at 7 micron thick) for RNA extraction
 - 6-10 Additional slides for IHC
 - H&E (4 micron thick) last slide

The 5-7 selected tissue sections for RNA extraction then underwent deparaffinization, macrodissection and processing (RecoverAll™ Total Nucleic Acid Isolation Kit AM1975 protocol) (Figure 3.5). Quality and quantity of extracted RNA was assessed using NanoDrop-2000 Spectrophotometer and Agilent RNA-6000 Bioanalyzer systems, respectively.

Figure 3.5 Macrodissection Process



For the Verona cohort similar processes were followed but samples were not macrodissected. Here Allprep Qiagen was used for 184 fresh frozen samples and GuSCN for 16 fresh frozen samples as previously described¹³⁵. For the FFPE samples RecoverAll™ was used, as in the RM samples.

RNA was diluted for the NanoString experiments. 100ng RNA was loaded in 5 μ L (dilution 20ng/ μ L) when possible. However, for the RM samples 70ng in 7 μ L was used (dilution 10ng/ μ L) due to the quantity of RNA available.

nCounter Elements™ Process

Oligonucleotide probe pools were created and hybridized to reporter/capture Tags and these Tags were hybridized to the RNA target, according to the NanoString Elements™ manual (version 2, Sept 2016) as previously described^{136,137}. Following hybridization, samples were purified, orientated and immobilised in their cartridge using the nCounter Prep Station before being loaded into the Digital Analyser (Figure 3.2). The

molecular barcodes were counted and decoded, results stored as a Reporter Code Count (RCC) file. The RCC files were analysed alongside the Reporter Library Files (RLFs), containing details of the custom probes and housekeeping genes selected.

RNA sequencing (RNAseq) (n=98)

In the Verona RNAseq samples, gene expression was assessed by RNAseq as previously described¹³⁸. RNAseq was carried out by the Mayo Clinic Core Facility, Rochester. RNA was diluted (200ng/20uL) and quantity and quality assessed using Qubit® Fluorometer and Agilent RNA 6000 Bioanalyzer. A column based DNA extraction method was used before RNAseq libraries were prepared using PolyA selection and RNA library prep using NEBNext-Ultra RNA Directional kit to produce Illumina compatible libraries. The libraries were sequenced using a HighSeq2500 with Paired-Ends 2x100 and targeted depth of 50 million reads/sample.

3.2.4 Bioinformatics Techniques

nSolver™ v3.0 analysis

The nSolver™ software analysis package was used to perform Quality Control (QC) and normalisation of the expression data from the NanoString assays. QC steps included assessment of assay metrics (field of view counts/binding density), internal Code Set controls (6 positive and 8 negative controls to assess variations in expression level according to concentration and to correct background noise respectively) and principal component analysis to assess batch effect. Following QC steps, raw data were normalised to housekeeping genes selected using the geNorm algorithm within nSolver™.

Integrative Latent Variable Model (iLVM)

The Integrative Latent Variable Model (iLVM) was used to measure concordance between subtyping using the microarray and NanoString platforms. The 19 samples from the Microarray cohort which overlapped with the Verona cohort were used for this analysis. Specifically, we assessed the concordance of subtypes attributed using the novel

NanoString assay with those previously attributed to these 19 samples using the PanNETassigner multi-omics signature and microarray data. Subtypes were attributed in the 19 Verona cohort samples using NanoString gene expression data and the Integrative Latent Variable Model Method (iLVM). iLVM is a dimension reduction method, which uses latent/unobserved variables to identify clusters within data, designed in house (Gift Nyamundanda). It was chosen as a method here as it is good at finding clusters in data even when only small numbers of variables are available (n=19).

Assignment of Subtypes using 228 gene PanNETassigner NanoString Assay (n=144)

Normalised expression data was \log_2 transformed and median centred. Genes with $\geq 20\%$ zero expression were removed to overcome background artefact/noise as described¹³⁹. To assess potential batch (or technical) effects between different runs of NanoString assay experiments we used our *exploBATCH* computational tool¹⁴⁰. *exploBATCH* contains a tool *findBATCH*, which uses probabilistic principal component analysis with covariates, to assess batch effects by identifying those principal components that are associated with the given batch information. Those principal components with 95% confidence interval (CI) not containing zero will inform significant batch effect in the data and are corrected with ComBat¹⁴¹.

ComBat estimates how much each gene's expression is proportional to the batch for every gene. A regression model is then applied to remove this effect. A form of unsupervised clustering, Non-negative Matrix Factorisation (NMF), was subsequently used to determine PanNETassigner subtypes, applied using the R/BioConductor platform as previously described^{142,143}.

Refinement of 228 Gene PanNETassigner NanoString Assay

A smaller, robust panel of differentially expressed genes was derived from the 228 gene panel using Significance Analysis of Microarrays (SAM). SAM, distributed by Stanford University in an R-package, is a non-

parametric statistical technique using multiple permutations to assess whether gene expression changes are statistically significant¹⁴⁴. 78 genes were selected for the Refined PanNETassigner NanoString assay, named the Nano-PanNET assay. Prediction Analysis for Microarrays (PAM) centroids were then created for every gene for each PanNETassigner subtype using these 78 genes. The PAM centroid may be considered as the average expression of a particular gene in that subtype, scaled by variability¹⁴⁵. PAM centroids can be used for single sample prediction and PAM analysis was performed using R-based *pamr* tool.

Validation of Refined 78 gene Nano-PanNETAssay

The same bioinformatics techniques were used in the validation samples, to assess and correct batch. Pearson Correlation was then used to score each sample's gene expression data against the PAM centroids, giving a Pearson Correlation score for each subtype and subtypes were assigned. Concordance was then assessed both across platforms and between FFPE and fresh frozen samples.

Survival Analyses

OS according to molecular subtype attributed by the PanNETassigner and Nano-PanNET assays was assessed using Kaplan Meier methods and Cox regression was used to compare survival rates between subtypes and investigate if grade and molecular subtype were independent prognostic variables. R statistical computing (<http://www.r-project.org>) was used for all calculations.

3.2.5 Overview of my role

PanNEN patient samples and Clinical Data

The tissue samples and clinical data utilised in the development of the Nano-PanNET assay are from the PanNEN registry. My role in the set-up and management of this registry is described in detail in Chapter 2.

228 gene PanNETassigner NanoString Assay Development

Based on our lab's PanNETassigner signature, I selected a panel of subtyping and housekeeping genes for the 228 gene PanNETassigner NanoString assay. I worked with NanoString to arrange the design of target specific probes for the novel panel. I checked all 228 probes using the Basic Local Alignment Search Tool (BLAST), an algorithm for comparing biological sequence information with established sequence databases, to confirm identity and optimum isoform coverage. I then selected the final probes, with the support of Anguraj Sadanandam, and ordered them from Integrated DNA Technologies alongside the TagSets from NanoString.

Wet Lab Work

With the support of Chanthirika Ragulan (Higher Scientific Officer), I carried out the following lab work:

- All NanoString work for 144 samples analysed using the 228 gene assay
- NanoString work for 44 fresh frozen samples using the 78 gene Nano-PanNET assay (NanoString work for 36/44 FFPE samples using 78 gene assay was carried out by Krisha Desai, Post-Doctoral Training Fellow, after I had taught her the processes involved)
- Sourced quotes for RNAseq work and prepared samples for RNAseq (including appropriate RNA dilutions and quality control)
- Visited ICR core facility to watch and understand the RNAseq workflow

- All RM cohort sample work including macrodissection, RNA extraction, quality and quantity assessments and NanoString work using 78 gene Nano-PanNET assay

Bioinformatics Work

With the support of Gift Nyamundanda, Kate Eason and Anguraj Sadanandam (Bioinformaticians), I carried out the following bioinformatics work:

- NSolver and nCounter Advanced analyses for NanoString data, including all quality control assessments (validated by Chanthirika Ragulan)
- Used TreeView and Cluster 3.0 to assess gene expression
- Survival Analyses (validated by Gift Nyamundanda)
- Liaised with bioinformaticians to select appropriate clinical data for multivariate analyses and interpreted the results
- Generated figures in Adobe Illustrator and PowerPoint

The remainder of the bioinformatics work was carried out by Gift Nyamundanda and validated by Anguraj Sadanandam.

Communication of Results

I have communicated data from this chapter as follows:

- I presented this project as a poster at the NIHR Research Leaders of the Future meeting, Leeds 2016. (A translational study in Gastroenteropancreatic Neuroendocrine tumours (GEP-NETs) to validate and assess a new molecular classification (PaNACeA)).
- With Anguraj Sadanandam, I wrote an abstract based on data from this chapter, selected for oral presentation at ENETs 2018.

(Development of a multiplex biomarker assay to subtype pancreatic neuroendocrine tumours (PanNETs) with distinct prognosis and mutations).

- I presented this project at the ICR Conference as an oral presentation, London 2018. (A translational study in Pancreatic Neuroendocrine tumours (PanNETs)).
- I am in the process of preparing a manuscript (including figures/tables) for submission, with support from the co-authors.

3.3 Results

3.3.1 Initial Testing of 228 gene PanNETassigner NanoString Assay (n=48)

228 gene PanNETassigner NanoString assay

The 228 gene assay PanNETassigner NanoString assay, hereafter referred to as the 228 gene assay, was successfully developed as described in methods. The final 228 genes and those genes removed following BLAST analysis are detailed in Supplementary Table 3.1 (Appendix 3).

Quality and Quantity of RNA for Fresh Frozen samples from Verona Cohort (n=144)

For the 144 samples processed with the 228 gene assay the median RNA concentration was 222ng/μL, range 2.8 to 4099ng/μL. RNA Integrity number (RIN) ranged from 6.5 to 10.

228 gene assay Test Set (n=48)

The 228 gene assay was effectively performed on a test set of 48 fresh frozen samples from the Verona cohort. Gene expression data was successfully generated and analysed within nSolver. All samples formally passed the nSolver QC steps as described in methods. However, 4 samples were flagged for review and these were omitted from further analysis. 3 samples were flagged due to just lower than threshold (0.95) linearity on positive controls which was thought to be caused by RNA purification issues. 1 sample was flagged due to having a slightly increased binding density (2.4) which was attributed to an excess of RNA.

3.3.2 Suitability of the NanoString platform

As described in methods, subtyping details were already available for 19/48 from the test set, from microarray data used in our previous Cancer Discovery publication⁵¹. Before developing the assay further we wished to confirm that the NanoString platform could be used to accurately assign PanNETassigner subtypes. We therefore assessed the concordance between subtypes previously assigned using microarray data and subtypes assigned here using the novel 228 gene assay. We used iLVM to cluster

the NanoString gene expression data to assign subtypes, as the low number of samples available (n=19) made other techniques such as PAM and Pearson correlation less reliable.

Using the NanoString gene expression data for the 19 samples, iLVM identified 3 clusters, corresponding to the Insulinoma-like, the Intermediate and the MLP PanNETassigner subtypes. The concordance between the subtypes assigned using iLVM with the original subtypes was assessed. The misclassification error rate was 5% with 18/19 samples correctly classified (Figure 3.6 and Table 3.1).

Figure 3.6 Strong Concordance between subtypes derived from Microarray data and NanoString data (iLVM)

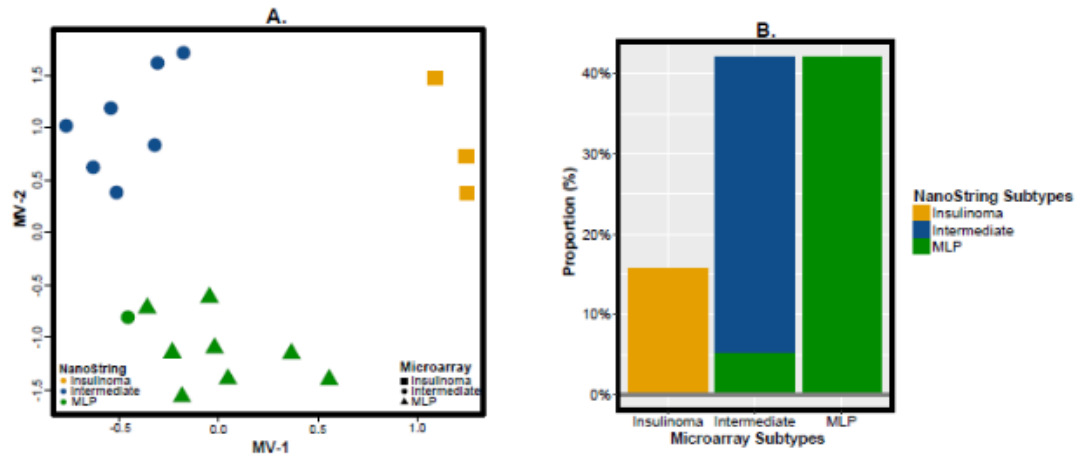


Figure A 1/19 samples assigned a different subtype by iLVM using 228 gene assay data vs. microarray data. This is seen as a green circle, representing a sample which was assigned as Intermediate according to microarray data but MLP according to NanoString data.

Figure B. This proportion plot highlights the 95% concordance seen with the 2 platforms, with just 1 sample misclassified.

Table 3.1 Subtypes Assigned using Microarray Data and 228 gene Assay (n=19)

Misclassified sample highlighted in red

Sample	Microarray Subtype	Nanostring iLVM Subtype
1634T	MLP	MLP
1635T	MLP	MLP
1637T	MLP	MLP
1638T	Intermediate	Intermediate
1644T	Insulinoma	Insulinoma
1649T	Intermediate	Intermediate
1650T	Intermediate	Intermediate
1656T	MLP	MLP
1657T*	Intermediate	MLP
1660T	MLP	MLP
1665T	Intermediate	Intermediate
1672T	Insulinoma	Insulinoma
1913T	MLP	MLP
1914T	MLP	MLP
1921T	Insulinoma	Insulinoma
1923T	Intermediate	Intermediate
1929T	MLP	MLP
1934T	Intermediate	Intermediate
1935T	Intermediate	Intermediate

3.3.3 Further Testing of the 228 Gene Assay (n=96)

Having demonstrated the suitability of the NanoString platform to assess PanNETassigner subtypes, we went on to perform the 228 gene assay on an additional 96 samples. Gene expression data was successfully generated and analysed within nSolver. All 96 samples formally passed the nSolver QC steps as described in methods with no flagged samples.

The data from the test set of 48 samples and from the additional 96 samples were then combined. The 144 samples overall included 6 replicates and 7 matched normal tissue samples. Heatmaps of the results for the tumour samples and replicates are shown below (Figures 3.7 and 3.8).

Figure 3.7 Heatmap of gene expression data from the 228 gene Assay
 (n= 127, 6 replicates, 7 normal and 4 flagged samples removed)

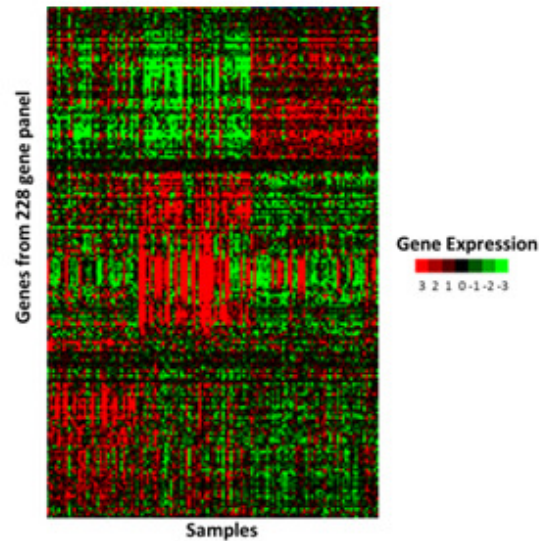
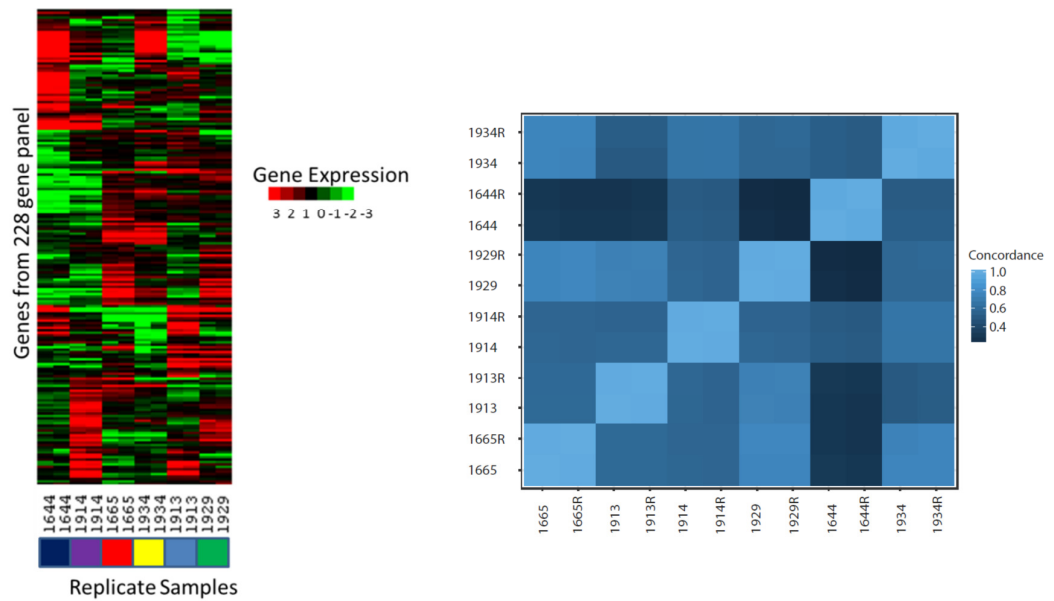


Figure 3.8 Technical Reproducibility of the 228 gene Assay
 (n=6 replicates)

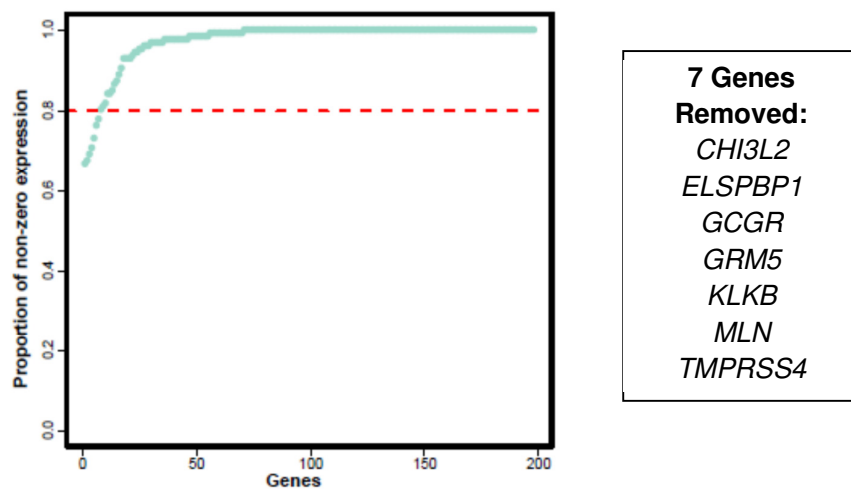


The 6 replicate samples were processed using the 228 gene assay 4 months apart. The replicates all demonstrated a high correlation of gene expression (~1), confirming the assay's technical reproducibility.

3.3.4 Subtyping using the 228 gene Assay (n=144)

We next used the NanoString gene expression data from the 144 samples to assign PanNETassigner subtypes. As described in methods only the genes with >80% non-zero expression were included. Here of the 198 genes (228 genes with the 30 housekeeping genes removed), 7 genes were removed from the subsequent analyses due to $\geq 20\%$ zero expression (Figure 3.9).

Figure 3.9 Genes with $\geq 20\%$ zero expression removed from analysis

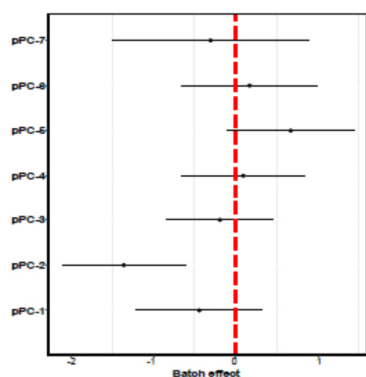


Batch Effect Assessment and Correction

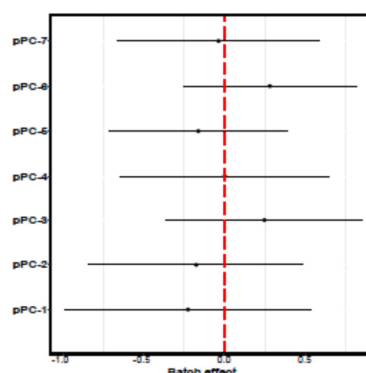
To assess any batch effects between different runs of nCounter platform experiments we used *exploBATCH* as described in methods (Figure 3.10)¹⁴⁰. As this did demonstrate a batch effect, ComBat was used to correct this.

Figure 3.10 exploBATCH analysis of batch effect for 228 Gene Assay

A Baseline



B After ComBat



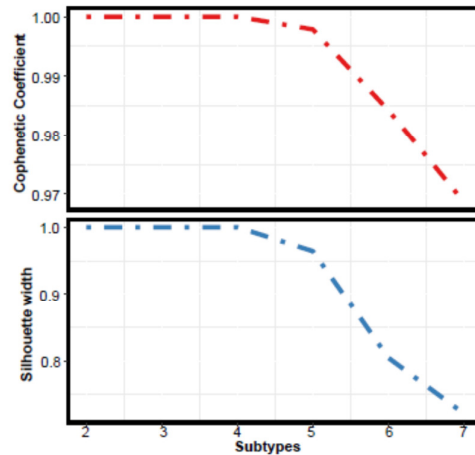
This figure shows probabilistic Principal Components (pPC) and their 95% confidence intervals. If the confidence interval crosses 0 then there is no batch effect. A Here pPC2's confidence interval doesn't cross 0, demonstrating a batch effect, which required correction B Demonstrates that the batch effect has been removed using ComBat.

Non-negative Matrix Factorisation (NMF) and Rank Survey

NMF was applied to the gene expression data for 127 samples (6 replicates, 7 matched normal samples and 4 flagged samples removed from the original 144 samples) across 191 genes (30 housekeeping and 7 genes with high levels of zero expression removed from original 228 genes)^{141,143,145}. This clustering paradigm revealed 4 subtypes.

The silhouette and cophenetic quality measures, which form part of the NMF analysis, support 4 subtypes (Figure 3.11). For each sample, the silhouette analysis considers the distance between each gene's expression level and the expression level for that gene in the subtype as a whole (the subtype's centroid). Following multiple runs (100), the number of subtypes chosen minimises the variability of gene expression between samples of the same subtype and maximises the variability between samples of different subtypes. The cophenetic analysis measures how robust the 4 subtypes are, considering if the process were repeated how many times each sample would be allocated to the same subtype.

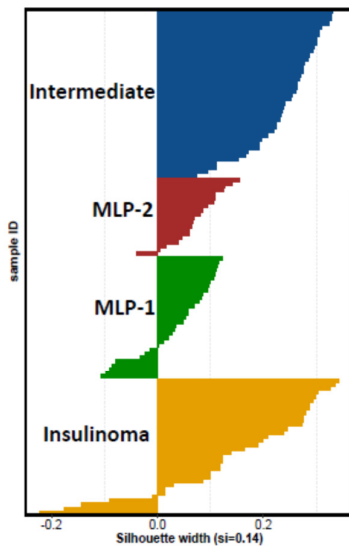
Figure 3.11 Cophenetic and Silhouette Analyses as part of NMF



Cophenetic and Silhouette analyses support 4 subtypes as both cophenetic coefficient and silhouette width fall for subtype numbers above 4.

Silhouette width was used again, this time from a single run, to determine the most representative samples for each subtype. Non-representative samples were removed as they may represent samples with mixed subtypes. Here 14 samples were removed, leaving the 113 most robust samples which were subsequently used to refine the 228 gene panel (Figure 3.12).

Figure 3.12 Single Run Silhouette to determine most representative samples for further analysis of PanNETassigner subtypes

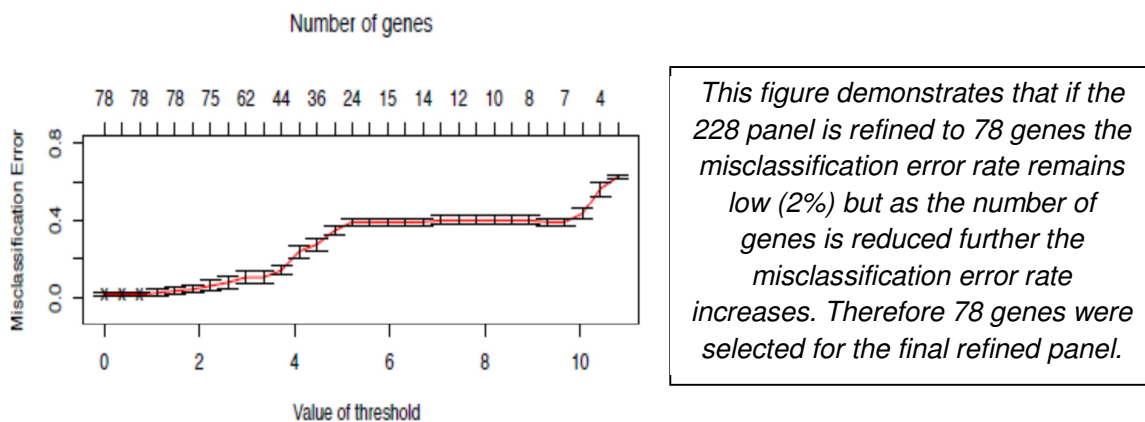


In the silhouette plot the samples with a silhouette width of <0 , on the left of the plot, represent potentially mixed samples and were removed before analyses were conducted to select the final genes for the refined panel

3.3.5 Development of the Refined 78 gene Nano-PanNET Assay

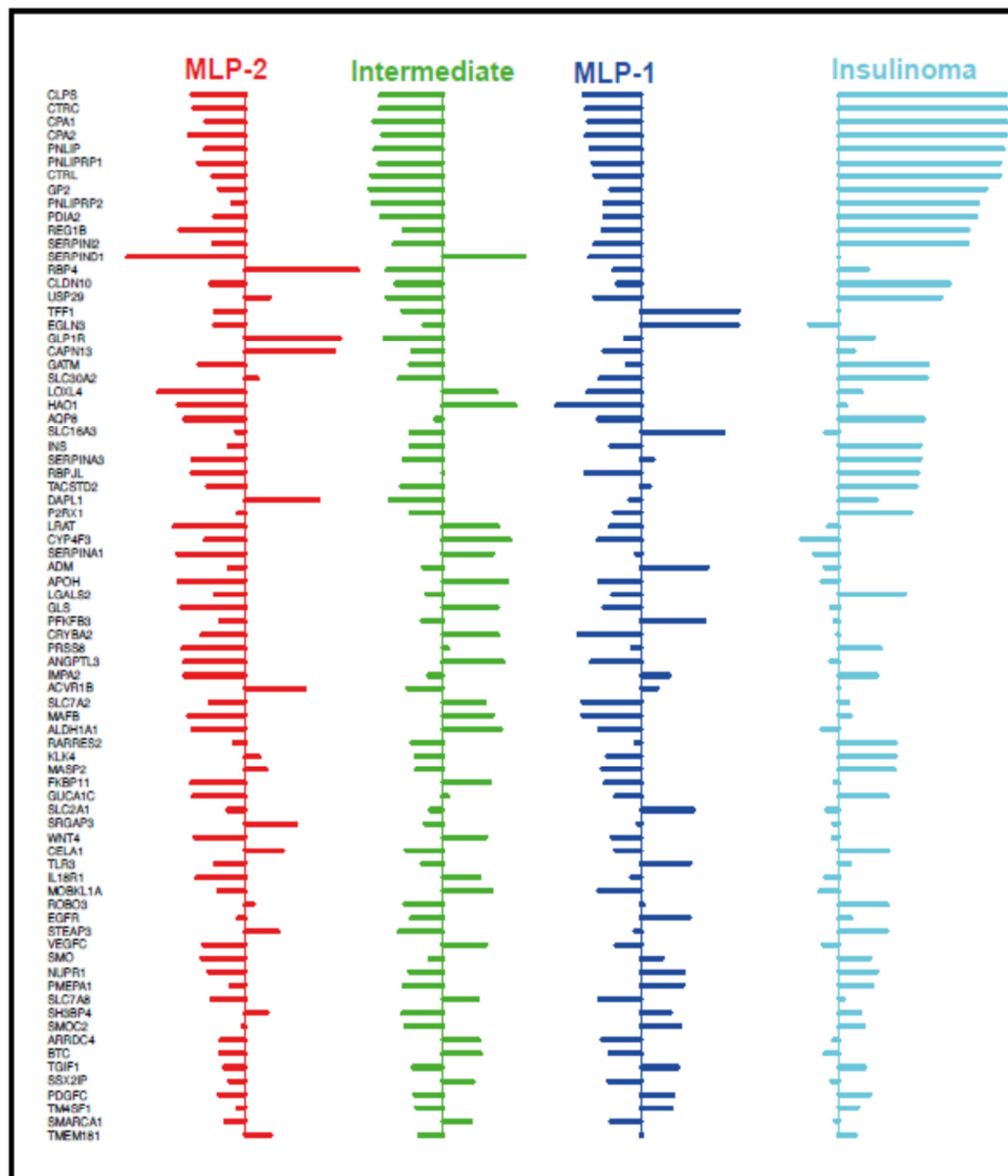
Gene expression data from the 113 remaining samples was then used to refine the 228 gene assay. SAM, a univariate approach to assess differentially expressed genes as described in methods, was used to select the smallest number of genes which could be used to differentiate the PanNETassigner subtypes (Figure 3.13)¹⁴⁴. This approach selected 78 genes (Supplementary Table 3.2, Appendix 3.2) for the Nano-PanNET assay.

Figure 3.13 SAM used to derive refined 78 gene Nano-PanNET Assay



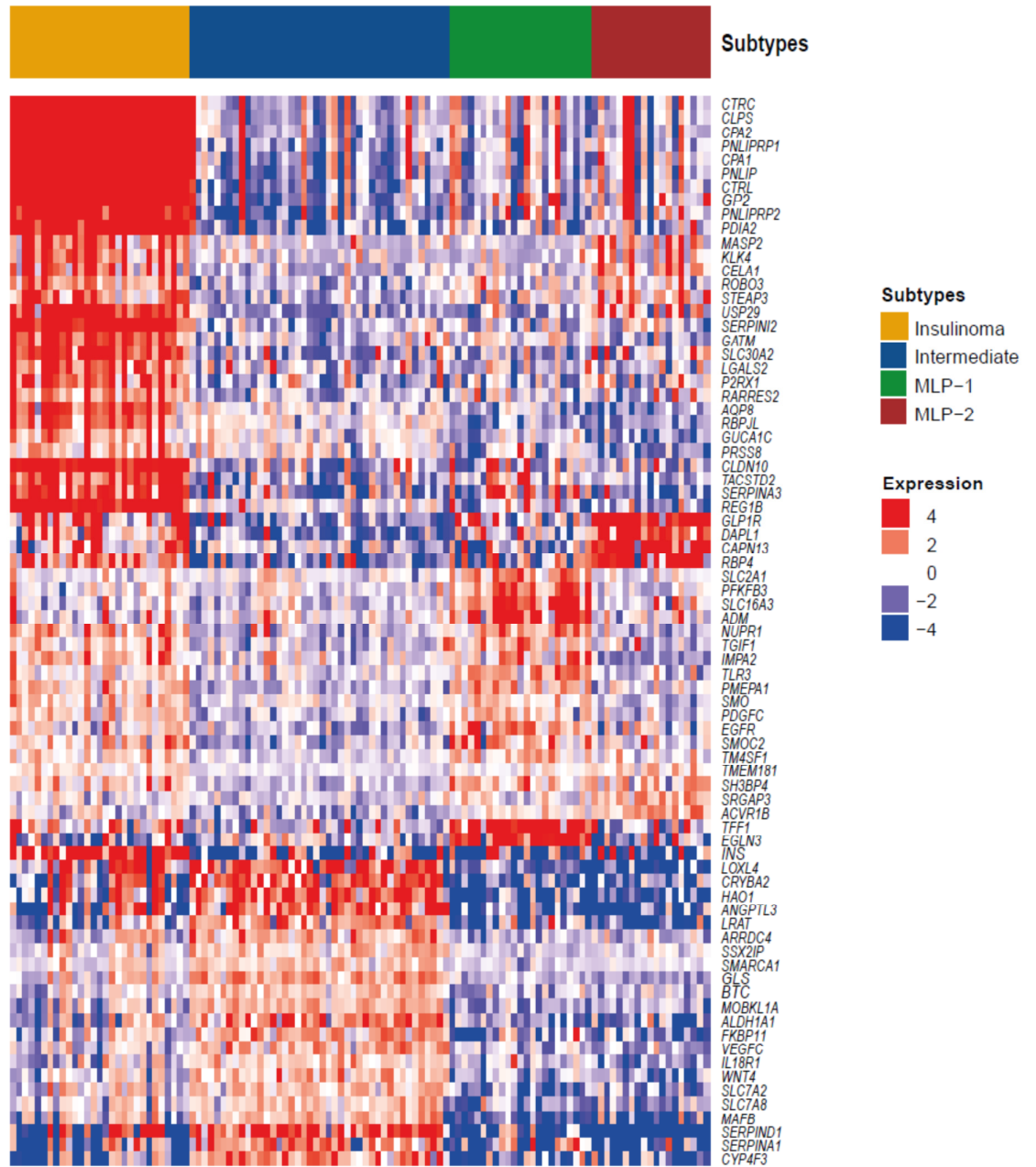
PAM was then used to derive centroids for each of the 78 genes in each of the 4 PanNETassigner subtypes (Figures 3.14 and 3.15)¹⁴⁵.

Figure 3.14 PAM Centroids for Refined 78 gene Nano-PanNET Assay



The PAM centroids represent the average expression pattern for each of the refined panel of 78 genes in each of the 4 subtypes

Figure 3.15 Heatmap of Expression of selected 78 genes (n=113)

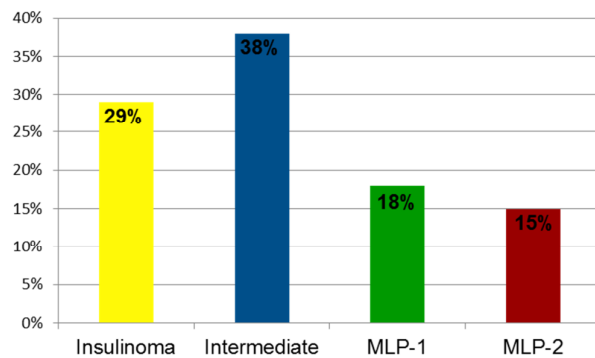


3.3.6 Survival Analysis according to PanNETassigner Subtype

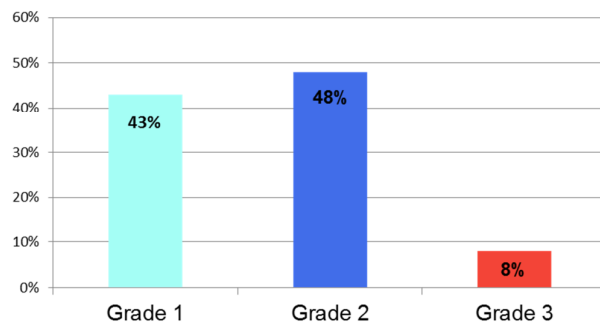
Having developed the refined 78 gene panel we wished to establish if the subtypes assigned had prognostic significance. Full clinical data was available for 97/113 of the patients whose samples were subtyped as above. The distribution of grades and subtypes across the cohort was assessed (Figure 3.16). The most frequently assigned subtype was Intermediate (38%), followed by Insulinoma-like (29%), with smaller percentages assigned to the MLP-1 and MLP-2 subtypes (18% and 15% respectively). Over 90% of patients had grade 1 or 2 disease. Of the 97 patients, 15 had functional disease. 10/15 functional cases were Insulinoma-like, 2/15 MLP-1 and 3/15 MLP-2 with 29% of the Insulinoma-like tumours being insulinomas.

Figure 3.16 Distribution of (A) PanNETassigner Subtypes and (B) WHO 2010 Grades (n=97)

A Distribution of PanNETassigner Subtypes



B Distribution of WHO 2010 Grades



Note percentages are rounded in these figures but original values to add up to 100%

OS according to PanNETassigner subtype was analysed, with the MLP-1 subtype demonstrating the poorest and the Insulinoma-like subtype the best survival ($p \leq 0.05$) (Figure 3.17). Median OS was 71 months (95% CI 56, NR) for the MLP-1 subtype but was not reached for the other PanNETassigner subtypes. Survival according to WHO 2010 grade was considered in the same cohort, with grade 3 patients having the worst prognosis and grade 1 the best, consistent with the literature ($p < 0.001$) (Figure 3.18).

Figure 3.17 OS according to PanNETassigner Subtype (n=97)

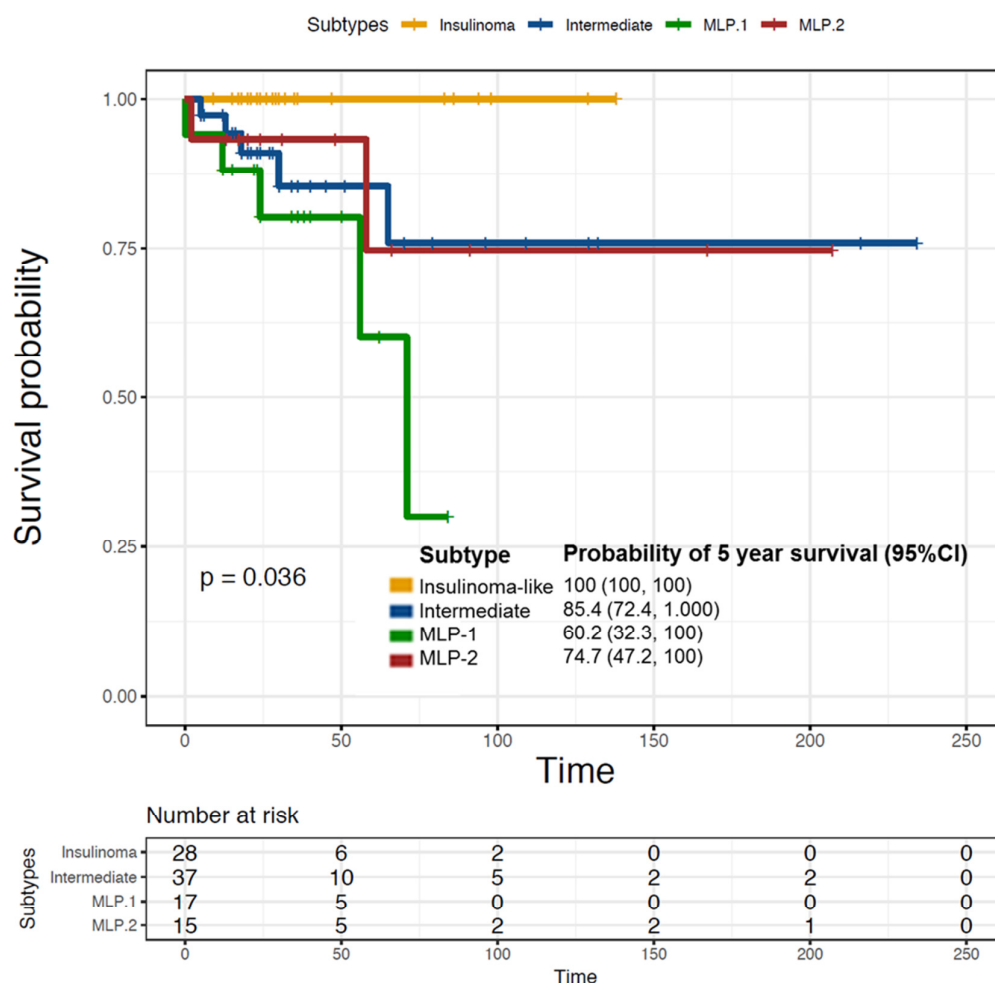
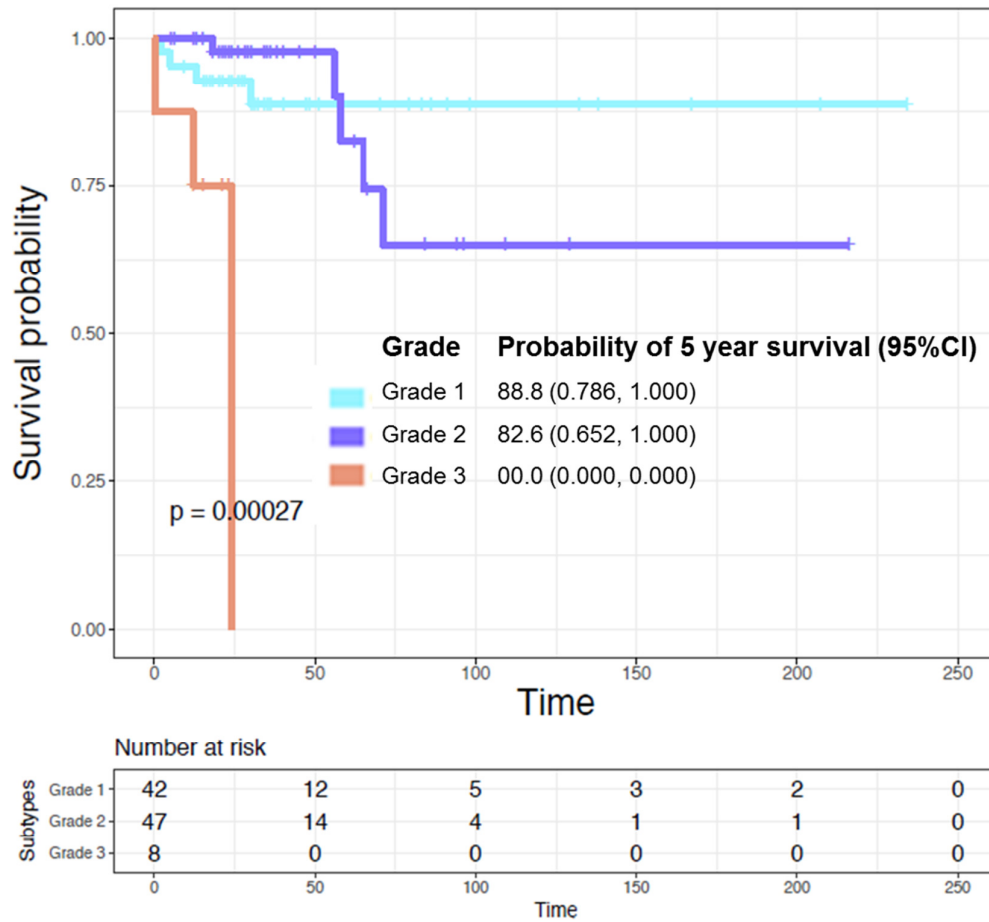
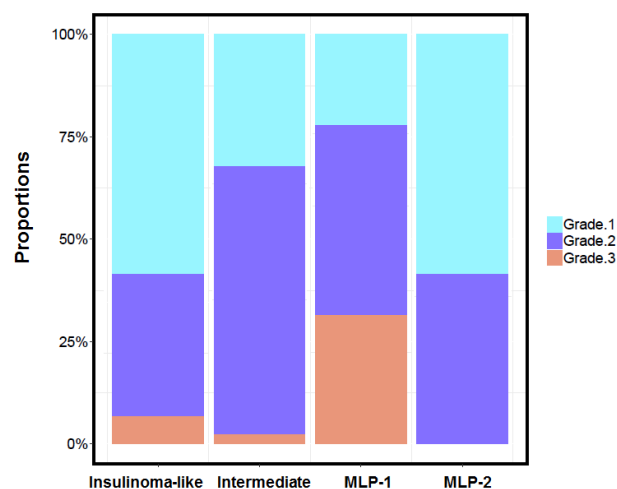


Figure 3.18 OS according to WHO 2010 Grade (n=97)



The distribution of grades across the PanNETassigner subtypes was analysed. All 3 grades were present in the Insulinoma-like, Intermediate and MLP-1 subtypes. The MLP-1 subtype was enriched for grade 3 patients compared to the other subtypes (29% of MLP-1 patients were grade 3). However, the majority of MLP-1 patients were grade 2 (47%) and grade 1 patients were also present (24%) (Figure 3.19).

Figure 3.19 WHO 2010 Grade according to PanNETassigner Subtype



We wanted to establish whether the PanNETassigner molecular subtypes could be used to stratify patients within grades. We therefore analysed OS according to PanNETassigner subtype for grade 1 and 2 patients separately (Figures 3.20 and 3.21). A major limitation here is that this division results in very small numbers of patients available for each analysis, making any statistical analysis challenging. Grade 3 was not similarly assessed as only 8 patients had grade 3 disease in this cohort. We also assessed survival for grade 1 and 2 patients combined, excluding the patients with more aggressive grade 3 disease, to establish if the same patterns were seen when the enrichment of grade 3 patients in the MLP-1 subtype was removed (Figure 3.22).

Within the 42 grade 1 patients, the 4 subtyped as MLP-1 were all censored as they were lost to follow up. The Insulinoma-like patients had a better prognosis than the Intermediate or MLP-2 patients, but this result did not reach statistical significance.

Within the 47 grade 2 patients, the 8 subtyped as MLP-1 and 6 as MLP-2 had a poorer prognosis but this was not statistically significant, possibly due to the small numbers available for analysis. Again the Insulinoma-like patients had the best prognosis.

When grade 3 patients were excluded and grade 1 and 2 patients were analysed together, a similar pattern was seen, with the MLP-1 patients having the poorest prognosis and insulinoma-like patients the best. However, this was not statistically significant.

Figure 3.20 OS according to PanNETassigner subtype for Grade 1 Patients

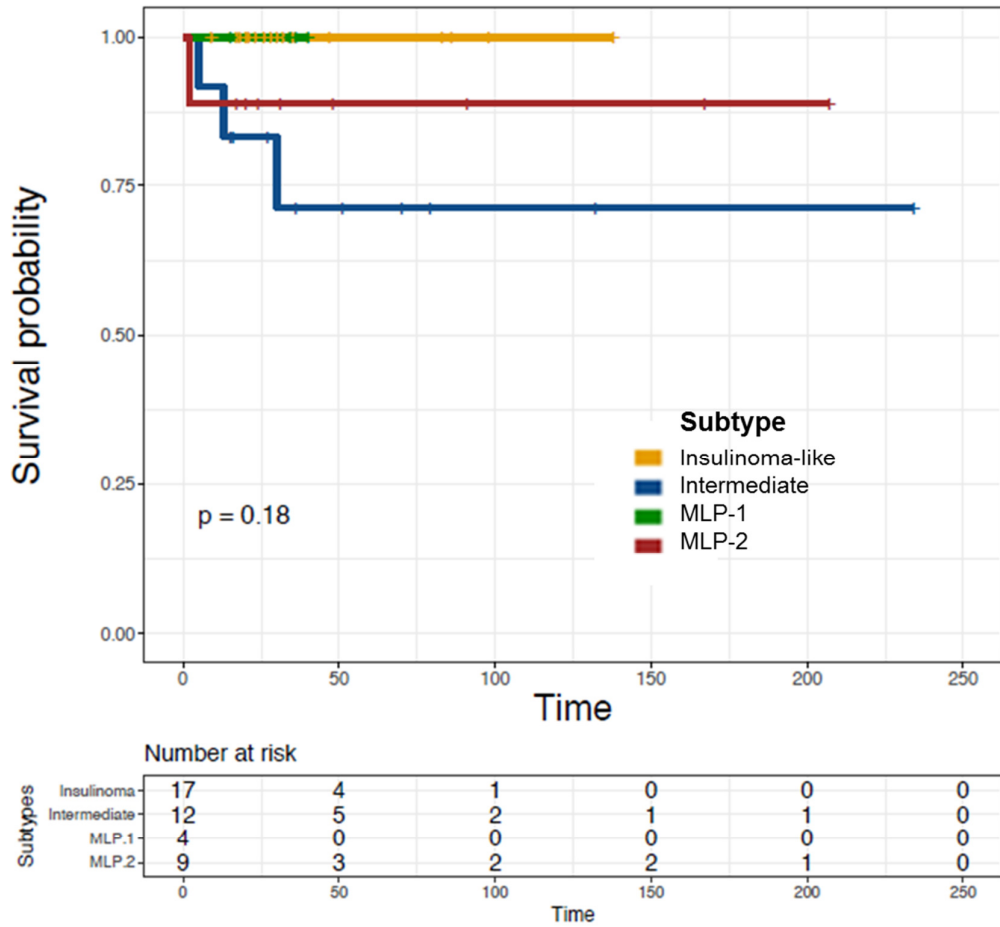


Figure 3.21 OS according to PanNETassigner subtype for Grade 2 patients

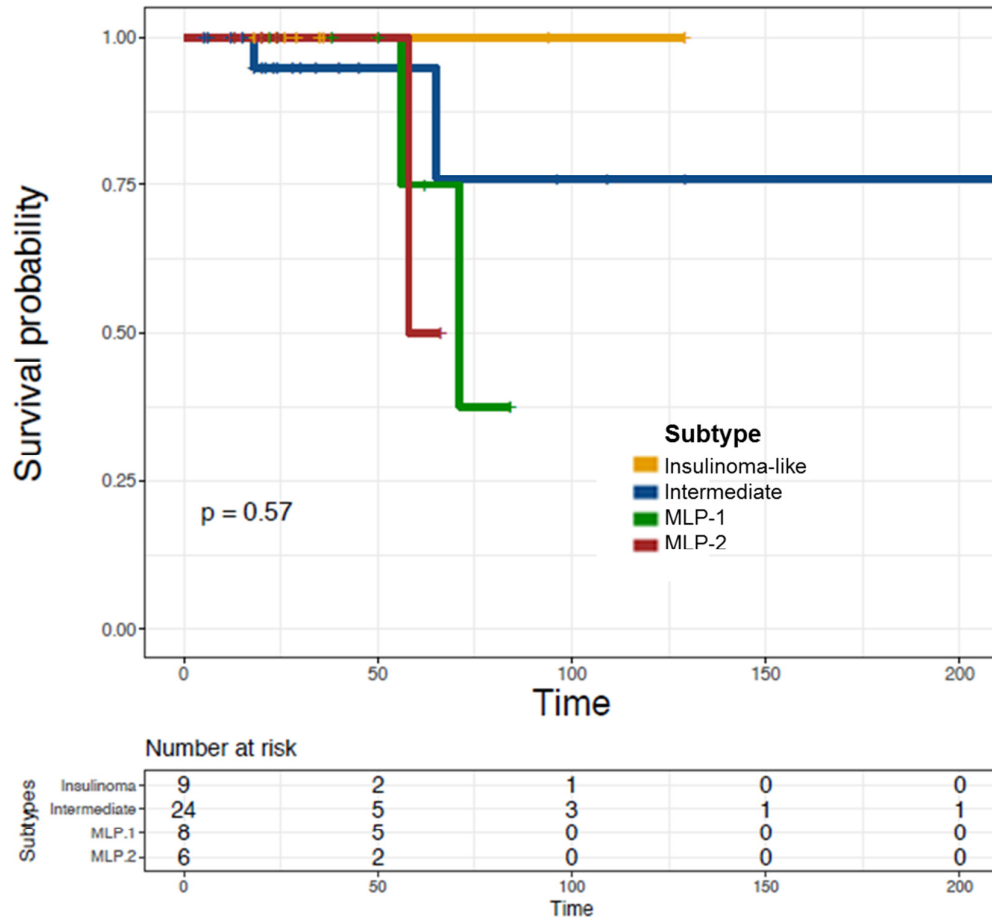
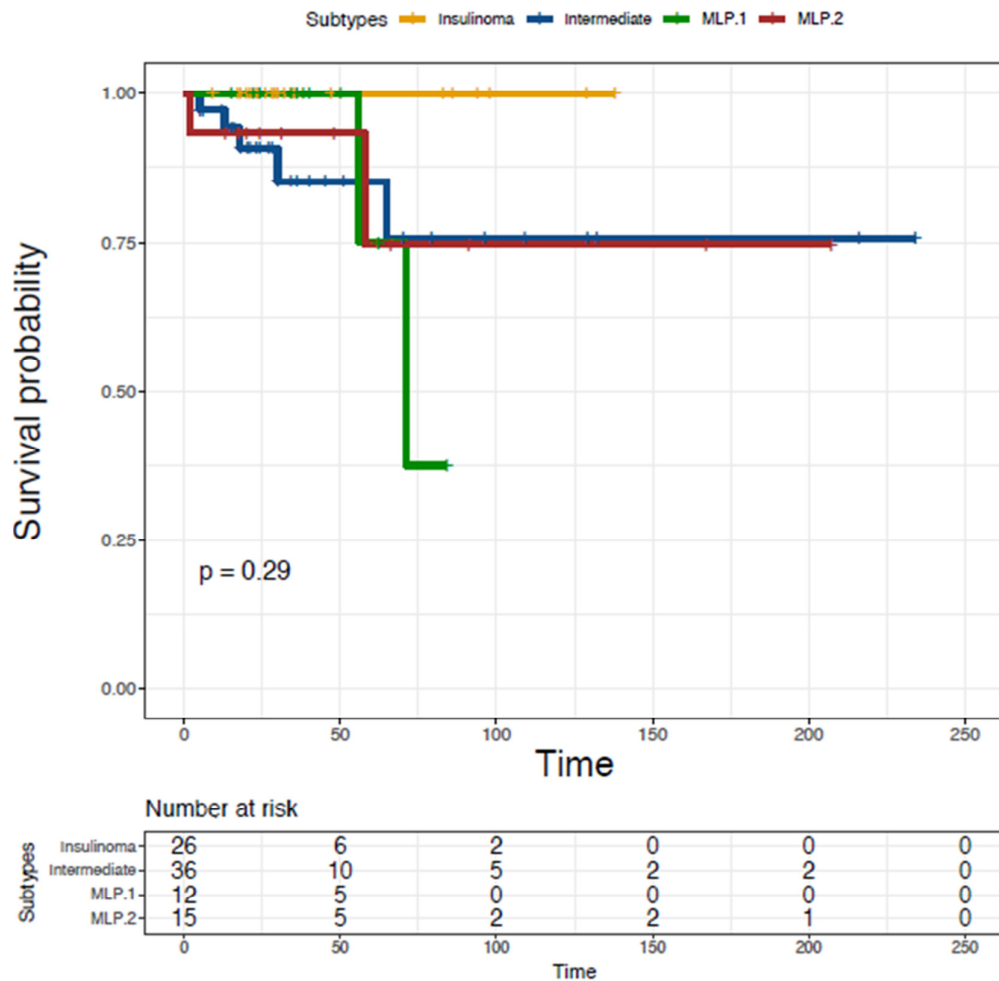


Figure 3.22 OS according to PanNETassigner subtype for Grade 1 and 2 patients

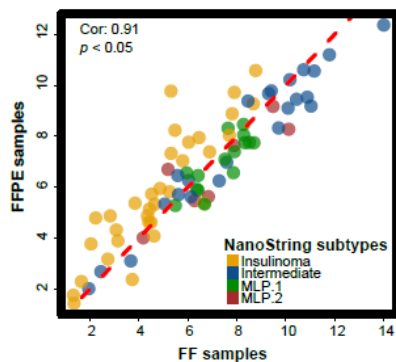


3.3.7 Validation of the 78 Gene Nano-PanNET Assay using FFPE samples from the Verona Cohort (n=44)

Having demonstrated that the PanNETassigner subtypes had prognostic significance, we sought to validate the refined 78 gene Nano-PanNET assay using additional patient samples. The assay was therefore tested in 44 FFPE PanNEN patient samples from the Verona cohort. All samples passed the NSolver QC steps. The same QC steps involving removal of genes with $\geq 20\%$ zero expression, assessing and correcting batch effect were completed as previously. Subtypes were successfully assigned using Pearson correlation to the previously derived 78 gene panel centroids.

37/44 of the FFPE samples overlapped with the 144 fresh frozen samples used to test the 228 gene assay. The correlation between gene expression results obtained using the fresh frozen versus the FFPE samples was 91% (Figure 3.22).

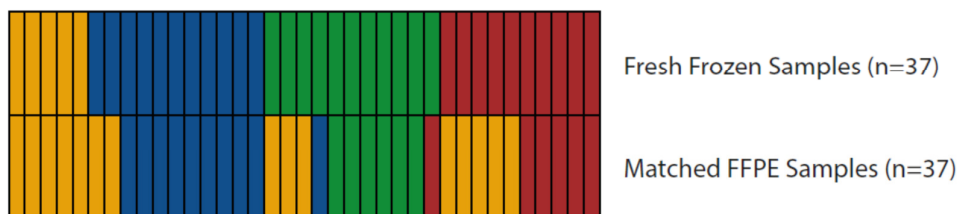
Figure 3.23 Correlation between the expression of the refined panel of 78 genes in fresh frozen and FFPE patient samples (n=37)



A scatter plot showing the median expression of the 78 genes, assessed by the NanoString platform, in fresh frozen and FFPE tissues (n=37). Colours indicate each gene's association with the PanNETassigner subtypes, according to the centroids derived for each gene.

The concordance of subtypes assigned in the FFPE samples with those assigned in the fresh frozen samples was also assessed, measured at 68% (Figure 3.23). The Insulinoma-like subtype was assigned more frequently in the FFPE than in the fresh frozen samples.

Figure 3.24 Concordance of PanNETassigner subtypes assigned using FFPE and Fresh Frozen Tissue by NanoString assay (n=37)



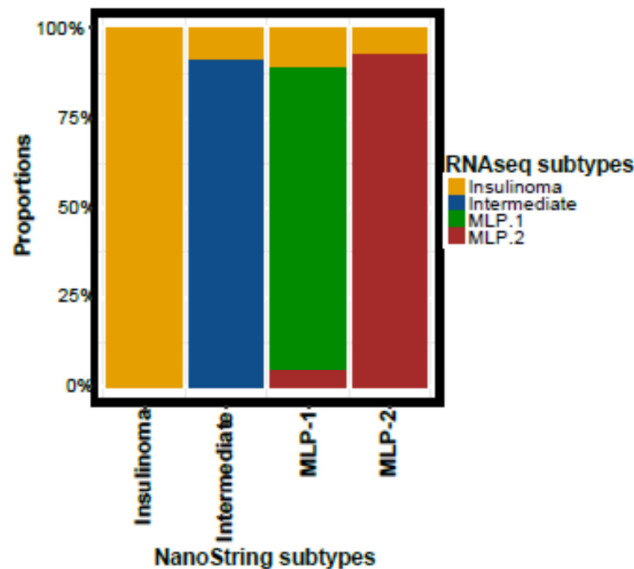
This figure demonstrates the concordance between subtypes assigned using fresh frozen versus FFPE tissue (25/37 subtypes matched, concordance 68%).

3.3.8 Validation of 78 gene panel centroids with RNAseq data (n=98)

The centroids for the refined 78 gene panel were assessed using RNAseq data from 98 fresh frozen samples from the Verona cohort. Here subtypes were successfully allocated based on gene expression data from RNAseq and using Pearson correlation to the 78 gene panel centroids.

The 98 RNAseq fresh frozen samples overlapped with 98/127 fresh frozen Verona samples originally subtyped (section 3.4.3) Concordance between the subtypes assigned using gene expression data from the two platforms, RNAseq and NanoString, was assessed (Figure 3.24). This analysis demonstrated a 93% concordance with 91/98 samples assigned the same subtypes using data from the 2 platforms. Here the Insulinoma-like subtype appeared to be more frequently assigned in the RNAseq samples.

Figure 3.25 Concordance between subtypes assigned using 78 gene panel centroids with RNAseq data (fresh frozen) and using NanoString assay data (fresh frozen) (n=98)



3.3.9 Validation of 78 gene Nano-PanNET Assay using FFPE samples from the Royal Marsden Cohort as a real world example (n=27)

Quality and Quantity of RNA from RM Cohort (n=27)

Available tissue was collected for RM patients in the PanACeA study as described in methods and in Chapter 2. Tumour samples were obtained for 57 of the 77 patients in the RM cohort. Of these 57, 30 samples did not have sufficient tissue for further analysis (Figure 2.2).

Ultimately, 29 FFPE tissue samples were available for 27 patients (2 patients had tissue available from both a pancreatic primary and a site of metastasis). 10 of the 29 samples were from pancreatic resection specimens and 19 were from biopsies (Supplementary Table 3.3, Appendix 3.3). All 10 resection specimens had adequate RNA concentrations for further analysis. Only 4/19 of the biopsy specimens had adequate RNA concentrations for further analysis. The 4 biopsy specimens with adequate RNA concentrations were all from pancreatic biopsies. None of the 10 liver biopsy specimens provided sufficient RNA for further analysis.

For the 14 samples ultimately processed with the 78 Gene Nano-PanNET assay the median RNA concentration was 122ng/μL, range 5.76 to 480ng/μL.

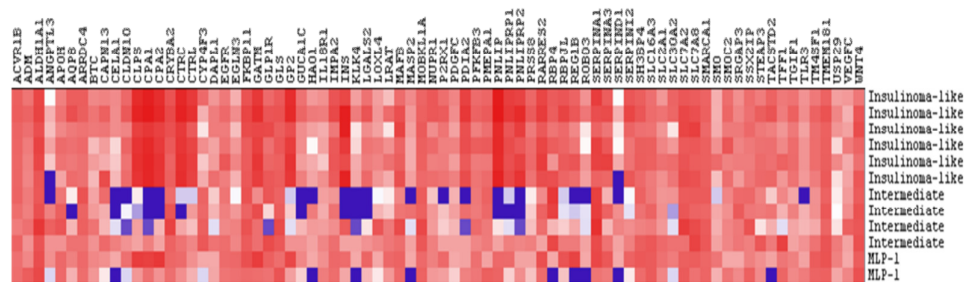
Refined 78 gene Nano-PanNET assay applied to RM cohort (n=14)

12/14 of the samples passed the QC steps as previously described and were successfully subtyped (Figure 3.25, Supplementary Table 3.3). 2/14 samples failed the normalisation QC step, due to content normalisation flags. One of the samples was a biopsy sample from 2005, the second oldest sample obtained, with a very low initial RNA concentration (5.92ng/μl). The other 3 successful biopsy samples in the RM cohort were from 2011, 2013 and 2014. As low amounts of intact RNA and sample degradation over time can cause a content normalisation flag, this may have been why this sample failed. The other failed sample was a resection specimen from 2010. It is less clear why this more recent sample failed. Low amounts of intact RNA may have contributed again as this sample had

a low initial RNA concentration (140ng/μl) compared to the mean concentration of the resection specimens overall (237ng/μl). Other potential causes include pipetting errors and inaccurate quantification.

In the RM cohort 70ng RNA in 7μL was used in the NanoString assay experiments, versus the 100ng in 5 μL used in the Verona samples. For the other 12 RM samples, acceptable gene expression results were obtained using 70ng RNA in 7μL and this dilution was not thought to be the cause for the 2 samples' QC failures.

Figure 3.26 78 gene Nano-PanNET Assay Results for RM Cohort (n=12)



3.3.10 Inclusion of 2 Erroneous Samples and Additional Bioinformatics Assessments Completed

Having completed the above analyses of the 228 gene and 78 NanoString assays, during collection of additional clinical data it was noted that 2 of the samples had been sent from Verona in error. These 2 samples were not PanNET samples but one pancreatic ductal adenocarcinoma (PDAC) sample (1579) and one sample from a patient with pancreatitis (1041). These samples were not included in the original analysis of subtype concordance using the 228 gene assay and the overlapping Microarray cohort subtypes (n=19). They were also not included in the survival analyses as there was no clinical data available (n=97). However, they were used in developing the refined 78 gene Nano-PanNET assay.

To check that the inclusion of these samples had not adversely affected the misclassification error rate of the refined 78 gene panel we repeated all of the analyses with these 2 samples excluded. This resulted in a refined

panel of 81 genes, with 77/81 genes overlapping with the original refined 78 gene panel. The 81 gene signature had a misclassification error rate of 1%. When the 77 gene signature was applied to the training cohort of 125 samples (i.e. the 127 samples with the 2 incorrect samples removed) the misclassification error rate remained unchanged at 1%. We therefore concluded that it was acceptable to proceed with the 78 gene signature.

3.4 Discussion

In this chapter I have described the successful development of a novel Nano-PanNET assay with potential prognostic significance. The initial 228 gene assay was demonstrated to achieve good-quality, reproducible results in fresh frozen samples with a high level of concordance with subtyping results achieved using microarray data (95%, n=19).

Having confirmed that the PanNETassigner subtypes could be reliably assigned using the nCounter platform, the 228 gene assay was refined to a 78 gene Nano-PanNET assay and corresponding centroids were developed (n=127). These centroids, representing the average gene expression of each of the 78 genes across the 4 subtypes, were validated using RNAseq data from fresh frozen samples, again with high concordance (93%, n=98).

For the majority of patients diagnosed with PanNEN however, fresh frozen tissue samples are not available. Although FFPE samples may contain only small concentrations of, or highly degraded, RNA, they are the most frequently available samples both for diagnosis and biomarker assessment. The 78 gene assay was therefore tested in FFPE samples both from the Verona and RM cohorts (n=58). Working with FFPE samples versus fresh frozen samples provided a number of challenges.

For the RM cohort, there was a predictable rate of attrition during sample retrieval. 77 PanNEN patients were selected for inclusion in the PanNEN registry and attempts made to collect tissue for 65 cases, as 12 patients had declined inclusion in translational work. The majority of these 65 patients had initially been diagnosed at their district general hospital before being referred to RM for treatment. Whilst histopathology samples had been reviewed at RM, they were subsequently returned to their referring centres, as per Royal College of Pathologist guidelines. 57/65 tissue samples were ultimately obtained but this was a lengthy process, highlighting the difficulties of such retrospective sample collection.

Following central histopathology review, 27/57 cases contained sufficient tissue for further analysis. Then, following macrodissection and RNA extraction, 14/27 had adequate RNA for NanoString analysis.

Of note, whilst all of the 10 resection specimens obtained had adequate RNA, only 4/19 biopsy samples did so. In particular not 1 of the 10 liver biopsies had sufficient concentrations of RNA for further analysis. This is an important observation as the liver is often chosen as a biopsy site in patients with advanced disease. From this data, noting the small sample size and the need for further validation, it appears that routine diagnostic liver biopsies may not yield sufficient RNA for additional translational work, , in PanNEN patients, as there is not sufficient tissue remaining following diagnostic tests.

In the Verona cohort, all of the samples were from resections and were carefully stored in the ARC-NET biobank. The FFPE samples were therefore both readily obtainable and were from larger resection specimens. All of the 44 FFPE samples from Verona had adequate RNA for further analysis. In addition to this being due to the nature of resection versus biopsy specimens, the samples in Verona had been carefully prepared and stored as part of a biobank, which was not the case for the diagnostic biopsies at various district general hospitals for the RM samples. As discussed in Chapter 2, such challenges highlight the need for prospective biobanks with robust protocols for obtaining and storing tissue, to enable high quality translational work.

Once available FFPE samples were obtained and adequate RNA extracted, the 78 gene assay was successfully performed, assigning subtypes in 56/58 FFPE samples (44 Verona and 14 RM FFPE samples). The ability to obtain robust results with low RNA concentrations on the nCounter platform is consistent with published data and is important when considering using the 78 gene assay in a real world setting¹²⁵.

The concordance between subtypes assigned using NanoString gene expression data in the Verona FFPE and fresh frozen samples was then assessed (n=37). Here concordance was 68%, although the correlation of

gene expression between FFPE and fresh frozen samples was higher at 91%. The subtype concordance between fresh frozen and FFPE samples is lower than the cross-platform concordance for fresh frozen samples reported with RNAseq and NanoString data, at 93% (n=98). The reason for the lower concordance between subtypes assigned in FFPE tissue and fresh frozen tissue is as yet uncertain. The challenges of obtaining good quality gene expression results with archived FFPE tissue are well documented, although a number of studies have demonstrated the advantages of NanoString in this setting^{126,147,148}. Further analyses investigating whether differences in sample cellularity may have contributed to this are on-going. The impact of storage time on the samples is also being investigated. RNA was extracted soon after resection for the fresh frozen samples but for the FFPE samples the extraction took place many years later. It is possible that RNA degradation over this time may have impacted upon these results¹⁴⁸.

The Verona FFPE samples were noted to be more frequently assigned the Insulinoma-like subtype than the fresh frozen samples when NanoString data was used (10 more were subtyped as Insulinoma-like in the FFPE than the fresh frozen samples, over 37 cases). The fresh frozen RNAseq samples were also more frequently assigned the Insulinoma-like subtype than the fresh frozen NanoString samples, although the level of discordance was lower within the fresh frozen samples (6 more were subtyped as Insulinoma-like in the RNAseq than the NanoString samples over 98 cases). The reason for this is also currently being investigated.

It is possible that genes relating to various normal pancreatic functions with high levels of expression in the Insulinoma-like centroids, such as *CLPS* and *CTRL*, may have been expressed in any associated normal pancreatic tissue present in the samples. The Verona FFPE samples were not macrodissected and as such small amounts of normal pancreas may potentially have been included in the samples and impacted subtyping. However, the RNAseq fresh frozen samples were prepared in the same way and at the same time as the NanoString fresh frozen samples so the slight increase in assignation of the Insulinoma-like subtype in the RNAseq

samples cannot be explained in this way. Our collaborators in Verona are currently looking back at the 6 samples from the RNAseq cohort, that were assigned Insulinoma-like using RNAseq data but not using NanoString data, to investigate this further.

If the 78 gene Nano-PanNET assay were to be taken forward and developed for use in clinic, the challenges of using FFPE samples in a real world setting would have to be carefully considered, both from the point of view of obtaining adequate RNA from biopsy samples and from ensuring that the Insulinoma-like subtype is not over assigned. In addition to the PAM50-based Prosigna Breast Cancer Prognostic Gene Signature Assay, our lab has recently successfully developed a NanoString assay to classify colorectal cancers (CRC), the CRCAssigner, which can also be used effectively in FFPE samples, demonstrating that this approach is achievable^{126,149}.

The 78 gene assay now requires further validation and optimisation, using additional FFPE and fresh frozen samples, to confirm whether macrodissection is required and the minimum RNA concentrations which could be used to provide robust results for PanNEN samples. I note that for the PAM50-based Prosigna Breast Cancer Prognostic Gene Signature NanoString Assay, macrodissection has been noted to be a key step to maximise diagnostic accuracy and the recommended RNA input is between 125 and 500ng RNA, although at validation reasonable results were achieved using lower inputs of 62.5ng¹⁵⁰.

In this project, all of the samples, whether in the Verona or RM cohort, are from baseline resections or biopsies. Using these samples we were unable to compare molecular subtypes between primary and metastatic tissues within the same patient or consider subtype evolution over time or following treatment. Ki-67 variability between primary and metastatic disease, as well as grade progression, have been reported in PanNET patients^{151,152,153,154}. Further, within a single PanNET patient, variable genomic profiles were noted in high versus low grade histological areas, with a progressive accumulation of genetic changes seen in the high grade regions¹⁵⁵. It is

therefore not unreasonable to consider that the PanNETassigner subtypes may also vary between primary and metastatic settings and over time, but this requires further study.

Considering such potential intra-patient and even intra-tumoural heterogeneity, the best approach to assigning a subtype or indeed subtypes for an individual patient will also have to be considered. It is unlikely to be acceptable for a patient to undergo multiple biopsies to assess potential subtypes present in different sites of disease or over time. It may be that, in the future, gene expression analysis of circulating tumour cells (CTCs) from liquid biopsies becomes an option to assess PanNETassigner subtypes and indeed such techniques are already being developed^{156,157,158,103}.

If these technical issues can be overcome, from the survival analyses presented here the PanNETassigner subtypes may potentially be used to provide additional prognostic information. In the survival analyses performed on 97 patients from the Verona cohort, the MLP-1 subtype was found to have a reduced median OS of 71 months ($p < 0.05$). Median OS was not reached for the other subtypes, with the Insulinoma-like subtype having the best predicted 5 year survival rate. Due to the low number of events it was not possible to carry out the planned multivariate analyses and attempts to stratify grade 1 and grade 2 patients by PanNETassigner subtype did not reach statistical significance, possibly due to the very small numbers of events which occurred and patients in each group.

As noted in Chapter 2, additional samples are now being made available for the PanNEN registry, from a Kings College cohort, and prospective PanNEN tissue samples are being collected in the RM sponsored PaC-MAN study. To obtain further additional samples, I, with the support of Anguraj Sadanandam, wrote a translational research proposal for the international SEQTOR trial of sequential everolimus or streptozocin/5FU (STZ/5FU) chemotherapy (Appendix 3.4). This proposal has now passed the appropriate regulatory steps and has been incorporated into substantial amendment 4 for the SEQTOR study. All of these additional FFPE and

fresh frozen samples will be used to further validate and optimise the 78 gene assay and to test the prognostic significance of the subtypes assigned in a larger cohort, with more events. If possible the predictive significance of the subtypes will be assessed with regards to treatment in the larger cohort.

The MLP-1 subtype having a poor prognosis is consistent with our labs' previous observations that the MLP tumours were enriched for metastases⁵¹. The MLP subtypes (MLP-1 and MLP-2) share a number of biological features which may contribute to this poor prognosis.

The first feature involves carbon metabolism, with significant differences previously described in the MLP versus the Insulinoma-like subtypes. Insulinoma-like tumours, which had a good prognosis in our data, were enriched for genes associated with the regulation of insulin and transporting glucose, as seen in mature β cells of the pancreas. MLP tumours, on the other hand, demonstrated increased expression of hexokinase (*HK1*) and lactate transporter (*MCT1/SLC2A2*) genes. These genes code for proteins which play important roles in glycolysis, with *HK1* driving high glycolytic activity and *MCT1* ensuring efflux of the lactic acid produced. The increased expression of such proteins associated with high levels of glycolytic activity has been associated with poorly differentiated and larger tumours, positive lymph node metastases, vascular invasion, advanced tumour stage and reduced survival across multiple solid tumours^{159,160,161}.

The ability to metabolise glucose anaerobically through glycolysis is an important feature for MLP tumours as they have been reported to be less vascularised than other subtypes and enriched for genes associated with hypoxia and hypoxia-inducible factor (HIF) signalling^{51,29}. Hypoxia and HIF signalling have in turn been linked to cancer stem cell renewal, immune suppression and the promotion of epithelial to mesenchymal transition (EMT) resulting in the development of metastases^{162,163,164,165}.

EMT provides cancer cells with an enhanced ability to metastasize, through the loosening of cell-cell adherences and through enriched invasive and migratory behaviours. MLP tumours were also previously noted to be

enriched for genes associated with EMT such as *Vim*⁵¹. Tumours which have undergone EMT are thought to be more aggressive, have increased stem-like features and are associated with increased inflammation, all of which again fit with the MLP-1 phenotype¹⁶⁶.

The MLP-1 tumours were enriched for patients with grade 3 disease compared to the other subtypes (29%) and such high grade disease is associated with reduced survival^{41,112}. Indeed, the inclusion of these NEC patients is a limitation of the study, as biologically such tumours are a distinct group compared to their well differentiated counterparts²⁷. Yet 71% MLP-1 patients had grade 1/2 disease and, within the grade 2 patients alone, a trend towards reduced survival for the MLP patients versus the other subtypes remained, although this was not statistically significant and requires validation. In the analyses planned using the aforementioned additional samples, the NEC and NET patients will be assessed separately to investigate whether the MLP-1 subtype maintains its poor prognosis, without the enrichment for grade 3 patients.

In the survival analyses, the Insulinoma-like subtype had the best prognosis. As discussed above, the Insulinoma-like subtype has been noted to be enriched for genes associated with mature β cells and appears to have a different cellular origin to the MLP subtypes⁵¹. 29% of the Insulinoma-like tumours assessed within the survival analyses were insulinomas, which are known to be less likely to metastasize and have a prolonged survival versus other PanNENs^{167,168}. However, 71% Insulinoma-like patients did not have insulinomas and 39% had grade 2 or 3 disease, highlighting that the PanNETassigner subtype may be able to provide supplementary information, additional to the clinical characteristics currently used, to inform prognostication

Following the work outlined in this chapter, further study is required to establish if the PanNETassigner subtypes remain prognostic in a larger cohort and on multivariate analyses, and this work is underway. Additional mechanistic studies in animal and cell line models, to confirm potential causes for these survival differences, are also planned. As discussed

above, the 78 gene Nano-PanNET assay developed here similarly requires further analytical and clinical validation. If these investigations confirm the prognostic significance and clinical utility of the PanNETassigner subtypes and assay, the 78 gene assay developed here could be deployed to analyse patient samples in trials or in clinic.

In the future, a model combining PanNETassigner subtype with stage and grade may be developed and would support a more disease biology based, personalised approach to treatment for PanNEN patients.

4 The Immune Landscape of PanNENs

Abstract

Objective

To date, little is known about the immune microenvironment in PanNENs. The aim of this chapter is to describe immune related gene expression in this disease and to consider possible causes for differential expression and the potential therapeutic opportunities this may afford.

Design

This study involved the analysis of immune related gene and protein expression from 320 PanNEN patient tumour samples (FFPE and fresh frozen) in this rare tumour type. Multiple platforms and various bioinformatics techniques were used including microarray, RNAseq, NanoString, multiplex IHC, Significance Analysis of Microarrays (SAM), Gene Set Enrichment Analysis (GSEA) and single sample Gene Set Enrichment Analysis (ssGSEA) and Cell type Identification By Estimating Relative Subsets Of known RNA Transcripts (CIBERSORT). Three main cohorts of patients were included, a training cohort (n=72) and two validation cohorts (n=146).

Results

This study demonstrated the differential expression of immune related genes, not by grade or other clinical parameters, but according to our previously described PanNETassigner molecular subtypes. The MLP-1 subtype was found to have an immune high phenotype, with the highest expression of and diversity of immune related gene expression. This phenotype was associated with larger hypoxic tumours, necroptosis and activity within the Damage Associated Molecular Pattern (DAMP) pathway in the MLP-1 samples.

Conclusion

This study provides comprehensive and novel phenotypic data regarding the immune microenvironment in PanNENs, identifying a subtype of patients with an immune high phenotype and a putative pathway to explain this enrichment with therapeutic potential.

4.1 Background and Rationale

Despite our improved understanding of the molecular nature of PanNENs, novel therapeutic approaches for patients remain elusive. One obvious area for exploration is immunotherapy and multiple trials of immune checkpoint blockade are underway in various NENs (NCT02923934/NCT03043664/NCT03095274). Interim results from a small number of studies suggest that a proportion of PanNEN patients may benefit from such treatments. The KEYNOTE 028 study of Pembrolizumab reported a clinical benefit in PD-L1 positive PanNEN patients (response rate 6%) (NCT02054806)⁵⁶ and anti-tumour activity was observed in PD-L1 unselected PanNEN patients with anti-PD-1 drugs JS001 (response rate 29%) (NCT03167853)¹⁶⁹ and Spartalizumab (response rate 3%) (NCT02955069)¹⁷⁰ (Table 4.1).

Notwithstanding these trials, however, little is known about the immune landscape of PanNENs. The few studies considering this subject have been small and retrospective in nature, considering just one or two biomarkers, and as yet no clear subgroup of potentially immunotherapy sensitive PanNEN patients has been defined (Table 4.2).

Comprehensive, detailed profiling and analysis is required to enable us to optimise and personalise patient selection approaches for immunotherapy, to ensure that PanNEN patients are given the best opportunity to respond to this treatment and to inform possible rational combination studies in the future.

To this end, this chapter focuses on the analysis of immune related gene expression in PanNEN patient tumour samples, across our previously described PanNETassigner molecular subtypes.

Table 4.1 Selected Immunotherapy Trials in PanNENs registered on ClinicalTrials.gov

NCT Number (Phase)	Population (n)	Treatment	Selection Criteria	Primary Endpoint	Results
NCT 02834013 (Phase II)	Rare Tumours (n=707)	Nivolumab and Ipilimumab	No specific PanNET criteria	Overall Response Rate	Ongoing
NCT 03147404 (Phase II)	GEP NEC (n=30)	Avelumab	Grade 3 NEC	Best Response	Ongoing
NCT 02923934 (Phase II)	Rare Tumours (n=120)	Nivolumab and Ipilimumab	No specific PanNET criteria	Clinical Benefit Rate	Ongoing
NCT 03095274 (Phase II)	GEP and Lung NET (n=126)	Durvalumab and Tremelimumab	Grade 1/2 PanNET	Clinical Benefit Rate	Ongoing
NCT 03043664 (Phase Ib/II)	GEP NET (n=26)	Pembrolizumab and Lanreotide Depot	Grade 1/2 NET	Overall Response Rate	Ongoing
NCT 03591731 (Phase II)	Advanced, Refractory Pulmonary or GEP Poorly Differentiated (NEC) (n=180)	Nivolumab Monotherapy or Nivolumab Plus Ipilimumab	Grade 3 NEC	Objective Response Rate	Ongoing
NCT 02939651 (Phase II)	Metastatic high-grade NET (n=21)	Pembrolizumab	Ki 67 > 20%	Objective Response Rate	Ongoing
NCT 03190213 (Phase II)	Metastatic/unresectable NEC of non-pulmonary origin (n=40)	Pembrolizumab	Ki-67 >20% and/or > 20 mitoses/10 hpf	Overall Response Rate	Ongoing
NCT 02054806 (Phase I)	Advanced Solid Tumours (n=477, 16 PanNET)	Pembrolizumab	PD-L1 +ve (≥ 1% modified proportion score, IHC QualTek)	Best Overall Response	Ongoing, PanNET Interim results ¹⁷¹ : ORR 6%, SD 88%
NCT 03167853 (Phase Ib)	Advanced NET (n=40, interim results n=23, 7 PanNETs)	JS001	Non-functional Ki 67 >10% Well/poorly differentiated	Overall Response Rate	Ongoing, Interim results ¹⁶⁹ : ORR 28.6%, DCR 47.6%
NCT 02955069 (Phase II)	Advanced or metastatic thoracic/GEP NET/NEC (n= 116, 33 PanNET)	Spartalizumab	Progressive Well or poorly differentiated Non-functional PanNET	Overall Response Rate	PanNET: PR 3%, SD 54.5%, DCR 57.6% GEP NEC:DCR 19% ¹⁷⁰

Table 4.2 Selected Studies of Potential Immune Biomarkers in GEP-NENs

Immune Biomarker	Results	N	Ref
PD-L1 expression and Grade in GEP NENs	PD-L1 expression associated with Grade. PD-L1 expressed in 29% poorly differentiated and 0% well differentiated GEP NENs	59 (24 PanNEN)	172
	PD-L1 expression and intensity directly correlated (P<0.001) with Grade increase from 1 to 3	57 (10 PanNEN)	173
PD-L1 expression in Metastatic GEP-NET	PD-L1 expressed in 22% tumours, associated with Grade 3 disease, PFS and OS	32 (14 PanNET)	174
PD-1 and PD-L1 expression in Midgut NET	PD-L1 expressed in 69% tumours, associated with a cytotoxic lymph node like structure (LLS) formation	32	175
PD-1, PD-L1 and PD-L2 expression in small bowel NET	30% expressed PD-L1 in tumour cells/ within TILs, 0% expressed PD-L2	62	176
PD-L1 expression in small cell NEC (pulmonary and extrapulmonary)	PD-L1 expression was not present in tumour cells but was present in tumour infiltrating macrophages (18.5%) and correlated with TILs	94 (33 extra-pulmonary)	177
Neutrophil/Lymphocyte ratio (peripheral blood) in resectable PanNETs	Pre-operative NLR independent prognostic factor for LN metastasis and Relapse Free Survival	95	178
T Cell Infiltrate in G1-G3 GEP NENs	PD-L1 expression only seen in Stage IV disease and in patients with Ki-67 >20%	52	179
FOXP3 + Regulatory T Cell in PanNETs	FOXP3+ Regulatory T Cell expression associated with reduced OS	101	180
T Cell Infiltrate in resectable intermediate grade NETs	Robust T cell infiltrate associated with improved RFS after resection Increased Regulatory T Cells associated with reduced survival after liver metastasis resection	87 NETs 39 NETs with liver mets	181
Tumour Mutational Burden (TMB)	4.2% high TMB, mean TMB 5.8 mutations/MB	75	182
	Mean TMB 0.82 mutations/MB	98	29
Microsatellite Instability (MSI)	PanNET did not demonstrate MSI-H status	75	182
	33% of sporadic insulinomas MSI-High	55	183
	0% mismatch repair deficiency in unselected PanNET cases	35	184

4.2 Methods

4.2.1 PanNEN Patient Samples

Figure 4.1 details the PanNEN samples included in this chapter and the analyses completed.

Preliminary work in NanoString cohort (n=48)

Immune gene profiling using the NanoString PanCancer Immune Profiling assay was carried out on a cohort of PanNEN tumour samples from the PanNEN registry, established as described in Chapter 2 (PaNACeA study, REC reference 16/LO/0984, CCR 4476, IRAS project ID 194534).

Microarray Training cohort (n=72)

PanNEN microarray gene expression data from work previously conducted by our lab was used as a training cohort. The gene expression data was originally from Missiaglia and colleagues, Verona (GEO Omnibus ID GSE73338; ref 34), and had been used by our lab previously in the original development of the PanNETassigner molecular subtypes^{51,80}. Gene expression in this cohort was assessed using an 18.5 K Human oligo-microarray from the Ohio State University Cancer Centre and analysed using R and Bioconductor as described^{132,133,134}. PanNETassigner molecular subtypes had already been assigned as previously described⁵¹.

Validation cohorts

Berlin cohort (n=26)

PanNEN microarray gene expression data from work previously conducted by our lab was used as a validation cohort. The gene expression data was from Wiedenmann and colleagues, Berlin, and had been used by our lab previously in the original development of the PanNETassigner molecular subtypes⁵¹. Gene expression was assessed using Affymetrix GeneChip Human array and analysed using R and Bioconductor with PanNETassigner subtypes already assigned as previously described⁵¹.

RNAseq cohort (n=120)

The second validation cohort consisted of samples from the Verona cohort in the PanNEN registry. All 48 of the NanoString cohort samples overlapped with this cohort and 10 samples overlapped between the NanoString, Microarray and RNAseq cohorts.

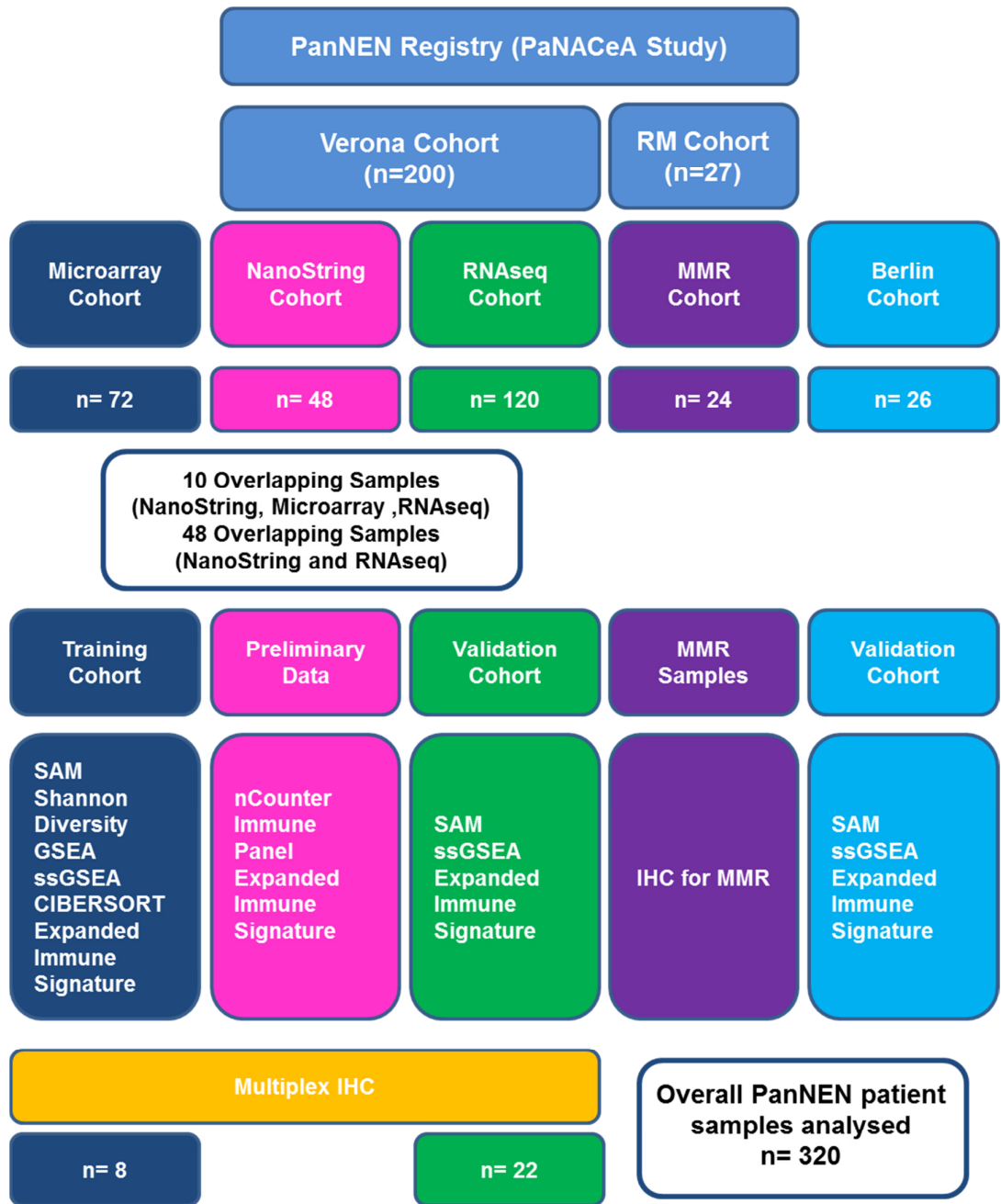
Mismatch Repair (MMR) cohort (n=24)

MMR was assessed in a cohort of PanNEN tumour samples from the RM cohort, again within the PanNEN registry.

Multiplex IHC cohort (n=30)

Multiplex IHC was conducted on a cohort including 8 FFPE samples from the Microarray cohort and an additional 22 FFPE samples from the RNAseq cohort.

Figure 4.1 Overview of PanNEN Samples and Analyses Conducted



4.2.2 Wet Lab Techniques

Standard nCounter Chemistry Process

The PanCancer Immune Profiling assay was ordered from NanoString Technologies. Hybridisation reactions were performed according to the nCounter® XT Assay Manual (Version 11, July 2016). The nCounter Prep Station, nCounter Digital Analyser and nSolver™ v3.0 analysis steps were carried out as previously described in Chapter 3.

RNA sequencing (RNAseq)

In the RNAseq cohort, gene expression was assessed by RNAseq as previously described¹³⁸. RNAseq was carried out by Eurofins Genomics (n=13) and at the Mayo Clinic Core Facility, Rochester (n=161). 120/174 samples sequenced were analysed here. RNA was diluted (200ng/20uL) and quantity and quality assessed using Qubit® Fluorometer and Agilent RNA 6000 Bioanalyzer. A column based DNA extraction method was used before RNAseq libraries were prepared using PolyA selection and RNA library prep using NEBNext-Ultra RNA Directional kit to produce Illumina compatible libraries. The libraries were sequenced using a HighSeq2500 with Paired-Ends 2x100. Targeted depth was 50 million reads/sample.

Multiplex IHC

Multiplex IHC was carried out in the Melcher Laboratory at the ICR, using the Opal™ 7 Solid Tumour Immunology Kit to detect 3 lymphocyte markers (CD8, CD20 and FOXP3), a macrophage marker (CD68), PanCK and DAPI in FFPE tissue slides. Slides were prepared according to the Opal™ 7 Solid Tumour Immunology manual (Version 3). The Vectra® fluorescent multispectral imaging system was used to analyse the 6 fluorophores *in situ*.

Mismatch Repair (MMR) analysis

Expression of MMR proteins was evaluated by IHC according to UK NEQAS guidelines. Tumours were dichotomised into MMR positive or negative. Tumours showing nuclear staining in the presence of satisfactory

internal controls, i.e. leucocytes, were interpreted as having preserved MMR expression. Tumours with an absence of nuclear staining in the presence of satisfactory internal controls were considered MMR negative.

PanNETassigner Subtype Allocation

To enable the assessment of immune related gene expression, multiplex IHC and MMR to be analysed according to PanNETassigner subtype, samples were subtyped, using PAM centroids and Pearson correlation, as outlined in Chapter 3, where possible.

4.2.3 Bioinformatics Techniques

nCounter Advanced Analysis

Analyses were carried out using the nCounter Advanced Analysis Plugin, including immune cell type profiling and immune pathway scoring, according to the nCounter Advanced Analysis Plugin for nSolver Software User Manual (MAN-10030-01 August 2016). Statistically significant differences between immune cell types profiled were assessed using Student TTest and corrected for multiple testing using Benjamini-Hochberg correction with a False Discovery Rate (FDR) of <0.05.

Significance Analysis of Microarrays (SAM)

Significance Analysis of Microarrays (SAM) was used to identify differentially expressed immune related genes from a panel of 600 immune related genes as previously described^{51,185,132,186,187}. The 600 genes had been selected to match the commercial nCounter® PanCancer Immune Profiling Panel of 730 genes used in the preliminary NanoString cohort. 600/730 genes were included in the microarray gene set. The statistical parameters applied to select the differentially expressed genes were false calls <1 and a FDR <0.05. This technique was used to identify differentially expressed immune genes according to various clinical parameters and PanNETassigner subtype in the Microarray cohort.

SAM was also used in the Berlin and RNAseq validation cohorts to analyse the differential expression of the 132 differentially expressed immune genes, selected using the SAM analysis of the Microarray cohort, again using a FDR of <0.05.

Shannon Entropy Plots of Diversity versus Specialisation

Using the immune related gene expression data from the Microarray cohort a Shannon Entropy analysis was conducted, measuring the diversity of gene expression and the specialization of gene expression, or average gene specificity, for each PanNETassigner subtype as previously described^{188,189}. Here the entropy of diversity and specificity were normalised between 0 and 1 as recommended in the R based bioconductor package BioQC.

Fantom5 CAGE Gene Set Analysis

To analyse the expression of genes associated with various cell types across the innate and adaptive immune systems, a set of transcriptomic cell type markers was chosen, based on the work of Rooney and colleagues according to analysis of Fantom5 CAGE data^{190,191}. Gene expression was analysed according to both PanNETassigner subtype and these immune cell type gene sets in the Microarray cohort. Of the 107 genes making up the transcriptomic cell type markers, 80 were represented in the microarray data. With a FDR of 0.2, 50/80 (62.5%) were statistically significantly differentially expressed across the PanNETassigner subtypes.

Molecular Signatures Database (MSigDB)

The Molecular Signatures Database (MSigDB) website (v6.3) was used to analyse overlaps between the 132 differentially expressed genes across the PanNETassigner subtypes and the Immunologic C7 MSigDB gene sets.

GSEA and ssGSEA

GSEA is a computational method that determines whether a particular gene set shows statistically significant differences in expression across a collection of samples within a particular dataset, according to their

phenotype¹⁹². A standalone GSEA package from GenePattern was used to analyse overlaps between differentially expressed genes across the PanNETassigner subtypes and the Immunologic C7 MSigDB gene sets.

ssGSEA calculates a separate enrichment score for each and every sample and gene set, independent of the sample's phenotype. This provides a gene set enrichment profile for every sample as previously described¹⁹³. ssGSEA was used on the Microarray cohort gene expression data to validate observations regarding immune related gene expression across the PanNETassigner subtypes. This analysis was repeated in the validation cohorts. Gene expression according to hypoxia (Hypoxia Hallmarks msigdb.gmt) and necroptosis (Necroptotic Process msigdb.gmt) gene sets was also assessed. This analysis was conducted using the ssGSEAProjection R package downloaded from GenePattern.

CIBERSORT

CIBERSORT, an analytical tool developed by Newman et al. using a gene expression based deconvolution algorithm, was used to provide an estimation of the abundances of immune cell types¹⁹⁴. CIBERSORT uses a signature matrix of 547 immune related genes to derive relative proportions of 22 types of immune cells. CIBERSORT was used to analyse the Microarray cohort gene expression data to validate our observations regarding immune related gene expression across the PanNETassigner subtypes. Of the 547 immune cell related genes, 441 were represented in the microarray data. CIBERSORT uses Monte Carlo sampling to derive a p-value for every sample. Cases with a FDR of <0.2 were considered.

RNAseq Analyses

The fastq results file was analysed for QC, mapping quality to the transcriptome (Q30) and genome and for intragenic RNA species. PCA was performed to identify outliers before further analysis. For downstream analyses, sequencing reads were mapped to transcripts using the RSEM (v1.2.29) software program¹⁹⁵, normalised, converted to counts per million, log₂ transformed and median centred. Samples were allocated

PanNETAssigner subtypes using a consensus clustering-based NMF R package as described in Chapter 3, based on a panel of genes selected from our initial Cancer Discovery paper⁵¹.

4.2.4 Overview of my role

Concept

Having worked with NanoString assays in the development of the PanNETAssigner assay, I proposed that our lab assess immune related gene expression in a cohort of PanNEN samples using the NanoString PanCancer Immune Profiling assay. The results of this initial preliminary experiment led to this chapter. I also suggested that multiplex IHC analyses be included in the project.

PanNET patient samples and Clinical Data

The tumour samples for the NanoString, RNAseq and MMR cohorts analysed here are from the PanNEN registry. My role in the set-up and management of this registry is described in detail in Chapter 2. The expression data for the Microarray and Berlin cohorts was already available from an earlier project within the Sadanandam lab.

Wet Lab Work

With the support of Chanthirika Ragulan (Higher Scientific Officer), I carried out the following lab work:

- All NanoString work, as previously described in Chapter 3
- Sourced quotes for RNAseq work and prepared samples for RNAseq (including appropriate RNA dilutions and quality control)
- Visited ICR core facility to observe and understand the RNAseq workflow
- Arranged for appropriate slides to be cut for mIHC work and assisted David Mansfield (Higher Scientific Officer) in performing the assays

- Arranged for appropriate slides to be cut and stained for MMR analysis, completed by Daniel Nava Rodrigues (Research Fellow in Histopathology)

Bioinformatics Work

With the support of Gift Nyamundanda, Kate Eason, Yatish Patil and Anguraj Sadanandam (Bioinformaticians), I carried out the following bioinformatics work:

- NSolver and nCounter Advanced analyses for NanoString data, including all quality control assessments, as previously described in Chapter 3 (validated by Chanthirika Ragulan)
- MSigDB work (validated by Yatish Patil)
- CIBERSORT work (validated by Yatish Patil and Anguraj Sadanandam)
- Liaised with the bioinformaticians to advise regarding selection of gene sets for analysis (e.g. expanded immune signature analysis/ genes of interest as targets for immunotherapy etc.)
- Interpreted the results for GSEA/ssGSEA/RNAseq analysis with bioinformaticians
- Analysed mIHC data to establish which proteins had significantly different expression levels across the PanNETassigner subtypes
- Generated figures in Adobe Illustrator and PowerPoint

The remainder of the bioinformatics work was carried out by Yatish Patil and validated by Anguraj Sadanandam.

Communication of Results

I have communicated data from this chapter as follows:

- I wrote the abstract, based on our preliminary NanoString data, selected for oral presentation at ESMO 2017 and presented at the conference. I was awarded an ESMO Travel Grant for the proffered oral paper.
- I have presented this project at the BRC GI Cancer PPI meeting as a mini-oral and poster. (Immune Landscape of Pancreatic Neuroendocrine Tumours, London 2018).
- I have written and prepared the manuscript (including figures/tables) for submission based on the remainder of the data, with support from the co-authors.

4.3 Results

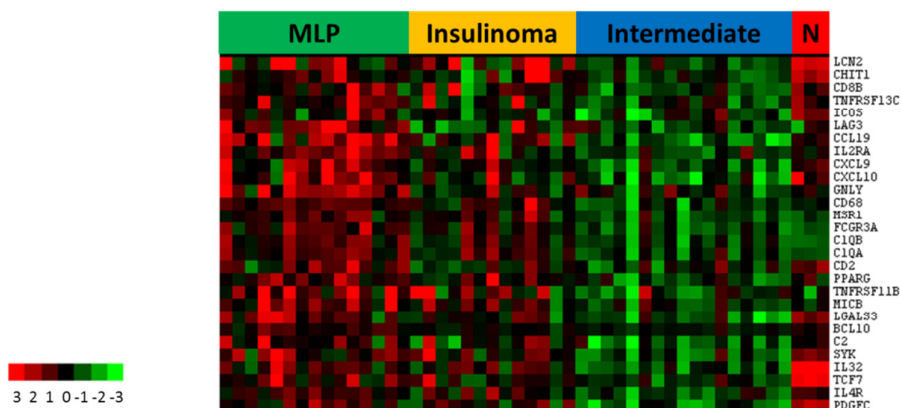
4.3.1 Preliminary Work: NanoString Immune Profiling Assay reveals differential immune gene expression across PanNETAssigner subtypes (n=48)

NanoString's Immune Profiling Assay was performed on 48 PanNEN samples (including 3 matched normal samples) and gene expression data was analysed according to PanNETAssigner subtype. This initial analysis combined MLP-1 and MLP-2 samples into 1 MLP subtype, due to the small number of samples. The analysis focused on the 2 non-functional subtypes, MLP and Intermediate, as it was felt that there was more of an unmet need for novel therapies in these patients (n=32).

308 immune-related genes were found to be differentially expressed between the MLP and Intermediate subtypes. 28/30 of the most differentially expressed genes had a higher expression in MLP vs. Intermediate (Figure 4.2).

Figure 4.2 Heatmap to demonstrate enrichment of the MLP Subtype for Immune Related Gene Expression

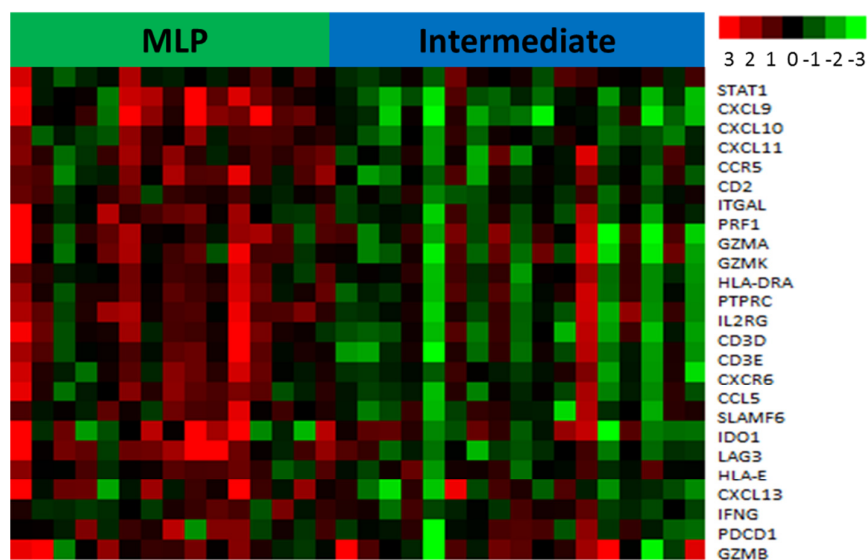
(n=48, 28/30 most differentially expressed genes shown)



Gene signatures thought to predict outcomes with checkpoint blockade, such as the expanded immune signature, were assessed and

demonstrated enrichment in the MLP vs. the Intermediate subtype (Figure 4.3). The expanded immune signature assessed here is based on the “preliminary expanded immune signature” of 28 genes defined by Ribas et al¹⁹⁶. Expression data for 25/28 genes was available in the NanoString panel.

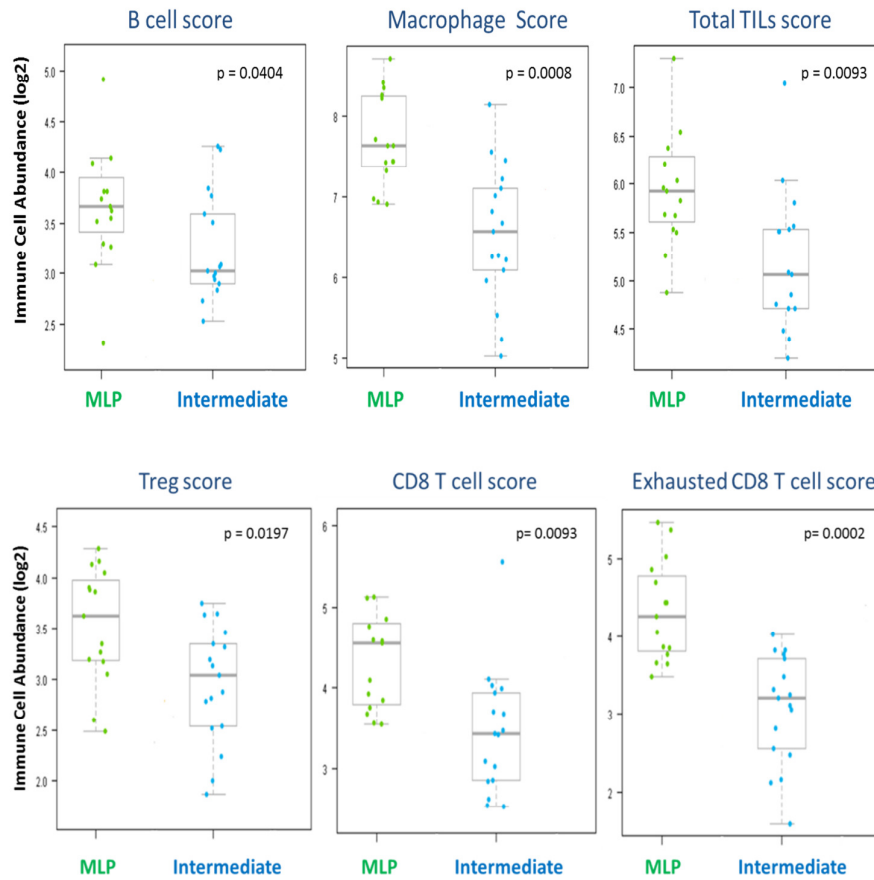
Figure 4.3 Heatmap to demonstrate the enrichment of the Preliminary Expanded Immune Signature in the MLP vs. the Intermediate Subtype (n=32)



4.3.2 Preliminary work: NanoString analyses reveal MLP subtype has a high Immune Cell Abundance and is enriched for multiple immune pathways

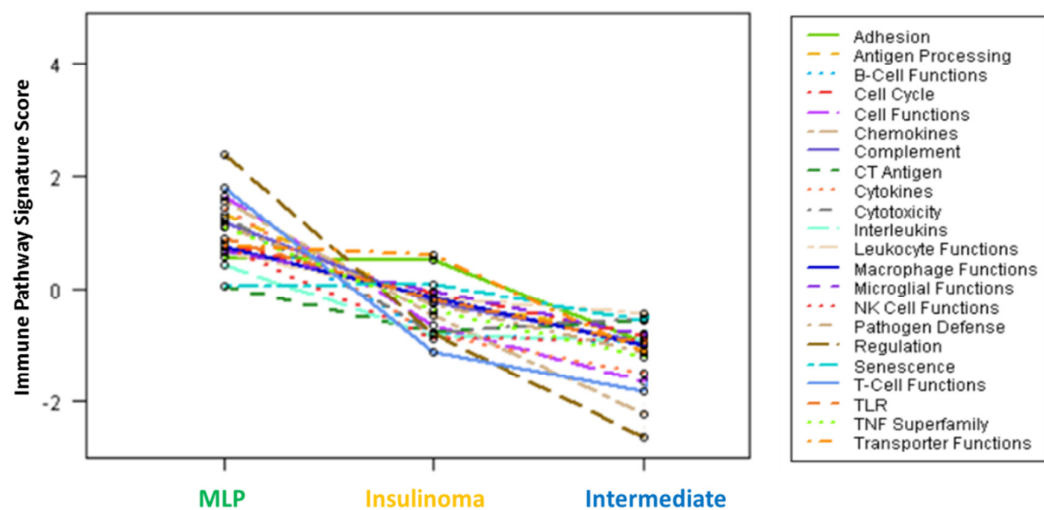
Immune cell abundance was assessed in the MLP and Intermediate subtypes using the NSolver analysis program as described in methods. Immune cell abundance was statistically significantly higher in the MLP vs. Intermediate samples across multiple cell types (Figure 4.4). These changes were found to translate into higher immune pathway scores, also assessed by NSolver and based on immune gene expression (Figure 4.5).

Figure 4.4 Box Plots to demonstrate enriched Immune Cell Abundance across multiple cell types in the MLP vs. Intermediate Subtype



**p* values calculated using Student TTest applied to MLP and Intermediate subtype data and corrected for multiple testing using Benjamini and Hochberg

Figure 4.5 NSolver Immune Pathway Scores increased in MLP subtype



These preliminary observations in the NanoString cohort led to the analyses described below being undertaken, to establish if other clinical parameters were linked to immune gene expression, to confirm whether the MLP subtype did indeed have an immune high phenotype, to establish possible causes for this and to consider potential therapeutic opportunities.

4.3.3 Immune related gene expression is not dependent upon grade of disease, liver metastases or genetic mutations

The expression of immune related genes was analysed according to clinical parameters of prognostic significance in PanNETs, specifically being grade of disease, the presence or absence of liver metastases and the presence or absence of key genetic mutations (specifically *MEN1*, *DAXX/ATRX* and *mTOR* pathway)^{28,29,46,197}. Associations with tumour grade were of particular interest as a number of on-going immunotherapy studies have restricted PanNET patient inclusion to grade 3 patients (NCT03591731, NCT02939651, NCT03190213).

To establish the distribution of immune related genes within these groups, data from the Microarray training cohort (n=72) was analysed using SAM and a panel of 600 immune related genes, as outlined in methods. The characteristics of this cohort are summarised in Table 4.3.

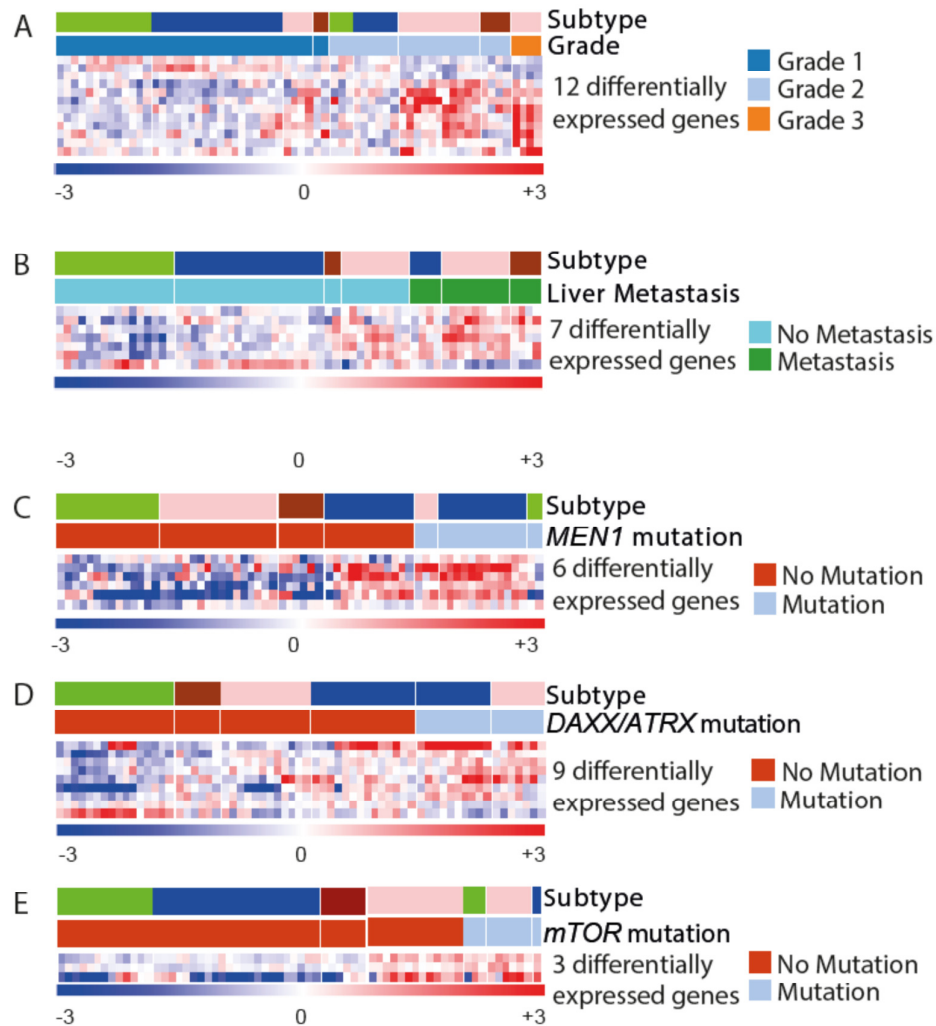
Table 4.3 Summary characteristics for Microarray Cohort

PanNET assigner subtypes	No. Samples (%)	Material used in expression profiling	Liver Metastases	WHO Grade
Insulinoma-like	16 (22%)	All primary tumours	0/16 (0%)	G1 13/16 (81%) G2 3/16 (19%)
Intermediate	25 (35%)	Primary 24/25 (96%) LN met 1/25 (4%)	5/25 (20%)	G1 18/24 (75%) G2 6/24 (25%)
MLP-1	20 (28%)	Primary 19/20 (95%) LN Met 1/20 (5%)	9/19 (47%)	G1 4/19 (21%) G2 11/19 (58%) G3 4/19 (21%)
MLP-2	11 (15%)	Primary 6/11 (55%) Met 5/11 (45%)	9/11 (82%)	G1 2/6 (33%) G2 4/6 (67%)
All Samples	72	65 (90%) Primary 7 (10%) Metastases	23/71 (32%)	G1 37/65 (57%) G2 24/65 (37%) G3 4/65 (6%)

To our surprise, only 12 genes (2% of 600 immune gene panel) were found to be differentially expressed according to grade of disease (Figure 4.6A). Even these 12 genes were not specific to a particular grade; a subset of grade 2 tumours sharing gene expression with grade 1 or 3 tumours. This suggests that, in itself, grade of disease is not a useful way to sub-divide patients when considering immune related gene expression.

When the data was assessed according to the presence or absence of liver metastases, 7 genes (1.2% of the 600 immune gene panel) were differentially expressed (Figure 4.6 B). 6 (1%) were differentially expressed according to *MEN1* mutations, 9 (1.5%) according to *DAXX/ATRX* mutations, and 3 (0.5%) according to *mTOR* pathway gene mutations (Figures 4.6 C, D and E). Therefore, as was the case with grade, liver metastases and genetic mutations do not provide a useful way to subgroup patients when considering immune related gene expression. This data suggests that our current methods of prognostication for PanNET patients do not provide a tool for differentiating patients according to immune related gene expression.

Figure 4.6 Immune Related Gene Expression According to Clinical Parameters of Importance and PanNETassigner Subtype



Subtypes (Top Bar)

- Insulinoma-Like
- Intermediate
- MLP-1
- MLP-2

SAM analysis of Microarray cohort (n=72) to determine the differential expression of immune related genes according to both clinical parameters and PanNETassigner subtypes, to establish which provided the dominant phenotype. In heatmaps A-E each column represents 1 of 72 patient samples and each row represents a differentially expressed gene. In the rainbow bar below the heatmap, red indicates elevated expression, blue decreased, and white no change. (Genes selected using SAM, FDR<0.05 and False Calls<1). Each sample's PanNETassigner subtype is also highlighted in top bar.

A Heat map of 12 differentially expressed immune related genes according to grade (1, 2 or 3). B Heat map of 7 differentially expressed immune related genes according to the presence or absence of liver metastases. C Heat map of 6 differentially expressed immune related genes according to MEN1 pathway mutations. D Heat map of 9 differentially expressed immune related genes according to DAXX/ATRX pathway mutations. E Heat map of 3 differentially expressed immune related genes according to mTOR pathway mutations.

4.3.4 Differential expression of immune related genes according to PanNETassigner subtype

Based on our preliminary NanoString work, we hypothesized that immune related gene expression may vary according to the PanNETassigner subtype. Indeed, the small numbers of genes differentially expressed according to grade, metastases or mutational status further segregated according to our previously published 4 PanNETassigner subtypes; Insulinoma-like, Intermediate, MLP-1 and MLP-2 (Figure 4.6 A-E).

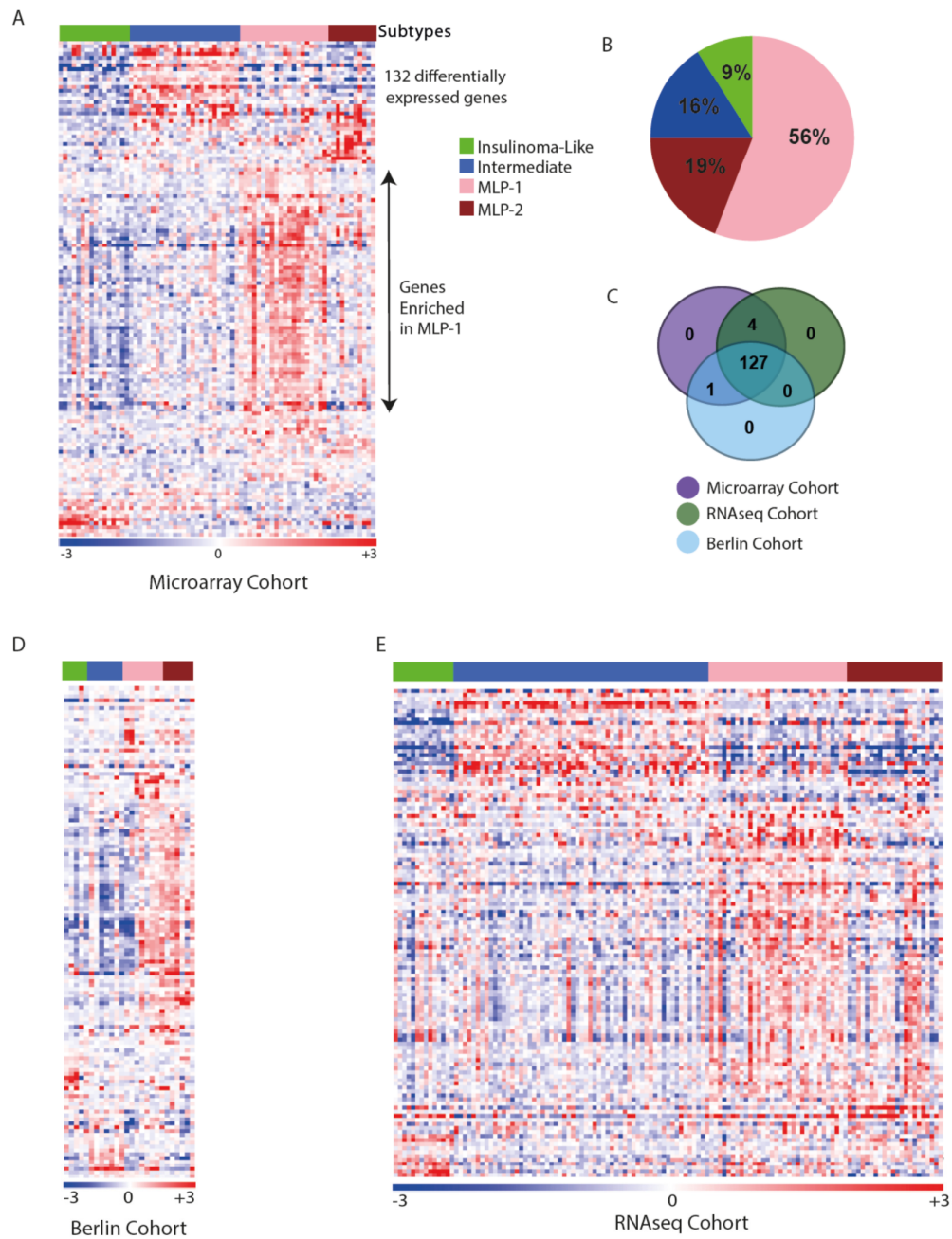
We next considered the PanNETassigner subtypes alone. Here 132 genes (22% of 600 immune related genes) were found to be statistically significantly differentially expressed between the 4 subtypes (Figure 4.7A and Supplementary Table 4.1). Of these 132 immune genes, MLP-1 was highly enriched for 74 (56%) genes, followed by MLP-2 with 25 (19%) and Intermediate 21 (16%) genes. Insulinoma-like samples appear to be immune-low, with only 12 (9%) enriched genes (Figure 4.7B).

These findings were validated using the Berlin (n=29) and RNAseq (n=120) validation cohorts. In the previous SAM analysis, 132 immune genes were differentially expressed in the Microarray cohort. SAM analyses were repeated to establish which of these 132 genes were differentially expressed according to PanNETassigner subtype in the validation cohorts. In the Berlin cohort, data for 129/132 of the genes was available and for 132/132 in the RNAseq cohort data. In the Berlin cohort 128/129 of the genes were differentially expressed across the PanNETassigner subtypes and 131/132 of the genes in the RNAseq cohort. Overall, 127/132 of the immune genes were common between all three cohorts demonstrating the

robustness of these genes in discriminating the immune landscape in PanNEN subtypes (Figure 4.7C). In both validation cohorts the MLP-1 subtype was enriched for immune related gene expression (Figures 4.7D and 4.7E).

Overall, these analyses show that the PanNETassigner MLP-1 subtype defines a group of patients enriched for immune related gene expression more successfully than clinical parameters of importance in PanNETs, including grade.

Figure 4.7 PanNETassigner Subtypes and Immune Related Gene Expression



A SAM analysis of Microarray cohort (n=72) determined 132 differentially expressed immune related genes according to PanNETassigner subtype alone. Each column represents one of 72 patient samples and each row represents a differentially expressed gene. In the rainbow bar below the heatmap red indicates elevated expression, blue decreased, and white no change. (FDR<0.05 and False Calls<1). B Pie chart demonstrating the proportions of differentially expressed immune related genes in each PanNETassigner subtype. 74 (56%) had the

highest level of expression in MLP-1, 25 (19%) in MLP-2, 21 (16%) in Intermediate and 12 (9%) in Insulinoma-like. C Vendiagram to demonstrate the overlap between the differentially expressed immune related genes according to PanNETassigner subtype in the Microarray cohort with the 2 validation cohorts (Berlin and RNAseq cohorts). Of the 132 differentially expressed immune related genes in the Microarray cohort, 127 were also differentially expressed in both validation cohorts (FDR 0.5). D HeatMap of differentially expressed immune related genes in the Berlin cohort which overlap with the 132 differentially expressed immune related genes in the Microarray cohort. E HeatMap of differentially expressed immune related genes in the RNAseq cohort which overlap with the 132 differentially expressed immune related genes in the Microarray cohort. Heatmap details as before.

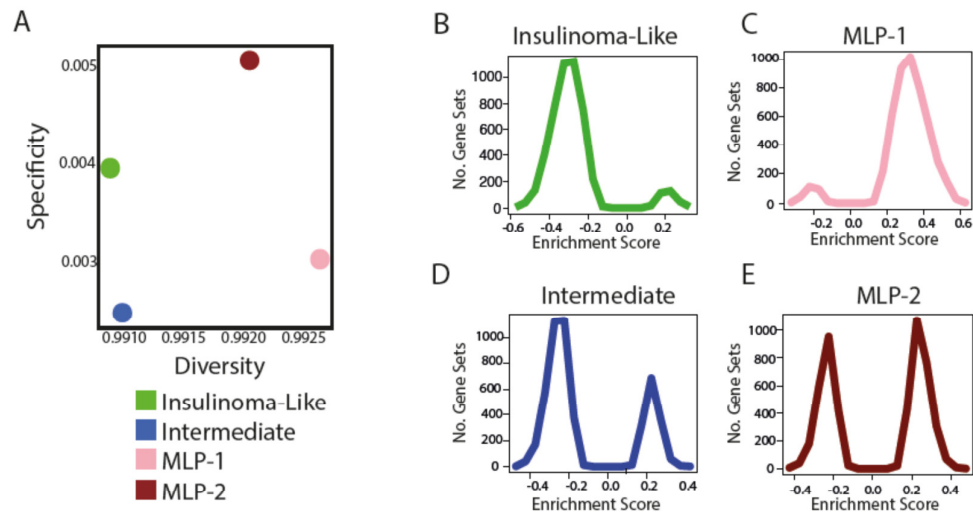
4.3.5 MLP-1 subtype demonstrates a highly diverse pattern of immune gene expression

Having noted that the MLP-1 subtype is enriched for immune related gene expression, we considered the pattern of this enrichment. A Shannon Entropy analysis was conducted to measure the diversity and specialisation of immune related gene expression across the PanNETassigner subtypes (Figure 4.8A). Typically, a highly diverse cancer type will not be specialised and vice versa. This analysis revealed that the MLP-1 subtype had the highest diversity of immune related gene expression with the second lowest specialisation. The MLP-2 subtype had the second highest diversity but was the most specialised. Both the Insulinoma-like and Intermediate subtypes demonstrated low diversity of immune related gene expression but the Insulinoma-like subtype had the second highest specificity whereas the Intermediate subtype had the lowest specificity.

To establish if the high diversity and low specialisation seen in the MLP-1 subtype translated into an increase in immune pathway and network activity, gene expression within the Microarray cohort tumour samples was analysed against the Immunologic C7 Molecular Signatures Database (MSigDB) gene set using the GSEA/MSigDB website (v6.3) as described¹⁹⁸. Whilst each of the subtypes except Insulinoma-like demonstrated some enrichment for a number of the Immunologic C7 gene sets, this positive enrichment was markedly higher in the MLP-1 and MLP-2 subtypes versus the others (Figure 4.8 B-E). Interestingly, while MLP-1

showed only positive enrichment of the gene sets, MLP-2 showed both positive and negative enrichments. This could be because MLP-2 is highly diverse (positive enrichment) but specialised (negative enrichment) as shown by the Shannon index. Overall, MLP-1 demonstrates highly diverse immune gene expression with enrichment of multiple immune pathways.

Figure 4.8 High Diversity of Immune Gene Expression in MLP-1 Subtype



A Shannon Entropy plot, measuring the diversity of gene expression and the specialisation of gene expression in each PanNETassigner molecular subtype. The MLP-1 subtype had the highest diversity of immune related gene expression with the second lowest specialisation. B-E GSEA analysis of gene expression within the Microarray cohort against the Immunologic C7 MSigDB gene set, according to PanNETassigner subtype. Positive enrichment was markedly higher in the MLP-1 subtype versus the other subtypes, suggesting a greater enrichment for immune related gene sets

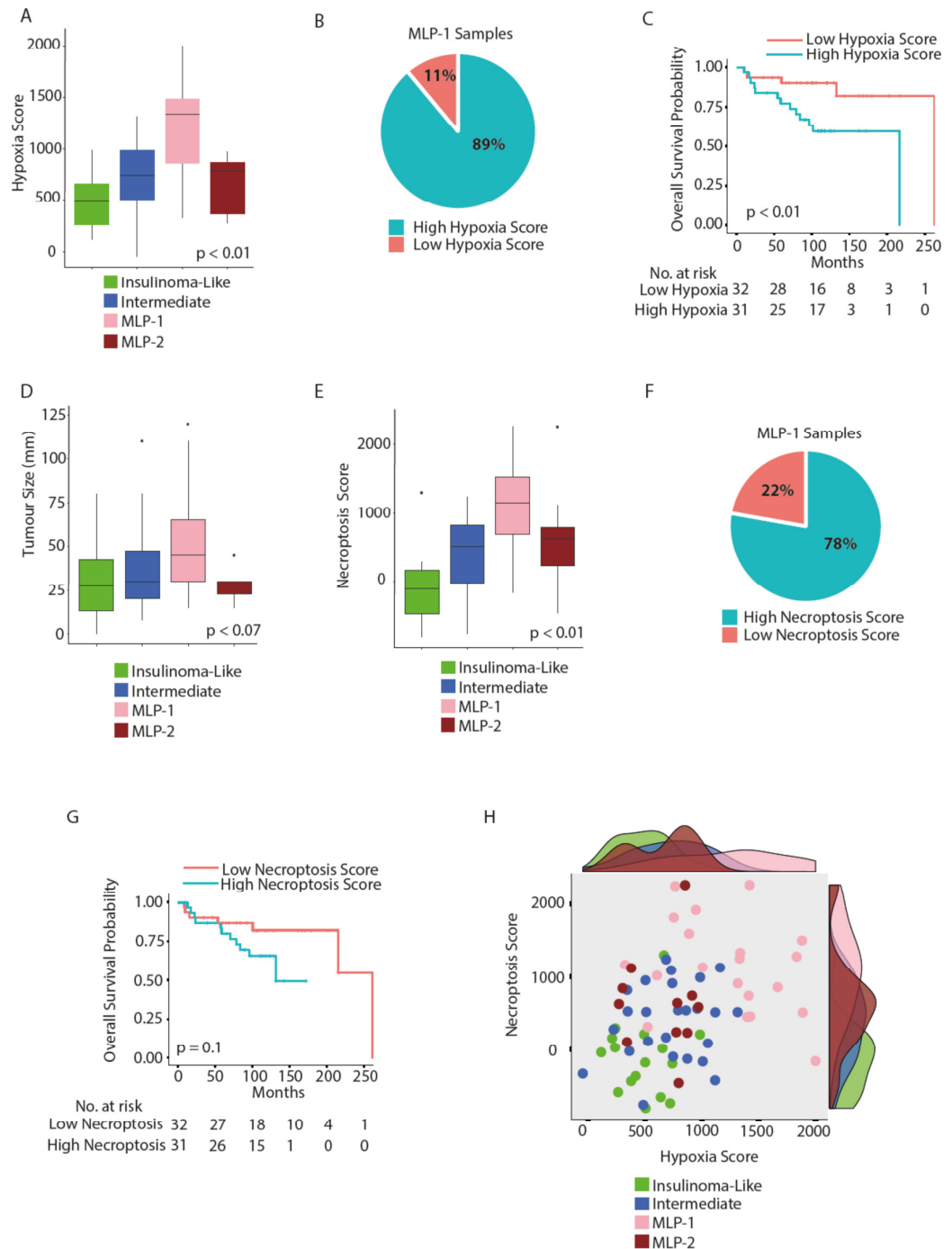
4.3.6 MLP-1 Subtype is enriched for Hypoxia and Necroptosis genes

We next considered potential causes for the MLP-1 subtype's immune reaction. In our initial description of MLP-1, and in Scarpa et al.'s subsequent analysis, it was noted to be less vascularised than other subtypes and enriched for genes associated with hypoxia and HIF signalling^{51,29}. We therefore considered whether a propensity for hypoxia could result in increased stimulation of the immune system resulting in MLP-1's immune enriched phenotype.

Using expression data from the Microarray cohort, MLP-1 was confirmed to be associated with a high hypoxia score versus the other subtypes (Figure 4.9A). Further, a large proportion of MLP-1 patients were found to have a high hypoxia score (Figure 4.9B), associated with a reduction in OS, suggesting that hypoxia may be a driving feature here (Figure 4.9C). This increase in hypoxia fits with the observation that MLP-1 tumours tend to be larger than tumours of other subtypes (Figure 4.9D), as larger tumours are more prone to hypoxia¹⁹⁹.

Hypoxia ultimately results in cell death in a variety of ways. Necroptosis is a form of programmed cell death associated both with such cellular metabolic stress and with promoting immune and inflammatory responses^{200,201,202}. We found that the MLP-1 subtype was associated with a high necroptosis score and that high score was associated with both a reduction in survival and was correlated with a high hypoxia score, especially in MLP-1 (Figures 4.9E-H). These results provide a possible link to explain why the hypoxic MLP-1 subtype may have an inflamed phenotype.

Figure 4.9 Enrichment of MLP-1 Subtype for Hypoxia and Necroptosis Genes



A Boxplot of ssGSEA Hypoxia Gene Set Score across the PanNETassigner subtypes with a significantly increased score in the MLP-1 subtype ($p < 0.01$ for a difference across all 4 subtypes). B Pie chart showing the proportion of MLP-1 samples with a high (89%) or low (11%) ssGSEA hypoxia score. C Kaplan Meier survival plot according to hypoxia score, demonstrating that patients with a high

hypoxia score have reduced survival vs. those patients with a low hypoxia score ($p < 0.01$). D Box Plot of Tumour size according to PanNETassigner subtype demonstrating that the MLP-1 subtype is enriched for larger tumours ($p < 0.07$ for a difference across all 4 subtypes). E Boxplot of ssGSEA necroptosis gene set score across the PanNETassigner subtypes with a significantly increased score in the MLP-1 subtype ($p < 0.01$ for a difference across all 4 subtypes). F Pie chart showing proportion of MLP-1 samples with a high (78%) or low (22%) necroptosis score. G Kaplan Meier survival plot according to necroptosis score, demonstrating that patients with a high necroptosis score have reduced survival vs. those patients with a low necroptosis score ($p = 0.1$). H Scatter plot of correlation between the hypoxia score and necroptosis score across the PanNETassigner subtypes

4.3.7 MLP-1 is enriched for genes associated with the DAMP pathway, Toll-Like Receptors and Dendritic Cells

Necroptosis results in an inflammatory phenotype through the release of DAMPs, which in turn elicit immune responses^{203,204,205,206}. We therefore analysed the expression of 14 key DAMP genes in the Microarray cohort. The expression of 12/14 of the genes was significantly enriched in the MLP-1 subtype (Figures 4.10A and B). In the MLP-1 samples, the expression of 11 of these 12 genes was positively correlated with the necroptosis score (Figure 4.10C). Only *Toll Like Receptor Adaptor Molecule 1's* (*TICAM1* or *TRIF*) expression was negatively correlated. *TICAM1* forms part of the toll-like receptor (TLR) signalling cascade, although possibly plays a more critical role in the pathogen associated molecular pattern (PAMP) pathway than the DAMP pathway²⁰⁴.

Toll Like Receptor 3 (*TLR3*) was the DAMP pathway gene most significantly enriched in MLP-1 (FDR=5.11E-05). High *TLR3* expression was associated with a reduction in OS in the Microarray cohort, with over 80% of the MLP-1 subtype having such high expression (Figures 4.10D and E). Expression of this receptor is seen in myeloid cells including dendritic cells (DCs), which are antigen presenting cells (APCs) and play a key role in activating the T cell-based adaptive immune system^{207,208,209}. The MLP-1 subtype was found to be enriched for the expression of genes linked to dendritic cells (Figure 4.10F). These observations provide a putative pathway to explain how the hypoxic MLP-1 tumour cells trigger the DAMP

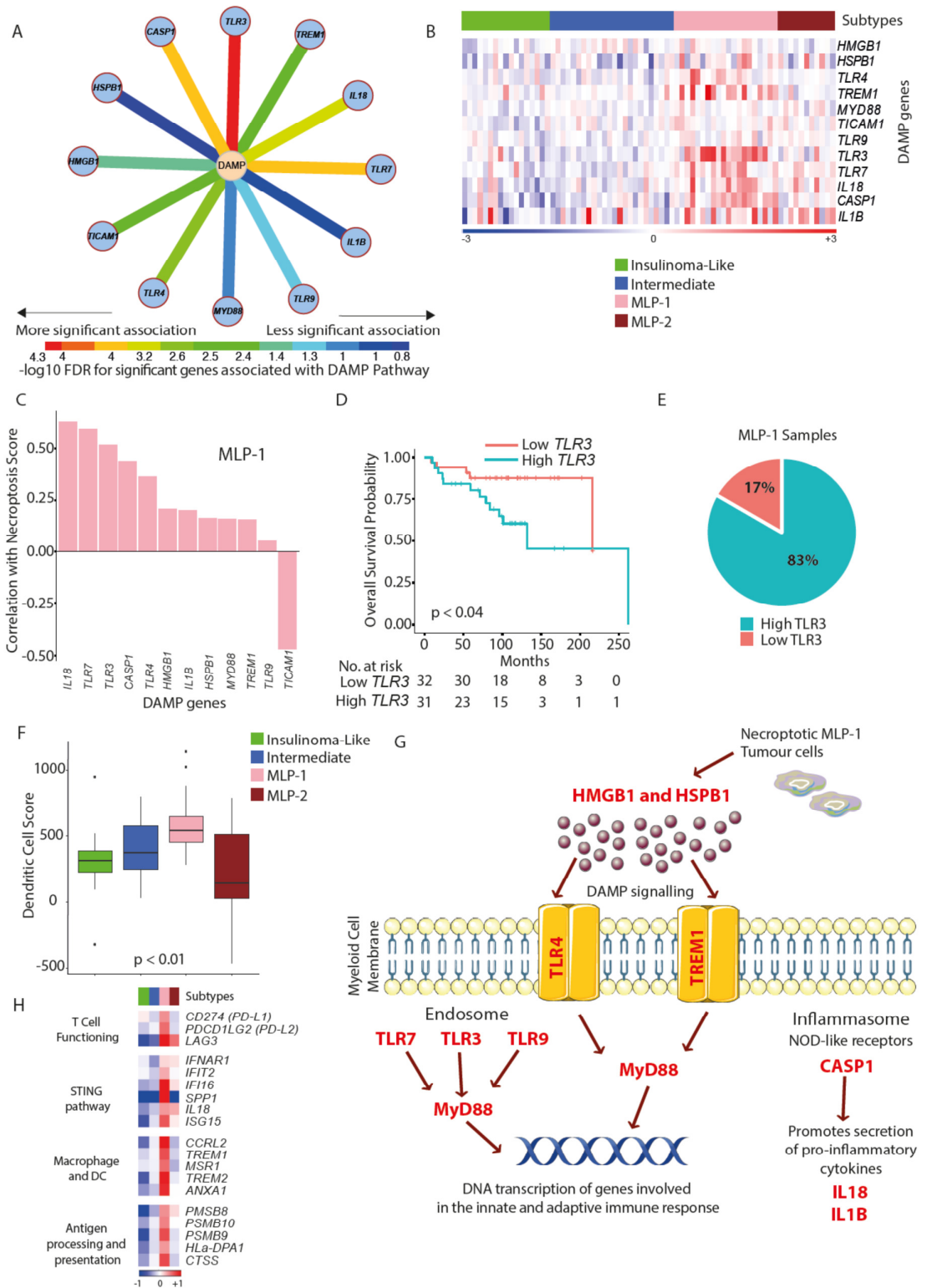
pathway, resulting in the increased transcription of multiple genes involved in immune responses (Figure 4.10G).

4.3.8 MLP-1 Subtype is enriched for genes associated with multiple aspects of the immune response

We next considered specific immune related genes highly expressed in MLP-1. We investigated the functions of the 74 SAM-determined differentially expressed genes with the highest expression in the MLP-1 subtype. Approximately 20 genes code for proteins which play a major role in T cell functioning and immune checkpoints (including *CD274/PD-L1*, *PDCD1LG2/PD-L2* and *LAG3*) and interferon signalling/the Stimulator of Interferon Genes (STING) pathway (*IFIT2*, *IFNAR1*, *IL18*, *IFI16*, *ISG15* and *SPP1*). Others code for proteins which are important in macrophage and DC functioning (*CCRL2*, *TREM1/2*, *ANXA1*, *MSR1* and numerous *TLRs*) and antigen processing and presentation (*PSMB9*, *PSMB10*, *PSMB8*, *CTSS* and *HLA-DPA1*) (Figure 4.10H).

We formally assessed these observations using GSEA to analyse overlaps between the set of 132 differentially expressed genes with increased expression in the MLP-1 subtype and the Immunologic C7 MSigDB gene sets. All 30 gene sets with FDR $q < 0.01$ were involved in T cell functioning, myeloid cell functioning or interferon signalling (Supplementary Table 4.2).

Figure 4.10 Enrichment of the MLP-1 pathway for DAMP pathway genes



A Node plot of 12/14 key DAMP pathway genes significantly enriched in the MLP-1 subtype. Expression of TLR3, TLR7 and CASP1 are most significantly enriched. B Heatmap of the 12 DAMP pathway genes, demonstrating enrichment in the MLP-1 subtype. In the rainbow bar below the heatmap red indicates elevated expression, blue decreased, and white no change. C Bar plot of DAMP pathway genes and their correlation with necroptosis score in the MLP-1 samples demonstrating a positive correlation in all but 1 gene (TICAM1). D Kaplan Meier survival plot according to TLR3 expression, demonstrating that patients with high TLR3 expression have reduced survival vs. patients with low TLR3 expression ($p < 0.04$). E Pie chart showing proportion of MLP-1 samples with high (83%) or low (17%) TLR3 expression. F Boxplot of ssGSEA DC gene set score across the PanNETassigner subtypes with a significantly increased score in the MLP-1 subtype ($p < 0.01$ for a difference across all 4 subtypes). G Schematic to demonstrate the potential significance of DAMP gene enrichment in the MLP-1 samples at a cellular level, with enriched genes highlighted in red. H Heat map to demonstrate enrichment of the MLP-1 subtype for genes associated with T Cell functioning, the STING pathway, macrophage and DC functioning and antigen processing and presentation

4.3.9 MLP-1 Subtype is enriched for the genes of multiple immune cell types

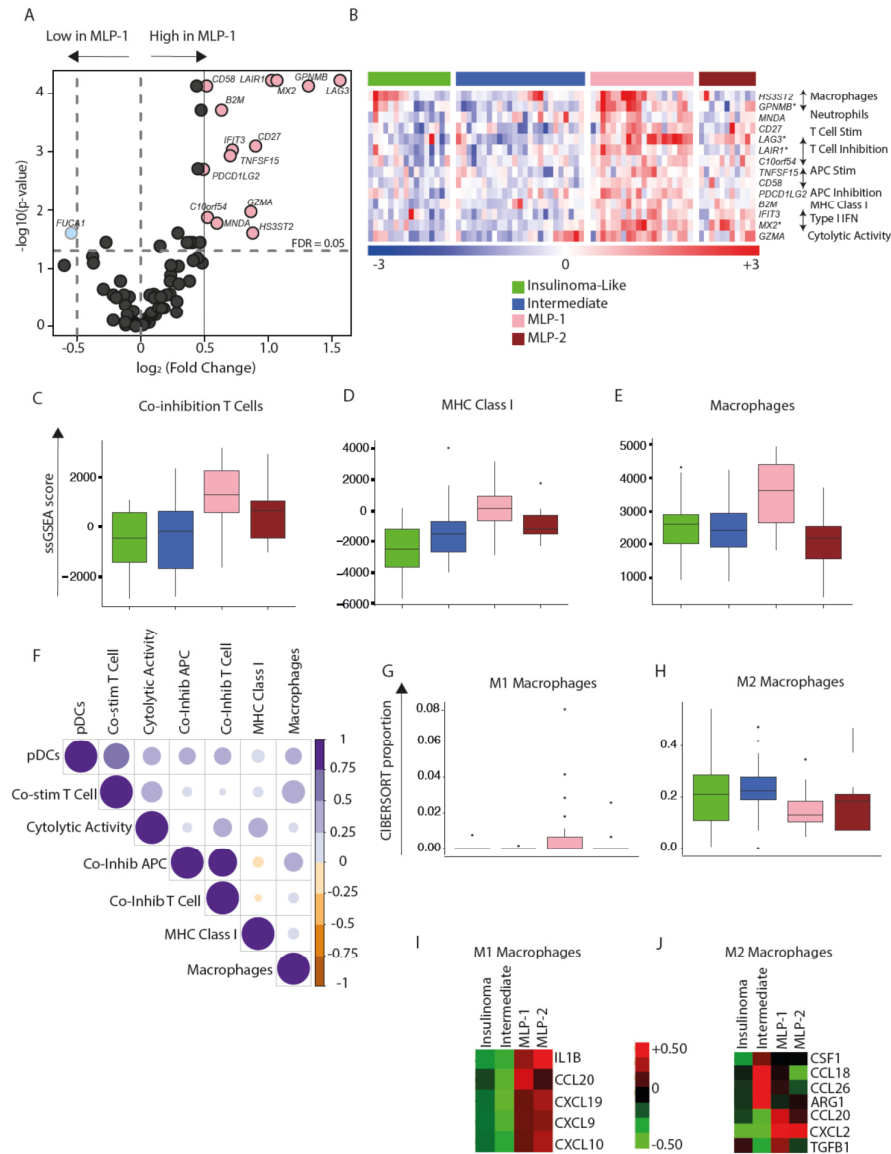
Having observed the above patterns of immune related gene expression in the MLP-1 subtype, we specifically investigated gene expression related to selected immune cell types. We chose a set of transcriptomic markers for genes associated with specific immune cell types, based on the work of Rooney and colleagues according to analysis of Fantom5 CAGE data^{190,191}. Gene expression was analysed according to the Rooney et al. immune cell type gene sets, across the PanNETassigner subtypes using ssGSEA and the Microarray cohort.

82% of the 80 genes from Rooney et al., were highly expressed in the MLP-1 subtype. 14 genes had significantly ($FDR < 0.05$) increased expression in the MLP-1 subtype versus the other PanNETassigner subtypes, with a fold change of ≥ 1.5 (Figure 4.11A). Just 1 of the transcriptomic cell type genes, FUCA1, had a significantly decreased expression in MLP-1 versus the other subtypes. FUCA1, a target of p53, encodes a protein involved in the degradation of fucose-containing glycoproteins and glycolipids. Reduced expression, as in the MLP-1 subtype, has been associated with poor prognosis in a number of cancers²¹⁰.

The pattern of increased expression in the MLP-1 subtype was observed across both myeloid cell specific and lymphoid cell specific genes. As predicted by the observations of gene functions (Figure 4.10H) and enrichment for components of the DAMP pathway (Figure 4.10A), here the MLP-1 subtype expressed genes associated with macrophages and neutrophils, cells involved in both T cell stimulation and inhibition and APC stimulation and inhibition, Major Histocompatibility Complex (MHC) Class I, a type I Interferon response and cytolytic activity (Figure 4.11B).

ssGSEA analyses were completed to confirm the statistical significance of the enrichment of immune cell types across the PanNETassigner subtypes. MLP-1 was enriched for co-inhibition of T cells, MHC Class I and macrophages (Figures 4.11C-E) along with the other cell types in Figure 4.11F, confirming the earlier findings.

Figure 4.11 Enrichment of the MLP-1 Subtype for genes associated with multiple immune cell types



A Volcano Plot to demonstrate differentially expressed immune genes within Rooney et al gene set in MLP-1. For fold change >1.5 and adjusted $p < 0.05$, 14 genes had significantly increased expression in MLP-1 versus the other PanNETassigner subtypes and 1 had significantly reduced expression. B Heat map of 14 Rooney et al genes with a fold change >1.5 and significantly increased expression, including 4 genes with a fold change > 2 (*). Immune cell types associated with the specific genes highlighted. In the rainbow bar below heatmap red indicates elevated expression, blue decreased, and white no change. C-E Boxplots of ssGSEA score across PanNETassigner subtypes with increased score in MLP-1. Using FDR < 0.01 , in MLP-1 there was a statistically significant increase in gene expression associated with co-inhibition of T cells, MHC Class I cells and macrophages. F Correlation plot for mean ssGSEA scores for MLP-1 cell types. G and H Boxplots of CIBERSORT proportions across PanNETassigner subtypes

with an increased score in MLP-1. Using FDR of <0.05, M1 macrophages demonstrated an increased abundance on CIBERSORT analysis in MLP-1 versus the other PanNETassigner subtypes, whereas M2 macrophages demonstrated a reduced abundance. I and J Heatmaps to demonstrate gene expression associated with M1 and M2 macrophages across PanNETassigner subtypes

4.3.10 MLP-1 tumours display elements of both immune stimulation and immunosuppression

We considered how the different immune cell types correlated with each other in the MLP-1 subtype and how such correlation could lead to immune activation or immunosuppression. Based on the positive correlation of ssGSEA scores between immune cell types (Figure 4.11F), our data suggests the presence of immune activation through APC (plasmacytoid dendritic cells; pDCs) induced T-cell co-stimulation and cytolytic activity, potentially through MHC class-I molecule expression by MLP-1 tumour cells (there is a high positive correlation between cytolytic activity and MHC class-I).

There was also a high positive correlation of ssGSEA scores between macrophages and the co-stimulation of T Cells in MLP-1 subtype (Figure 4.11F). Furthermore, there was an increase in the abundance of M1 macrophages (anti-tumorigenic) in the MLP-1 subtype and a reduction in M2 macrophages (pro-tumorigenic) by two different analyses (Figure 4.11 G-J). These analyses suggest the co-stimulation of T cells through M1 macrophages in the MLP-1 subtype.

On the other hand, cytolytic activity was highly correlated with the co-inhibition of T cells, suggesting a potential feedback mechanism leading to reduced adaptive T cell mediated immune-stimulation, which has been reported in other tumour types. This is further substantiated by the negative correlation between the co-inhibition of T cells and MHC class-I and between the co-inhibition of APC and MHC class-I. At the same time, the significantly high expression of immune check-point genes such as LAG3

and C10orf54 in the MLP-1 subtype suggests an immunosuppressive microenvironment in this poor prognostic subtype (Figure 4.11B)²¹¹.

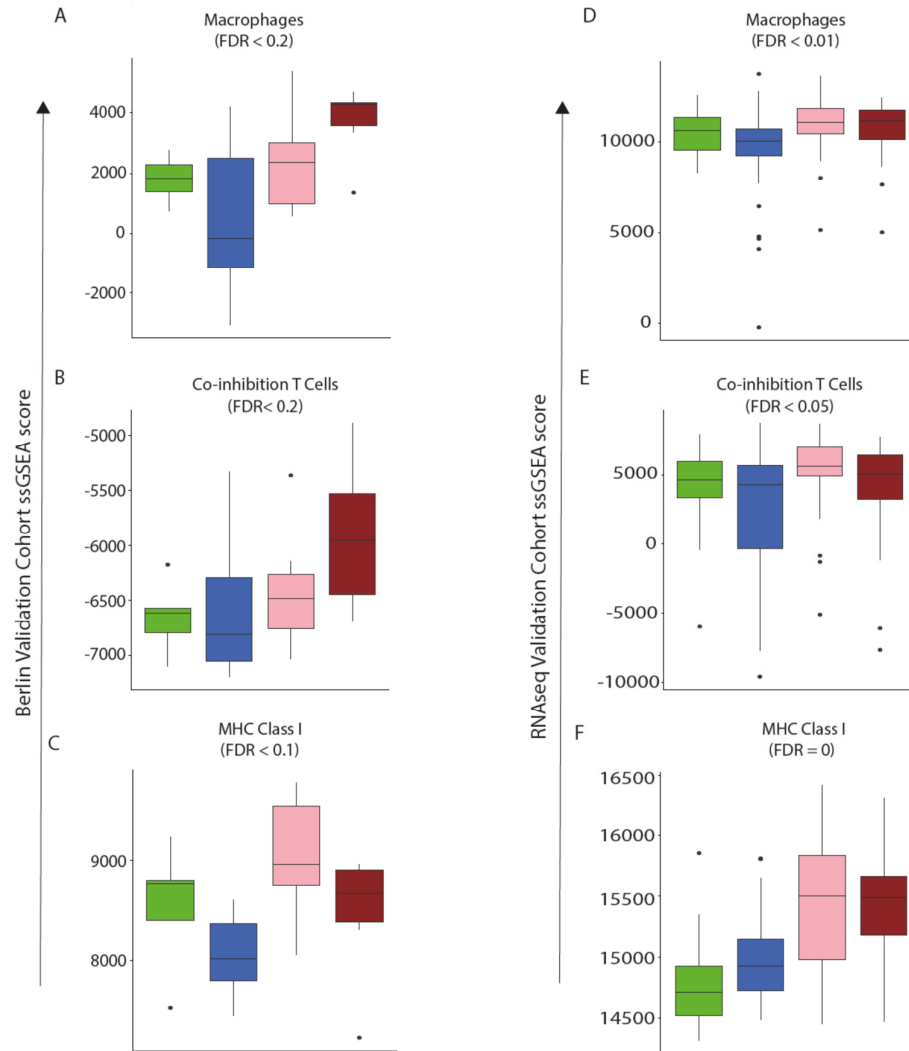
Overall, these data suggest that the MLP-1 subtype has elements of immune stimulation, modulated via myeloid cells (DC and M1 macrophage) and the DAMP pathway, leading to subsequent immunosuppression, in turn potentially leading to tumour progression and poor prognosis.

4.3.11 Validation Cohorts support patterns of immune cell gene expression in Microarray Cohort

Using ssGSEA analysis, we considered the presence of immune cell types across the PanNETassigner subtypes in the Berlin and RNAseq validation cohorts. Based on our Microarray cohort analysis, we specifically considered macrophages, co-inhibition of T Cells and MHC Class I. In both validation cohorts, as in the Microarray cohort, there was an elevated ssGSEA score for macrophages, the co-inhibition of T Cells and MHC Class I in the MLP-1 subtype versus the Insulinoma-like and the Intermediate subtypes (Figure 4.12A-F).

The difference in the validation cohorts is that the MLP-2 subtype samples also demonstrated an increased ssGSEA score for macrophages, co-inhibition of T cells and MHC Class I. These data are therefore supportive of the pattern of increased immune related gene expression in the MLP subtypes, as observed in the Microarray cohort.

Figure 4.12 ssGSEA Analyses for Validation Cohorts



ssGSEA analysis of Berlin validation cohort demonstrates increased scores in both MLP-1 and MLP-2 subtypes A-C Boxplots of ssGSEA scores of interest ($FDR \leq 0.2$) across PanNETassigner subtypes in the Berlin validation cohort ($n=26$). Here, as in the Microarray cohort, there was an elevated ssGSEA score for macrophages, the co-inhibition of T Cells and MHC Class I in the MLP-1 subtype vs. the Insulinoma-like and the Intermediate subtypes. The difference here is that the MLP-2 subtype samples also demonstrated increased ssGSEA score for macrophages and co-inhibition of T cells.

ssGSEA analysis of RNAseq validation cohort demonstrates increased scores in in both MLP-1 and MLP-2 subtypes D-F Boxplots of ssGSEA scores of interest ($FDR \leq 0.05$) across PanNETassigner subtypes in RNAseq validation cohort ($n=120$). Here, as in the Microarray cohort, there was an elevated ssGSEA score for macrophages, the co-inhibition of T Cells and MHC Class I in the MLP-1 subtype versus the Insulinoma-like and the Intermediate subtypes. The difference here is that the MLP-2 subtype samples also demonstrated increased ssGSEA score for macrophages and MHC Class I.

4.3.12 Other PanNETassigner subtypes demonstrate different enrichment patterns

We next assessed gene expression across the remaining 3 PanNETassigner subtypes, MLP-2, Intermediate and Insulinoma-like. We again looked at the Rooney et al. gene sets, ssGSEA and CIBERSORT analyses, according to PanNETassigner subtype.

The Insulinoma-like subtype had a low expression of immune related genes

Overall, the Insulinoma-like subtype had a low expression of the majority of the immune related genes. Using the Rooney et al. immune cell type gene set, 3 genes had increased and 4 genes had reduced expression in the Insulinoma-like subtype versus the other subtypes. However, on ssGSEA analysis there were no statistically significantly increased enrichment scores for the Insulinoma-like samples. Further, on CIBERSORT analysis the Insulinoma-like subtype did not have the highest abundance for any immune cell type.

The Intermediate subtype is enriched for B cells

Using the Rooney et al. immune cell type gene set, 4 genes had significantly increased and 4 genes had significantly reduced expression in the Intermediate subgroup versus the other PanNETassigner subtypes (Figure 4.13A). The 4 genes with increased expression play roles in B cell functioning, co-stimulation of APCs, a type II IFN response and neutrophil functioning (Figure 4.13B). Those with reduced expression all have increased expression in MLP-1 and are associated with macrophages, a type I IFN response and co-inhibition of T cells.

The ssGSEA analysis demonstrated a significant increase in the enrichment score for B cells (Figure 4.13C) and on CIBERSORT analysis there was a statistically significant increase in naïve B cell abundance and a reduction in memory B cell abundance (Figure 4.13D and E). We note that a high number of infiltrating naïve B cells has been associated with improved prognosis in a number of different cancers²¹².

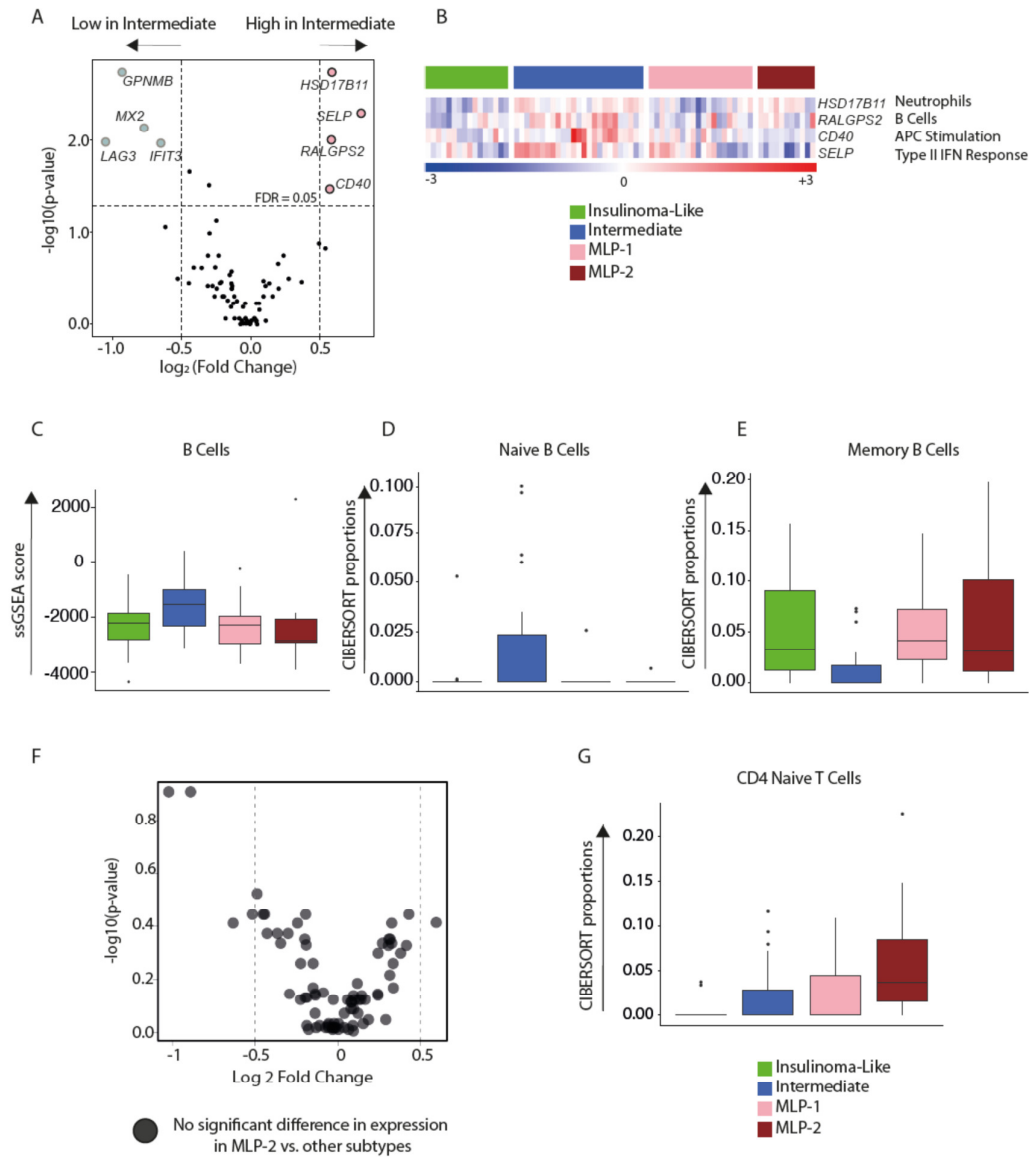
MLP-2 shares some features of enrichment with the MLP-1 subtype

Of the 132 differentially expressed immune related genes, 25 (19%) genes had the highest expression in the MLP-2 subtype. Using the Rooney et al. immune cell type gene sets, considering a fold change of 1.5 and an adjusted p value of <0.05 , none of the genes had a significantly increased fold change in the MLP-2 subtype versus the other PanNETassigner subtypes (Figure 4.13F).

In the ssGSEA analysis, the MLP-2 subtype was not seen to have the highest expression of any of the differentially expressed cell type gene sets. However, the MLP-2 subtype did have a higher expression of co-inhibition of T cell and MHC Class I genes than the Intermediate and Insulinoma-like subtypes (Figure 4.11 C and D). Further, in the validation cohorts the MLP-2 subtype was enriched for macrophages, co-inhibition of T cells and MHC Class I alongside the MLP-1 subtype (Figure 4.12).

On CIBERSORT analysis the MLP-2 subtype only demonstrated a high abundance of naïve CD4+ T cells with a FDR of < 0.05 and here the MLP-1 subtype also followed this pattern (Figure 4.13G).

Figure 4.13 Immune Enrichment Patterns in Intermediate and MLP-2



A Volcano plot to demonstrate differentially expressed immune genes within the Rooney et al. gene set in Intermediate. 4 genes had significantly increased and 4 had significantly reduced expression vs. other PanNETassigner subtypes (Fold change > 1.5 and FDR < 0.05). B Heat map of the 4 Rooney et al. genes with significantly increased expression in Intermediate. Associated cell types are highlighted and in the rainbow bar below the heatmap, red indicates elevated expression, blue decreased, and white no change. C Boxplot of ssGSEA score demonstrating an increase in gene expression associated with B Cells in Intermediate (FDR < 0.05). D and E Boxplots of CIBERSORT proportions demonstrating increased abundance of naive B cells in Intermediate, whereas memory B cells had reduced abundance (FDR < 0.05). F Volcano Plot demonstrating that no differentially expressed immune genes within the Rooney et al. gene set had increased expression in MLP-2 vs. the other subtypes. G Boxplot of CIBERSORT proportions demonstrating increased abundance of CD4 T cells in MLP-2 (FDR < 0.05)

4.3.13 Multiplex IHC demonstrates increased macrophage density in MLP-1

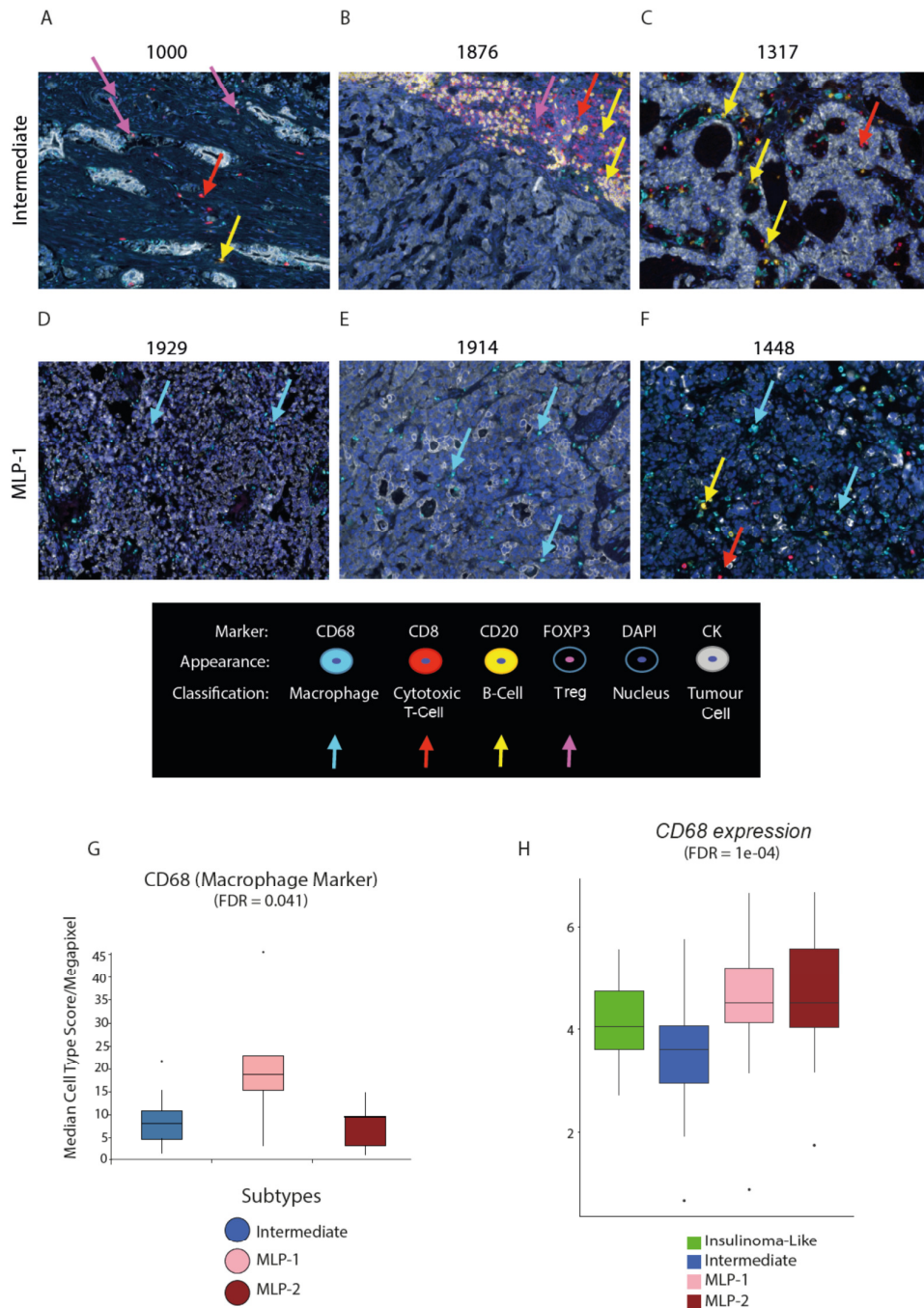
We sought to validate the patterns of immune related gene expression demonstrated in the PanNETassigner subtypes using immune related profiles of protein expression (Multiplex IHC). Using available matched FFPE samples (n=30 from Microarray and RNAseq cohorts), we assessed the number of cells stained positive for CD20 (B cell marker), CD68 (macrophage marker), CD8 (cytotoxic T cell marker), and FOXP3 (regulatory T cell marker) within the tumour tissue (Figure 4.14 A-F). Using a median score of cell type/megapixel for the tumour samples, we considered differences in protein expression across the PanNETassigner subtypes, excluding the Insulinoma-like samples as FFPE was only available for 2 cases.

The MLP-1 subtype demonstrated a statistically significant increased density of CD68 positive cells versus the Intermediate and MLP-2 subtypes (FDR=0.041) (Figure 4.14G). This is consistent with increased expression of the *CD68* gene in the MLP-1 subtype in the RNAseq cohort (Figure 4.14H).

There was no statistically significant difference in CD8 staining across the 3 subtypes which is consistent with the gene expression data. Similarly, there was increased staining for CD20 positive B cells in the Intermediate samples versus the MLP-1 and MLP-2 samples, but this did not reach statistical significance (FDR=0.5). Interestingly, the Intermediate subtype had a significantly increased density of FOXP3 positive cells versus the MLP-1 and MLP-2 subtypes (FDR=0.02).

These IHC-based protein expression findings are consistent with gene expression data, which validates both the techniques, describing enrichment for macrophages in the MLP-1 subtype and B cells in the Intermediate subtype.

Figure 4.14 Multiplex IHC (mIHC) supports Macrophage enrichment of MLP-1 subtype



A-C mIHC: Representative Slide Photos demonstrating protein expression of FOXP3 (Regulatory T Cell marker), CD8 (Cytotoxic T Cell marker) and CD20 (B Cell marker) in the Intermediate subtype samples. D-F mIHC: Representative Slide Photos demonstrating protein expression of CD68 (Macrophage marker), and to a lesser extent CD20 (B Cell Marker) and CD 8 (Cytotoxic T Cell marker) in the MLP-1 samples. G mIHC: Boxplot of median score of cell type/megapixel for each PanNETassigner subtype for macrophage marker CD68, demonstrating an

increased score in the MLP-1 subtype (FDR=0.041, for a difference across the 3 subtypes). H Boxplot of CD68 expression in RNAseq cohort demonstrating significantly increased expression in the MLP subtypes versus the Intermediate subtype, supporting the mIHC data.

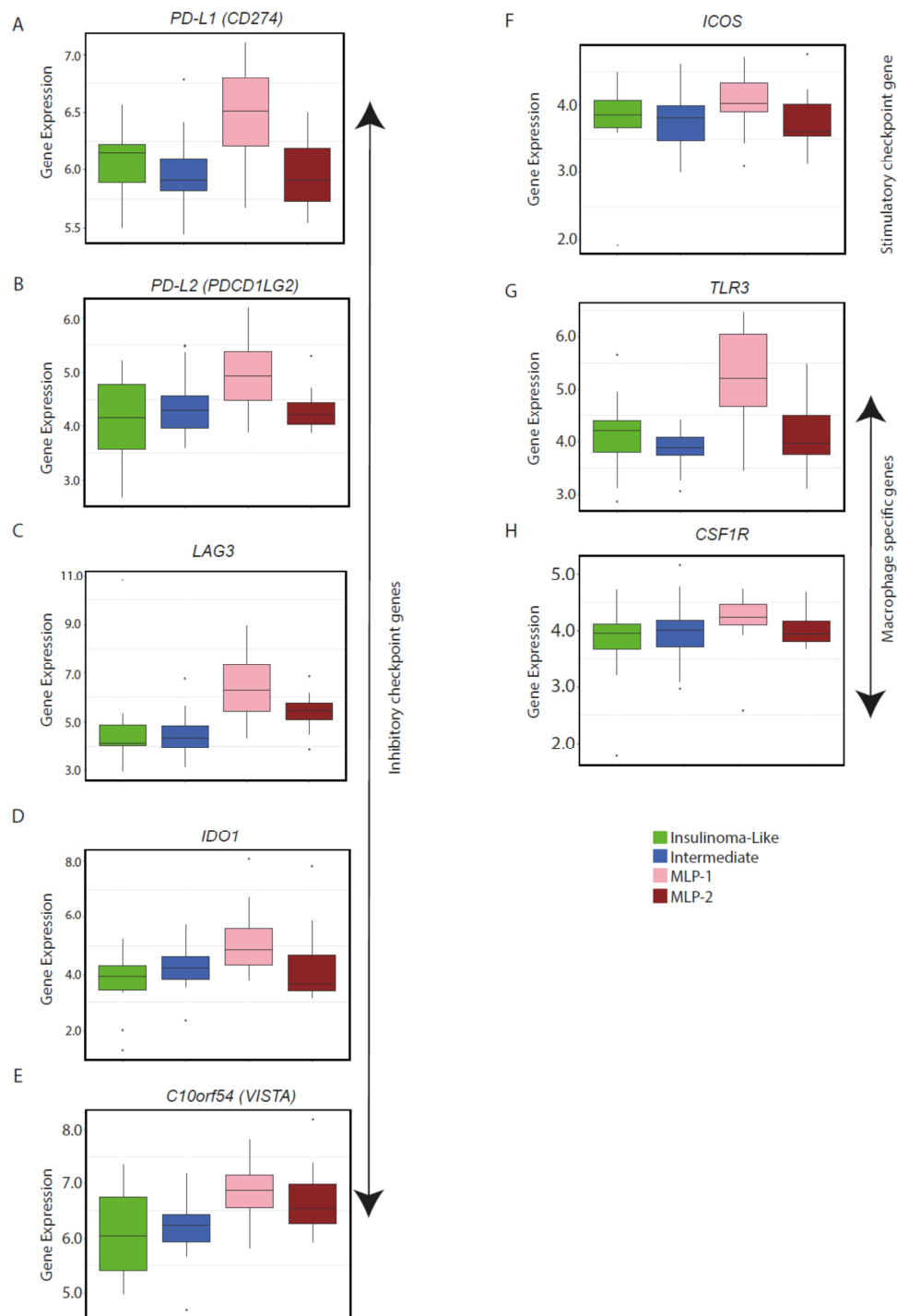
4.3.14 Key Immunotherapy Targets are enriched in MLP-1

To assess the potential clinical significance of the enrichment of immune related gene expression in the MLP-1 subtype, we next considered the expression of various known and potential immunotherapy targets across the PanNETassigner subtypes, using the Microarray cohort data. We first considered *PD-L1* expression, as *PD-L1* expression has been used as an inclusion criterion for clinical trials of immunotherapy in PanNET patients (NCT02054806). *PD-L1* (*CD274*) was differentially expressed according to PanNETassigner subtype, with expression enriched in the MLP-1 subtype (Figure 4.15A). *PD-L2* expression is similarly enriched in MLP-1, although *PD-1* is not (Figure 4.15B).

We next considered additional inhibitory immune checkpoints, *LAG3*, *IDO1* and *C10orf54* (*V-domain Ig suppressor of T cell activation, VISTA*), which were also enriched in the MLP-1 subtype (Figure 4.15C-E). The expression of *ICOS*, a stimulatory checkpoint gene highly expressed in Regulatory T Cells was likewise increased in the MLP-1 subtype, again likely to contribute to the immunosuppressive microenvironment²¹³ (Figure 4.15F).

In light of the association of the MLP-1 subtype with macrophages genes and the DAMP pathway, we also looked at the expression of *TLRs* and *CSF1R*. A number of *TLRs* (*TLRs 2, 3 and 4*) and *CSF1R* were all enriched in the MLP-1 subtype (Figure 4.15G and H).

Figure 4.15 Key Immunotherapy Targets enriched in the MLP-1 subtype



A-E Boxplots of Inhibitory Checkpoint gene expression in the Microarray cohort, demonstrating a significant increase in the MLP-1 samples vs. the other subtypes ($FDR < 0.005$ for a difference across all 4 subtypes). *F* Boxplot of Stimulatory Checkpoint ICOS expression in Microarray cohort demonstrating significantly increased expression in the MLP-1 ($FDR < 0.05$ for a difference across all 4

subtypes) G-H Boxplots of Gene expression linked to Macrophage Functioning in Microarray cohort demonstrating increased expression in the MLP-1 subtype (FDR < 0.01 for a difference across all 4 subtypes)

4.3.15 Deficient Mismatch Repair (MMR) not associated with PanNETassigner subtypes

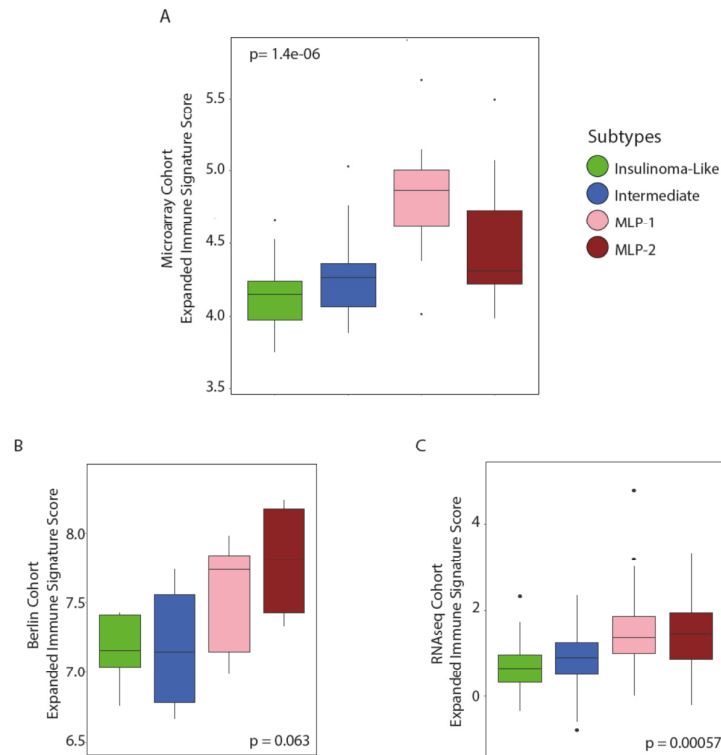
As Microsatellite instability has been postulated as a biomarker for immunotherapy in a number of solid tumours, we assessed MMR using immunohistochemistry in a cohort of 24 FFPE PanNEN samples from the RM cohort. We assessed staining of the 4 MMR proteins MSH2, MSH6, MLH1 and PMS2. Only 2/24 of the samples demonstrated MMR deficiency, both with loss of expression of MSH6 (Appendix 4, Supplementary Table 4.3). 1 of the MMR deficient samples was Insulinoma-like and the other Intermediate, demonstrating no association with the PanNETassigner subtypes, although noting this is a small sample size.

4.3.16 MLP Subtype enriched for Expanded Immune Signature across all cohorts

We finally analysed the expanded immune signature across the PanNETassigner subtypes, as this signature has been demonstrated to predict response to PD-L1 blockade in a number of different solid tumours. Here the expanded immune signature used was based on the final 18 gene profile, developed by Ribas et al¹³¹.

This analysis demonstrated enrichment of the expanded immune signature with a statistically significant increase in score in the MLP-1 subtype versus the other PanNETassigner subtypes in the Microarray cohort (Figure 4.16A). The enrichment of the MLP-1 subtype versus the Insulinoma-like and Intermediate subtypes is also seen in the Berlin and the RNAseq cohorts (Figure 4.16 B and C). In both the Berlin and the RNASeq cohorts, the MLP-2 subtype is also enriched, supporting their previously noted similarities.

Figure 4.16 Expanded Immune Signature Enrichment in MLP-1 and MLP-2

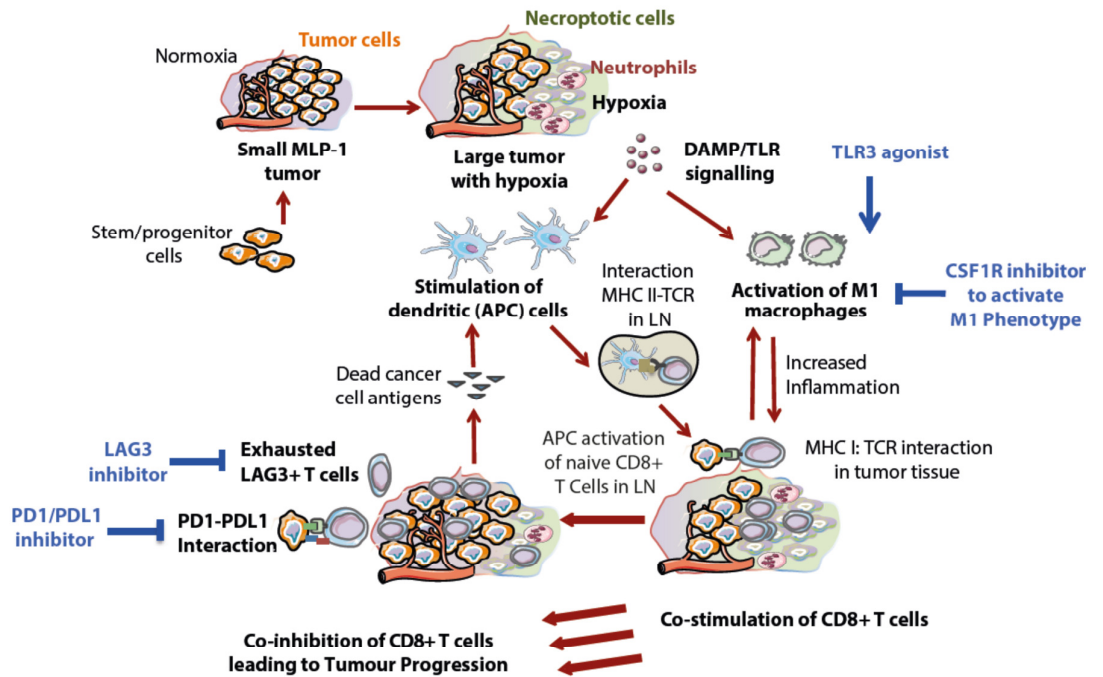


A Expanded immune signature score for Microarray cohort (note expression data for 13/18 genes in signature available in the Microarray cohort). B and C Expanded immune signature score in validation cohorts (for both validation cohorts data for all genes was available). As in the Microarray training cohort, the MLP-1 samples had higher scores than the Intermediate or Insulinoma-like samples. Here the MLP-2 samples also had high scores.

Overall, these data generate the hypothesis that the MLP-1 subtype, with the highest and most diverse expression of immune related genes, enrichment for immunologic gene sets, DAMP pathway genes, multiple elements of the immune system and the expanded immune signature, may potentially be more vulnerable to immunotherapeutic approaches, compared to other PanNETassigner subtypes. The pathways which may be involved in generating this immune high phenotype from hypoxia and necroptosis, to myeloid cell activation via DAMP signalling and T cell co-stimulation with a subsequent shift to T cell co-inhibition, provide a number of putative potential therapeutic targets (Figure 4.17 and Table 4.4).

Figure 4.17 Pathways of Immune Enrichment and Potential Therapeutic Opportunities in the MLP-1 Subtype

A



Schematic of a putative pathway explaining the enrichment of immune gene expression in the MLP-1 subtype. Large MLP-1 tumours are prone to hypoxia and through necroptosis and subsequent stimulation of the DAMP pathway innate and adaptive immune response are activated. The consequences of the activation depend upon the balance between stimulation and inhibition of the immune response, particularly the T Cell response. Potential targets for therapy are highlighted in blue.

Table 4.4 PanNETassigner Subtypes, Immune Properties and Potential Treatment Approaches

PanNETassigner Subtype	Selected Enriched Immune Genes	Enriched Immune Cell Type/ Function	Potential Immunotherapy Approach
Insulinoma-like	STAT2	None	
	STAT4		
	IFIT1		
Intermediate	RALGPS2	B Cells	B Cell directed therapy
	CCL26	Eosinophils	Regulatory T cell inhibition
	CCL13	Regulatory T Cells	Combination therapy
	CD46	NK Cell	
	IL32		
	IL4		
MLP-1	PD-L1	T Cells	Anti-PD-L1
	PD-L2	APCs	Anti- PD-1
	LAG3	Macrophages	Anti-LAG 3
	IDO-1	Neutrophils	IDO-1 Inhibitors
	CSF1R	Dendritic Cells	CSF1R inhibitors
	IFI16	IFN Response	TLR agonists
	TLRs		STING agonists
	DAMP pathway		Combination therapy
MLP-2	CXCL10	T Cell	Anti-PD-L1
	LTK	NK Cell	Anti- PD-1
	PVR	Complement	Combination therapy
	CCL19	MAC	
	C1S/C1R		
	C8G		
	C9		

4.4 Discussion

Whilst trials of immunotherapy are on-going in PanNENs, the immune landscape of this disease is largely uncertain. In this chapter, I have outlined how we sought to describe immune related gene expression in PanNENs and consider how this may impact upon immune cell type distribution and functioning. Having previously described molecular subtypes in PanNENs, we specifically considered immune related gene expression across our PanNETassigner subtypes, to provide insights into the heterogeneity of the immune microenvironment in this disease, to consider potential causes for this heterogeneity, to assess whether a particular subtype of patients may be more amenable to an immunotherapeutic approach and to highlight potential immunotherapeutic targets.

In this study, we demonstrated a differential expression of immune related genes across PanNEN patient tumour samples. This differential expression was not well described according to known clinical parameters of importance such as grade of disease, the presence of liver metastases or specific genetic mutations. However, PanNETassigner molecular subtypes could be used to divide patients into groups with varied immune related gene expression, with the MLP-1 subtype (approximately 20% of PanNEN patients) demonstrating a particularly immune-high phenotype.

In light of our lab's expertise in subtyping, this study focuses on the differential expression of immune related genes across our molecular subtypes. We recognise that it would also be of benefit to analyse the immune landscape of these tumours in a non-biased manner, and plan to undertake this as part of a future project.

The MLP-1 subtype is enriched for genes involved in Hypoxia Inducible Factor (HIF) signalling^{51,29}. HIF signalling has been linked to many aspects of immunity in the tumour microenvironment (TME), including up-regulation of immune checkpoints such as PD-L1 and CTLA-4²¹⁴. Hypoxic cell

damage may also result in necroptosis and subsequent signalling through the DAMP and STING pathways, with myeloid cell recruitment, all demonstrated here to be enriched in the MLP-1 subtype^{204,215}. These pathways are of great interest in cancer medicine as they provides links between cell damage, danger signals and an adaptive immune response^{204,205,203}. Whilst much remains to be learnt about these pathways and their potential to either promote or inhibit tumour progression, they provide a plausible explanation for the MLP-1 subtype's immune high phenotype. If, following mechanistic testing in animal models and cell lines, these pathways are confirmed to play a key role, a number of possible therapeutic targets such as TLR3 and HMGB1 may be identified.

The immune genes highly expressed in MLP-1 covered both the lymphoid and myeloid cellular compartments and a broad range of innate and adaptive immune cellular activities. The analyses here support the presence of a co-ordinated immune response within the MLP-1 tumours, with enrichment for genes involved in antigen presentation, MHC Class-I, co-stimulation of T cells and cytolytic activity. As would be expected, such cytolytic activity was also associated with enrichment for genes involved in the corresponding inhibitory pathways, including checkpoint pathways (PD-L1/CD274, LAG-3 and C10orf54/VISTA). We suggest that tumour progression occurs when the negative feedback outweighs anti-tumour cytotoxic activity. This enrichment of genes involved in inhibitory pathways provides a rationale for investigating whether the MLP-1 subtype patients are more likely to benefit from immune checkpoint inhibitor therapies than patients in other subtypes.

A number of checkpoint inhibitor trials in NEN patients have used PD-L1 positivity as an inclusion criterion. Earlier studies have shown that PD-L1 (CD274) is expressed in GEP-NENs and that expression is associated with both grade and survival^{173,174,175,182}. The largest of these studies in PanNENs (n=70) reported that 11% of patients were PD-L1 positive with a cut-off of 1% tumour cell staining and 3% with a cut-off of 5% tumour cells staining¹⁸². In our study, *PD-L1* was differentially expressed across our

PanNETassigner subtypes with the MLP-1 subtype demonstrating the highest expression, again suggesting that investigating checkpoint inhibitor therapy may be appealing in this subtype.

However, not all MLP-1 samples expressed PD-L1 and yet retained other aspects of the immune high phenotype. Further, experience to date with other solid tumours has informed us that PD-L1 expression alone is not always a reliable biomarker for checkpoint blockade, highlighting the need for other more reliable predictive biomarkers for immunotherapy treatments. These observations led us to consider the potential of other putative predictive biomarkers for immunotherapy in PanNEN patients, such as tumour mutational load or burden (TML/TMB), microsatellite instability and IFN- γ -related mRNA profiles, as well as the possibility of using our PanNETassigner subtypes^{216,217,218,131}.

PanNENs have been reported to have a low TMB, of either 5.8 mutations/megabase¹⁸² or 0.82 mutations/megabase²⁹ in different publications. Both of these figures are significantly lower than those reported for the tumour types most sensitive to immune checkpoint blockade, such as melanoma or lung cancer, which have approximately 10 mutations/ megabase, making it unlikely that TML/TMB will provide a useful predictive biomarker for immunotherapy in PanNETs and we therefore did not assess this here.

There are limited and contradictory reports of MSI in PanNETs, with one paper reporting 33% of sporadic insulinomas to be MSI-High¹⁸³ and another reporting no cases of MMR deficiency in 35 unselected PanNET cases¹⁸⁴. In our study 8% (2/24) of the samples tested demonstrated a MMR deficiency, suggesting there may be a small percentage of PanNET patients for whom MSI may provide a potential biomarker, although this observation requires additional investigation in a larger patient sample and in patients treated with immunotherapy.

Various IFN- γ -related signatures have been demonstrated to predict response to PD-L1 blockade in a number of different solid tumours¹³¹. When we analysed the expanded immune signature across our PanNETassigner subtypes, a proportion of the samples demonstrated high levels of IFN- γ -related gene expression, suggesting that this signature should be investigated as part of the on-going clinical trials of immunotherapy in PanNEN patients to establish its potential predictive role here. The MLP-1 subtype demonstrated particular enrichment of IFN- γ -related gene expression, again supporting the consideration of trials of immune checkpoint inhibitors in this group of patients.

In our analysis, we also considered other aspects of the immune system, beyond immune checkpoints, with a view to improving understanding of, and providing a sound scientific rationale for, potential future combination studies of immunotherapy agents.

Both on a transcriptomic and proteomic level, the MLP-1 cohort samples were consistently enriched for the expression of macrophage related genes and protein, suggesting an increased level of tumour associated macrophages (TAMs). The CIBERSORT analysis predicted a polarisation towards M1 macrophages with a reduction in M2 macrophage abundance and this was confirmed with a wider gene panel. Whilst this binary classification of macrophages is no doubt overly simplistic, M1 macrophages are often considered anti-tumorigenic whereas M2 macrophages are considered pro-tumorigenic. This polarisation requires further confirmation, but fits with the pro-inflammatory, cytotoxic phenotype displayed by these baseline MLP-1 samples.

It would be interesting to assess how this macrophage polarisation varies over time, in metastases versus the primary disease and with treatment, noting our MLP-1 samples were almost all taken from the primary disease (95%) and were all taken pre-treatment. Over time, this high abundance of macrophages in the MLP-1 samples may become polarised towards M2 macrophages. Such a switch in polarisation could contribute to the high

levels of invasion and migration characteristically seen in MLP-1 tumours. If this hypothesis were demonstrated to be correct, a treatment targeting TAMs, such as a CSF1R inhibitor, or one which can re-educate TAMs to an anti-tumorigenic phenotype may be worthy of investigation. We also note the MLP-1 samples were enriched for the expression of CSF1R, again making this a potentially appealing target for investigation.

Similarly, DCs and the TLRs which activate them, also enriched in the MLP-1 subtype, are thought to play a critical role regulating the immune system²¹⁹. Tumour associated DCs have been described as dysfunctional, causing up-regulation of immune checkpoints, an increase in regulatory T cells and decreased OS in various tumours^{220,221,222,223}. As both DC-targeted and TLR-targeting treatment strategies are in development, this is another area which warrants consideration in MLP-1 patients²²⁴.

Overall, the MLP-1 subtype appears to be enriched for gene expression relating to multiple aspects of the immune system. The MLP-2 subtype also demonstrated a greater level of enrichment for immune related gene expression than the Intermediate or Insulinoma-like subtypes. In the Berlin and RNAseq cohorts, the MLP-2 subtype was most enriched for the expanded immune signature versus the Intermediate and Insulinoma-like subtypes. Indeed, in the validation cohorts, the MLP-2 subtype also demonstrated an immune high phenotype, alongside the MLP-1 subtype. In the Microarray cohort, the MLP-2 subtype had the second highest level of expression of the differentially expressed immune related genes, after the MLP-1 subtype, and on multiple occasions demonstrated increased gene expression versus the Intermediate and Insulinoma-like subtypes (for example in cytolytic activity, co-inhibition of T cell genes and MHC Class I genes). Further, the MLP-2 subtype had the second highest level of diversity of immune related gene expression, after MLP-1, on the Shannon Entropy analysis. These findings are consistent with the many shared features these two subtypes demonstrate⁵¹.

MLP tumours are enriched for genes associated with epithelial to mesenchymal transition (EMT). EMT has been associated with the expression of immune checkpoints in multiple cancer types, including lung, kidney and cholangiocarcinoma^{166,225,226}. Moreover a pan-cancer EMT signature has been associated with immune activation and high levels of expression of immune checkpoints and other immune targets, such as PD1, PD-L1, CTLA4, OX40L, and PD-L2²²⁷. EMT has also been linked to a hypoxia, another important feature of MLP-1 tumours^{164,165}.

As MLP-1 and MLP-2 together make up approximately 30% of PanNEN patients, their immune high phenotype is worthy of further investigation to establish if these patients may be more amenable to an immunotherapeutic approach.

In contrast to the MLP subtypes, the Intermediate subtype demonstrated particular enrichment for B cells, also with an increase in CD20 staining on multiplex IHC. Evidence is mounting that B cells may also have an important role to play^{228,229}. As reported in patients with liver cancer, the increased tumour infiltrating B cells in our Intermediate subtype were associated with an increase in IFN- γ , CD40, a low Ki-67 and improved survival^{51, 230, 231}. The significance of tumour infiltrating B cells in PanNENs requires further investigation, but as CD40 activated B cells can be potent APCs, this is an area worthy of consideration for Intermediate subtype PanNEN patients.

As with the MLP subtypes, some of the observations regarding the Intermediate subtype fit with previously noted characteristics. The Intermediate subtype is known to be associated with MEN1 mutations, with 50% of this subtype having a mutation versus <13% in the MLP and Insulinoma-like subtypes⁵¹. MEN1 codes for the tumour suppressor menin which plays a critical role in regulating CD4 +ve T cell senescence and preventing CD8+ve T cell dysfunction through limiting mTORC 1 activity^{232,233}. Loss of menin has been linked to CD8+ve T cell senescence, in turn associated with a senescence-associated secretory phenotype with increased pro-inflammatory cytokines and chemokines and matrix

remodelling alongside impaired immune memory formation. As discussed above, in our study the Intermediate subtype was enriched for pro-inflammatory type II IFN (IFN- γ), and whilst the CIBERSORT analysis reported increased naïve B cells, there was a reduced abundance of memory B cells.

Our study has a number of limitations. We recognise that compared to studies in other tumour types the sample size is relatively small. However, it should be acknowledged that in this rare tumour type, a study of 320 tumour samples is a large study. The study is retrospective and includes samples taken at a single time-point, at baseline. The immune system is known to be highly dynamic and the best time to study immune related gene expression is unclear. Ideally, we would be able to analyse tissue and other samples prospectively, at multiple time-points, in primary and metastatic disease and in patients undergoing immunotherapy treatment. This would enable us to assess the impact of clonal evolution, inter-tumour heterogeneity and the impact of treatment. Such a study would also enable the analysis of additional data, such as TMB, the proteome, the role of liquid biopsies and the microbiome, as well as considering the transcriptome, however such analyses are beyond the scope of this study.

This study has demonstrated that the MLP-1 subtype of PanNEN patients has an immune high phenotype, associated with an increased tumour size, hypoxia, necroptosis and DAMP/STING/TLR pathway activation. We have highlighted particular features of the immune system which may provide future treatment targets for investigation for these patients, noting that there is a level of heterogeneity within MLP-1 tumour samples.

There is a complex interplay between tumour cells, and the immune system in PanNEN. The data presented here may serve as a spring-board for further investigation to understand this interplay, as outlined above. However, once this complexity has been elucidated, it seems likely that there will be a role for immunotherapy or its combination with other treatments, perhaps such as Peptide Receptor Radionuclide Therapy,

oncolytic viruses or targeted therapies in selected PanNEN patients. Following further investigation in prospective clinical trials as well as mechanistic studies, the PanNETassigner molecular subtypes may potentially play a role, providing putative predictive biomarkers for such immune therapies.

5 Conclusions

The standardisation of PanNEN grading and staging, with the adoption of the WHO classification and ENETs/8th edition AJCC staging paradigms respectively, is an important step forward in the management of this rare disease. The current classification paradigm enables patients to be grouped into 4 grades and 4 stages of disease and has, without doubt, improved PanNEN management and facilitated patient stratification for clinical trials. Whilst these variables have prognostic significance, there remains a wide range of disease behaviour encompassed within each grade or stage. This is particularly apparent in the advanced disease setting, especially for grade 2 patients. This range of behaviour is likely due to heterogeneity in tumour biology which is not captured by the current classification paradigm. There is a well-recognised unmet clinical need for biomarkers to enable improved PanNEN patient stratification and treatment personalisation.

The aims of my thesis were shaped by this unmet need. Large, well annotated datasets are required to facilitate translational work and biomarker development. To this end, this MD(Res) project succeeded in established a large international PanNEN registry, which currently includes 282 patients and will increase in size with the addition of the Kings College cohort (Aim 1). The clinical phenotyping performed has confirmed that the registry patients are representative of PanNEN patients more generally and therefore provide a robust sample set for translational work and biomarker correlation (Aim 2). Further, to try and overcome some of the challenges experienced with retrospective tissue and data collection and with archived FFPE samples in the PanNEN registry, the RM sponsored Pac-MAN biobanking study has been developed. This study, which opened in January 2019, will enable the prospective collection of tissue and other biological specimens from PanNEN patients at multiple time-points, facilitating additional translational work in the future.

Molecular biomarkers have played an increasingly important role in prognostication and guiding treatment decisions across multiple tumour types in recent years^{234,235,236,237}. Organisations such as Cancer Research

UK (CRUK) have developed roadmaps to describe how a newly discovered potential biomarker may be developed into an assay, suitable for the clinic²³⁸. To be incorporated into clinical practice, assays detecting such prognostic or predictive biomarkers must be robust, reproducible and have undergone rigorous analytical and clinical validation, as well as demonstrating clinical utility and value for money²³⁹.

Our lab had previously defined 4 molecular subtypes in PanNEN, based on an integrated multi-omics analysis, collectively named the PanNETassigner signature⁵¹. The prognostic significance of the subtypes was previously unknown, but the association of one of the subtypes, MLP, with metastases led to the hypothesis that these subtypes may have prognostic significance and potentially could be developed as a molecular biomarker for PanNENs.

My thesis therefore sought to develop an assay based on the PanNETassigner subtypes which could be readily deployed to analyse trial samples or in clinic, using the low cost nCounter Elements platform (Aim 3). The PanNETassigner assay was successfully developed and refined into a 78 gene assay, the Nano-PanNET assay. The subtypes assigned by the assay were demonstrated to be reliable and reproducible. Further, the assay was able to assign PanNETassigner subtypes in both fresh frozen and more clinically available FFPE tumour samples, although further validation and optimisation is required in the FFPE setting in particular. The work described here is an essential preliminary step along the analytical validation pathway for the Nano-PanNET assay.

Having demonstrated that it was possible to ascribe PanNETassigner subtypes using the 78 gene assay, my thesis also considered the prognostic significance of the subtypes assigned. Survival analyses revealed that the MLP-1 subtype (approximately 20% of PanNEN patients) was associated with a statistically significant reduction in OS, whereas the Insulinoma-like subtype (approximately 30% of PanNEN patients) had a prolonged OS, with the Intermediate and MLP-2 subtypes being in the middle (Aim 4). As has been a problem for many PanNEN studies, the prolonged survival, and subsequent low number of events in the patients

analysed, meant that multivariate analyses were not possible here. As described above, it is hoped that the results presented here will be validated and further interrogated in a larger patient sample in due course.

Predictive as well as prognostic biomarkers are an unmet need in PanNENs. The first trials of immunotherapy are underway and, as for other tumour sites, biomarkers will be required to predict those patients who may benefit. A detailed understanding of the immune microenvironment in this disease is lacking and the last aim of my thesis was therefore to describe immune related gene expression, across our PanNETassigner subtypes (Aim 5).

This analysis demonstrated that the clinical parameters used to direct standard therapies, such as grade of disease or the presence of liver metastases did not segregate patients according to immune related gene expression. Conversely, our PanNETassigner subtypes were able to subdivide patients by differential immune gene expression, a finding which was confirmed in two separate validation cohorts. The poor prognosis MLP-1 subtype demonstrated both the highest level and diversity of immune-related gene expression, associated with hypoxic tumours and signalling within the DAMP pathway. The immune gene expression profile demonstrated generates the hypothesis that the MLP-1 subtype may be more amenable to an immunotherapeutic approach than other subtypes. The theories outlined in this chapter now require further investigation in mechanistic studies and prospective clinical trials.

Despite the limitations outlined in the discussions of each chapter, chiefly the retrospective nature of the PanNEN registry, the challenges of using FFPE tissue for molecular analyses and of survival analyses with limited events and the use of primarily baseline surgical resection specimens when assessing the dynamic immune system, the research presented here contributes significantly to the field. The large PanNEN registry, with additional samples still being collected, provides a useful platform for future clinical and biomarker studies in this setting. The PanNETassigner molecular subtypes have been identified as a potential future prognostic

biomarker, subject to validation, and the Nano-PanNET assay may provide a means for assigning these subtypes in clinic. Novel phenotypic data has been presented regarding the immune microenvironment in PanNENs which will hopefully lead to additional mechanistic studies and prospective clinical trials.

Overall, my thesis demonstrates that molecular subtyping can be used to provide valuable additional information both regarding prognosis and the immune microenvironment in PanNENs. With the further validation and investigation outlined, the PanNETassigner subtypes may pave a way forward for a more personalised, disease biology directed approach for patients with this rare tumour type.

References

1. Modlin IM, Lye KD, Kidd M. A 5-decade analysis of 13,715 carcinoid tumors. *Cancer*. 2003;97(4):934-959. doi:10.1002/cncr.11105.
2. Yao JC, Hassan M, Phan A, et al. One hundred years after "carcinoid": epidemiology of and prognostic factors for neuroendocrine tumors in 35,825 cases in the United States. *J Clin Oncol*. 2008;26(18):3063-3072. doi:10.1200/JCO.2007.15.4377.
3. Dasari A, Shen C, Halperin D, et al. Trends in the Incidence, Prevalence, and Survival Outcomes in Patients With Neuroendocrine Tumors in the United States. *JAMA Oncol*. 2017;3(10):1335-1342. doi:10.1001/jamaoncol.2017.0589.
4. Fraenkel M, Kim M, Faggiano A, de Herder WW, Valk GD, Incidence of gastroenteropancreatic neuroendocrine tumours: a systematic review of the literature. *Endocr Relat Cancer*. 2014;21(3):R153-R163. doi:10.1530/ERC-13-0125.
5. Hallet J, Law CHL, Cukier M, Saskin R, Liu N, Singh S. Exploring the rising incidence of neuroendocrine tumors: A population-based analysis of epidemiology, metastatic presentation, and outcomes. *Cancer*. 2015;121(4):589-597. doi:10.1002/cncr.29099.
6. Lee MR, Harris C, Baeg KJ, Aronson A, Wisnivesky JP, Kim MK. Incidence Trends of Gastroenteropancreatic Neuroendocrine Tumors in the United States. *Clin Gastroenterol Hepatol*. December 2018. doi:10.1016/j.cgh.2018.12.017.
7. Palepu J, Shrikhande S V., Bhaduri D, et al. Trends in diagnosis of gastroenteropancreatic neuroendocrine tumors (GEP-NETs) in India: A report of multicenter data from a web-based registry. *Indian J Gastroenterol*. 2017;36(6):445-451. doi:10.1007/s12664-017-0808-7.
8. Scherübl H, Streller B, Stabenow R, et al. Clinically detected gastroenteropancreatic neuroendocrine tumors are on the rise: Epidemiological changes in Germany. *World J Gastroenterol*. 2013;19(47):9012. doi:10.3748/wjg.v19.i47.9012.
9. Guo L-J, Wang C-H, Tang C-W. Epidemiological features of gastroenteropancreatic neuroendocrine tumors in Chengdu city with a population of 14 million based on data from a single institution. *Asia Pac J Clin Oncol*. 2016;12(3):284-288. doi:10.1111/ajco.12498.
10. Bosman, F.T., Carneiro, F., Hruban, R.H., Theise ND, IARC. *WHO Classification of Tumours 4th Edition, Volume 3 IARC*.; 2010.
11. Ekeblad S, Skogseid B, Dunder K, Oberg K, Eriksson B. Prognostic Factors and Survival in 324 Patients with Pancreatic Endocrine Tumor Treated at a Single Institution. *Clin Cancer Res*.

2008;14(23):7798-7803. doi:10.1158/1078-0432.CCR-08-0734.

12. International Agency for Research on Cancer, Lloyd R V., Osamura RY, Kloppel G. *Who Classification of Tumours of Endocrine Organs*. World Health Organization; 2017. <http://publications.iarc.fr/Book-And-Report-Series/Who-Iarc-Classification-Of-Tumours/Who-Classification-Of-Tumours-Of-Endocrine-Organs-2017>. Accessed October 23, 2017.
13. Falconi M, Eriksson B, Kaltsas G, et al. ENETS Consensus Guidelines Update for the Management of Patients with Functional Pancreatic Neuroendocrine Tumors and Non-Functional Pancreatic Neuroendocrine Tumors. *Neuroendocrinology*. 2016;103(2):153-171. doi:10.1159/000443171.
14. Modlin IM, Lye KD, Kidd M. A 5-decade analysis of 13,715 carcinoid tumors. *Cancer*. 2003;97(4):934-959. doi:10.1002/cncr.11105.
15. Oberg K, Knigge U, Kwekkeboom D, Perren A, ESMO Guidelines Working Group. Neuroendocrine gastro-entero-pancreatic tumors: ESMO Clinical Practice Guidelines for diagnosis, treatment and follow-up. *Ann Oncol*. 2012;23(suppl 7):vii124-vii130. doi:10.1093/annonc/mds295.
16. Basuroy R, Bouvier C, Ramage JK, Sissons M, Kent A, Srirajakanthan R. Presenting Symptoms and Delay in Diagnosis of Gastrointestinal and Pancreatic Neuroendocrine Tumours. *Neuroendocrinology*. 2018;107(1):42-49. doi:10.1159/000488510.
17. Kaltsas GA, Besser GM, Grossman AB. The Diagnosis and Medical Management of Advanced Neuroendocrine Tumors. *Endocr Rev*. 2004;25(3):458-511. doi:10.1210/er.2003-0014.
18. Modlin IM, Oberg K, Chung DC, et al. Gastroenteropancreatic neuroendocrine tumours. *Lancet Oncol*. 2008;9(1):61-72. doi:10.1016/S1470-2045(07)70410-2.
19. Young K, Iyer R, Morganstein D, Chau I, Cunningham D, Starling N. Pancreatic neuroendocrine tumors: a review. *Futur Oncol*. 2015;11(5):853-864. doi:10.2217/fo.14.285.
20. Garcia-Carbonero R, Sorbye H, Baudin E, et al. ENETS Consensus Guidelines for High-Grade Gastroenteropancreatic Neuroendocrine Tumors and Neuroendocrine Carcinomas. *Neuroendocrinology*. 2016;103(2):186-194. doi:10.1159/000443172.
21. Kunz PL, Reidy-Lagunes D, Anthony LB, et al. Consensus Guidelines for the Management and Treatment of Neuroendocrine Tumors. *Pancreas*. 2013;42(4):557-577. doi:10.1097/MPA.0b013e31828e34a4.
22. Rindi G, Klöppel G, Alhman H, et al. TNM staging of foregut (neuro)endocrine tumors: a consensus proposal including a grading system. *Virchows Arch*. 2006;449(4):395-401. doi:10.1007/s00428-

006-0250-1.

23. Li X, Gou S, Liu Z, Ye Z, Wang C. Assessment of the American Joint Commission on Cancer 8th Edition Staging System for Patients with Pancreatic Neuroendocrine Tumors: A Surveillance, Epidemiology, and End Results analysis. *Cancer Med.* 2018;7(3):626-634. doi:10.1002/cam4.1336.
24. Luo G, Javed A, Strosberg JR, et al. Modified Staging Classification for Pancreatic Neuroendocrine Tumors on the Basis of the American Joint Committee on Cancer and European Neuroendocrine Tumor Society Systems. *J Clin Oncol.* 2017;35(3):274-280. doi:10.1200/JCO.2016.67.8193.
25. Klöppel G, La Rosa S. Ki67 labeling index: assessment and prognostic role in gastroenteropancreatic neuroendocrine neoplasms. *Virchows Arch.* 2018;472(3):341-349. doi:10.1007/s00428-017-2258-0.
26. Scarpa A, Mantovani W, Capelli P, et al. Pancreatic endocrine tumors: improved TNM staging and histopathological grading permit a clinically efficient prognostic stratification of patients. *Mod Pathol.* 2010;23(6):824-833. doi:10.1038/modpathol.2010.58.
27. Yachida S, Vakiani E, White CM, et al. Small Cell and Large Cell Neuroendocrine Carcinomas of the Pancreas are Genetically Similar and Distinct From Well-differentiated Pancreatic Neuroendocrine Tumors. *Am J Surg Pathol.* 2012;36(2):173-184. doi:10.1097/PAS.0b013e3182417d36.
28. Jiao Y, Shi C, Edil BH, et al. DAXX/ATRX, MEN1, and mTOR pathway genes are frequently altered in pancreatic neuroendocrine tumors. *Science.* 2011;331(6021):1199-1203. doi:10.1126/science.1200609.
29. Scarpa A, Chang DK, Nones K, et al. Whole-genome landscape of pancreatic neuroendocrine tumours. *Nature.* 2017;543(7643):65-71. doi:10.1038/nature21063.
30. Ricci C, Casadei R, Taffurelli G, et al. WHO 2010 classification of pancreatic endocrine tumors. is the new always better than the old? *Pancreatology.* 14(6):539-541. doi:10.1016/j.pan.2014.09.005.
31. Hauck L, Bitzer M, Malek N, Plentz RR. Subgroup analysis of patients with G2 gastroenteropancreatic neuroendocrine tumors. *Scand J Gastroenterol.* July 2015:1-5. doi:10.3109/00365521.2015.1064994.
32. Reid MD, Balci S, Saka B, Adsay NV. Neuroendocrine tumors of the pancreas: current concepts and controversies. *Endocr Pathol.* 2014;25(1):65-79. doi:10.1007/s12022-013-9295-2.
33. Basturk O, Yang Z, Tang LH, et al. The High-grade (WHO G3) Pancreatic Neuroendocrine Tumor Category Is Morphologically and Biologically Heterogenous and Includes Both Well Differentiated and

Poorly Differentiated Neoplasms. *Am J Surg Pathol*. 2015;39(5):683-690. doi:10.1097/PAS.0000000000000408.

34. La Rosa S, Sessa F, Capella C, et al. Prognostic criteria in nonfunctioning pancreatic endocrine tumours. *Virchows Arch*. 1996;429(6):323-333. <http://www.ncbi.nlm.nih.gov/pubmed/8982376>. Accessed May 31, 2019.
35. Pape U, Jann H, Müller-Nordhorn J, et al. Prognostic relevance of a novel TNM classification system for upper gastroenteropancreatic neuroendocrine tumors. *Cancer*. 2008;113(2):256-265. doi:10.1002/cncr.23549.
36. Garcia-Carbonero R, Capdevila J, Crespo-Herrero G, et al. Incidence, patterns of care and prognostic factors for outcome of gastroenteropancreatic neuroendocrine tumors (GEP-NETs): results from the National Cancer Registry of Spain (RGETNE). *Ann Oncol*. 2010;21(9):1794-1803. doi:10.1093/annonc/mdq022.
37. Khan MS, Luong T V, Watkins J, Toumpanakis C, Caplin ME, Meyer T. A comparison of Ki-67 and mitotic count as prognostic markers for metastatic pancreatic and midgut neuroendocrine neoplasms. *Br J Cancer*. 2013;108(9):1838-1845. doi:10.1038/bjc.2013.156.
38. Bu J, Youn S, Kwon W, et al. Prognostic factors of non-functioning pancreatic neuroendocrine tumor revisited: The value of WHO 2010 classification. *Ann hepato-biliary-pancreatic Surg*. 2018;22(1):66-74. doi:10.14701/ahbps.2018.22.1.66.
39. Pelosi G, Bresaola E, Bogina G, et al. Endocrine tumors of the pancreas: Ki-67 immunoreactivity on paraffin sections is an independent predictor for malignancy: a comparative study with proliferating-cell nuclear antigen and progesterone receptor protein immunostaining, mitotic index, and othe. *Hum Pathol*. 1996;27(11):1124-1134. <http://www.ncbi.nlm.nih.gov/pubmed/8912819>. Accessed May 26, 2019.
40. Panzuto F, Boninsegna L, Fazio N, et al. Metastatic and locally advanced pancreatic endocrine carcinomas: analysis of factors associated with disease progression. *J Clin Oncol*. 2011;29(17):2372-2377. doi:10.1200/JCO.2010.33.0688.
41. Rindi G, Falconi M, Klersy C, et al. TNM staging of neoplasms of the endocrine pancreas: results from a large international cohort study. *J Natl Cancer Inst*. 2012;104(10):764-777. doi:10.1093/jnci/djs208.
42. Sorbye H, Welin S, Langer SW, et al. Predictive and prognostic factors for treatment and survival in 305 patients with advanced gastrointestinal neuroendocrine carcinoma (WHO G3): the NORDIC NEC study. *Ann Oncol*. 2013;24(1):152-160. doi:10.1093/annonc/mds276.

43. Karpathakis A, Dibra H, Pipinikas C, et al. Prognostic Impact of Novel Molecular Subtypes of Small Intestinal Neuroendocrine Tumor. *Clin Cancer Res.* 22(1):250-258. doi:10.1158/1078-0432.CCR-15-0373.
44. Yao J, Garg A, Chen D, et al. Genomic profiling of NETs: a comprehensive analysis of the RADIANT trials. *Endocr Relat Cancer.* 2019;26(4):391-403. doi:10.1530/ERC-18-0332.
45. Chan DL, Clarke SJ, Diakos CI, et al. Prognostic and predictive biomarkers in neuroendocrine tumours. *Crit Rev Oncol.* 2017;113:268-282. doi:10.1016/j.critrevonc.2017.03.017.
46. Marinoni I, Kurrer AS, Vassella E, et al. Loss of DAXX and ATRX are associated with chromosome instability and reduced survival of patients with pancreatic neuroendocrine tumors. *Gastroenterology.* 2014;146(2):453-60.e5. doi:10.1053/j.gastro.2013.10.020.
47. Singhi AD, Liu T-C, Roncaioli JL, et al. Alternative Lengthening of Telomeres and Loss of DAXX/ATRX Expression Predicts Metastatic Disease and Poor Survival in Patients with Pancreatic Neuroendocrine Tumors. *Clin Cancer Res.* 2017;23(2):600-609. doi:10.1158/1078-0432.CCR-16-1113.
48. Park JK, Paik WH, Lee K, Ryu JK, Lee SH, Kim Y-T. DAXX/ATRX and MEN1 genes are strong prognostic markers in pancreatic neuroendocrine tumors. *Oncotarget.* 2017;8(30):49796-49806. doi:10.18632/oncotarget.17964.
49. Duerr E-M, Mizukami Y, Ng A, et al. Defining molecular classifications and targets in gastroenteropancreatic neuroendocrine tumors through DNA microarray analysis. *Endocr Relat Cancer.* 2008;15(1):243-256. doi:10.1677/ERC-07-0194.
50. Simbolo M, Barbi S, Fassan M, et al. Gene expression profiling of lung atypical carcinoids and large cell neuroendocrine carcinomas identifies three transcriptomic subtypes with specific genomic alterations. *J Thorac Oncol.* May 2019. doi:10.1016/j.jtho.2019.05.003.
51. Sadanandam A, Wulschleger S, Lyssiotis CA, et al. A Cross-Species Analysis in Pancreatic Neuroendocrine Tumors Reveals Molecular Subtypes with Distinctive Clinical, Metastatic, Developmental, and Metabolic Characteristics. *Cancer Discov.* 2015;5(12):1296-1313. doi:10.1158/2159-8290.CD-15-0068.
52. Ramage JK, Ahmed A, Ardill J, et al. Guidelines for the management of gastroenteropancreatic neuroendocrine (including carcinoid) tumours (NETs). *Gut.* 2012;61(1):6-32. doi:10.1136/gutjnl-2011-300831.
53. Pavel M, O'Toole D, Costa F, et al. ENETS Consensus Guidelines Update for the Management of Distant Metastatic Disease of Intestinal, Pancreatic, Bronchial Neuroendocrine Neoplasms (NEN)

and NEN of Unknown Primary Site. *Neuroendocrinology*. 2016;103(2):172-185. doi:10.1159/000443167.

54. Hendifar AE, Dhall D, Strosberg JR. The Evolving Treatment Algorithm for Advanced Neuroendocrine Neoplasms: Diversity and Commonalities Across Tumor Types. *Oncologist*. 2019;24(1):54-61. doi:10.1634/theoncologist.2018-0187.
55. Kaderli RM, Spanjol M, Kollár A, et al. Therapeutic Options for Neuroendocrine Tumors: A Systematic Review and Network Meta-analysis. *JAMA Oncol*. 2019;5(4):480. doi:10.1001/jamaoncol.2018.6720.
56. Mehnert JM, Rugo HS, O'Neil BH, et al. 427OPembrolizumab for patients with PD-L1–positive advanced carcinoid or pancreatic neuroendocrine tumors: Results from the KEYNOTE-028 study. *Ann Oncol*. 2017;28(suppl_5). doi:10.1093/annonc/mdx368.
57. Oberg K, Modlin IM, De Herder W, et al. Consensus on biomarkers for neuroendocrine tumour disease. *Lancet Oncol*. 2015. doi:10.1016/S1470-2045(15)00186-2.
58. Jensen RT, Bodei L, Capdevila J, et al. Unmet Needs in Functional and Nonfunctional Pancreatic Neuroendocrine Neoplasms. *Neuroendocrinology*. 2019;108(1):26-36. doi:10.1159/000494258.
59. Rinke A, Müller H-H, Schade-Brittinger C, et al. Placebo-controlled, double-blind, prospective, randomized study on the effect of octreotide LAR in the control of tumor growth in patients with metastatic neuroendocrine midgut tumors: a report from the PROMID Study Group. *J Clin Oncol*. 2009;27(28):4656-4663. doi:10.1200/JCO.2009.22.8510.
60. Caplin ME, Pavel M, Ćwikła JB, et al. Lanreotide in Metastatic Enteropancreatic Neuroendocrine Tumors. *N Engl J Med*. 2014;371(3):224-233. doi:10.1056/NEJMoa1316158.
61. Raymond E, Dahan L, Raoul J-L, et al. Sunitinib Malate for the Treatment of Pancreatic Neuroendocrine Tumors. *N Engl J Med*. 2011;364(6):501-513. doi:10.1056/NEJMoa1003825.
62. Pavel ME, Baudin E, Öberg KE, et al. Efficacy of everolimus plus octreotide LAR in patients with advanced neuroendocrine tumor and carcinoid syndrome: final overall survival from the randomized, placebo-controlled phase 3 RADIANT-2 study. *Ann Oncol*. 2017;28(7):1569-1575. doi:10.1093/annonc/mdx193.
63. Yao JC, Shah MH, Ito T, et al. Everolimus for Advanced Pancreatic Neuroendocrine Tumors. *N Engl J Med*. 2011;364(6):514-523. doi:10.1056/NEJMoa1009290.
64. Moertel CG, Lefkopoulo M, Lipsitz S, Hahn RG, Klaassen D. Streptozocin–Doxorubicin, Streptozocin–Fluorouracil, or Chlorozotocin in the Treatment of Advanced Islet-Cell Carcinoma. *N*

Engl J Med. 1992;326(8):519-523.
doi:10.1056/NEJM199202203260804.

65. Moertel CG, Hanley JA, Johnson LA. Streptozocin Alone Compared with Streptozocin plus Fluorouracil in the Treatment of Advanced Islet-Cell Carcinoma. *N Engl J Med.* 1980;303(21):1189-1194. doi:10.1056/NEJM198011203032101.
66. Kouvaraki MA, Ajani JA, Hoff P, et al. Fluorouracil, Doxorubicin, and Streptozocin in the Treatment of Patients With Locally Advanced and Metastatic Pancreatic Endocrine Carcinomas. *J Clin Oncol.* 2004;22(23):4762-4771. doi:10.1200/JCO.2004.04.024.
67. Dilz L-M, Denecke T, Steffen IG, et al. Streptozocin/5-fluorouracil chemotherapy is associated with durable response in patients with advanced pancreatic neuroendocrine tumours. *Eur J Cancer.* 2015;51(10):1253-1262. doi:10.1016/j.ejca.2015.04.005.
68. Kunz PL, Catalano PJ, Nimeiri H, et al. A randomized study of temozolomide or temozolomide and capecitabine in patients with advanced pancreatic neuroendocrine tumors: A trial of the ECOG-ACRIN Cancer Research Group (E2211). *J Clin Oncol.* 2018;36(15_suppl):4004-4004. doi:10.1200/JCO.2018.36.15_suppl.4004.
69. Strosberg JR, Wolin EM, Chasen B, et al. NETTER-1 phase III: Efficacy and safety results in patients with midgut neuroendocrine tumors treated with ¹⁷⁷Lu-DOTATATE. *J Clin Oncol.* 2016;34(15_suppl):4005-4005. doi:10.1200/JCO.2016.34.15_suppl.4005.
70. Brabander T, van der Zwan WA, Teunissen JJM, et al. Long-Term Efficacy, Survival, and Safety of [177Lu-DOTA0,Tyr3]octreotate in Patients with Gastroenteropancreatic and Bronchial Neuroendocrine Tumors. *Clin Cancer Res.* 2017;23(16):4617-4624. doi:10.1158/1078-0432.CCR-16-2743.
71. de Baere T, Deschamps F, Tselikas L, et al. GEP-NETS UPDATE: Interventional radiology: role in the treatment of liver metastases from GEP-NETs. *Eur J Endocrinol.* 2015;172(4):R151-R166. doi:10.1530/EJE-14-0630.
72. Shah H, Benson AB, Lurie RH, et al. **Manisha NCCN Guidelines Panel Disclosures Continue NCCN Guidelines Version 1.2019 Neuroendocrine and Adrenal Tumors.*; 2019. www.nccn.org/patients. Accessed June 10, 2019.
73. Herrera-Martínez AD, Hofland LJ, Gálvez Moreno MA, Castaño JP, de Herder WW, Feelders RA. Neuroendocrine neoplasms: current and potential diagnostic, predictive and prognostic markers. *Endocr Relat Cancer.* 2019;26(3):R157-R179. doi:10.1530/ERC-18-0354.
74. Yao JC, Pavel M, Phan AT, et al. Chromogranin A and Neuron-

Specific Enolase as Prognostic Markers in Patients with Advanced pNET Treated with Everolimus. *J Clin Endocrinol Metab.* 2011;96(12):3741-3749. doi:10.1210/jc.2011-0666.

75. Ter-Minassian M, Chan JA, Hooshmand SM, et al. Clinical presentation, recurrence, and survival in patients with neuroendocrine tumors: results from a prospective institutional database. *Endocr Relat Cancer.* 2013;20(2):187-196. doi:10.1530/ERC-12-0340.
76. Khan MS, Kirkwood AA, Tsigani T, et al. Early Changes in Circulating Tumor Cells Are Associated with Response and Survival Following Treatment of Metastatic Neuroendocrine Neoplasms. *Clin Cancer Res.* 2016;22(1):79-85. doi:10.1158/1078-0432.CCR-15-1008.
77. Sherman SK, Maxwell JE, O'Dorisio MS, O'Dorisio TM, Howe JR. Pancreastatin predicts survival in neuroendocrine tumors. *Ann Surg Oncol.* 2014;21(9):2971-2980. doi:10.1245/s10434-014-3728-0.
78. Strosberg D, Schneider EB, Onesti J, et al. Prognostic Impact of Serum Pancreastatin Following Chemoembolization for Neuroendocrine Tumors. *Ann Surg Oncol.* 2018;25(12):3613-3620. doi:10.1245/s10434-018-6741-x.
79. Qian ZR, Ter-Minassian M, Chan JA, et al. Prognostic Significance of MTOR Pathway Component Expression in Neuroendocrine Tumors. *J Clin Oncol.* 2013;31(27):3418-3425. doi:10.1200/JCO.2012.46.6946.
80. Missiaglia E, Dalai I, Barbi S, et al. Pancreatic endocrine tumors: expression profiling evidences a role for AKT-mTOR pathway. *J Clin Oncol.* 2010;28(2):245-255. doi:10.1200/JCO.2008.21.5988.
81. Kim HS, Lee HS, Nam KH, Choi J, Kim WH. p27 Loss Is Associated with Poor Prognosis in Gastroenteropancreatic Neuroendocrine Tumors. *Cancer Res Treat.* 2014;46(4):383-392. doi:10.4143/crt.2013.102.
82. Khan MS, Kirkwood A, Tsigani T, et al. Circulating Tumor Cells As Prognostic Markers in Neuroendocrine Tumors. *J Clin Oncol.* 2013;31(3):365-372. doi:10.1200/JCO.2012.44.2905.
83. La Rosa S, Rigoli E, Uccella S, Novario R, Capella C. Prognostic and biological significance of cytokeratin 19 in pancreatic endocrine tumours. *Histopathology.* 2007;50(5):597-606. doi:10.1111/j.1365-2559.2007.02662.x.
84. Son E-M, Kim JY, An S, et al. Clinical and Prognostic Significances of Cytokeratin 19 and KIT Expression in Surgically Resectable Pancreatic Neuroendocrine Tumors. *J Pathol Transl Med.* 2015;49(1):30-36. doi:10.4132/jptm.2014.10.23.
85. Mehta S, de Reuver PR, Gill P, et al. Somatostatin Receptor SSTR-2a Expression Is a Stronger Predictor for Survival Than Ki-67 in Pancreatic Neuroendocrine Tumors. *Medicine (Baltimore).*

2015;94(40):e1281. doi:10.1097/MD.0000000000001281.

86. Roldo C, Missiaglia E, Hagan JP, et al. MicroRNA expression abnormalities in pancreatic endocrine and acinar tumors are associated with distinctive pathologic features and clinical behavior. *J Clin Oncol.* 2006;24(29):4677-4684. doi:10.1200/JCO.2005.05.5194.
87. Malczewska A, Kidd M, Matar S, Kos-Kudla B, Modlin IM. A Comprehensive Assessment of the Role of miRNAs as Biomarkers in Gastroenteropancreatic Neuroendocrine Tumors. *Neuroendocrinology.* 2018;107(1):73-90. doi:10.1159/000487326.
88. Treglia G, Castaldi P, Rindi G, Giordano A, Rufini V. Diagnostic performance of Gallium-68 somatostatin receptor PET and PET/CT in patients with thoracic and gastroenteropancreatic neuroendocrine tumours: a meta-analysis. *Endocrine.* 2012;42(1):80-87. doi:10.1007/s12020-012-9631-1.
89. Ambrosini V, Campana D, Polverari G, et al. Prognostic Value of 68Ga-DOTANOC PET/CT SUVmax in Patients with Neuroendocrine Tumors of the Pancreas. *J Nucl Med.* 2015;56(12):1843-1848. doi:10.2967/jnumed.115.162719.
90. Campana D, Ambrosini V, Pezzilli R, et al. Standardized Uptake Values of 68Ga-DOTANOC PET: A Promising Prognostic Tool in Neuroendocrine Tumors. *J Nucl Med.* 2010;51(3):353-359. doi:10.2967/jnumed.109.066662.
91. Tirosh A, Papadakis GZ, Millo C, et al. Prognostic Utility of Total 68 Ga-DOTATATE-Avid Tumor Volume in Patients With Neuroendocrine Tumors. *Gastroenterology.* 2018;154(4):998-1008.e1. doi:10.1053/j.gastro.2017.11.008.
92. Bahri H, Laurence L, Edeline J, et al. High prognostic value of 18F-FDG PET for metastatic gastroenteropancreatic neuroendocrine tumors: a long-term evaluation. *J Nucl Med.* 2014;55(11):1786-1790. doi:10.2967/jnumed.114.144386.
93. Garin E, Le Jeune F, Devillers A, et al. Predictive Value of 18F-FDG PET and Somatostatin Receptor Scintigraphy in Patients with Metastatic Endocrine Tumors. *J Nucl Med.* 2009;50(6):858-864. doi:10.2967/jnumed.108.057505.
94. Chan DL, Pavlakis N, Schembri GP, et al. Dual Somatostatin Receptor/FDG PET/CT Imaging in Metastatic Neuroendocrine Tumours: Proposal for a Novel Grading Scheme with Prognostic Significance. *Theranostics.* 2017;7(5):1149-1158. doi:10.7150/thno.18068.
95. Zurita AJ, Khajavi M, Wu H-K, et al. Circulating cytokines and monocyte subpopulations as biomarkers of outcome and biological activity in sunitinib-treated patients with advanced neuroendocrine tumours. *Br J Cancer.* 2015;112(7):1199-1205.

doi:10.1038/bjc.2015.73.

96. Yao JC, Shah M, Panneerselvam ; Ashok, et al. *The VEGF Pathway in Pancreatic Neuroendocrine Tumors: Prognostic and Predictive Capacity of Baseline Biomarker Levels on Efficacy of Everolimus Analyzed From the RADIANT-3 Study*. <https://nanets.net/abstracts-archive/2012/220-c51-the-vegf-pathway-in-pancreatic-neuroendocrine-tumors-prognostic-and-predictive-capacity-of-baseline-biomarker-levels-on-efficacy-of-everolimus-analyzed-from-the-radiant-3-study/file>. Accessed June 10, 2019.
97. Falletta S, Partelli S, Rubini C, et al. mTOR inhibitors response and mTOR pathway in pancreatic neuroendocrine tumors. *Endocr Relat Cancer*. 2016;23(11):883-891. doi:10.1530/ERC-16-0329.
98. Gerson SL. Clinical Relevance of *MGMT* in the Treatment of Cancer. *J Clin Oncol*. 2002;20(9):2388-2399. doi:10.1200/JCO.2002.06.110.
99. Schmitt AM, Pavel M, Rudolph T, et al. Prognostic and predictive roles of *MGMT* protein expression and promoter methylation in sporadic pancreatic neuroendocrine neoplasms. *Neuroendocrinology*. 2014;100(1):35-44. doi:10.1159/000365514.
100. Cros J, Hentic O, Rebours V, et al. *MGMT* expression predicts response to temozolomide in pancreatic neuroendocrine tumors. *Endocr Relat Cancer*. 2016;23(8):625-633. doi:10.1530/ERC-16-0117.
101. Brigliadori G, Foca F, Dall'Agata M, et al. Defining the cutoff value of *MGMT* gene promoter methylation and its predictive capacity in glioblastoma. *J Neurooncol*. 2016;128(2):333-339. doi:10.1007/s11060-016-2116-y.
102. Drozdov I, Kidd M, Nadler B, et al. Predicting neuroendocrine tumor (carcinoid) neoplasia using gene expression profiling and supervised machine learning. *Cancer*. 2009;115(8):1638-1650. doi:10.1002/cncr.24180.
103. Modlin IM, Kidd M, Malczewska A, et al. The NETest. *Endocrinol Metab Clin North Am*. 2018;47(3):485-504. doi:10.1016/j.ecl.2018.05.002.
104. Modlin IM, Kidd M, Bodei L, Drozdov I, Aslanian H. The clinical utility of a novel blood-based multi-transcriptome assay for the diagnosis of neuroendocrine tumors of the gastrointestinal tract. *Am J Gastroenterol*. 2015;110(8):1223-1232. doi:10.1038/ajg.2015.160.
105. Modlin IM, Frilling A, Salem RR, et al. Blood measurement of neuroendocrine gene transcripts defines the effectiveness of operative resection and ablation strategies. *Surgery*. 2016;159(1):336-347. doi:10.1016/j.surg.2015.06.056.
106. Ćwikła JB, Bodei L, Kolasinska-Ćwikła A, Sankowski A, Modlin IM, Kidd M. Circulating Transcript Analysis (NETest) in GEP-NETs

Treated With Somatostatin Analogs Defines Therapy. *J Clin Endocrinol Metab.* 2015;100(11):E1437-E1445. doi:10.1210/jc.2015-2792.

107. Bodei L, Kidd M, Modlin IM, et al. Measurement of circulating transcripts and gene cluster analysis predicts and defines therapeutic efficacy of peptide receptor radionuclide therapy (PRRT) in neuroendocrine tumors. *Eur J Nucl Med Mol Imaging.* 2016;43(5):839-851. doi:10.1007/s00259-015-3250-z.
108. Kinross JM, Drymoussis P, Jiménez B, Frilling A. Metabonomic profiling: a novel approach in neuroendocrine neoplasias. *Surgery.* 2013;154(6):1185-92-3. <http://www.ncbi.nlm.nih.gov/pubmed/24383116>. Accessed June 7, 2019.
109. Komatsubara KM, Carvajal RD. The promise and challenges of rare cancer research. *Lancet Oncol.* 2016;17(2):136-138. doi:10.1016/S1470-2045(15)00485-4.
110. Scarpa A. The landscape of molecular alterations in pancreatic and small intestinal neuroendocrine tumours. *Ann Endocrinol (Paris).* 2019;80(3):153-158. doi:10.1016/j.ando.2019.04.010.
111. Foubert F, Salimon M, Dumars C, et al. Survival and prognostic factors analysis of 151 intestinal and pancreatic neuroendocrine tumors: a single center experience. *J Gastrointest Oncol.* 2018;10(1):103-111. doi:10.21037/jgo.2018.09.13.
112. Rindi G, Klersy C, Albarello L, et al. Competitive Testing of the WHO 2010 versus the WHO 2017 Grading of Pancreatic Neuroendocrine Neoplasms: Data from a Large International Cohort Study. *Neuroendocrinology.* 2018;107(4):375-386. doi:10.1159/000494355.
113. Panzuto F, Boninsegna L, Fazio N, et al. Metastatic and locally advanced pancreatic endocrine carcinomas: analysis of factors associated with disease progression. *J Clin Oncol.* 2011;29(17):2372-2377. doi:10.1200/JCO.2010.33.0688.
114. Riihimäki M, Hemminki A, Sundquist K, Sundquist J, Hemminki K. The epidemiology of metastases in neuroendocrine tumors. *Int J Cancer.* 2016;139(12):2679-2686. doi:10.1002/ijc.30400.
115. Monaghan PJ, Lamarca A, Valle JW, et al. Routine measurement of plasma chromogranin B has limited clinical utility in the management of patients with neuroendocrine tumours. *Clin Endocrinol (Oxf).* 2016;84(3):348-352. doi:10.1111/cen.12985.
116. Marotta V, Zatelli MC, Sciammarella C, et al. Chromogranin A as circulating marker for diagnosis and management of neuroendocrine neoplasms: more flaws than fame. *Endocr Relat Cancer.* 2018;25(1):R11-R29. doi:10.1530/ERC-17-0269.
117. Kidd M, Bodei L, Modlin IM. Chromogranin A. *Curr Opin Endocrinol*

Diabetes Obes. 2016;23(1):28-37.
doi:10.1097/MED.0000000000000215.

118. Kruljac I, Vurnek I, Maasberg S, et al. A score derived from routine biochemical parameters increases the diagnostic accuracy of chromogranin A in detecting patients with neuroendocrine neoplasms. *Endocrine.* 2018;60(3):395-406. doi:10.1007/s12020-018-1592-6.
119. Scarpa A, Mantovani W, Capelli P, et al. Pancreatic endocrine tumors: improved TNM staging and histopathological grading permit a clinically efficient prognostic stratification of patients. *Mod Pathol.* 2010;23(6):824-833. doi:10.1038/modpathol.2010.58.
120. Cavalcanti MS, Gönen M, Klimstra DS. The ENETS/WHO grading system for neuroendocrine neoplasms of the gastroenteropancreatic system: a review of the current state, limitations and proposals for modifications. *Int J Endocr Oncol.* 2016;3(3):203. doi:10.2217/IJE-2016-0006.
121. Klimstra DS, Modlin IR, Adsay NV, et al. Pathology Reporting of Neuroendocrine Tumors: Application of the Delphic Consensus Process to the Development of a Minimum Pathology Data Set. *Am J Surg Pathol.* 2010;34(3):300-313. doi:10.1097/PAS.0b013e3181ce1447.
122. Nielsen TO, Parker JS, Leung S, et al. A comparison of PAM50 intrinsic subtyping with immunohistochemistry and clinical prognostic factors in tamoxifen-treated estrogen receptor-positive breast cancer. *Clin Cancer Res.* 2010;16(21):5222-5232. doi:10.1158/1078-0432.CCR-10-1282.
123. Metzger Filho O, Ignatiadis M, Sotiriou C. Genomic Grade Index: An important tool for assessing breast cancer tumor grade and prognosis. *Crit Rev Oncol Hematol.* 2011;77(1):20-29. doi:10.1016/j.critrevonc.2010.01.011.
124. Ma X-J, Salunga R, Dahiya S, et al. A five-gene molecular grade index and HOXB13:IL17BR are complementary prognostic factors in early stage breast cancer. *Clin Cancer Res.* 2008;14(9):2601-2608. doi:10.1158/1078-0432.CCR-07-5026.
125. Veldman-Jones MH, Brant R, Rooney C, et al. Evaluating Robustness and Sensitivity of the NanoString Technologies nCounter Platform to Enable Multiplexed Gene Expression Analysis of Clinical Samples. *Cancer Res.* 2015;75(13):2587-2593. doi:10.1158/0008-5472.CAN-15-0262.
126. Nielsen T, Wallden B, Schaper C, et al. Analytical validation of the PAM50-based Prosigna Breast Cancer Prognostic Gene Signature Assay and nCounter Analysis System using formalin-fixed paraffin-embedded breast tumor specimens. *BMC Cancer.* 2014;14(1):177. doi:10.1186/1471-2407-14-177.

127. Kim ST, Do I-G, Lee J, Sohn I, Kim K-M, Kang WK. The NanoString-based multigene assay as a novel platform to screen EGFR, HER2, and MET in patients with advanced gastric cancer. *Clin Transl Oncol*. 2015;17(6):462-468. doi:10.1007/s12094-014-1258-7.
128. Chang KTE, Goytain A, Tucker T, et al. Development and Evaluation of a Pan-Sarcoma Fusion Gene Detection Assay Using the NanoString nCounter Platform. *J Mol Diagnostics*. 2018;20(1):63-77. doi:10.1016/j.jmoldx.2017.09.007.
129. Lira ME, Choi Y-L, Lim SM, et al. A single-tube multiplexed assay for detecting ALK, ROS1, and RET fusions in lung cancer. *J Mol Diagn*. 2014;16(2):229-243. doi:10.1016/j.jmoldx.2013.11.007.
130. Scott DW, Chan FC, Hong F, et al. Gene Expression–Based Model Using Formalin-Fixed Paraffin-Embedded Biopsies Predicts Overall Survival in Advanced-Stage Classical Hodgkin Lymphoma. *J Clin Oncol*. 2013;31(6):692-700. doi:10.1200/JCO.2012.43.4589.
131. Ayers M, Lunceford J, Nebozhyn M, et al. IFN- γ -related mRNA profile predicts clinical response to PD-1 blockade. *J Clin Invest*. 2017;127(8):2930-2940. doi:10.1172/JCI91190.
132. Collisson EA, Sadanandam A, Olson P, et al. Subtypes of pancreatic ductal adenocarcinoma and their differing responses to therapy. *Nat Med*. 2011;17(4):500-503. doi:10.1038/nm.2344.
133. Gentleman RC, Carey VJ, Bates DM, et al. Bioconductor: open software development for computational biology and bioinformatics. *Genome Biol*. 2004;5(10):R80. doi:10.1186/gb-2004-5-10-r80.
134. Sadanandam A, Lyssiotis CA, Homicsko K, et al. A colorectal cancer classification system that associates cellular phenotype and responses to therapy. *Nat Med*. 2013;19(5):619-625. doi:10.1038/nm.3175.
135. Ali N, Rampazzo R de CP, Costa ADT, Krieger MA. Current Nucleic Acid Extraction Methods and Their Implications to Point-of-Care Diagnostics. *Biomed Res Int*. 2017;2017:9306564. doi:10.1155/2017/9306564.
136. Kulkarni MM. Digital Multiplexed Gene Expression Analysis Using the NanoString nCounter System. In: *Current Protocols in Molecular Biology*. Vol Chapter 25. Hoboken, NJ, USA: John Wiley & Sons, Inc.; 2011:Unit25B.10. doi:10.1002/0471142727.mb25b10s94.
137. Geiss GK, Bumgarner RE, Birditt B, et al. Direct multiplexed measurement of gene expression with color-coded probe pairs. *Nat Biotechnol*. 2008;26(3):317-325. doi:10.1038/nbt1385.
138. Bailey P, Chang DK, Nones K, et al. Genomic analyses identify molecular subtypes of pancreatic cancer. *Nature*. 2016;531(7592):47-52. doi:10.1038/nature16965.

139. Smyth EC, Nyamundanda G, Cunningham D, et al. A seven-Gene Signature assay improves prognostic risk stratification of perioperative chemotherapy treated gastroesophageal cancer patients from the MAGIC trial. *Ann Oncol.* 2018;29(12):2356-2362. doi:10.1093/annonc/mdy407.
140. Nyamundanda G, Poudel P, Patil Y, Sadanandam A. A Novel Statistical Method to Diagnose, Quantify and Correct Batch Effects in Genomic Studies. *Sci Rep.* 2017;7(1):10849. doi:10.1038/s41598-017-11110-6.
141. Chen C, Grennan K, Badner J, et al. Removing Batch Effects in Analysis of Expression Microarray Data: An Evaluation of Six Batch Adjustment Methods. Kliebenstein D, ed. *PLoS One.* 2011;6(2):e17238. doi:10.1371/journal.pone.0017238.
142. Devarajan K. Nonnegative Matrix Factorization: An Analytical and Interpretive Tool in Computational Biology. *PLoS Comput Biol.* 2008;4(7):e1000029. doi:10.1371/JOURNAL.PCBI.1000029.
143. Gaujoux R, Seoighe C. A flexible R package for nonnegative matrix factorization. *BMC Bioinformatics.* 2010;11(1):367. doi:10.1186/1471-2105-11-367.
144. Tusher VG, Tibshirani R, Chu G. Significance analysis of microarrays applied to the ionizing radiation response. *Proc Natl Acad Sci.* 2001;98(9):5116-5121. doi:10.1073/pnas.091062498.
145. Tibshirani R, Hastie T, Narasimhan B, Chu G. Diagnosis of multiple cancer types by shrunken centroids of gene expression. *Proc Natl Acad Sci.* 2002;99(10):6567-6572. doi:10.1073/pnas.082099299.
146. Taslamani L, Nilsson B. A framework for regularized non-negative matrix factorization, with application to the analysis of gene expression data. *PLoS One.* 2012;7(11):e46331. doi:10.1371/journal.pone.0046331.
147. Reis PP, Waldron L, Goswami RS, et al. mRNA transcript quantification in archival samples using multiplexed, color-coded probes. *BMC Biotechnol.* 2011;11(1):46. doi:10.1186/1472-6750-11-46.
148. von Ahlfen S, Missel A, Bendrat K, Schlumpberger M. Determinants of RNA quality from FFPE samples. *PLoS One.* 2007;2(12):e1261. doi:10.1371/journal.pone.0001261.
149. Ragulan C, Eason K, Fontana E, et al. Analytical Validation of Multiplex Biomarker Assay to Stratify Colorectal Cancer into Molecular Subtypes. *Sci Rep.* 2019;9(1):7665. doi:10.1038/s41598-019-43492-0.
150. Nielsen T, Wallden B, Schaper C, et al. Analytical validation of the PAM50-based Prosigna Breast Cancer Prognostic Gene Signature Assay and nCounter Analysis System using formalin-fixed paraffin-

embedded breast tumor specimens. *BMC Cancer*. 2014;14(1):177. doi:10.1186/1471-2407-14-177.

151. Panzuto F, Cicchese N, Partelli S, et al. Impact of Ki67 re-assessment at time of disease progression in patients with pancreatic neuroendocrine neoplasms. Luque RM, ed. *PLoS One*. 2017;12(6):e0179445. doi:10.1371/journal.pone.0179445.
152. Shi H, Zhang Q, Han C, Zhen D, Lin R. Variability of the Ki-67 proliferation index in gastroenteropancreatic neuroendocrine neoplasms - a single-center retrospective study. *BMC Endocr Disord*. 2018;18(1):51. doi:10.1186/S12902-018-0274-Y.
153. Miller HC, Drymoussis P, Flora R, Goldin R, Spalding D, Frilling A. Role of Ki-67 proliferation index in the assessment of patients with neuroendocrine neoplasias regarding the stage of disease. *World J Surg*. 2014;38(6):1353-1361. doi:10.1007/s00268-014-2451-0.
154. Singh S, Hallet J, Rowsell C, Law CHL. Variability of Ki67 labeling index in multiple neuroendocrine tumors specimens over the course of the disease. *Eur J Surg Oncol*. 2014;40(11):1517-1522. doi:10.1016/j.ejso.2014.06.016.
155. Martin DR, LaBauve E, Pomo JM, Chiu VK, Hanson JA, Gullapalli RR. Site-Specific Genomic Alterations in a Well-Differentiated Pancreatic Neuroendocrine Tumor With High-Grade Progression. *Pancreas*. 2018;47(4):502-510. doi:10.1097/MPA.0000000000001030.
156. Gorges TM, Kuske A, Röck K, et al. Accession of Tumor Heterogeneity by Multiplex Transcriptome Profiling of Single Circulating Tumor Cells. *Clin Chem*. 2016;62(11):1504-1515. doi:10.1373/clinchem.2016.260299.
157. Porras TB, Kaur P, Ring A, Schechter N, Lang JE. Challenges in using liquid biopsies for gene expression profiling. *Oncotarget*. 2018;9(6):7036-7053. doi:10.18632/oncotarget.24140.
158. Rizzo FM, Meyer T. Liquid Biopsies for Neuroendocrine Tumors: Circulating Tumor Cells, DNA, and MicroRNAs. *Endocrinol Metab Clin North Am*. 2018;47(3):471-483. doi:10.1016/j.ecl.2018.04.002.
159. Yu M, Chen S, Hong W, et al. Prognostic role of glycolysis for cancer outcome: evidence from 86 studies. *J Cancer Res Clin Oncol*. 2019;145(4):967-999. doi:10.1007/s00432-019-02847-w.
160. He X, Lin X, Cai M, et al. Overexpression of Hexokinase 1 as a poor prognosticator in human colorectal cancer. *Tumor Biol*. 2016;37(3):3887-3895. doi:10.1007/s13277-015-4255-8.
161. Smith TA. Mammalian hexokinases and their abnormal expression in cancer. *Br J Biomed Sci*. 2000;57(2):170-178. <http://www.ncbi.nlm.nih.gov/pubmed/10912295>. Accessed May 22, 2019.

162. Philip B, Ito K, Moreno-Sanchez R, Ralph SJ. HIF expression and the role of hypoxic microenvironments within primary tumours as protective sites driving cancer stem cell renewal and metastatic progression. *Carcinogenesis*. 2013;34(8):1699-1707. doi:10.1093/carcin/bgt209.
163. Balamurugan K. HIF-1 at the crossroads of hypoxia, inflammation, and cancer. *Int J Cancer*. 2016;138(5):1058-1066. doi:10.1002/ijc.29519.
164. Jain RK. Antiangiogenesis Strategies Revisited: From Starving Tumors to Alleviating Hypoxia. *Cancer Cell*. 2014;26(5):605-622. doi:10.1016/j.ccell.2014.10.006.
165. Lewis DM, Pruitt H, Jain N, et al. A Feedback Loop between Hypoxia and Matrix Stress Relaxation Increases Oxygen-Axis Migration and Metastasis in Sarcoma. *Cancer Res*. 2019;79(8):1981-1995. doi:10.1158/0008-5472.CAN-18-1984.
166. Chae YK, Chang S, Ko T, et al. Epithelial-mesenchymal transition (EMT) signature is inversely associated with T-cell infiltration in non-small cell lung cancer (NSCLC). *Sci Rep*. 2018;8(1):2918. doi:10.1038/s41598-018-21061-1.
167. Lo CY, Lam KY, Kung AW, Lam KS, Tung PH, Fan ST. Pancreatic insulinomas. A 15-year experience. *Arch Surg*. 1997;132(8):926-930. <http://www.ncbi.nlm.nih.gov/pubmed/9267281>. Accessed June 19, 2019.
168. Nikfarjam M, Warshaw AL, Axelrod L, et al. Improved contemporary surgical management of insulinomas: a 25-year experience at the Massachusetts General Hospital. *Ann Surg*. 2008;247(1):165-172. doi:10.1097/SLA.0b013e31815792ed.
169. Zhang P, Lu M, Li J, Shen L. 1309OEfficacy and safety of PD-1 blockade with JS001 in patients with advanced neuroendocrine neoplasms: A non-randomized, open-label, phase Ib trial. *Ann Oncol*. 2018;29(suppl_8). doi:10.1093/annonc/mdy293.002.
170. Yao JC, Strosberg J, Fazio N, et al. 1308OActivity & safety of spartalizumab (PDR001) in patients (pts) with advanced neuroendocrine tumors (NET) of pancreatic (Pan), gastrointestinal (GI), or thoracic (T) origin, & gastroenteropancreatic neuroendocrine carcinoma (GEP NEC) who have p. *Ann Oncol*. 2018;29(suppl_8). doi:10.1093/annonc/mdy293.001.
171. Mehnert JM, Rugo HS, O'Neil BH, et al. 427OPembrolizumab for patients with PD-L1–positive advanced carcinoid or pancreatic neuroendocrine tumors: Results from the KEYNOTE-028 study. *Ann Oncol*. 2017;28(suppl_5). doi:10.1093/annonc/mdx368.
172. Li Z, Leng J, Wang H, Li S, Lu M, Zhou L, Huang X, Jia L, Kang Q, Li J, Shen L. LD. PD-L1 Expression is Associated with Grade of

Neuroendocrine Tumors. In: *ENETs*. ; 2016.
<https://www.enets.org/abstracts.1290.html>.

173. Cavalcanti E, Armentano R, Valentini AM, Chieppa M, Caruso ML. Role of PD-L1 expression as a biomarker for GEP neuroendocrine neoplasm grading. *Cell Death Dis*. 2017;8(8):e3004. doi:10.1038/cddis.2017.401.
174. Kim ST, Ha SY, Lee S, et al. The Impact of PD-L1 Expression in Patients with Metastatic GEP-NETs. *J Cancer*. 2016;7(5):484-489. doi:10.7150/jca.13711.
175. Cives M., Strosberg J. CD. PD1 and PDL1 Expression in Midgut Neuroendocrine Tumors. *Neuroendocrinology*. 2016;103((suppl 1)):1-128.
176. Lamarca A, Nonaka D, Breitwieser W, et al. PD-L1 expression and presence of TILs in small intestinal neuroendocrine tumours. *Oncotarget*. 2018;9(19):14922-14938. doi:10.18632/oncotarget.24464.
177. Schultheis AM, Scheel AH, Ozretić L, et al. PD-L1 expression in small cell neuroendocrine carcinomas. *Eur J Cancer*. 2015;51(3):421-426. doi:10.1016/j.ejca.2014.12.006.
178. Tong Z, Liu L, Zheng Y, et al. Predictive value of preoperative peripheral blood neutrophil/lymphocyte ratio for lymph node metastasis in patients of resectable pancreatic neuroendocrine tumors: a nomogram-based study. *World J Surg Oncol*. 2017;15(1):108. doi:10.1186/s12957-017-1169-5.
179. Milione M, Pellegrinelli A, Centonze G, Dominoni F, Pusceddu S, Giacomelli L, Buzzoni R, Coppa J, Mazzaferro V, Anichini A DBF. Distribution of T-Cell Infiltrate in G1, G2 and G3 NENs. *Neuroendocrinology*. <https://www.enets.org/distribution-of-t-cell-infiltrate-in-g1-g2-and-g3-nens.html>. Published 2016. Accessed April 24, 2019.
180. De Reuver PR, Mehta S, Gill P, et al. Immunoregulatory Forkhead Box Protein p3-Positive Lymphocytes Are Associated with Overall Survival in Patients with Pancreatic Neuroendocrine Tumors. 2016. doi:10.1016/j.jamcollsurg.2015.12.008.
181. Katz SC, Donkor C, Glasgow K, et al. T cell infiltrate and outcome following resection of intermediate-grade primary neuroendocrine tumours and liver metastases. doi:10.1111/j.1477-2574.2010.00231.x.
182. Salem ME, Puccini A, Grothey A, et al. Landscape of Tumor Mutation Load, Mismatch Repair Deficiency, and PD-L1 Expression in a Large Patient Cohort of Gastrointestinal Cancers. *Mol Cancer Res*. 2018;16(5):805-812. doi:10.1158/1541-7786.MCR-17-0735.
183. Mei M, Deng D, Liu T-H, et al. Clinical implications of microsatellite

instability and MLH1 gene inactivation in sporadic insulinomas. *J Clin Endocrinol Metab.* 2009;94(9):3448-3457. doi:10.1210/jc.2009-0173.

184. Arnason T, Sapp HL, Rayson D, et al. Loss of Expression of DNA Mismatch Repair Proteins Is Rare in Pancreatic and Small Intestinal Neuroendocrine Tumors. *Arch Pathol Lab Med.* 2011;135. doi:10.5858/arpa.2010-0560-OA.
185. Guinney J, Dienstmann R, Wang X, et al. The consensus molecular subtypes of colorectal cancer. *Nat Med.* 2015;21(11):1350-1356. doi:10.1038/nm.3967.
186. Braconi C, Valeri N, Gasparini P, et al. Hepatitis C virus proteins modulate microRNA expression and chemosensitivity in malignant hepatocytes. *Clin Cancer Res.* 2010;16(3):957-966. doi:10.1158/1078-0432.CCR-09-2123.
187. Tusher VG, Tibshirani R, Chu G. Significance analysis of microarrays applied to the ionizing radiation response. *Proc Natl Acad Sci.* 2001;98(9):5116-5121. doi:10.1073/pnas.091062498.
188. Martinez O, Reyes-Valdes MH. Defining diversity, specialization, and gene specificity in transcriptomes through information theory. *Proc Natl Acad Sci.* 2008;105(28):9709-9714. doi:10.1073/pnas.0803479105.
189. Martínez O, Reyes-Valdés MH, Herrera-Estrella L. Cancer Reduces Transcriptome Specialization. Shiu S-H, ed. *PLoS One.* 2010;5(5):e10398. doi:10.1371/journal.pone.0010398.
190. Rooney MS, Shukla SA, Wu CJ, Getz G, Hacohen N. Molecular and Genetic Properties of Tumors Associated with Local Immune Cytolytic Activity. *Cell.* 2015;160(1-2):48-61. doi:10.1016/j.cell.2014.12.033.
191. (DGT) TFC and the RP and C, Forrest ARR, Kawaji H, et al. A promoter-level mammalian expression atlas. *Nature.* 2014;507(7493):462-470. doi:10.1038/nature13182.
192. Subramanian A, Tamayo P, Mootha VK, et al. Gene set enrichment analysis: a knowledge-based approach for interpreting genome-wide expression profiles. *Proc Natl Acad Sci U S A.* 2005;102(43):15545-15550. doi:10.1073/pnas.0506580102.
193. Barbie DA, Tamayo P, Boehm JS, et al. Systematic RNA interference reveals that oncogenic KRAS-driven cancers require TBK1. *Nature.* 2009;462(7269):108-112. doi:10.1038/nature08460.
194. Newman AM, Liu CL, Green MR, et al. Robust enumeration of cell subsets from tissue expression profiles. *Nat Methods.* 2015;12(5):453-457. doi:10.1038/nmeth.3337.
195. Li B, Dewey CN. RSEM: accurate transcript quantification from RNA-Seq data with or without a reference genome. *BMC Bioinformatics.*

2011;12(1):323. doi:10.1186/1471-2105-12-323.

196. Ribas A, Robert C, Hodi FS, et al. Association of response to programmed death receptor 1 (PD-1) blockade with pembrolizumab (MK-3475) with an interferon-inflammatory immune gene signature. *J Clin Oncol.* 2015;33(15_suppl):3001-3001. doi:10.1200/jco.2015.33.15_suppl.3001.
197. Teo RYA, Teo TZ, Tai DWM, Tan DM, Ong S, Goh BKP. Systematic review of current prognostication systems for pancreatic neuroendocrine neoplasms. *Surgery.* December 2018. doi:10.1016/j.surg.2018.10.031.
198. Godec J, Tan Y, Liberzon A, et al. Compendium of Immune Signatures Identifies Conserved and Species-Specific Biology in Response to Inflammation. *Immunity.* 2016;44(1):194-206. doi:10.1016/j.immuni.2015.12.006.
199. Jain RK, Martin JD, Stylianopoulos T. The role of mechanical forces in tumor growth and therapy. *Annu Rev Biomed Eng.* 2014;16(1):321-346. doi:10.1146/annurev-bioeng-071813-105259.
200. Galluzzi L, Vitale I. Molecular mechanisms of cell death: recommendations of the Nomenclature Committee on Cell Death 2018. *Cell Death Differ.* 2018;25:486-541. doi:10.1038/s41418-017-0012-4.
201. Najafov A, Chen H, Yuan J. Necroptosis and Cancer. *Trends in cancer.* 2017;3(4):294-301. doi:10.1016/j.trecan.2017.03.002.
202. Tang D, Kang R, Berghe T Vanden, Vandenabeele P, Kroemer G. The molecular machinery of regulated cell death. doi:10.1038/s41422-019-0164-5.
203. Hernandez C, Huebener P, Schwabe RF. Damage-associated molecular patterns in cancer: a double-edged sword. *Oncogene.* 2016;35(46):5931-5941. doi:10.1038/onc.2016.104.
204. Tang D, Kang R, Coyne CB, Zeh HJ, Lotze MT. PAMPs and DAMPs: signal 0s that spur autophagy and immunity. *Immunol Rev.* 2012;249(1):158-175. doi:10.1111/j.1600-065X.2012.01146.x.
205. He Y, Zha J, Wang Y, Liu W, Yang X, Yu P. Tissue Damage-Associated "Danger Signals" Influence T-cell Responses That Promote the Progression of Preneoplasia to Cancer. *Cancer Res.* 2013;73(2):629-639. doi:10.1158/0008-5472.CAN-12-2704.
206. Qin X, Ma D, Tan Y, Wang H, Cai Z. The role of necroptosis in cancer: A double-edged sword? *Biochim Biophys Acta - Rev Cancer.* 2019;1871(2):259-266. doi:10.1016/j.bbcan.2019.01.006.
207. Rakoff-Nahoum S, Medzhitov R. Toll-like receptors and cancer. *Nat Rev Cancer.* 2009;9(1):57-63. doi:10.1038/nrc2541.

208. Roselli E, Araya P, Núñez NG, et al. TLR3 Activation of Intratumoral CD103+ Dendritic Cells Modifies the Tumor Infiltrate Conferring Anti-tumor Immunity. *Front Immunol*. 2019;10. doi:10.3389/fimmu.2019.00503.
209. Wu D-D, Li T, Ji X-Y. Dendritic Cells in Sepsis: Pathological Alterations and Therapeutic Implications. *J Immunol Res*. 2017;2017:1-9. doi:10.1155/2017/3591248.
210. Ezawa I, Sawai Y, Kawase T, et al. Novel p53 target gene *FUCA1* encodes a fucosidase and regulates growth and survival of cancer cells. *Cancer Sci*. 2016;107(6):734-745. doi:10.1111/cas.12933.
211. Sadanandam A, Young K, Nyamundanda G, Ragulan C, Lawlor R SA. Development of Multiplex Biomarker Assay to Subtype Pancreatic Neuroendocrine Tumors (PanNETs) with Distinct Prognosis and Mutations. *Neuroendocrinology*. 2018;Vol. 106((suppl 1)). <https://www.enets.org/development-of-multiplex-biomarker-assay-to-subtype-pancreatic-neuroendocrine-tumors-pannets-with-distinct-prognosis-and-mutations.html>.
212. Wouters MCA, Nelson BH. Prognostic Significance of Tumor-Infiltrating B Cells and Plasma Cells in Human Cancer. *Clin Cancer Res*. 2018;24(24):6125-6135. doi:10.1158/1078-0432.CCR-18-1481.
213. Chen Q, Mo L, Cai X, et al. ICOS signal facilitates Foxp3 transcription to favor suppressive function of regulatory T cells. *Int J Med Sci*. 2018;15(7):666-673. doi:10.7150/ijms.23940.
214. Palazon A, Goldrath AW, Nizet V, Johnson RS. HIF Transcription Factors, Inflammation, and Immunity. *Immunity*. 2014;41:518-528. doi:10.1016/j.immuni.2014.09.008.
215. He L, Xiao X, Yang X, Zhang Z, Wu L, Liu Z. STING signaling in tumorigenesis and cancer therapy: A friend or foe? *Cancer Lett*. 2017;402:203-212. doi:10.1016/j.canlet.2017.05.026.
216. Rizvi NA, Hellmann MD, Snyder A, et al. Mutational landscape determines sensitivity to PD-1 blockade in non-small cell lung cancer. *Science (80-)*. 2015;348(6230):124-128. doi:10.1126/science.aaa1348.
217. Snyder A, Makarov V, Merghoub T, et al. Genetic Basis for Clinical Response to CTLA-4 Blockade in Melanoma. *N Engl J Med*. 2014;371(23):2189-2199. doi:10.1056/NEJMoa1406498.
218. Le DT, Uram JN, Wang H, et al. PD-1 Blockade in Tumors with Mismatch-Repair Deficiency. *N Engl J Med*. 2015;372(26):2509-2520. doi:10.1056/NEJMoa1500596.
219. Mitchell D, Chintala S, Dey M. Plasmacytoid dendritic cell in immunity and cancer. *J Neuroimmunol*. 2018;322:63-73. doi:10.1016/j.jneuroim.2018.06.012.

220. Aspod C, Leccia M-T, Charles J, Plumas J. Plasmacytoid dendritic cells support melanoma progression by promoting Th2 and regulatory immunity through OX40L and ICOSL. *Cancer Immunol Res*. 2013;1(6):402-415. doi:10.1158/2326-6066.CIR-13-0114-T.
221. Aspod C, Leccia M-T, Charles J, Plumas J. Melanoma hijacks plasmacytoid dendritic cells to promote its own progression. *Oncoimmunology*. 2014;3(1):e27402. doi:10.4161/onci.27402.
222. Gousias K, von Ruecker A, Voulgari P, Simon M. Phenotypical analysis, relation to malignancy and prognostic relevance of ICOS + T regulatory and dendritic cells in patients with gliomas. *J Neuroimmunol*. 2013;264(1-2):84-90. doi:10.1016/J.JNEUROIM.2013.09.001.
223. Sisirak V, Vey N, Goutagny N, et al. Breast cancer-derived transforming growth factor- β and tumor necrosis factor- α compromise interferon- α production by tumor-associated plasmacytoid dendritic cells. *Int J Cancer*. 2013;133(3):771-778. doi:10.1002/ijc.28072.
224. Shi M, Chen X, Ye K, Yao Y, Li Y. Application potential of toll-like receptors in cancer immunotherapy: Systematic review. *Medicine (Baltimore)*. 2016;95(25):e3951. doi:10.1097/MD.0000000000003951.
225. Liang J, Liu Z, Zou Z, et al. The Correlation Between the Immune and Epithelial-Mesenchymal Transition Signatures Suggests Potential Therapeutic Targets and Prognosis Prediction Approaches in Kidney Cancer. *Sci Rep*. 2018;8(1):6570. doi:10.1038/s41598-018-25002-w.
226. Ueno T, Tsuchikawa T, Hatanaka KC, et al. Prognostic impact of programmed cell death ligand 1 (PD-L1) expression and its association with epithelial-mesenchymal transition in extrahepatic cholangiocarcinoma. *Oncotarget*. 2018;9(28):20034-20047. doi:10.18632/oncotarget.25050.
227. Mak MP, Tong P, Diao L, et al. A Patient-Derived, Pan-Cancer EMT Signature Identifies Global Molecular Alterations and Immune Target Enrichment Following Epithelial-to-Mesenchymal Transition. *Clin Cancer Res*. 2016;22(3):609-620. doi:10.1158/1078-0432.CCR-15-0876.
228. Sarvaria A, Madrigal JA, Saudemont A. B cell regulation in cancer and anti-tumor immunity. *Cell Mol Immunol*. 2017;14(8):662-674. doi:10.1038/cmi.2017.35.
229. Guy T V., Terry AM, Bolton HA, Hancock DG, Shklovskaya E, Fazekas de St Groth B. Pro- and anti-tumour effects of B cells and antibodies in cancer: a comparison of clinical studies and preclinical models. *Cancer Immunol Immunother*. 2016;65(8):885-896. doi:10.1007/s00262-016-1848-z.
230. Garnelo M, Tan A, Her Z, et al. Interaction between tumour-infiltrating

B cells and T cells controls the progression of hepatocellular carcinoma. *Gut*. 2017;66(2):342-351. doi:10.1136/gutjnl-2015-310814.

231. Sadanandam A, Young K, Nyamundanda G, Ragulan C, Lawlor R SA. Development of Multiplex Biomarker Assay to Subtype Pancreatic Neuroendocrine Tumors (PanNETs) with Distinct Prognosis and Mutations. *Neuroendocrinology*.:15th Annual ENETS conference (2018). <https://www.enets.org/development-of-multiplex-biomarker-assay-to-subtype-pancreatic-neuroendocrine-tumors-pannets-with-distinct-prognosis-and-mutations.html>. Accessed April 28, 2019.
232. Kuwahara M, Suzuki J, Tofukuji S, et al. The Menin-Bach2 axis is critical for regulating CD4 T-cell senescence and cytokine homeostasis. *Nat Commun*. 2014;5(1):3555. doi:10.1038/ncomms4555.
233. Suzuki J, Yamada T, Inoue K, et al. The tumor suppressor menin prevents effector CD8 T-cell dysfunction by targeting mTORC1-dependent metabolic activation. *Nat Commun*. 2018;9(1):3296. doi:10.1038/s41467-018-05854-6.
234. Henry NL, Hayes DF. Cancer biomarkers. *Mol Oncol*. 2012;6(2):140-146. doi:10.1016/j.molonc.2012.01.010.
235. Sepulveda AR, Hamilton SR, Allegra CJ, et al. Molecular Biomarkers for the Evaluation of Colorectal Cancer: Guideline From the American Society for Clinical Pathology, College of American Pathologists, Association for Molecular Pathology, and the American Society of Clinical Oncology. *J Clin Oncol*. 2017;35(13):1453-1486. doi:10.1200/JCO.2016.71.9807.
236. Tsang JYS, Tse GM. Molecular Classification of Breast Cancer. *Adv Anat Pathol*. April 2019:1. doi:10.1097/PAP.000000000000232.
237. Oberndorfer F, Müllauer L. Molecular pathology of lung cancer. *Curr Opin Oncol*. December 2017:1. doi:10.1097/CCO.0000000000000429.
238. Lioumi M, Newell D. CR-UK biomarker roadmaps. In: *Other Molecular Diagnostics Studies*. Vol 16. American Association for Cancer Research; 2010:B33-B33. doi:10.1158/DIAG-10-B33.
239. Teutsch SM, Bradley LA, Palomaki GE, et al. The Evaluation of Genomic Applications in Practice and Prevention (EGAPP) initiative: methods of the EGAPP Working Group. *Genet Med*. 2009;11(1):3-14. doi:10.1097/GIM.0b013e318184137c.
240. Sadanandam A, Wang X, de Sousa E Melo F, et al. Reconciliation of classification systems defining molecular subtypes of colorectal cancer: interrelationships and clinical implications. *Cell Cycle*. 2014;13(3):353-357. doi:10.4161/cc.27769.

Acknowledgements

It would not have been possible to complete this MD(Res.) thesis without the help and support of many people.

Firstly, I would like to thank my supervisors Naureen Starling and Anguraj Sadanandam, for their invaluable support and advice. Prof David Cunningham, Dr Ian Chau and Dr Daniel Morganstein have been similarly helpful and supportive throughout my entire MD(Res.) program.

I would also like to acknowledge financial support from Professor Cunningham's Research Fund, the Swire Charitable Trust and the RM/ICR NIHR BRC.

I am indebted to Ruwaida Begum and her Biological Specimens Coordinating Team and the histopathology team, Dr Monica Terlizzo and Dr Daniel Nava Rodrigues. I would also like to thank Jacqui Oates, the Operational Head of the GI and Lymphoma Research Unit, and the entire team in the trials office, specifically Sijy Pillai, Bijal Patel and Richard Crux who worked on the PaNACeA study and the statistical team (Clare Peckitt, Ria Kalaitzaki, Kyriakous Kouvelakis and Henry Nanji). Their endless patience and support has been key to the successful completion of this thesis.

I would like to thank all of the members of the Sadanandam lab. Chanthirika Ragulan for teaching me fundamental lab techniques, Gift Nyamundanda, Kate Eason and Yatish Patil for their support with bioinformatics, Elisa Fontana for learning the techniques with me and not mocking my wet-lab skills too much and our collaborators in Verona, particularly Rita Lawlor, and at Kings College Hospital. Without their patience and kindness the lab work aspects of this thesis would have been impossible.

There are many others who contributed to this work. I would like to thank all the staff in the GI and Lymphoma Unit at the Royal Marsden Hospital including Consultants, Clinical Trial Coordinators, Research Nurses and Data Managers as well as the patients who gave their time to the patient focus group and the patients who contributed tissue.

A special acknowledgment goes to all of the Clinical Research Fellows with whom I have had the pleasure to work with and share successes and failures throughout the duration of my MD(Res) project.

Finally, I would like to thank my family and particularly my husband Richard and our sons, Jack and Tom. I dedicate this thesis to them, as their love, endless patience and constant support are deeply appreciated.

Appendices

Appendix 1

Appendix 1.1 Abbreviations used in this thesis

Abbreviation	Definition
5HIAA	5-hydroxyindoleacetic acid
ACTH	Adrenocorticotrophic hormone
AJCC	American Joint Committee on Cancer
ALT	Alternative Lengthening of Telomeres
APCs	Antigen Presenting Cells
BLAST	Basic Local Alignment Search Tool
BRC	Biomedical Research Council
CCR	Committee for Clinical Research
cDNA	Complementary DNA
CgA	Chromogranin A
CgB	Chromogranin B
CI	Chief Investigator
	Cell type Identification By Estimating Relative Subsets Of known RNA
CIBERSORT	Transcripts
CIN	Chromosomal Instability
CoE	Centres of Excellence
CRC	Colorectal Cancer
CRUK	Cancer Research UK
CTCs	Circulating Tumour Cells
DAMP	Damage Associated Molecular Pattern
DAPI	4',6-diamidino-2-phenylindole
DC	Dendritic Cells
DNA	Deoxyribonucleic acid
EMT	Epithelial to Mesenchymal Transition
ENETs	European Neuroendocrine Tumour Society
EPC	Exocrine Pancreatic Cancer

ESMO	European Society for Medical Oncology
EUS	Endoscopic Ultrasound Scans
FDG	Fluorodeoxyglucose
FDR	False Discovery Rate
FFPE	Formalin Fixed Paraffin Embedded
Ga	Gallium
GI	Gastrointestinal
GRF	Growth hormone releasing factor
GSEA	Gene Set Enrichment Analysis
H&E	Haematoxylin and Eosin
HIF	Hypoxia Inducible Factor
HPF	High Powered Field
HRA	Health Research Authority
ICF	Informed Consent Form
ICR	Institute for Cancer Research
IFN	Interferon
IL-8	Interleukin-8
iLVM	Integrative Latent Variable Model
IQR	Inter Quartile Range
IRAS	Integrated Research Application System
MDT	Multidisciplinary team
MEN1	Multiple Endocrine Neoplasia
MGMT	O-6-methylguanine-DNA methyltransferase
MHC	Major Histocompatibility Complex
MI	Mitotic Index
miR	MicroRNA
MMR	Mismatch Repair
MRI	Magnetic Resonance Imaging
mRNA	Messenger RNA
MSigDB	Molecular Signatures Database
NET	Neuroendocrine Tumour
ng/ μ L	nanograms/ microlitre
NGS	Next Generation sequencing
NIHR	National Institute of Health Research

NSE	Neuron Specific Enolase
OS	Overall Survival
PAM	Prediction Analysis for Microarrays
PAMP	Pathogen Associated Molecular Pattern
PanCK	Pan Cytokeratin
PanNEC	Pancreatic Neuroendocrine Carcinoma
PanNEN	Pancreatic Neuroendocrine Neoplasm
PanNET	Pancreatic Neuroendocrine Tumour
PCR	Polymerase Chain Reaction
PDAC	Pancreatic Ductal Adenocarcinoma
PET	Positron Emission Tomography
PFS	Progression Free Survival
PIS	Patient Information Sheet
PIGF	Placental Growth Factor
PP	Pancreatic Peptide
pPC	Probabalistic Principal Component
PPI	Patient and Public Involvement
PPI	Proton Pump Inhibitor
PPQ	PRRT predictive quotient
PTHrP	Parathyroid hormone related peptide
QC	Quality Control
RCC	Reporter Code Count File
REC	Research Ethics Committee
RECIST	Response Evaluation Criteria In Solid Tumours
RIN	RNA Integrity number
RLF	Reporter Library File
RMH	Royal Marsden Hospital
RNA	Ribonucleic acid
RNAseq	RNA Sequencing
SA	Substantial Amendment
SAM	Significance analysis of Microarrays
SAP	Statistical Analysis Plan
SDF-1 α	Stromal cell-derived factor-1 α
SEER	Surveillance, Epidemiology and End Results

SI-NET	Small Intestinal NET
SOPs	Standard Operating Procedures
SRS	Somatostatin Receptor Scintigraphy
ssGSEA	single sample Gene Set Enrichment Analysis
SSTR	Somatostatin Receptor
STING	Stimulator of Interferon Genes
sVEGFR	Soluble Vascular Endothelial Growth Factor
TAMs	Tumour Associated Macrophages
TLR	Toll Like Receptor
TMB	Tumour Mutational Burden
TME	Tumour Microenvironment
TMG	Trial Management Group
TML	Tumour Mutational Load
UICC	Union for International Cancer Control
ULN	Upper Limit of Normal
VHL	Von Hippel Lindau
VIP	Vasointestinal polypeptide
vs	Versus
WHO	World Health Organisation

Appendix 2.

Appendix 2.1 PaNACeA Study Protocol

A TRANSLATIONAL STUDY IN GASTROENTERO-PANCREATIC NEUROENDOCRINE TUMOURS (GEP-NETs) TO VALIDATE AND ASSESS A NOVEL MOLECULAR CLASSIFICATION (PaNACeA)

Chief Investigator:	Dr Naureen Starling
Lead Scientist:	Dr Anguraj Sadanandam
Co - Investigator:	Dr Kate Young
Co - Investigator:	Dr Daniel Morganstein
Co - Investigator:	Dr Ian Chau
Co – Investigator:	Dr David Watkins
Co – Investigator:	Dr Sheela Rao
Co - Investigator:	Prof David Cunningham
Study Coordinator:	Sijy Pillai/Angela Gillbanks
Histopathologist:	Pathologists from Prof Scarpa’s group (University of Verona, Italy) and Prof Bertram Wiedenmann’s group (Charite Hospital, Berlin, Germany)
Tissue Coordinator:	Ms Ruwaida Begun
Statistician:	Ms Ria Kalaitzaki
Bioinformatician:	Mr Gift Nyamundanda
Database development:	Dr Federica Morano Dr Kate Young
Protocol development:	Dr Andrea Lanese Dr Kate Young
Study Sponsor:	The Royal Marsden NHS Foundation Trust
Collaborators:	Prof Aldo Scarpa, Verona Dr Rajaventhana Srirajaskanthan, Kings
Trial Management Group:	Dr Naureen Starling Dr Anguraj Sadanandam Dr Kate Young Ms Ria Kalaitzaki Sijy Pillai/Angela Gillbanks

TABLE OF CONTENTS:**Page**

Protocol signature page.....	3
1. Protocol synopsis.....	4
2. Background.....	6
3. Study rationale.....	8
4. Study design.....	10
4.1 Inclusion criteria.....	10
4.2 Exclusion criteria.....	10
5. Study endpoints.....	11
5.1 Primary endpoint.....	11
5.2 Secondary endpoints.....	11
6. Statistical considerations.....	11
6.1 Sample size.....	11
6.2 Statistical endpoints and data analysis.....	12
7. Study procedures and assessment.....	14
7.1 Collection and storage of tissue.....	14
7.2 Molecular analyses.....	14
8. Reporting.....	16
8.1 Annual reporting to REC.....	16
8.2 Quality assurance/audit.....	16
9. Confidentiality.....	16
10. Informed consent.....	17
11. Sample labelling, storage and destruction.....	17
12. Use of information.....	17
13. Publications.....	18
14. Trial management group.....	18
15. References.....	19

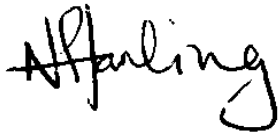
Protocol signature page:

Study title: A TRANSLATIONAL STUDY IN GASTROENETROPANCREATIC
NEUROENDOCRINE TUMOURS (GEP-NETs) TO VALIDATE AND ASSESS THE
CLINICAL UTILITY OF A NOVEL MOLECULAR CLASSIFICATION (PaNACeA)

Protocol version: 2.0

Version date: 25th April 2018

Approved by Chief Investigator: Dr Naureen Starling

A handwritten signature in black ink, appearing to read 'Naureen Starling', written in a cursive style.

Investigator's agreement

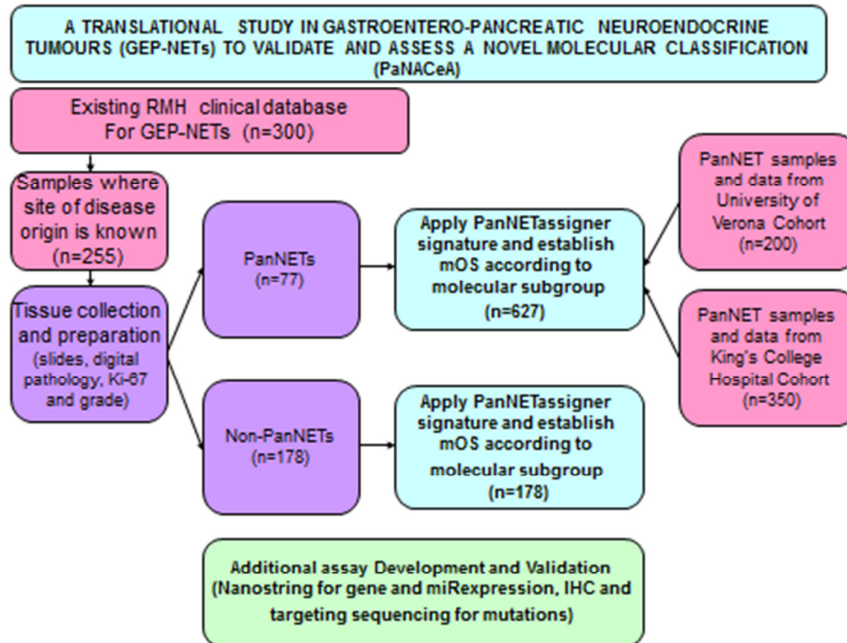
1. Protocol synopsis

Title of study:	A translational study in gastroenteropancreatic neuroendocrine tumours (GEP- NETs) to validate and assess the clinical utility of a novel molecular classification
Chief Investigators:	Dr Naureen Starling
No. of study centres:	3 (Royal Marsden Hospital, ARC-NET Verona and King's College Hospital)
Study period:	1 st August 2016- July 8 th 2020
Primary objective:	To explore overall survival in pancreatic neuroendocrine patients according to PanNET molecular subtype attributed by the PanNETassigner signature
Secondary Objectives:	<ol style="list-style-type: none">1. To assess the association of grade, molecular subtypes, or a combined Model with prognosis of PanNET tumours2. To establish if non-pancreatic GEP-NETs can be classified by the PanNETassigner signature3. To further develop diagnostic assays (including Nanostring Technologies for gene and miR expression, IHC for protein expression and targeting sequencing for mutations) applicable in the clinic (this objective will not be addressed statistically)4. To assess overall survival according to different treatment modalities according to PanNET molecular subtypes
Methodology:	Tissue samples from patients treated for gastroenteropancreatic neuroendocrine neoplasm over the last 10 years at Royal Marsden NHS Foundation Trust and at the University of Verona will be collected and transported for storage at The Royal Marsden NHS Foundation Trust. Molecular analyses including, among others, nCounter assay (Nanostring Technique), Ion AmpliSeq custom panel and Ion Torrent Personal Genome Machine, RNA isolation, real-

time RT PCR using specific primers, IHC will be performed. Targeted sequencing will be carried out using the facilities from the University of Verona, Italy and their established protocol. The Centre for Molecular Pathology's (CMP) Research Diagnostic facilities may also be used for this purpose. The molecular analyses data will be collected in a link-anonymised fashion and correlated to clinical outcome data. Tissue from a further cohort of PanNET patients treated at King's College Hospital, London, with matched clinical data will also be transported to the Royal Marsden for storage and subsequent analysis.

- Number of patients:** Total: Approximately 805 GEP-NET samples with matched clinical data
Approximately 77 PanNET samples with matched clinical data from Royal Marsden Cohort.
Approximately 200 PanNET samples with matched clinical data from University of Verona Cohort.
Approximately 350 PanNET samples with matched clinical data from the Kings Hospital Cohort.
Approximately 178 non-pancreatic GEP-NET samples with matched clinical data from Royal Marsden Cohort.
- Main inclusion criteria:** Patients with gastroenteropancreatic neuroendocrine neoplasm treated at The Royal Marsden NHS Foundation Trust , the University of Verona and King's College Hospital, and whose tissue samples are available
- Primary Endpoint:** Overall survival (OS), defined as time from the date of diagnosis to death of any cause, according to PanNET molecular subtype attributed by the PanNETassigner signature.
- Secondary Endpoints:**
1. OS by grade and molecular subtype.
 2. OS according to PanNET molecular subtype in non-pancreatic GEP-NETs.
 3. OS according to different treatment modalities and molecular subtype.

Schema:



2. Background

Neuroendocrine neoplasms (NEN) are a very heterogenous group of tumours which are thought to originate from pluripotential progenitor cells that develop neuroendocrine characteristics. Although they are considered a rare neoplasm, their incidence has been increasing over the last 30 years, probably due to an ageing population, improved detection and increased awareness of the disease. Indeed, using data from the Surveillance, Epidemiology, and End Result (SEER) database a retrospective analysis conducted in USA showed a significant increase in the incidence of NENs from 1.9 persons per 100.000 in 1973 to 5.25 per 100.000 in 2004 (Yao JC, 2008). A more recent comprehensive systematic review that included also patients from United States and Western Europe, confirmed this data. Furthermore, it reported that the age-adjusted incidence of gastroenteropancreatic neuroendocrine tumours (GEP-NETs) has increased steadily over the past four decades (1973 – 2007), increasing 3.65-fold in the USA and 3.8- to 4.8-fold in the UK (Fraenkel M, 2014).

NENs may arise in different organs. The most common site of origin is the lung, followed by small intestine, pancreas, appendix and rectum (Yao JC, 2008). Our study

will focus on gastric, bowel and pancreatic tumours, which are grouped together as the GEP-NETs.

Historically, NETs were classified into foregut (bronchi, stomach, pancreas, gallbladder, duodenum), midgut (jejunum, ileum, appendix, right colon) and hindgut (left colon and rectum) tumours according to their embryological origin, but in 2010 the World Health Organisation (WHO) reclassified NETs according to grade and stage. Grading is performed on the basis of morphological criteria and the proliferative activity of the tumour (Ki-67 index), while staging is according to the tumour, node, metastasis (TNM) staging system.

As a result, NENs have been divided into neuroendocrine tumours (NETs), which included the grade 1 and 2 well differentiated neoplasms, and neuroendocrine carcinomas (NECs), which consist of the poorly differentiated Grade 3 tumours. Grade 1 tumours have a ki-67 of less than 3%, grade 2 between 3 – 20% and grade 3 of more than 20% (*Bosman FT, 2010*).

The prognostic relevance of the WHO classification has since been established. GEP-NETs tend to be slow-growing tumours with a 5-years overall survival of approximately 75%, that drops to 27-43% in patients with a pancreatic primary (*Hauso O, 2008 ; Pape UF, 2008*). Using the WHO classification, the 5-year survival rate varies according to grade, with a rate of 96%, 73% and 28% for grades 1, 2 and 3 respectively. Survival also varies with stage, with 100% of patients with stage I disease and only 55% of patients with stage IV disease alive at 5 years (*Pape UF, 2008*).

Multiple different treatments are currently available to treat GEP-NETs. However, there is neither a clear gold standard treatment nor a treatment paradigm to guide the order in which treatments are given. Currently, the choice of 1st line treatment is often based on the WHO classification (*Ramage JK, 2012 ; Young K, 2015*).

Surgery remains the only curative approach, and may be used even in oligometastatic disease (*Pathak S, 2013*). However, patients frequently present with advanced disease where surgery is not possible. In the palliative setting, patients with grade 1 or 2 disease are frequently treated with a less aggressive approach, initially with a combination of watchful waiting and somatostatin analogues before more intensive treatment when initial treatment fails with chemotherapy (including streptozocin, dacarbazine, doxorubicin, 5FU/capecitabine and temozolomide), targeted agents in PanNETs (sunitinib and everolimus), peptide receptor radionuclide therapy/radiolabelled somatostatin analogues and liver directed treatments for

metastases. There is no strong evidence base to determine which patients would benefit from the more aggressive treatment options earlier, according to clinical, pathological or molecular characteristics. Patients with grade 3 disease tend to be treated more aggressively upfront with immediate platinum based chemotherapy doublets.

Due to the limited evidence available, a general consensus on the best approach to these patients, including the best order of these treatments, is hard to reach, and a clear standard of care is still lacking. This is especially true for the grade 2 NETs, whose behaviour is often unpredictable in clinical practice (sometimes closer to grade 1, sometimes more similar to grade 3), making it difficult to predict which patient would benefit from a more aggressive treatment approach up front.

3. Study rationale

There is a clear unmet clinical need for markers to complement grade to predict prognosis and guide treatment decisions in GEP-NET. One of the hallmarks of PanNETs is its high molecular heterogeneity and the absence of oncogenic drivers, which could serve as prognostic indicators or be used for therapeutic purposes. Recurrent alterations have been described in a series of genes in sporadic PanNETs (n=58) including *MEN1*, *DAXX/ATRX*, *TSC2*, *PTEN* and *ATM* (Jiao, 2011). Large sample size studies that aim to better define the molecular characteristics of PanNET, to identify potentially targetable molecular alterations and to implement a stratified treatment approach for this disease, are urgently needed.

However, for the first time, we have divided PanNETs into 3 distinct molecular subtypes based on an integrated analysis of gene expression (221 genes), microRNA (miR; 30 miRs) and mutations (targeted mutational profiles of *MEN1*, *DAXX/ATRX*, *TSC2*, *PTEN* and *ATM*), collectively named the **PanNETassigner signature** (Sadanandam, 2015):

- 1. Metastases-like primary tumours** (MLP primary tumours enriched for distant metastasis and associated with *DAXX/ATRX*, *TSC2*, *PTEN* and *ATM* mutations)
- 2. MEN1-like/intermediate tumours** (primarily enriched for *MEN1* mutations; however, also for *DAXX/ATRX*)
- 3. Insulinoma-like tumours** (enriched for insulinomas with mutations in *TSC2*, *PTEN* and *ATM*)

The MLP subtype shows a high expression of mesenchymal phenotype-, stem cell-, glycolysis- and hypoxia-related genes. The MEN1-like/intermediate subtype has molecular characteristics in between insulinomas and MLPs. We have also determined the association between these molecular subtypes and grade of disease, according to Ki-67 expression. Grade 1 and 2 PanNETs are heterogeneous, variably associating with all three molecular subtypes, whereas higher grade 3 tumours are exclusively associated with the MLP subtype.

In addition to the PanNET assigner signature, we have also identified a protein biomarker, ENPP2 that is highly expressed in a non-functional subset of MLP and intermediate subtype PanNETs, and may serve as a biomarker to distinguish PanNET subtypes.

These data suggest that this molecular classification of PanNET into three subtypes may provide a useful tool for patient stratification and treatment selection over and above the current classification.

A similar approach has been used in breast cancer. The Prosigna test measures risk of recurrence (ROR) as a ROR score, although here we will not be looking at a score to assess risk of recurrence but to assess prognosis and potentially to guide treatment (*Nielsen, 2010*). Further, Liedtke et al. demonstrated that the breast cancer genomic grade index, which is a 97-gene signature to stratify histological tumour grade into high and low risk groups, predicts response to chemotherapy and separates intrinsic subtypes of breast cancer (*Filho, 2011*). Similarly, the Breast Cancer Index (BCI) which combines HOXB13:IL17BR (H:I) and molecular grade index (MGI; based on tumour grade), stratifies breast cancer patients into three risk groups and provides assessment of tumour recurrence (*Ma, 2008*). In this proposal, we attempt to develop a similar index for GEP-NETs to improve patient prognostication and potentially guide treatment selection.

This retrospective translational tissue collection study is intended to utilise an existing clinical database of RMH PanNET patients and tumour tissue alongside tissue with matched clinical data from Italy, where we have an active collaboration with Prof. Aldo Scarpa, the Head of Department of Pathology and Diagnostics at University of Verona and the Director of the Centre of Applied Research on Cancer (ARC-NET) in pancreatic cancer. An additional cohort of PanNET samples with matched clinical data from King's College Hospital, London will also be analysed. These datasets will enable us to assess the validity of the PanNETassigner signature in a large well annotated clinical dataset of NET patients in 3 high volume tertiary centres. This is

with a view to establish if the signature can be used to stratify PanNET patients for prognosis and potentially to guide treatment. Furthermore, we will assess the same molecular classification in non-pancreatic GEP-NETs (stomach and bowel) to establish if these tumours can be divided into similar molecular subtypes, which will be novel.

We hope that results from this study may promote the implementation of a more selective therapeutic approach to patients with PanNET through the acquisition of useful information on the biology of PanNET using the PanNETassigner (gene, miR and mutation) signatures and the development of biomarker assays, which predict prognosis and response to treatment.

4. Study design

This is a retrospective translational tissue collection study. The study will utilise an existing clinical database of RMH patients treated for GEP-NETs over the last 10 years. Tissue will be collected for these 255 patients and this dataset will then be combined with a dataset of 200 new PanNET samples from Italy and 350 PanNET samples from King's College Hospital. The combined dataset (n=627 PanNET samples and n=178 non-pancreatic GEP-NET samples) will then be used to answer the primary and secondary endpoints.

4.1 Inclusion criteria

Patients with:

- Histological diagnosis of GEP-NET with known site of disease origin (RMH/University of Verona/King's College Hospital Cohorts)
- Tissue sample available
- Matched Clinical data available

4.2 Exclusion criteria

Patients with:

- Other primary cancer at or before diagnosis
- All treatment received elsewhere, other than RMH/University of Verona/King's

5. Study endpoints

5.1 Primary endpoint

Overall survival (OS), defined as time from the date of diagnosis to death of any cause, according to PanNET molecular subtype attributed by the PanNETassigner signature.

5.2 Secondary Endpoints

1. OS by grade and investigate the combined model of grade and molecular subtype to predict prognosis.
2. OS according to PanNET molecular subtype in non-pancreatic GEP-NETs.
3. OS according to different treatment modalities and molecular subtype.

6. Statistical consideration

6.1 Sample size

The sample size is limited by the number of patients who have been treated for GEP-NETs at the Royal Marsden Hospital, the University of Verona and at King's College Hospital and for whom tissue is available for molecular analyses. We are expecting to retrieve tissue from approximately 627 PanNET samples and 178 non-pancreatic GEP-NET samples.

The distribution of the molecular subtypes is currently unknown but if we assume approximately equal distribution and a 2 year OS of around 57% (based on PanNET patient data from the RMH clinical database) across all molecular subtypes and then further assume a difference in OS around this, then with 627 PanNET samples and:

- 80% power
- 2-sided 1.5% significance level (based on 3 tests, subtype 1v2, 1v3 and 2v3, standard p-value of 0.05 divided by 3 to account for this),

we can detect a difference of at least 16% (or more) in 2 year OS from 38% to 54% (HR = 0.64) between any 2 molecular subtypes (nQuery software- log-rank test for survival). A 16% difference is felt to be reasonable as according to

published data there is a 45% difference in 5 year survival between grade 2 and grade 3 GEP-NET (Ramage JK, 2012).

Even after allowing for a 40% loss of tissue (n=376) we can still detect a difference of 22% in 2 year OS from 38% to 60% (HR = 0.53) between any 2 molecular subtypes.

Similarly, in the non-pancreatic samples (GEP-NET, n=178), with 80% power and 2-sided 1.5% significance level, we can detect a difference of at least 32% (or more) in 2 year OS from 38% to 70% (HR = 0.37) between any 2 molecular subtypes (nQuery software- log-rank test for survival).

6.2 Statistical analysis:

Due to the anticipated low number of events and patients all results will be interpreted with caution and with hypothesis-generating intention. A formal Statistical Analysis Plan (SAP) will be drafted and approved prior to any analysis.

Primary Endpoint

The survival distributions of molecular subtypes will be estimated using the Kaplan-Meier method. Groups will be compared using Cox regression model.

Secondary Endpoint 1

Cox proportional hazards models will explore the independent prognostic value of grade and subsequently in a multivariable model we will investigate grade and molecular subtype in combination. This analysis may adjust for other known pre-defined prognostic factors. The proportionality assumption of the Cox model will be tested with Schoenfeld residuals.

Secondary Endpoint 2

To explore OS according to PanNET molecular subtype in non-pancreatic GEP-NETs. It is known that PanNET clinical characteristics are similar to those of the other GEP-NETs. Hence, in this objective we will use the 178 non-pancreatic GEP-NETs to evaluate if our molecular PanNET subtypes are applicable in non-pancreatic GEP-NETs. The Kaplan-Meier method will be used to present the

survival estimates whilst Cox regression model will be used to compare the survival rates between groups.

Secondary Endpoint 3

PanNET samples from the RMH dataset will be used to test well-defined PanNETassigner gene and miR signatures from our previous study (Sadanandam et al., 2015; *Cancer Discovery, under revision*) with IHC markers using Cox regression analysis.

Secondary Endpoint 4

Interaction tests will be used to investigate whether there was a differential treatment effect within molecular subtype defined subgroups. Again, Cox proportional hazards models will be used for this multivariable analysis which may adjust for pre-defined prognostic factors.

7 Study procedure and assessments

7.1 Collection and storage of tissue

Tissue collected from the University of Verona, by Prof. Scarpa's group, is already available at the Royal Marsden NHS Foundation Trust for analysis (n=200 PanNET).

We will locate and retrieve the remaining samples for the patients from the Royal Marsden database (n=77 PanNET, n=178 non-pancreatic GEP-NET).

We will locate and retrieve the samples for the King's College Cohort with our collaborators at King's College Hospital (n=350), who will also provide matched clinical data.

Formalin-fixed, paraffin-embedded (FFPE) tissues from PanNETs and GEP-NETs will be reviewed for quality and tumour content before conducting the analysis.

7.2 Molecular analyses

The following procedures will be followed to perform the analysis of gene and miR expression in the study population. We will use nCounter assay (Nanostring

Technologies) of the matched patient samples. These will be subjected to computational subtype identification methods as described below. For the purpose of molecular subtyping a minimal sample size of 63 was estimated using pilot PanNETassigner gene profile data from 86 PanNET samples. Since a gene is either differentially expressed or not, we used a method that assumes that each of these tests has a Bernoulli distribution. The statistical power was set at 0.8 and the false discovery rate at 5%. The subtypes identified from gene and miR profiles will be reconciled using different sample enrichment analysis methods developed by us including our published hypergeometric test (*Sadanandam A, 2014*) and other methods such as frequency-distance metrics and prototype vector (*Eason and Sadanandam, unpublished*).

Procedures including but not limited to the following will be conducted to perform the analysis of the human DNA samples, which will be analysed with a panel targeting all coding sequences of *MEN1*, *ATRX*, *DAXX*, *PTEN*, *TSC2* and *ATM*. DNA will be prepared from human tumour tissue after neoplastic cell enrichment to about 70%. Next-generation targeted sequencing will be performed using an Ion AmpliSeq custom panel (Life Technologies) and Ion Torrent Personal Genome Machine (PGM, Life Technologies). Data analysis will be done using the Torrent Suite Software v.3.6 (Life Technologies). This analysis will assign each sample to a particular molecular subtype.

PanNET samples from the RMH dataset will also be used to test well-defined PanNETassigner gene and miR signatures from our previous study (*Sadanandam A, 2015; Cancer Discovery, under revision*) using nCounter platform (Nanostring Technology; gene and miR all in one assay), RT-PCR (<10 genes or miRs), and immunohistochemistry (IHC for 4 selected protein markers). We have previously published a proof-of-concept RT-PCR and IHC assays for colorectal cancer subtyping (*Sadanandam A, 2013*). Moreover, we have a dedicated nCounter analysis system available in CMP (shared with Dr Valeri lab, ICR). For analysing the nCounter assay data (including 50 genes and 30 miRs), technical normalization will be performed using the synthetic positive controls to adjust the counts for each gene in that assay after performing the quality controls using nSolver analysis software. Then biological normalization will be performed to correct for differences in sample abundances. Each sample will be normalized to the geometric mean of the top 20 most highly expressed genes. Student *t-test* will be used on normalized counts to calculate statistical significances of pair-wise comparisons. R statistical computing (<http://www.r-project.org>) will be used for all

the calculations. RNA isolation and real-time RT-PCR using specific primers (already designed and optimised) for the biomarkers will be performed as described (*Sadanandam A, 2014*). For classification purpose using RT-PCR a standard curve using linearized plasmid containing the target sequence will be created for each gene or miR expression (*Sadanandam A, 2014*). Finally, the gene-specific copy number will be calculated according to the standard curve followed by normalization and mean-centring of the data to assign each sample to a subtype as described (*Sadanandam A, 2014*). We will also test the use of up to 8 house-keeping genes for normalization. We will perform IHC using a selected set of validated antibodies as described in our previous publication (*Collisson EA, 2011*). The resulting sample classifications from these analyses will then be compared to see concordance in classification using different methods. The significance of these classifications will be tested using *Chi-Squared* statistical test.

Targeted sequencing will be done using the facilities from the University of Verona, Italy, as they have an established protocol. We will also involve pathologists from Italy and from Germany, who are already working on the GEP-NET subtypes and grades.

Analyses will be performed at the Royal Marsden and the institute of Cancer Research. However, some of the analyses may involve researchers outside the Royal Marsden and the Institute of Cancer Research including workers in commercial companies, or other health and research organizations, but this will be on the understanding that the sample is anonymised (see section 9 and 10)

8 Reporting

8.1 Annual reporting to REC

The Ethics Committee will be notified of all projects receiving tissue and data from the tissue bank.

8.2 Quality assurance/audit

Systems of quality assurance, including all elements described in this protocol will be implemented. Quality control is applied to each stage of data handling to ensure that data are accurate, reliable and processed correctly. All data and documentation related to this study will be available for GCP audit and inspection by competent authorities. All research staff will assist in all aspects of audit/inspection

9 Confidentiality & Data Handling

This trial should be conducted according to the approved protocol and its amendments, in accordance with The Medicines for Human Use (Clinical Trials) Regulations 2004 as amended, the Research Governance Framework for Health and Social Care and the principles of GCP.

In this study anonymisation will be carried out by a third party (not directly involved in this translational research) who will access the trial database and allocate a trial number for tissue samples which can be linked with a trial number for patient outcome, all patient identifiers will be removed. Tissue samples will be coded on entry to the study so that in all circumstances researchers carrying out the analysis will not have access to details that identify the patient and will see all data in an anonymised form.

Data will be collected and maintained according to ICH-GCP standards and entered into the study password protected CRS Web database where it will be stored. Source documents will be maintained for 5 years and will be available for inspection by authorised staff including the Chief Investigator, Study Coordinator, and Statistician. Source documents will be made available if requested for monitoring and audit purposes to the Ethics and Research and Development departments and for inspection by regulatory bodies.

10 Informed consent

In this study the data & tissue will be link-anonymised and all analyses will be performed on archived diagnostic tissue. The Human Tissue Authority (HTA) code of practice for consent states that if the tissue is anonymised then tissue taken from living patients that does not have consent for future research may be used in ethically approved research projects without the patient's consent. Hence we would not routinely seek specific consent for the purpose of this study. (Reference: HTA: Code of Practice 1 on Consent, from paragraph 127 to 129).

11 Sample labelling, storage and destruction

In order to protect patient identity all samples will not be labelled with any information that may lead to the direct identification of the patient concerned, including patients name, date of birth, or National Health Service (NHS) or hospital

number. Instead, tissue specimens from each patient will be labelled with the study name, the patient's study number (assigned at registration) and initials.

Tissue samples will be stored indefinitely in secure facilities at the RMH. However, the patient retains the right to have the sample material returned or destroyed at any time.

The sponsor will be the exclusive owner of any data, discoveries, or derivative materials from the sample materials and is responsible, via the chief investigator, for the destruction of the sample(s) at the request of the research patient.

12 Use of information

All unpublished information relating to this study is considered confidential.

13 Publication

The investigators will co-ordinate publication strategies, presentations and peer review publication.

14 Trial management group

The role of the Trial Management Group (TMG) is to monitor all the aspects of the conduct and progress of the study, ensure that the protocol is adhered to.

The TMG will develop and approve the molecular analysis plan

15 Amendments

<u>Changes from v1 to v2</u>		
PAGE NUMBER	V1	V2
1		Trial Team updated to include Sijy Pillai, Angela Gillbanks, Prof Aldo Scarpa and Dr Rajaventhana Srirajaskanthan
<u>4</u>		Number of trial centres changed from 1 to 2 with the addition of King's College Hospital Study duration extended to July 2020
5-16		Throughout protocol updated to reflect the addition of a further 150 patient samples from the Verona Cohort
5-16		Throughout protocol updated to reflect the addition of approximately a further 350 patient samples from the King's College Hospital cohort
12		Inclusion criteria updated to allow patients treated over 10 years ago to be included

Appendix 3

Appendix 3.1 Supplementary Table 3.1 228 Gene Panel for PanNETassigner Nanostring Assay

Original Gene Panel selected from PanNETassigner Paper	Panel with genes removed after BLAST analysis	Final Panel with housekeeping (highlighted blue)
A1CF	A1CF	A1CF
ABI3BP	ABI3BP	ABI3BP
ACAD9	ACAD9	ACAD9
ACADSB	ACADSB	ACADSB
ACE	ACE	ACE
ACVR1B	ACVR1B	ACVR1B
ADAM28	ADAM28	ADAM28
ADAMTS2	ADAMTS2	ADAMTS2
ADAMTS7	ADAMTS7	ADAMTS7
ADM	ADM	ADM
AFG3L1	AFG3L1	AFG3L1
AKR1C4	AKR1C4	AKR1C4
ALDH1A1	ALDH1A1	ALDH1A1
ANGPTL3	ANGPTL3	ANGPTL3
APLP1	APOH	APOH
APOH	AQP8	AQP8
AQP8	ARRDC4	ARRDC4
ARRDC4	BTC	BTC
ATHL1	C19orf77	C19orf77
BCAT1	C20orf46	C20orf46
BID	C7orf68	C7orf68
BTC	CAPN13	CAPN13
C19orf77	CAPNS1	CAPNS1
C20orf46	CASR	CASR
C7orf68	CDS1	CDS1
CADPS	CEACAM1	CEACAM1
CAPN13	CELA1	CELA1
CAPNS1	CHI3L2	CHI3L2
CASP1	CHST1	CHST1
CASR	CHST8	CHST8
CDS1	CKS2	CKS2
CEACAM1	CLCA1	CLCA1
CELA1	CLDN1	CLDN1
CHI3L2	CLDN10	CLDN10
CHST1	CLDN11	CLDN11
CHST8	CLPS	CLPS

CKS2	CNPY2	CNPY2
CLCA1	COL1A2	COL1A2
CLDN1	COL5A2	COL5A2
CLDN10	COL8A1	COL8A1
CLDN11	COPE	COPE
CLPS	CPA1	CPA1
CNPY2	CPA2	CPA2
COL1A2	CRYBA2	CRYBA2
COL5A2	CTRC	CTRC
COL8A1	CTRL	CTRL
COPE	CXCR4	CXCR4
CPA1	CXCR7	CXCR7
CPA2	CYP4F3	CYP4F3
CRYBA2	DAPL1	DAPL1
CSDA	DEFB1	DEFB1
CTRB1	DLL1	DLL1
CTRC	EFNA1	EFNA1
CTRL	EGFR	EGFR
CUZD1	EGLN3	EGLN3
CXCR4	ELMO1	ELMO1
CXCR7	ELSPBP1	ELSPBP1
CYP4F3	ENC1	ENC1
DAPL1	ENTPD3	ENTPD3
DEFB1	ERBB3	ERBB3
DLL1	F10	F10
EFNA1	F12	F12
EGFR	F7	F7
EGLN3	FAM19A5	FAM19A5
ELMO1	FGB	FGB
ELSPBP1	FGD1	FGD1
ENC1	FKBP11	FKBP11
ENTPD3	FMNL1	FMNL1
ERBB3	FOXO4	FOXO4
F10	GAL3ST4	GAL3ST4
F12	GATM	GATM
F7	GCGR	GCGR
FAM19A5	GLP1R	GLP1R
FCGR1A	GLRA2	GLRA2
FGB	GLS	GLS
FGD1	GP2	GP2
FKBP11	GRM5	GRM5
FMNL1	GRSF1	GRSF1
FOXO4	GUCA1C	GUCA1C
GAL3ST4	HAO1	HAO1
GATM	HGD	HGD
GCGR	HR	HR
GLP1R	HSD11B2	HSD11B2

GLRA2	IDS	IDS
GLS	IFI44	IFI44
GP2	IL18R1	IL18R1
GRM5	IL20RA	IL20RA
GRSF1	IL22RA1	IL22RA1
GUCA1C	IMPA2	IMPA2
HAO1	INS	INS
HERC5	IP6K2	IP6K2
HGD	KIT	KIT
HR	KLK4	KLK4
HSD11B2	KLK8	KLK8
IDS	LEF1	LEF1
IFI44	LGALS2	LGALS2
IL18R1	LGALS4	LGALS4
IL20RA	LOXL4	LOXL4
IL22RA1	LRAT	LRAT
IMPA2	MAFB	MAFB
INPP5F	MAP3K14	MAP3K14
INS	MASP2	MASP2
IP6K2	MBP	MBP
KIT	MIA2	MIA2
KLK4	MLN	MLN
KLK8	MMP1	MMP1
LEF1	MNX1	MNX1
LGALS2	MOBKL1A	MOBKL1A
LGALS4	MX2	MX2
LOXL4	MXRA5	MXRA5
LRAT	NAAA	NAAA
MAFB	NDC80	NDC80
MAP3K14	NEFM	NEFM
MASP2	NEK6	NEK6
MBP	NETO2	NETO2
MIA2	NUDT5	NUDT5
MLN	NUPR1	NUPR1
MMP1	P2RX1	P2RX1
MNX1	PAFAH1B3	PAFAH1B3
MOBKL1A	PDGFC	PDGFC
MTP18	PDIA2	PDIA2
MX2	PEMT	PEMT
MXRA5	PFKFB2	PFKFB2
NAAA	PFKFB3	PFKFB3
NDC80	PLA1A	PLA1A
NEFM	PLCE1	PLCE1
NEK6	PLIN3	PLIN3
NETO2	PLXDC1	PLXDC1
NUDT5	PMEPA1	PMEPA1
NUPR1	PMM1	PMM1

P2RX1	PNLIP	PNLIP
PAFAH1B3	PNLIPRP1	PNLIPRP1
PDE4DIP	PNLIPRP2	PNLIPRP2
PDGFC	POSTN	POSTN
PDIA2	PPEF1	PPEF1
PEMT	PRLR	PRLR
PFKFB2	PRSS22	PRSS22
PFKFB3	PRSS8	PRSS8
PIF1	PSMB9	PSMB9
PLA1A	PTPLA	PTPLA
PLCE1	PVRL4	PVRL4
PLIN3	RAB17	RAB17
PLXDC1	RAB7L1	RAB7L1
PMEPA1	RARRES2	RARRES2
PMM1	RBP4	RBP4
PNLIP	RBPJL	RBPJL
PNLIPRP1	REG1B	REG1B
PNLIPRP2	ROBO3	ROBO3
POSTN	SCD5	SCD5
PPEF1	SERPINA1	SERPINA1
PRLR	SERPINA3	SERPINA3
PRSS1	SERPIND1	SERPIND1
PRSS2	SERPINI2	SERPINI2
PRSS22	SH3BP4	SH3BP4
PRSS3	SLC12A7	SLC12A7
PRSS8	SLC16A3	SLC16A3
PSMB9	SLC2A1	SLC2A1
PTPLA	SLC30A2	SLC30A2
PTTG1	SLC7A2	SLC7A2
PVRL4	SLC7A8	SLC7A8
RAB17	SMARCA1	SMARCA1
RAB20	SMEK1	SMEK1
RAB7L1	SMO	SMO
RARRES2	SMOC2	SMOC2
RBP4	SPAG4	SPAG4
RBPJL	SRGAP3	SRGAP3
REG1B	SSX2IP	SSX2IP
ROBO3	STEAP3	STEAP3
SCD5	SUSD5	SUSD5
SERPINA1	TACSTD2	TACSTD2
SERPINA3	TAPBPL	TAPBPL
SERPIND1	TBC1D24	TBC1D24
SERPINI2	TECR	TECR
SH3BP4	TFF1	TFF1
SLC12A7	TGFBR3	TGFBR3
SLC16A3	TGIF1	TGIF1
SLC2A1	THBS2	THBS2

SLC30A2	TLE2	TLE2
SLC7A2	TLR3	TLR3
SLC7A8	TM4SF1	TM4SF1
SLC8A2	TM4SF4	TM4SF4
SMARCA1	TM4SF5	TM4SF5
SMEK1	TMEM176B	TMEM176B
SMO	TMEM181	TMEM181
SMOC2	TMEM90B	TMEM90B
SPAG4	TMPRSS15	TMPRSS15
SRGAP3	TMPRSS4	TMPRSS4
SSX2IP	TNFAIP6	TNFAIP6
STEAP1	TOP2A	TOP2A
STEAP3	TSC2	TSC2
SUSD5	TSHZ3	TSHZ3
TACSTD2	TWIST1	TWIST1
TAPBPL	TYMS	TYMS
TBC1D24	USP29	USP29
TECR	VEGFC	VEGFC
TFF1	VIPR2	VIPR2
TGFBR3	WNT4	WNT4
TGIF1	ZNF521	ZNF521
THBS2		AGK
TLE2		AMMECR1L
TLR3		CC2D1B
TM4SF1		CNOT10
TM4SF4		CNOT4
TM4SF5		COG7
TMEM176B		DDX50
TMEM181		DHX16
TMEM51		DNAJC14
TMEM90B		EDC3
TMPRSS15		EIF2B4
TMPRSS4		ERCC3
TNFAIP6		FCF1
TOP2A		GPATCH3
TSC2		HDAC3
TSHZ3		MRPS5
TWIST1		MTMR14
TYMS		NOL7
USP29		NUBP1
VEGFC		PRPF38A
VIPR2		SAP130
WNT4		SF3A3
ZNF521		TLK2
		TMUB2
		TRIM39
		USP39

		ZC3H14
		ZKSCAN5
		ZNF143
		ZNF346

Appendix 3.2 Supplementary Table 3.2 Refined 78 Gene PanNETassigner Panel and Centroids

Gene ID	Insulinoma-like	Intermediate	MLP-1	MLP-2
CLPS	1.7291	-0.6349	-0.5751	-0.5395
CTRC	1.7024	-0.6376	-0.5535	-0.519
CPA1	1.692	-0.6985	-0.5317	-0.3949
CPA2	1.6891	-0.6103	-0.5477	-0.5661
PNLIP	1.6669	-0.6912	-0.5098	-0.3992
PNLIPRP1	1.6271	-0.6449	-0.4872	-0.4681
CTRL	1.6233	-0.719	-0.4651	-0.3252
GP2	1.4843	-0.7414	-0.3024	-0.2604
PNLIPRP2	1.4047	-0.7112	-0.3687	-0.1255
PDIA2	1.39	-0.6192	-0.3686	-0.3066
REG1B	1.3047	-0.3919	-0.3827	-0.6619
SERPINI2	1.2992	-0.4979	-0.4648	-0.3196
SERPIND1	-0.0027	0.8235	-0.5206	-1.1861
RBP4	0.2889	-0.5673	-0.2673	1.1367
CLDN10	1.1139	-0.4771	-0.2451	-0.3489
USP29	1.0346	-0.5693	-0.4623	0.2389
TFF1	0.0031	-0.4046	0.9858	-0.3037
EGLN3	-0.299	-0.1904	0.9789	-0.3076
GLP1R	0.3482	-0.5853	-0.1588	0.9546
CAPN13	0.1531	-0.3075	-0.374	0.8988
GATM	0.8948	-0.3308	-0.1407	-0.4641
SLC30A2	0.8837	-0.4404	-0.4117	0.123
LOXL4	0.2272	0.5328	-0.5412	-0.8694
HAO1	0.0719	0.7249	-0.8575	-0.6741
AQP8	0.8541	-0.0756	-0.4266	-0.6199
SLC16A3	-0.131	-0.3289	0.836	-0.0851
INS	0.8221	-0.3271	-0.3037	-0.164
SERPINA3	0.8209	-0.3938	0.1213	-0.5292
RBPJL	0.7974	2.00E-04	-0.5601	-0.5395
TACSTD2	0.7854	-0.4172	0.0852	-0.3797
DAPL1	0.3791	-0.5345	-0.1134	0.74
P2RX1	0.7278	-0.3267	-0.2653	-0.0676
LRAT	-0.0986	0.5567	-0.3045	-0.7115
CYP4F3	-0.3759	0.6789	-0.4276	-0.4094
SERPINA1	-0.251	0.5052	-0.0459	-0.6781
ADM	-0.1361	-0.2008	0.6746	-0.1651
APOH	-0.1671	0.6489	-0.4204	-0.6705
LGALS2	0.6624	-0.164	-0.2861	-0.3024
GLS	-0.0749	0.5494	-0.3771	-0.6436

Gene ID	Insulinoma-like	Intermediate	MLP-1	MLP-2
PFKFB3	-0.0387	-0.21	0.6416	-0.2534
CRYBA2	-0.0123	0.5533	-0.6322	-0.439
PRSS8	0.4144	0.0454	-0.0892	-0.6249
ANGPTL3	-0.0804	0.6109	-0.5034	-0.6184
IMPA2	0.3784	-0.1409	0.2876	-0.6144
ACVR1B	-6.00E-04	-0.3588	0.1591	0.6016
SLC7A2	0.0949	0.4198	-0.592	-0.356
MAFB	0.1145	0.5008	-0.5857	-0.5727
ALDH1A1	-0.1662	0.5828	-0.419	-0.5275
RARRES2	0.5732	-0.3157	-0.0524	-0.1137
KLK4	0.5702	-0.2726	-0.3365	0.1396
MASP2	0.5584	-0.2663	-0.389	0.2073
FKBP11	-0.0429	0.474	-0.3653	-0.54
GUCA1C	0.4919	0.0412	-0.2562	-0.5317
SLC2A1	-0.1256	-0.1196	0.5261	-0.1807
SRGAP3	-0.0512	-0.1841	-0.0242	0.5143
WNT4	-0.0595	0.4323	-0.2939	-0.5092
CELA1	0.5017	-0.3757	-0.2567	0.3755
TLR3	0.1089	-0.2092	0.4951	-0.3031
IL18R1	-0.1315	0.3657	-0.0974	-0.4899
MOBKL1A	-0.1914	0.4872	-0.4285	-0.2662
ROBO3	0.4868	-0.3831	0.0197	0.0801
EGFR	0.1232	-0.3177	0.4863	-0.0744
STEAP3	0.4806	-0.4499	-0.0554	0.3282
VEGFC	-0.1643	0.4374	-0.2474	-0.4165
SMO	0.3166	-0.136	0.2099	-0.4367
NUPR1	0.3869	-0.3347	0.43	-0.3711
PMEPA1	0.3344	-0.3983	0.4272	-0.1472
SLC7A8	0.0439	0.3496	-0.4165	-0.3356
SH3BP4	0.2141	-0.4081	0.2954	0.2178
SMOC2	0.2505	-0.3794	0.3959	-0.0229
ARRDC4	-0.053	0.3601	-0.3912	-0.2415
BTC	-0.1347	0.3799	-0.3153	-0.2524
TGIF1	0.2655	-0.2955	0.3788	-0.2105
SSX2IP	-0.0643	0.3003	-0.3327	-0.1628
PDGFC	0.3183	-0.2814	0.3275	-0.2602
TM4SF1	0.1945	-0.27	0.3088	-0.0739
SMARCA1	-0.0349	0.2789	-0.3038	-0.1953
TMEM181	0.1668	-0.2359	0.0081	0.257

Appendix 3.3 Supplementary Table 3.3 RM Cohort FFPE Sample Details

Sample ID	Original conc (ng/ μ L)	Source of Tissue	Date of Sample	78 Gene Assay	Subtype
1242 P	5.76	Biopsy (pancreas)	21/05/2014	Completed	Intermediate
1068	5.92	Biopsy (pancreas)	17/06/2005	Failed QC	
1225	7.46	Biopsy (pancreas)	28/06/2013	Completed	MLP-1
1181	35.2	Biopsy (pancreas)	01/03/2011	Completed	Insulinoma-like
1025	50.2	Resection	28/07/2007	Completed	Intermediate
1141	104	Resection	18/03/2009	Completed	Intermediate
1161	104	Resection	03/07/2010	Completed	Insulinoma-like
1148	140	Resection	25/01/2010	Failed QC	
1078	212	Resection	25/10/2004	Completed	Insulinoma-like
1279	220	Resection	04/06/2007	Completed	MLP-1
1138	316	Resection	06/02/2013	Completed	Insulinoma-like
1024	348	Resection	21/05/2008	Completed	Intermediate
1185	400	Resection	27/04/2011	Completed	Insulinoma-like
1137	480	Resection	12/03/2008	Completed	Insulinoma-like
1242 M	Out of range	Biopsy (sub hepatic mass)	21/05/2014		
1272	Out of range	Biopsy (liver)	30/09/2005		
1285	Out of range	Biopsy (liver)	15/01/2008		
1315	Out of range	Biopsy (liver)	20/08/2010		
1174	Out of range	Biopsy (liver)	02/09/2010		
1188	Out of range	Biopsy (liver)	05/07/2011		
1196	Out of range	Biopsy (liver)	21/12/2011		
1139 P	Out of range	Biopsy (pancreas)	09/03/2012		
1139 M	Out of range	Biopsy (liver)	09/03/2012		
1053	Out of range	Biopsy (liver)	29/09/2005		

Sample ID	Original conc (ng/μL)	Source of Tissue	Date of Sample	78 Gene Assay	Subtype
1258	Out of range	Biopsy (peritoneum)	27/05/2011		
1033	Out of range	Biopsy (pancreas)	08/05/2007		
1169	Out of range	Biopsy (liver)	26/08/2010		
1226	Out of range	Biopsy (liver)	17/07/2013		
1235	Out of range	Biopsy (spleen)	10/02/2014		

Appendix 3.4 SEQTOR study Translational Project documents.

ANNEX VI: SEQTOR SUB-STUDY

PanNETassigner Molecular Subtypes Assay

Version 1.0, 7th August 2018

Sponsors: Laboratory of Systems and Precision Cancer Medicine
Division of Molecular Pathology
The Institute of Cancer Research

Institut Català d'Oncologia.
Institut d'Investigació Biomèdica de Bellvitge (IDIBELL).
Universitat de Barcelona (UB)

Team Leader/Principal Investigator
Anguraj Sadanandam
Laboratory of Systems and Precision Cancer Medicine
Division of Molecular Pathology
The Institute of Cancer Research
anguraj.sadanandam@icr.ac.uk

Clinical Research Fellow
Kate Young
GI and Lymphoma Research Unit
Royal Marsden Hospital
Kate.young@rmh.nhs.uk

Funding

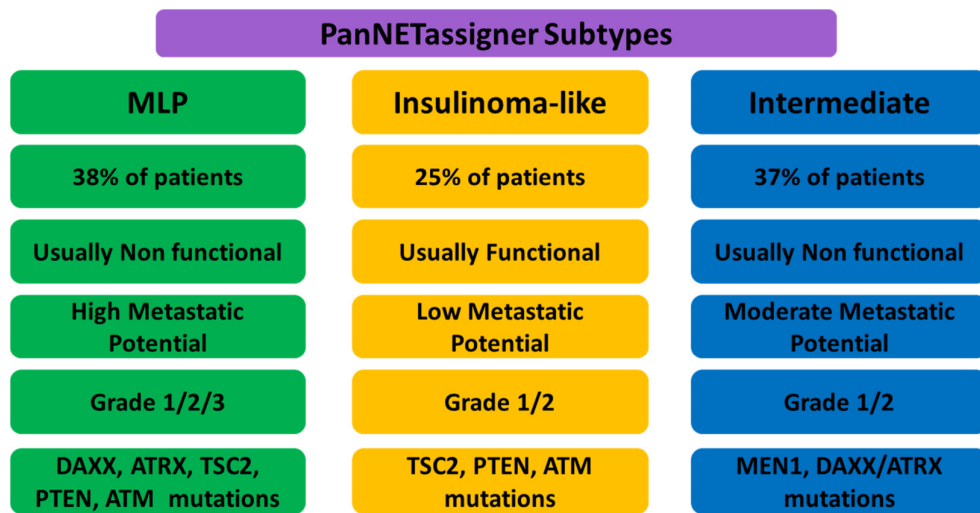
Funding is available for the first 40 samples from Anguraj Sadanandam's laboratory at the Institute of Cancer Research. An application to an international funding organisation for the remaining samples is planned following this pilot study.

Scientific Background

Our lab previously defined three molecular subtypes in sporadic Pancreatic Neuroendocrine tumours (PanNETs) based on an integrated analysis of gene expression (221 genes), microRNA (30 miRs) and mutations (targeted mutational profiles of *MEN1*, *DAXX/ATRX*, *TSC2*, *PTEN* and *ATM*), collectively named the PanNETassigner signature⁵¹. The existence of three such subtypes was supported by Scarpa et al. who reported three similar transcriptomic subtypes using RNA-sequencing²⁹.

The three PanNETassigner subtypes, Metastasis-like-primary (MLP), Insulinoma-like and Intermediate, each have specific biology and clinical features as described in the figure below.

Figure 1. PanNETassigner Molecular Subtypes



Grade 1/2 PanNETs are heterogeneous, associated with all three molecular subtypes, whereas Grade 3 tumours are predominantly associated with the MLP subtype. These observations suggest that subtyping using the PanNETassigner signature may facilitate patient stratification, potentially being able to select those Grade 1/2 patients falling into the MLP subtype, whose disease may behave more aggressively than would be expected according to grade alone.

Indeed, as we presented at ENETS 2018, the PanNETassigner subtypes are prognostic²¹, with the MLP subtype being an independent predictor for a poor prognosis. As yet the predictive value of this assay has not been assessed.

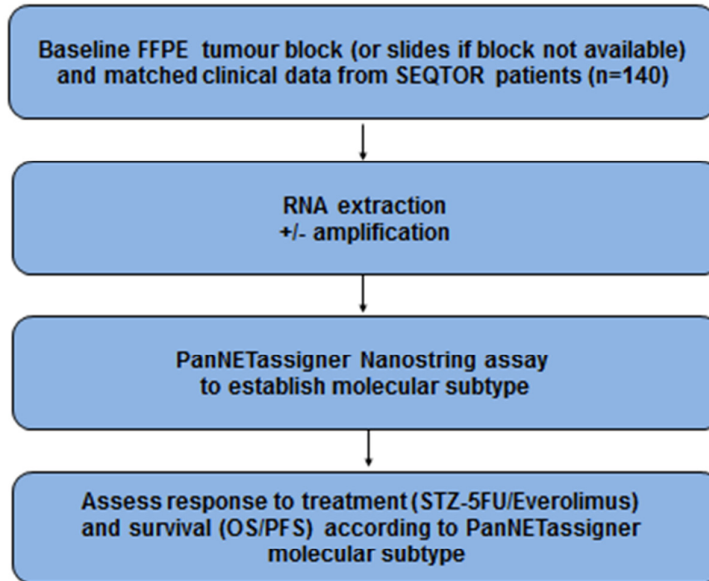
Based on our multi-omics PanNETassigner signature we have now developed a robust reproducible low cost PanNETassigner assay using the NanoString™ platform to take forward to the clinic. Expression signatures have been used extensively in other tumour types, particularly breast cancer. The Prosigna test measures risk of recurrence¹²² and the breast cancer Genomic Grade Index predicts response to chemotherapy and separates subtypes of breast cancer¹²³. The Breast Cancer Index (BCI) stratifies breast cancer patients into three risk groups and provides an assessment of tumour recurrence¹²⁴. A similar index for GEP-NETs, to improve patient prognostication and classification and potentially to predict treatment response would be highly clinically relevant. The tissue and matched patient data from the SEQTOR study provide an opportunity to test the predictive value of the PanNETassigner assay for patients undergoing treatment with chemotherapy and everolimus.

Hypothesis

The PanNETassigner molecular subtypes may be used to predict response to treatment with everolimus or streptozocin/5FU (STZ/5FU) chemotherapy in patients with grade 1 or 2 PanNETs.

Study Design

Schema



Primary Objective

To determine progression free survival according to PanNETassigner molecular subtype for first line treatment with STZ-5FU or everolimus

Secondary Objectives

To determine progression free survival according to PanNETassigner molecular subtype for second line treatment with STZ-5FU or everolimus

To determine response rate according to PanNETassigner molecular subtype for first/ second line treatment with STZ-5FU or everolimus

Exploratory Objectives

Where tissue quantity and quality allows, to investigate further potential predictive or prognostic biomarkers using additional techniques including other high throughput genomic analyses and/or microarray

Methods

Samples

The PanNETassigner Molecular Subtypes Assay will be performed on the samples sent to Dr Aldo Scarpa (Annex IV: Tumor Block analysis sub-study of SEQTOR). Patients must have given their informed and written consent to donate their samples for this sub-study.

Nucleic Acid Extraction and quality/quantity assessment

Following histopathologist assessment, selected tissue sections/slides will undergo deparaffinization, macrodissection and processing (RecoverAll™ Total Nucleic Acid Isolation Kit AM1975 protocol). Quality and quantity of extracted RNA will be assessed using NanoDrop-2000 Spectrophotometer and Agilent RNA-6000 Bioanalyzer systems respectively.

NanoString probe development, process and analysis (PanNETassigner assay)

We have selected a panel of genes for a NanoString Elements™ assay based on our PanNETassigner signature⁵¹. Oligonucleotide probe pools will be created and hybridized to reporter/capture Tags and these Tags will be hybridized to the RNA target, according to the NanoString Elements™ manual (version 2, Sept 2016) as previously described^{136,137}. Following hybridization, samples will be purified, orientated and immobilised in their cartridge using the nCounter Prep Station before being loaded into the Digital Analyser. The molecular barcodes will be counted and decoded, results stored as a Reporter Code Count (RCC) file. The RCC file may be analysed alongside the Reporter Library File (RLF) containing details of the custom probes and housekeeping genes selected.

Statistics and Analysis

Statistics

A minimal sample size of 40 was estimated using pilot PanNETassigner gene profile data from 86 PanNET samples to classify given data into four PanNET subtypes – MLP-1, MLP-2, insulinoma and intermediate. Since a gene is either differentially expressed or not, we used a method that assumes that each of these tests has a Bernoulli distribution. The statistical power was set at 0.8 and the false discovery rate at 5%.

nSolver™ analysis

The nSolver™ software analysis package will be used to perform QC and normalisation of the expression data. QC steps included assessment of assay metrics (field of view counts/binding density), internal CodeSet controls (6 positive, 8 negative controls to assess variations in expression level according to concentration and correct background noise respectively) and principal component analysis to assess batch effect. Following QC steps raw data will be normalised to housekeeping genes selected using the geNorm algorithm within nSolver™.

Assignment of Molecular Subtype and Refinement of 228 gene NanoString Assay

The normalised expression data will be log2 transformed and median centred. PanNETassigner subtypes will be assigned using Pearson correlation.

SEQTOR Translational Research Proposal Lay Summary

PanNETassigner Molecular Subtypes Assay

Pancreatic neuroendocrine tumours (PanNETs) are a rare group of tumours and their behaviour is highly variable. The SEQTOR study is trying to find out the best order in which to give two of the commonly used treatments for PanNETs, streptozotocin based chemotherapy and the mTOR inhibitor, everolimus. It would also be very helpful to be able to predict which patients are more likely to respond to which treatments but as yet this is not possible.

The aim of our study is to evaluate a new test, the PanNETassigner assay. This test uses molecular technologies, looking at changes in RNA seen in tumour samples, to divide PanNET patients into different molecular subtypes. We will use the PanNETassigner assay on tumour samples to divide patients from the SEQTOR study into the different molecular subtypes.

The PanNETassigner assay has been developed by Dr Sadanandam's lab at the Institute for Cancer Research in Sutton (UK). If you consent to take part the tumour tissue you have already provided for the SEQTOR study will be sent from the Centre for Applied Research on Cancer in Verona (Italy) to the Institute of Cancer Research in Sutton (UK). It will not be possible to directly identify you from any information included with this sample as the samples will be anonymised.

We will combine the molecular subtype results from the PanNETassigner assay test with the clinical data from the SEQTOR study to see if this test can be used to predict which patients are more likely to respond to which treatments. We will also assess if the molecular subtypes can predict how aggressively disease may behave and if the subtypes can predict overall prognosis.

If successful the tests assessed in this project could be taken forward into the clinic and, combined with current approaches, improve the prediction of prognosis for PanNET patients and help guide treatment decisions.

Appendix 4

Appendix 4.1 Supplementary Table 4.1 132 differentially expressed immune genes according to PanNETassigner subtype, classified according to subtype with highest expression

Genes	Subtype
TNFRSF11A	Insulinoma-like
STAT2	Insulinoma-like
THBD	Insulinoma-like
GTF3C1	Insulinoma-like
NEFL	Insulinoma-like
ALCAM	Insulinoma-like
IFIT1	Insulinoma-like
ENG	Insulinoma-like
TFEB	Insulinoma-like
CCND3	Insulinoma-like
STAT4	Insulinoma-like
MNX1	Insulinoma-like

Genes	Subtype
BID	Intermediate
TNFRSF1A	Intermediate
ITGA2	Intermediate
CD55	Intermediate
TNFSF10	Intermediate
LAMP2	Intermediate
IL18R1	Intermediate
VEGFC	Intermediate
CD63	Intermediate
C8B	Intermediate
CEACAM1	Intermediate
CD46	Intermediate
IL13RA2	Intermediate
MRC1	Intermediate
CD164	Intermediate
CCL13	Intermediate
S100A7	Intermediate
CCL26	Intermediate
ARG1	Intermediate
IL6R	Intermediate
CLU	Intermediate

Genes	Subtype
SPP1	MLP-1
CXCR4	MLP-1
PDGFC	MLP-1
LIF	MLP-1
FCGR1A	MLP-1
ADA	MLP-1
TLR3	MLP-1
KIT	MLP-1
LY96	MLP-1
LAG3	MLP-1
TNFSF13B	MLP-1
COL3A1	MLP-1
CDK1	MLP-1
IFI16	MLP-1
ENTPD1	MLP-1
CCRL2	MLP-1
PSMB9	MLP-1
CASP1	MLP-1
PBK	MLP-1
MAP4K2	MLP-1
CTSS	MLP-1
ISG15	MLP-1
C1QA	MLP-1
NCF4	MLP-1
THBS1	MLP-1
IL8	MLP-1
ANXA1	MLP-1
TLR2	MLP-1
DUSP6	MLP-1
TREM2	MLP-1
PSMB8	MLP-1
FCER1G	MLP-1
TREM1	MLP-1
FAS	MLP-1
CCL5	MLP-1
FN1	MLP-1
CASP10	MLP-1

Genes	Subtype
CCR7	MLP-1
POU2AF1	MLP-1
PTPRC	MLP-1
APOE	MLP-1
IL2RB	MLP-1
CFI	MLP-1
CTAG1B	MLP-1
MSR1	MLP-1
BLNK	MLP-1
TLR7	MLP-1
PYCARD	MLP-1
CCR5	MLP-1
IL18	MLP-1
PDCD1LG2	MLP-1
PPARG	MLP-1
HLA-DPA1	MLP-1
TLR4	MLP-1
C1QB	MLP-1
TRAF6	MLP-1
MCAM	MLP-1
CD53	MLP-1
RIPK2	MLP-1
GATA3	MLP-1
PSMB10	MLP-1
PDGFRB	MLP-1
CD274	MLP-1
ITGA5	MLP-1
IL10RA	MLP-1
CD58	MLP-1
LCK	MLP-1
IFIT2	MLP-1
CEACAM6	MLP-1
MAP3K1	MLP-1
DPP4	MLP-1
IFNAR1	MLP-1
DUSP4	MLP-1
CLEC4A	MLP-1

Genes	Subtype
HSD11B1	MLP-2
C1S	MLP-2
C1R	MLP-2
CCL19	MLP-2
NFATC2	MLP-2
INPP5D	MLP-2
CXCL10	MLP-2
LTK	MLP-2
IL15RA	MLP-2
F12	MLP-2
IL13RA1	MLP-2
ST6GAL1	MLP-2
TXNIP	MLP-2
C4BPA	MLP-2
IL12A	MLP-2
ITK	MLP-2
MPPED1	MLP-2
C8A	MLP-2
ICAM4	MLP-2
C8G	MLP-2
PVR	MLP-2
C9	MLP-2
CCL15	MLP-2
NOD2	MLP-2
CYLD	MLP-2

Appendix 4.2 Supplementary Table 4.2 GSEA Report for MLP-1 using C7
Gene Sets

Gene Set Name	FDR q-value
GSE3203_INFLUENZA_INF_VS_IFNB_TREATED_LN_BCELL_UP	0.007
GSE9650_NAIVE_VS_EFF_CD8_TCELL_DN	0.007
GSE3039_ALPHAALPHA_VS_ALPHABETA_CD8_TCELL_UP	0.008
GSE35825_UNTREATED_VS_IFNA_STIM_MACROPHAGE_DN	0.008
GSE3039_ALPHAALPHA_VS_ALPHABETA_CD8_TCELL_UP	0.008
GSE35825_UNTREATED_VS_IFNA_STIM_MACROPHAGE_DN	0.008
GSE18804_SPLEEN_MACROPHAGE_VS_COLON_TUMORAL_MACROPHAGE_UP	0.008
GSE45739_NRAS_KO_VS_WT_UNSTIM_CD4_TCELL_UP	0.008
GSE22935_WT_VS_MYD88_KO_MACROPHAGE_UP	0.008
GSE14699_DELETIONAL_TOLERANCE_VS_ACTIVATED_CD8_TCELL_UP	0.008
GSE29618_MONOCYTE_VS_PDC_UP	0.008
GSE43955_TH0_VS_TGFB_IL6_TH17_ACT_CD4_TCELL_4H_UP	0.008
GSE10325_CD4_TCELL_VS_MYELOID_DN	0.008
GOLDRATH_NAIVE_VS_EFF_CD8_TCELL_DN	0.008
GSE40685_TREG_VS_FOXP3_KO_TREG_PRECURSOR_DN	0.008
GSE15930_STIM_VS_STIM_AND_IL-12_24H_CD8_T_CELL_UP	0.008
GSE3982_NEUTROPHIL_VS_NKCELL_UP	0.008
GSE6259_CD4_TCELL_VS_CD8_TCELL_UP	0.008
GSE18804_SPLEEN_MACROPHAGE_VS_COLON_TUMORAL_MACROPHAGE_UP	0.008
GSE45739_NRAS_KO_VS_WT_UNSTIM_CD4_TCELL_UP	0.008
GSE22935_WT_VS_MYD88_KO_MACROPHAGE_UP	0.008
GSE14699_DELETIONAL_TOLERANCE_VS_ACTIVATED_CD8_TCELL_UP	0.008
GSE29618_MONOCYTE_VS_PDC_UP	0.008
GSE43955_TH0_VS_TGFB_IL6_TH17_ACT_CD4_TCELL_4H_UP	0.008
GSE10325_CD4_TCELL_VS_MYELOID_DN	0.008
GOLDRATH_NAIVE_VS_EFF_CD8_TCELL_DN	0.008
GSE40685_TREG_VS_FOXP3_KO_TREG_PRECURSOR_DN	0.008
GSE15930_STIM_VS_STIM_AND_IL-12_24H_CD8_T_CELL_UP	0.008
GSE3982_NEUTROPHIL_VS_NKCELL_UP	0.008
GSE6259_CD4_TCELL_VS_CD8_TCELL_UP	0.008

Appendix 4.3 Supplementary Table 4.3 MMR status for RMH PanNET cohort (n=24)

Pt trial ID	PanNET assigner Subtype	MSH2	MSH6	MLH1	PMS2	Proficient or Deficient? (P/D)
1226		(+)	(+)	(+)	(+)	P
1078		(+)	(+)	(+)	(+)	P
1024		(+)	(+)	(+)	(+)	P
1137	Insulinoma	(+)	(-)	(+)	(+)	D
1138		(+)	(+)	(+)	(+)	P
1148		(+)	(+)	(+)	(+)	P
1161		(+)	(+)	(+)	(+)	P
1185		(+)	(+)	(+)	(+)	P
1235		(+)	(+)	(+)	(+)	P
1242		(+)	(+)	(+)	(+)	P
1242		(+)	(+)	(+)	(+)	P
1258		(+)	(+)	(+)	(+)	P
1272		(+)	(+)	(+)	(+)	P
1315		(+)	(+)	(+)	(+)	P
1025		(+)	(+)	(+)	(+)	P
1033		(+)	(+)	(+)	(+)	P
1068		(+)	(+)	(+)	(+)	P
1141	Intermediate	(+)	(-)	(+)	(+)	D
1174		(+)	(+)	(+)	(+)	P
1181		(+)	(+)	(+)	(+)	P
1188		(+)	(+)	(+)	(+)	P
1196		(+)	(+)	(+)	(+)	P
1139		(+)	(+)	(+)	(+)	P
1279		(+)	(+)	(+)	(+)	P